國立臺灣大學醫學院臨床醫學研究所

博士論文

Graduate Institute of Clinical Medicine

College of Medicine

National Taiwan University

Doctoral Dissertation

多囊性卵巢症候群之臨床表徵與致病機轉

The Clinical features and Pathophysiology of Polycystic Ovarian Syndrome

黃楚珺

Chu-Chun Huang

臨床指導教授：陳美州教授、楊友仕教授

Advisor: Prof. Mei-Jou Chen, Prof. Yu-Shih Yang

基礎指導教授：陳沛隆副教授

Advisor: A.P. Pei-Lung Chen

中華民國 109 年 1 月

January 2020

doi:10.6342/NTU202000313

國立臺灣大學博士學位論文
口試委員會審定書

多囊性卵巢症候群之臨床表徵與致病機轉

The Clinical features and Pathophysiology of Polycystic Ovarian Syndrome

本論文係黃楚珺君（D02421008）在國立臺灣大學臨床醫學研究所完成之博士學位論文，於民國 108 年 12 月 11 日承下列考試委員審查通過及口試及格，特此證明

口試委員：楊友仕 陳美州 陳沛隆（簽名）

（指導教授）

黃婉婉 林偉勁

徐明義

系主任、所長 林偉勁（簽名）

（是否須簽章依各院系所規定）

doi:10.6342/NTU202000313

致謝

首先最想感謝的，是帶領我踏入多囊性卵巢症候群研究領域的指導老師陳美州教授，若不是站在巨人的肩膀上，博士班畢業之路遙遙無期。老師以自身作為學生最完美的榜樣，身為兩個孩子的母親，令人由衷敬佩地兼顧了家庭、研究和臨床醫療工作，展現了對研究無比的積極熱忱和嚴謹正直，對於學生則是完全無私的指導和支持，學生必當繼續努力，向恩師看齊。

同樣由衷感謝另外兩位博士班指導老師楊友仕教授和陳沛隆副教授這些年來的諄諄教導，論文委員會楊偉勛所長、黃娟娟教授、徐明義教授給予許多寶貴的建議，部主任陳思原教授以及其他台大婦產科恩師們和學長姐學弟妹的支持與鼓勵,台大生殖醫學中心諮詢員和技術員同仁們在臨床醫療和研究收案的大力協助，生殖內分泌實驗室周佳宏博士、黃薏璇助理、藍晨瑋博士、吳佳恩博士、柯昀菽助理...等諸多同仁在檢體收集處理、動物和細胞實驗上的種種幫忙，我才能有今天小小的成果。

這些年來除了努力生產畢業論文，在家庭方面也是有所「生產」,感恩暄暄出現在我的生命中，讓我體認人生最神奇而美好的一種幸福。也要感謝我的先生和公婆極大的育兒協助和體諒支持，否則要兼顧家庭、研究和臨床工作簡直是不可能的任務。也謝謝弟弟妹妹和其他家人的陪伴，緩解了研究不順時的許多壓力。最後，要將這份榮耀獻給我的父母還有在天上的阿嬤，從出生那刻開始，直到現在和將來，您們都是我生命中最大的力量，謝謝您們。

doi:10.6342/NTU202000313

中文摘要

多囊性卵巢症候群 (Polycystic ovarian syndrome, 簡稱 PCOS) 是育齡婦女最常見的內分泌疾病，其臨床表徵十分多元且個體變異性極高，在青少年時期，病患可能出現無月經或者月經不規則、多毛症、嚴重痤瘡、肥胖、雄性禿等症狀；到了生育年齡則可能面臨不孕，並在懷孕期間出現較高機率的流產、妊娠糖尿病、子癲前症、早產等風險；在新陳代謝方面，胰島素阻抗或第二型糖尿病、高血壓、高血脂等代謝症候群的發生率顯著上升，子宮內膜增生或者子宮內膜癌的機率也增加，因此對婦女健康的影響極為廣泛而深遠。而此複雜疾病無論是從診斷標準、致病機轉、治療方針甚至於長期預後，都尚有許多未解之謎題仍待進一步研究釐清，因此博士班期間將針對此疾病進行一系列臨床與基礎研究。

在第一個研究中，為了進一步釐清此複雜症候群之臨床表徵分群模式，並針對其新陳代謝風險找出預後危險因子，我們使用了強大且創新的統計學圖表分析法--廣義相關圖（generalized association plots，GAP），來分析多囊性卵巢症候群病患的症狀模式和特徵分群。我們首先運用關聯性分析，找出與多囊性卵巢症候群之新陳代謝異常最為相關的四個內分泌指標 (FSH, LH, free androgen index, DHEA-S)，接著依照這四個內分泌指標表現值相近度，將總共 460 名多囊性卵巢症候群患者分為四個次族群，每個次族群中的個體即這四個內分泌指標表現最相近的一群病患。結果可發現，所分出的四個次族群，不僅各自具有獨特的內分泌表徵，也同時具有顯著不同的新陳代謝異常風險。當病患出現高 free androgen index 數值且低 LH 濃度時，將會是罹患新陳代謝症候群的高風險群，這些患者可更密集地接受新陳代謝相關追蹤檢查，倘若病患出現低 free androgen index 數值且高 LH 濃度時，則可告知病患日後得到新陳代謝異常風險與同齡女性無異，應可降低不必要的追蹤檢測和健保花費，也可降低病患之焦慮不安。我們的研究成功的將患者進行了良好分組，也找出了與新陳代謝風險相關的內分泌特徵。

在第二個研究中我們針對多囊性卵巢症候群的致病機轉進行研究，由於多囊性卵巢症候群最重要的臨床症狀之一是濾泡成長異常和排卵失調，而卵巢濾泡液的生成也是濾泡成長過程重要的一環，故我們首先分析了卵巢濾泡

doi:10.6342/NTU202000313

液是如何調控相鄰內皮細胞之通透性，並針對其成分進行分析。我們先以單層人類臍靜脈內皮細胞裝置分析 11 位多囊性卵巢症候群和 9 位對照組受試者卵巢濾泡液對於內皮細胞通透性的調節，發現多囊性卵巢症候群患者的濾泡液會使得相鄰內皮細胞通透性顯著下降，由於細胞通透性與血管生成因子有關，故進一步以晶片分析 13 位多囊性卵巢症候群和 11 位對照組受試者卵巢濾泡液中的血管生成因子濃度，晶片所偵測的 55 種血管生成因子中，我們發現多囊性卵巢症候群病患的濾泡液表現較高濃度的 Platelet factor 4(PF4)，且 PF4 會與 IL-8 進行拮抗性結合，抑制細胞間隙的生成並降低相鄰內皮細胞的通透性，我們的發現不僅提供了多囊性卵巢症候群致病機轉的另一種新解釋，而且也讓我們對於 PF4 與卵巢功能相關之細胞生理機轉有更進一步的了解。

多囊性卵巢症候群具有高度遺傳性，但在過去眾多基因關聯性研究中卻找不出顯著致病基因，故被認為可能是一個多基因遺傳疾病。然而針對其高度遺傳性的另一個可能解釋是超基因調控 (epigenetics)，過去相關文獻甚少，故在第三個致病機轉相關研究中，我們將針對超基因調控其中一種重要機轉 – DNA 甲基化進行研究，針對卵巢顆粒細胞運用晶片分析全基因體 DNA 甲基化表現，試圖釐清多囊性卵巢症候群和對照組之間是否有顯著 DNA 甲基化差異。在這個研究中我們分析了兩種卵巢顆粒細胞，一種是成人卵巢顆粒細胞，代表成熟的疾病細胞，另一種是從誘導性多功能幹細胞 (induced pluripotent stem cells, iPSCs) 再次分化衍生出的卵巢顆粒細胞(分化第十二天)，代表處於剛分化階段的初始細胞。DNA 甲基化晶片的分析結果顯示多囊性卵巢症候群患者的 iPSC 衍生顆粒細胞和成人顆粒細胞均出現 CREB 訊息傳導路徑過度活化的情形，後續的西方墨點法亦驗證了多囊性卵巢症候群組有較高的 CREB 蛋白和 CBP 蛋白表現量，此發現可為多囊性卵巢症候群的致病機轉和臨床表徵提供嶄新而合理的解釋。

由於微小核醣核酸 (miRNA) 調節也是超基因調控重要的機轉之一，且血液游離微小核醣核酸的表現在許多疾病研究中已經被證實有良好的臨床診斷及預測預後功效，故在第四個研究中，我們欲分析血液游離微小核醣核酸是否可以作為多囊性卵巢症候群的臨床診斷和療效預測之生物指標。我們從文獻中選擇了 14 種可能與多囊性卵巢症候群致病機轉相關的標的微小核醣核酸，在 75 個多囊性卵巢症候群病患和 20 個對照組受試者的周邊血液進行逆轉錄

doi:10.6342/NTU202000313

聚合酶鏈式反應 (rtPCR) 測量。在第一個階段的標的微小核醣核酸測量中，我們發現多囊性卵巢症候群患者與對照組受試者的血液游離微小核醣核酸表現模式有顯著不同，多囊性卵巢症候群患者的血液 miR-93, miR-132, miR-221, miR-223, miR-27a, miR-212 表現值相較於對照組顯著較高，而 miR-222 和 miR-320a 表現值顯著較低。此外，metformin 藥物在臨床上可改善 50%患者的排卵功能和月經週期，然而目前並無方法可預測其療效，故我們分析了 metformin 治療有效和無效兩組之間的微小核醣核酸表現，亦發現有顯著差異。第二個階段為模型建立，我們以 miR-93、miR-132、miR-222、miR-27a、miR-125b、miR-212 這六個最具顯著差異的微小核醣核酸表現值，建立了多囊性卵巢症候群的診斷模型，其接收者操作特徵 (receiver operating characteristic, ROC) 曲線下面積 (area under curve, AUC) 高達 0.96，對於受試者是否符合多囊性卵巢症候群臨床診斷有極佳的預測性。此外我們針對 metformin 是否具有改善排卵的臨床療效，也以 miR-132, miR-27a, miR-222, miR-93 這四個微小核醣核酸表現值建立了預測模型，並成功在另一個獨立的多囊性卵巢症候群病患族群中驗證其預測效果，藉由此預測模型，可以幫忙預測患者是否可以在接受 metformin 治療後，出現排卵功能及月經週期上的改善，對於臨床治療的療效預測和藥物選擇有所助益。

總結以上四個研究所獲得的成果，從病患卵巢濾泡液、卵巢顆粒細胞、血液檢體、到病患專一性 iPSC 細胞株的建立，透過各種分析方法，在臨床症狀、疾病診斷、疾病預後、致病機轉以及臨床治療上都有許多新的發現，包括：臨床症狀的分組解析和新陳代謝症候群危險因子的探尋、濾泡液中血管生成因子與其潛在影響內皮細胞通透性之機轉解析、病患專一性及多囊性卵巢症候群特異性 iPSC 之建立與再分化研究、全基因體 DNA 甲基化分析所發現之 CREB 訊息調控路徑異常對於致病機轉之可能影響、以血液游離微小核醣核酸建立之多囊性卵巢症候群診斷模型和 metformin 療效預測模型，無論是研究過程所積累的經驗，或者是所獲得的種種研究成果，都為日後多囊性卵巢症候群相關基礎或臨床研究提供了大量的工具和材料，在臨床醫療的診斷和治療也有諸多貢獻。

關鍵字：多囊性卵巢症候群、誘導性多功能幹細胞、細胞通透性、DNA 甲基化、微小核醣核酸、超基因調控、顆粒細胞、CREB、platelet factor 4。

doi:10.6342/NTU202000313

英文摘要 English Abstract

Polycystic ovarian syndrome (PCOS) is the most common endocrine disorder in women with reproductive age. There is a broad spectrum of clinical presentations and the heterogeneity of symptoms is extremely high. In adolescence, the common presentations include amenorrhea, irregular menstruation, hirsutism, severe acne, obesity and alopecia. The patients of childbearing age have higher risks of infertility and pregnancy complications, such as abortion, gestational diabetes, preeclampsia and preterm delivery. And they also have higher risk of metabolic aberrations such as insulin resistance, type II diabetes, hypertension and dyslipidemia. Therefore its impact on women health is huge and lifelong. Until now, there are still many unanswered questions regarding to its diagnostic criteria, pathophysiology, treatment and screen strategies, and long-term prognosis. Therefore the aim of the proposal is to conduct series of basic and clinical researches on PCOS.

In the first study, we applyed a matrix visualization and clustering approach, generalized association plots (GAP), to divide 460 PCOS patients into four distinct clusters according to the correlation of four endocrine parameters. Each cluster exhibited specific endocrine characteristics and the prevalence of metabolic syndrome (MS) was significantly different among each cluster ($P < 0.0001$). A common endocrine characteristic of the metabolically unhealthy clusters was relatively lower LH level. While high FAI level did correlate with more severe metabolic aberrations, high LH level (>15 mIU/ml) during early follicular phase showed better predictive value than low FAI level to become a metabolically healthy cluster. Our results could stratify women with PCOS into meaningful subtypes and provide a better understanding of related risk factors. This could potentially enable the design and delivery of more effective screening and treatment intervention.

The second study was focusing on the pathogenesis of PCOS. Abnormal folliculogenesis is one of the cardinal presentations of PCOS and the formation of follicular fluid (FF) have been proposed to be involved in the normal follicular growth. However, whether or not there is a change in intrafollicular angiogenetic/angiostatic factors and in endothelial permeability underlies PCOS is unknown. Therefore we collected the FF from 13 PCOS and 11 ovulatory control subjects. The influence of FF on endothelial cell permeability was evaluated using a human umbilical vein

doi:10.6342/NTU202000313

endothelial cell monolayer permeability assay. The FF from PCOS patients caused significantly poorer endothelial cell permeability comparing with the effect of FF from the control group. The intrafollicular expression profiles of angiogenesis-related proteins were analyzed using a Human Angiogenesis Protein Array Kit. Among the 55 angiogenesis-related proteins tested, there was a significantly higher level of intrafollicular platelet factor 4 (PF4) and PF4/IL-8 complex in the PCOS group ($p = 0.004$). The anti-permeability effect of PF4 was related to the decrease in the intercellular gaps and antagonistic binding with IL-8. Our study provided the first evidence of the pathophysiologic contribution of the well-known angiostatic protein, PF4, on human reproductive biology. The increase of the intrafollicular PF4 and its anti-permeability effect might affect the formation of FF and folliculogenesis in PCOS.

In the third study, we wanted to elucidate whether and how the pathogenesis of PCOS is related to epigenetic aberrations. We established patient-specific induced pluripotent stem cells (iPSCs) from skin fibroblasts through the application of nonviral episomal reprogramming and were differentiated into ovarian granulosa cells (GCs) with the use of a cocktail of growth factors. This could serve as a valuable model to evaluate the presymptomatic pathogenic events in early cellular differentiation and developmental status. The combination of DNA methylomic analysis in the adult GCs and iPSC-derived GCs revealed several differentially methylated genes and differentially expressed pathways between the PCOS and control groups, and a preserved persistent hyperactivation of the CREB signaling pathway might be involved in the pathogenesis of PCOS. CREB and its coactivators are known to be critical sensors for both hormonal and metabolic signals, and it is possible that the aberration of the CREB signaling pathway could be related to complex hormonal and metabolic disorders such as PCOS. These results could have implications on the early developmental origin, familial nature, and environmental interaction effects of this disease, providing possible therapeutic targets in the future.

The aim of the fourth study is to investigate the role of microRNAs (miRNAs) in the pathogenesis of PCOS, and to evaluate the feasibility of miRNA expression as clinical diagnostic biomarkers for PCOS. We selected 14 targeted miRNAs which had been reported to be related with glucose metabolism or diabetes, ovarian or pituitary function in the literatures. Totally 75 patients with PCOS and 20 control subjects had their plasma sent for rtPCR analysis. The results showed that the expression levels of

doi:10.6342/NTU202000313

miR-93, miR-132, mR-221, miR-223, miR-27a and miR-212 were significantly higher in PCOS and the levels of miR-222 and miR-320a were significantly lower in PCOS group. The prediction model for the diagnosis of PCOS was further established according to six discriminative miRNAs and the area under curve (AUC) was as high as 0.96. The second part of the study is to evaluate the feasibility of circulatory miRNAs as the predictive biomarkers for the therapeutic effect of metformin. Clinically about 50% of PCOS patients showed improvements in ovulation and menstrual cyclicity when taking metformin. Therefore we compared the expression level of circulatory miRNAs between metformin-effective and metformin-effective patients. And then we established a predictive model for the therapeutic effects of metformin according to the expression level of four discriminative miRNAs (miR-93、miR-222、miR-223、miR-429). The AUC was 0.72 and could be validated with another separate PCOS cohort. Our study showed that the expression pattern of circulatory miRNAs could be effective prediction models for the diagnosis of PCOS and the therapeutic effect of metformin. The pathophysiological contribution of the differentially expressed miRNAs to PCOS needs further researches to elucidate.

In summary, the GAP analysis stratified women with PCOS into meaningful subtypes and provide a better understanding of related risk factors. There was an increase in the level of intrafollicular PF4 protein and its anti-permeability effect might affect the formation of FF and folliculogenesis in PCOS. The aberrant epigenetic regulation was shown to be involved in the pathogenesis of PCOS, including differentially expressed DNA methylation involving CREB signaling pathway. The differential levels of circulatory miRNAs between PCOS and control group could be an excellent diagnostic tool for PCOS and the regulatory roles of these miRNAs on PCOS deserved further studies. The above results provide considerable contributions for both the basic researches and clinical practices in PCOS.

Keywords：Polycystic ovarian syndrome、induced pluripotent stem cells、permeability、DNA methylation、miRNA、epigenetics、granulosa cells、CREB、platelet factor 4.

doi:10.6342/NTU202000313

目　錄

doi:10.6342/NTU202000313

doi:10.6342/NTU202000313

圖目錄

doi:10.6342/NTU202000313

表目錄

doi:10.6342/NTU202000313

第一章　緒論

第一節 多囊性卵巢症候群簡介

多囊性卵巢症候群 (Polycystic ovarian syndrome, 簡稱 PCOS) 是育齡婦女最常見的內分泌疾病，不同文獻所報告之發生率有所不同，可高達 5.5-19.9% (Azziz *et al.*, 2016)，對婦女健康的影響極為顯著。

(一) 歷史淵源

遠在兩千五百年前的古希臘時代，現代醫學之父希波克拉底醫師 (Hippocrates, 460 B.C.-377 B.C.) 就曾在其著作中描述過這樣的女性病患：「But those women whose menstruation is less than three days or is meagre, are robust, with a healthy complexion and a masculine appearance; yet they are not concerned about bearing children nor do they become pregnant. -- Diseases of Women 1.6」(Azziz *et al.*, 2011)，這段文字描述與多囊性卵巢症候群的關鍵症狀可說十分雷同，包括月經量少、男性化外型，以及不容易懷孕，只差在當時並沒有對於卵巢的型態進行描述。而真正把這個疾病的多囊性卵巢型態和臨床症狀同時定義出來的學者，則是 1935 年發表在美國婦產科學期刊(American Journal of Obstetrics & Gynecology)的 Irving Stein 醫師和 Michael Leventhal 醫師，其”Amenorrhea associated with bilateral polycystic ovaries”一文中描述了七個女性病患，出現共同的症狀包括：無月經、多毛症、肥胖和多囊性卵巢外觀，可說是多囊性卵巢症候群這個重要疾病被清楚界定的開始。然而其論文發表至今已經超過 80 年，即便歷經了多年研究，對於此複雜症候群仍有許多未明之處，包括確切的致病機轉、最佳的診斷與治療方式、其與基因或者超基因調控的相

doi:10.6342/NTU202000313

關性、在不同年齡層的診斷依據和影響層面.....等等，目前都尚未有定論，因此也啟發了博士班研究進一步深入探索的契機。

以演化的觀點來說，多囊性卵巢症候群被認為與糖尿病和肥胖一樣，可能都與「節儉基因」的表現有關 (thrifty genotypes and phenotypes)。 在古早時代，由於人類面臨的嚴苛的生存環境且必須進行長時間的體能活動，飲食能量缺乏，因此節儉基因的表現是有利於當時生存的，使得這個疾病的基因型和表徵在源遠流長的演化之河中被流傳下來，然而在現代社會因飲食過度充裕和體能活動下降，使得節儉基因型不再是現代人類的生存優勢，反而造成相關疾病如糖尿病、肥胖、心血管疾病的發生率大增，而多囊性卵巢症候群也被認為與這些疾病高度相關。

(二) 診斷標準

多囊性卵巢症候群的診斷方式至今沒有全世界統一的標準，目前最廣為各學者所接受的診斷標準之一是 2003 年制訂的鹿特丹標準 (Rotterdam criteria) (Rotterdam ESHRE/ASRM-Sponsored PCOS Consensus Workshop Group, 2004)，首先必須排除其他造成排卵異常或雄性荷爾蒙增加之內分泌疾患，包括：先天性腎上腺增生症 (congenital adrenal hyperplasia)、庫欣氏症候群 (Cushing's syndrome)、高泌乳激素血症 (hyperprolactinemia)、甲狀腺亢進或低下 (hyper- or hypo-thyroidism)、肢端肥大症 (acromegaly)、卵巢早發性衰竭 (premature ovarian failure)、單純肥胖、分泌雄性荷爾蒙之腫瘤等疾病，接著必須符合以下三項診斷條件之任兩項以上，即可符合多囊性卵巢症候群之診斷：(1) 慢性無排卵 (Chronic anovulation, 簡稱 AO)：定義為每年的自發性月經少於九次；(2) 高雄性荷爾蒙症 (Hyperandrogenism, 簡稱 HA)：包含血清雄性荷爾蒙過高，或者臨床上出現多毛症、嚴重痤瘡、雄性禿等雄性荷爾蒙過高的表徵；(3) 多囊性卵巢型態 (Polycystic ovarian morphology, 簡稱 PCOM)：在超音波檢查下，單側或雙側之卵巢出現超過 20 顆之 2-9 毫米大小之濾泡。

doi:10.6342/NTU202000313

其他通用的診斷標準至少還包括 1990 年美國國家衛生研究院 (National Institutes of Health, NIH) 所制定的 NIH 標準 (Zawadzki and Dunaif, 1992) ，病患必須同時符合上述慢性無排卵和高雄性荷爾蒙症兩項條件，至於多囊性卵巢型態並不在診斷條件當中。較晚被提出的另一個診斷標準是雄性荷爾蒙過高暨多囊性卵巢症候群協會(Androgen Excess and PCOS Society, AE-PCOS Society) 於 2006 年所制定的 AE-PCOS 標準 (Azziz *et al.*, 2006)，高雄性荷爾蒙症是必備條件，然後再加上慢性無排卵或者多囊性卵巢型態任一條件即可符合診斷。目前台大醫院所使用的是鹿特丹標準，也可說是現行文獻中最廣為使用的診斷標準，然而由此診斷方式會出現四個不同組合的臨床表現：(1) 完全表現型 (full-blown phenotype, phenotype A)：三項診斷條件均符合；(2) 非多囊性卵巢型 (non-PCO phenotype, phenotype B)：符合慢性無排卵和高雄性荷爾蒙症，但無多囊性卵巢型態；(3) 排卵型 (ovulatory phenotype, phenotype C)：符合高雄性荷爾蒙症和多囊性卵巢型態，但排卵正常；(4) 非高雄性荷爾蒙症 (non-hyperandrogenic phenotype, phenotype D)；符合慢性無排卵和多囊性卵巢型態，但雄性荷爾蒙正常。每一個子群的臨床表現都不相同，如此診斷出來的族群十分多樣化且不同個體間的變異性很高，也進一步造成研究上和臨床治療上的歧異和困難。

(三) 臨床表徵

多囊性卵巢症候群的臨床表徵十分多元且個體變異性極高，在青少年時期，病患可能出現無月經或者月經不規則、多毛症、嚴重痤瘡、肥胖、雄性禿等症狀；到了生育年齡則約七成患者不孕，並可能在懷孕期間出現較高機率的流產、妊娠糖尿病、子癲前症、早產等風險；過了生育年齡後，胰島素阻抗或第二型糖尿病、高血壓、高血脂等新陳代謝症候群的發生率上升，子宮內膜增生或者子宮內膜癌的機率也增加 (Diamanti-Kandarakis and Papavassiliou, 2006; Randeva *et al.*, 2012)，因此這個複雜疾病對於婦女的健康影響，可說是層面廣泛且長久深遠。針對其各種臨床表徵一一詳述如下：

doi:10.6342/NTU202000313

(1) 皮膚外觀表徵

多毛症和雄性禿是高雄性荷爾蒙症最具代表性的症狀。在過去的臨床研究顯示，65-75%的多囊性卵巢症候群患者會出現多毛症，這比非多囊性卵巢症候群婦女的發病率顯著增加（0-2%） (Azziz *et al.*, 2009)。多數研究對於多毛症的診斷，通常以 modified Ferriman-Gallwey（mFG）分數大於等於 6 分作為標準，這個數值是對應到一般女性族群 95%高標的分數，然而也有其他研究認為 mFG 分數大於等於 3 就應視為異常 (DeUgarte *et al.*, 2006)。另一個研究則發現，針對 228 名臨床顯示為輕微毛髮過量的患者（mFG 分數小於等於 5），進一步的驗血和超音波檢查後，卻有超過一半符合高雄性荷爾蒙症，並有百分之五十的患者符合多囊性卵巢症候群 (Souter *et al.*, 2004) 。因此，究竟多毛症的最佳診斷標準為何亦尚未有定論，且可能隨不同種族而異，一般亞裔患者的多毛症狀較高加索人種輕微，而被認為應要採用較低的 mFG 分數標準。至於痤瘡是否可以作為多囊性卵巢症候群的高雄性荷爾蒙症診斷標準之一，在不同研究的看法不一，一般而言多囊性卵巢症候群患者罹患痤瘡的比率約 15–25%，然而痤瘡在非多囊性卵巢症候群族群的一般青少年患病率就非常高，因此究竟痤瘡的發生率在多囊性卵巢症候群患者是否有顯著上升，而且罹患痤瘡是否可以符合高雄性荷爾蒙症的診斷條件，目前仍有爭議。

(2) 新陳代謝異常

許多文獻均顯示多囊性卵巢症候群並不只是單純內分泌疾病，而是與新陳代謝異常有強烈的相關性，包括了血脂異常 (dyslipidemia)、胰島素阻抗 (insulin resistance)、中央型肥胖 (central obesity 或 abdominal obesity)、第二型糖尿病、高血壓等疾病 (Chen *et al.*, 2007; Moran *et al.*, 2010; Diamanti-Kandarakis and Dunaif, 2012; Wild *et al.*, 2010)。然而，依照鹿特丹診斷標準的不同組合，可將多囊性卵巢症候群病患分成四個不同次族群如前述，這些病患是否都具有相同的新陳代謝風險？要如何篩選出真正具有新陳代謝高風險的病患？近年來也有不少文獻試圖探討這些問題。有些研究認為高雄性荷爾蒙症與新陳代謝異常之高風險存在正相關 (Shroff *et al.*, 2007; Chae *et al.*, 2008)，然而也有許多研究分

doi:10.6342/NTU202000313

析鹿特丹標準之四個不同次族群的新陳代謝異常發生率，結果顯示並沒有出現統計上顯著差異 (Hassa *et al.*, 2006; Kauffman *et al.*, 2008; Wijeyaratne *et al.*, 2011; Li *et al.*, 2013; Hosseinpanah *et al.*, 2014)。此外，除了睪固酮 (testosterone) 以外，其他荷爾蒙如硫酸脫氫表雄酮 (dehydroepiandrosterone sulfate, DHEA-S) 和黃體化激素(luteinizing hormone, LH) 也曾被報告與新陳代謝異常的發生率有相關聯性(Chen *et al.*, 2006; Lawson *et al.*, 2008; Lerchbaum *et al.*, 2012)。因此如何針對每個病患不同的臨床表徵來評估其新陳代謝異常的風險變成了臨床上極為重要的課題，假如我們能夠篩選出新陳代謝低風險的病患，便可減少不必要的追蹤治療，降低醫療花費，並降低病患不必要的焦慮，增進其生活品質，另一方面，若能篩選出新陳代謝高風險的病患，便可及早給予積極的追蹤治療，甚至達到初級預防 (primary prevention) 之效果，幫助病患正視自己的高風險並及早建立健康的生活型態以降低日後發生新陳代謝症候群之機率。因此在博士班研究的第一階段，將全面分析多囊性卵巢症候群病患的各個荷爾蒙指標，希望可以將臨床表現變異性極高的病患進行良好的分組，並試圖找出與新陳代謝異常最相關的臨床指標，不僅有助於進一步解析其與新陳代謝異常相關之致病機轉，更有助於臨床上預測預後並追蹤治療。

(3) 肥胖

肥胖對多囊性卵巢症候群的影響，以及反過來說，多囊性卵巢症候群對肥胖的影響，十分地複雜，有著密不可分的交互作用。儘管多囊性卵巢症候群在肥胖和纖瘦的女性都會發生，但近年一個囊括 15129 名女性的系統性回顧分析顯示，肥胖症在多囊性卵巢症候群女性的罹患率，仍比非多囊性卵巢症候群的女性顯著上升，且因種族而異，亞裔患者的肥胖率是對照組的 2.3 倍，高加索裔患者的肥胖率是對照組的 10.8 倍 (Lim *et al.*, 2012)，顯示高加索裔患者在肥胖這個徵狀上是更加嚴重的。然而，大多數研究均從大型醫院或診所召募多囊性卵巢症候群患者，而這當中很可能會出現轉診偏差(referral bias)，亦即較為肥胖的多囊性卵巢症候群患者可能比較傾向於花費較高的時間與金錢成本前往大型醫院規則就診，導致這些研究的多囊性卵巢症候群患者肥胖比例較高。事實上，另外兩個並非從醫院召募病患而是從一般女性群眾進行診斷的研究顯示，從醫

doi:10.6342/NTU202000313

院召募的多囊性卵巢症候群患者明顯比從一般人群召募的多囊性卵巢症候群患者還要肥胖，而從一般人群招募的患者比起未罹病者的肥胖機率並無顯著差異 (Ezeh *et al.*, 2013; Luque‐Ramirez *et al.*, 2015)。這些研究顯示，肥胖的多囊性卵巢症候群患者相較於瘦的多囊性卵巢症候群患者，顯然有較強的驅動力促使其就診，這也造成了多數在醫院進行的研究對於肥胖和多囊性卵巢症候群的相關性可能是高估的。

此外，肥胖這個因素是否會單獨引起多囊性卵巢症候群的發生仍然是有爭議的。在一個西班牙的全國出生登記回溯性研究 (Alvarez‐Blasco *et al.*, 2006) 和一個澳洲的社區型縱向觀察研究 (Teede *et al.*, 2013) 顯示，罹患肥胖症的女性有較高的機率得到多囊性卵巢症候群。然而，一個在未挑選族群 (unselected population) 的美國研究中，不同身體質量指數 (body mass index, BMI) 的婦女得到多囊性卵巢症候群診斷的機率並沒有顯著差異 (Yildiz *et al.*, 2008) ，另一個類似的土耳其研究卻又顯示高身體質量指數的婦女有更高的多囊性卵巢症候群罹患率 (Yildiz *et al.*, 2012)，可以說各家研究眾說紛紜。而另一個反對肥胖會單獨誘發多囊性卵巢症候群的觀點是，不同國家或不同地區的居民其平均身體質量指數顯著不同，但是這些地區的多囊性卵巢症候群盛行率卻沒有顯著差異 (Lizneva *et al.*, 2016)，由此推測肥胖對於多囊性卵巢症候群盛行率並無顯著影響。另外，過去的基因研究也並沒有找到已知與肥胖相關的基因變異出現在多囊性卵巢症候群病患中 (Cai *et al.*, 2014)。

儘管肥胖無法單獨促成或者完全解釋多囊性卵巢症候群的胰島素阻抗和新陳代謝異常，但是卻會加重其症狀嚴重度 (Moran *et al.*, 2015)。一個在美國長期追蹤 18 年共 1127 位年輕多囊性卵巢候群患者的族群研究顯示 (Wang *et al.*, 2011)，肥胖的年輕多囊性卵巢症候群患者，日後罹患第二型糖尿病的比率高達 23.1%，相較於身體質量指數正常者的糖尿病罹病率僅 13.1%，顯著地上升。高血脂的發病率也是在肥胖的多囊性卵巢症候群患者顯著較高 (41.9% v.s. 27.7%)。我們在臨床上也經常可以觀察到，患者只要減少 5-10%的體重，便能在血糖、血脂肪、雄性荷爾蒙、甚至是無排卵等症狀都出現顯著改善，如同過

doi:10.6342/NTU202000313

去文獻所報告的一樣 (Nicholson *et al.*, 2010)。

(4) 不孕

多囊性卵巢症候群是無排卵性不孕的主要原因，為社會增添了沉重的健康和經濟負擔；然而，多囊性卵巢症候群相關的不孕症研究依然會受到轉診偏差的影響，多數研究是在大型醫院甚至醫學中心執行而非針對社區之多囊性卵巢症候群病患執行，因此許多研究不見得能夠反應多囊性卵巢症候群之不孕症診斷和治療方式的全貌。在一個澳洲的社區執行大型橫斷性研究 (community-based cross-sectional analysis) 中，總共分析了 4856 名自述罹患多囊性卵巢症候群的女性，其中有 72%罹患不孕症，而未自述罹患多囊性卵巢症候群的女性則只有 16%出現不孕（P 值 < 0.001）(Joham *et al.*, 2015)。另一個美國的回溯性研究則是根據醫院病歷追蹤了 786 名被診斷多囊性卵巢症候群超過 30 年的病患(Wild *et al.*, 2010)，結果 66%的女性罹患不孕症。總之，不孕症與多囊性卵巢症候群的相關性是非常顯著的。

(5) 精神疾患

過去的研究顯示，多囊性卵巢症候群病患比未罹患多囊性卵巢症候群的女性更加普遍而嚴重地出現憂鬱和焦慮等精神疾病(Teede *et al.*, 2011; Dokras *et al.*, 2011; Veltman‐Verhulst *et al.*, 2012)，而無論是哪一種表型，或者無論是否肥胖，精神疾患的發生率都顯著增加 (Dokras *et al.*, 2011; Moran *et al.*, 2012)。特別的是，這些病患憂鬱的程度與胰島素阻抗的程度似乎呈現正相關 (Cinar *et al.*, 2011)。在一個分析了 28 個研究 (包括 2,384 例多囊性卵巢症候群患者和 2,705 例對照組)的統合研究(metaanalysis)中，同樣發現多囊性卵巢症候群患者比起對照組會出現更嚴重的情緒困擾 (Veltman‐Verhulst *et al.*, 2012)。然而，儘管多毛症、肥胖和不孕症都被報告可能會在某種程度上造成多囊性卵巢症候群病患的情緒困擾，沒有單一因素可以完全並一致性地解釋多囊性卵巢症候群患者的精神疾病，顯示其影響可能是多因素的(Veltman‐Verhulst *et al.*, 2012)。

doi:10.6342/NTU202000313

(6) 懷孕與生產併發症

多囊性卵巢症候群患者有較高風險在懷孕期間發生併發症。一個瑞典的大型病例對照研究 (Roos *et al.*, 2011) 分析了出生登記資料庫中，在 1995 年到 2007 年之間，總共 3,787 名生下單胞胎的多囊性卵巢症候群產婦，以及超過 100 萬名非多囊性卵巢症候群之對照組產婦，結果顯示多囊性卵巢症候群孕產婦罹患子癇前症、嚴重早產（定義為早於 32 週的生產）和妊娠糖尿病的機率均顯著上升。而多囊性卵巢症候群產婦所生的嬰兒，也有顯著較高的風險出現體重過大、胎便吸入症候群和低 Apgar score（<7 分）。其他研究也證實了這些發現(Sterling *et al.*, 2016; Pan *et al.*, 2015; Palomba *et al.*, 2015)，而且即使使用了其他診斷標準來診斷多囊性卵巢症候群都得到一致的結果，顯見多囊性卵巢症候群不僅會增加患者懷孕生產時的風險，亦會增加對胎兒的風險。

(7) 心血管疾病併發症

雖然多囊性卵巢症候群病患發生心血管疾病的實際風險比對照組增加多少尚不明確，然而多數研究均顯示，與心血管疾病相關的風險因子之發生率顯著較高，這樣的結果顯示多囊性卵巢症候群病患可能有更高的風險發生心血管疾病 (Carmina *et al.*, 2014)。例如：與健康對照組相比，多囊性卵巢症候群病患出現更嚴重的冠狀動脈鈣化(Christian *et al.*, 2003; Talbott *et al.*, 2004)，其頸動脈內壁厚度也顯著增加(Luque‐Ramirez *et al.*, 2007; Lass *et al.*, 2011)。但是這些危險因子的發生是否實際增加了多囊性卵巢症候群病患心血管疾病的死亡率，則尚未有定論。在一般族群當中，超過 50 歲以後，心血管疾病 (例如心肌梗塞) 的發生率就開始增加，然而多囊性卵巢症候群病患增加的程度與對照組相比並未出現顯著差異。過去有少數研究分析了在接近更年期時的多囊性卵巢症候群病患，進行年齡配對之後，其心血管疾病的發生率並未高於對照組(Carmina *et al.*, 2013; Ramezani *et al.*, 2015; Bairey *et al.*, 2016)，一個可能的問題在於這些研究中，長期追蹤的病患人數太少，且發生心血管疾病的事件數太少，而難以檢測到微小的差異。此外，種族差異、不同的診斷標準和研究設計都可能影響了研究結果。

doi:10.6342/NTU202000313

(8) 癌症

過去已有許多文獻報告指出，多囊性卵巢症候群病患得到子宮內膜癌的機率顯著增加（勝算比：2.7 倍），其背後機轉可能與慢性無排卵和高胰島素血症有關，至於其與卵巢癌和乳腺癌的風險則無顯著關聯性(Dumesic *et al.*, 2013)。

(四) 致病機轉

多囊性卵巢症候群的病理生理學和致病機轉相當複雜，許多分子機轉彼此交互影響，其發生順序和因果關係至今仍無法完全釐清。曾被提出的相關致病機轉如下：

(1) 高雄性荷爾蒙症 Hyperandrogenism

高雄性荷爾蒙症在鹿特丹診斷標準中雖然非必備條件，但卻是 AE-PCOS 標準和 NIH 標準的必備診斷條件，也可以說是多囊性卵巢症候群最重要的臨床表徵之一，在致病機轉上扮演極為關鍵的角色。正常的生理機轉下，女性體內的雄性荷爾蒙約一半來自於卵巢濾泡鞘細胞 (theca cell) 所分泌，另一半則是來自於腎上腺 (Rosenfield and Ehrmann, 2016)，而多囊性卵巢症候群病患體內分泌過多的雄性荷爾蒙，約 70-80%被認為是來自於卵巢的過度分泌，其餘 20-30%的多囊性卵巢症候群病患，則是以腎上腺分泌過多的雄性荷爾蒙來表現，腎上腺皮質會受到促腎上腺皮質激素 (adrenocorticotropic hormone, ACTH) 的刺激，將膽固醇轉換成黃體素和雄性荷爾蒙的前驅物，最後在腎上腺皮質網狀區 (zona reticularis) 製造出睪固酮。而腎上腺特有的 Sulfotransferase 2A1 酵素可以將去氫皮質酮酮 (Dehydroepiandrosterone, DHEA) 快速轉換為硫酸去氫皮質酮 (Dehydroepiandrosterone sulfate, DHEA-S)，因此臨床上可藉由測量 DHEA-S 得知腎上腺製造雄性荷爾蒙的產量高低。

而在卵巢濾泡鞘細胞當中，雄性荷爾蒙合成途徑的許多酵素之過度表現，

doi:10.6342/NTU202000313

都曾被報告和多囊性卵巢症候群有所相關。例如在合成雄性荷爾蒙過程的一個關鍵速率酵素 (rate-limiting enzyme) CYP17A1 (17α-hydroxylase)，被發現在多囊性卵巢症候群病患的卵巢濾泡鞘細胞的表現顯著增加，進而可能導致更多黃體素前驅物被轉換為雄性荷爾蒙 (McAllister *et al.*, 2015)。從多囊性卵巢症候群病患分離出的卵巢濾泡鞘細胞，受到胰島素和黃體化激素刺激產生的雄性荷爾蒙也比正常女性較多 (Nestler *et al.*, 1998)。多囊性卵巢症候群病患除了雄性荷爾蒙的生成異常增加之外，還有一個雄性荷爾蒙表現過高的因素在於性激素結合球蛋白 (Sex hormone binding globulin, SHBG) 在肝臟的生成，會受到高胰島素血症的影響而下降，進而導致具有生物活性的游離睪固酮 (free testosterone) 增加 (Diamanti-Kandarakis and Dunaif, 2012)，並使體內器官組織更加受到雄性荷爾蒙的刺激而進一步出現相關臨床表徵，例如：多毛症、嚴重痤瘡、雄性禿等症狀，甚至加重其他新陳代謝方面的異常，包括：高胰島素血症、中央型肥胖、高血壓、肝功能異常.....等等，因此高雄性荷爾蒙可說是多囊性卵巢症候群最關鍵的臨床表徵也是致病機轉之一。總歸來說，高雄性荷爾蒙症產生的原因，與腦下垂體分泌過多黃體化激素、卵巢睪固酮合成異常、高胰島素血症、性激素結合球蛋白減少.....等多種因素皆有關。

(2) 胰島素阻抗 Insulin resistance 和高胰島素血症 Hyperinsulinemia

過去的研究發現，多囊性卵巢症候群病患整體來說約有 85%會出現胰島素阻抗，而且並非只有肥胖的多囊性卵巢症候群病患，連瘦的多囊性卵巢症候群病患也會發生胰島素阻抗 (發生率高達 75%)。而肥胖則是會加重胰島素阻抗的程度，在多囊性卵巢症候群病患比起非多囊性卵巢症候群婦女還要更加顯著 (Stepto *et al.*, 2013)。這當中的分子機轉被認為與胰島素受體 (insulin receptor) 下游的訊息傳導異常有關，在多囊性卵巢症候群病患的肌肉細胞中，MEK1/2 持續活化，使得胰島素受體和胰島素受體受質(insulin receptor substrate 1, IRS1)的絲氨酸(serine)磷酸化增加，進一步使下游的 PI3K 活性下降，並使得後續代謝路徑受到抑制，而影響了胰島素在周邊組織的敏感性 (Azziz *et al.*, 2016)。

除了肌肉細胞外，多囊性卵巢症候群病患的脂肪細胞也同樣出現胰島素阻

doi:10.6342/NTU202000313

抗的情形。脂肪細胞雖然只影響了人體 10%的糖分吸收，但對於血糖調節仍十分重要，不僅調控游離脂肪酸的代謝，也分泌許多種脂肪激素 (adipokines)，影響著胰島素的功能、能量平衡和新陳代謝的穩定(Azziz *et al.*, 2016)。多囊性卵巢症候群病患的脂肪細胞除了胰島素受體訊息傳遞異常以外，細胞所製造的葡萄糖運輸蛋白(glucose transporter 4 , GLUT4) 也顯著下降，而發炎性細胞激素例如腫瘤壞死因子(tumor necrosis factor, TNF)和白細胞介素 6 (interleukin-6, IL-6)的分泌也使得脂肪細胞吸收糖分的功能受到抑制，種種機轉導致多囊性卵巢症候群的脂肪細胞也出現胰島素阻抗之情形。

在胰島素阻抗的情況下，多囊性卵巢症候群病患的基礎胰島素分泌量增加而出現高胰島素血症，高胰島素血症又會進一步刺激卵巢濾泡鞘細胞分泌更多雄性荷爾蒙，並且抑制肝臟分泌性激素結合球蛋白，因此患者的胰島素阻抗和高雄性荷爾蒙症可說是息息相關。

(3) 卵巢濾泡發育異常 Abnormal folliculogenesis

卵巢濾泡發育異常以及其所造成的排卵異常，可說是年輕女性最常見且困擾的症狀之一，在多囊性卵巢症候群的發生率高達 70-90% (Balen *et al.*, 1995)，特別是在亞洲族群的病患，由於肥胖比例和多毛症的情況不如西方國家那麼顯著，排卵異常是最常見甚至有時是唯一的臨床症狀。與排卵異常相關的病徵包括：空腔濾泡 (antral follicle) 和前空腔濾泡 (preantral follicle) 數量增加、空腔濾泡發育停滯 (arrest)、主濾泡 (dominant follicle) 篩選失調、無法排卵、卵巢顆粒細胞 (granulosa cell) 生長發育異常和荷爾蒙分泌異常 (Franks *et al.*, 2008; Chang *et al.*, 2013; Dumesic *et al.*, 2013)。而造成濾泡發育異常的原因眾說紛紜，有一說是由於卵巢顆粒細胞過早表現出黃體化激素受體而提前黃體化 (premature luteinization) ，進而導致濾泡生長中止(Jonard and Dewailly, 2004)；也有一說是由於濾泡刺激素 (follicle-stimulating hormone, FSH) 分泌不足，此外，高胰島素血症和高雄性荷爾蒙都會干擾腦下垂體和卵巢所分泌之荷爾蒙，進而可能導致濾泡生長異常(Franks *et al.*, 2008; Jonard and Dewailly, 2004)。

doi:10.6342/NTU202000313

另一個濾泡生長異常的可能解釋是卵巢血管生成失調。血管上皮生長因子(vascular endothelial growth factor, VEGF)是調控濾泡生長和黃體生成最重要的分子之一 (Tamanini and De Ambrogi, 2004)，也曾被報告與卵巢過度刺激症候群(ovarian hyperstimulation syndrome, OHSS) 的致病機轉有重要相關 (Chen *et al.*, 2008, 2010)，而過去的研究發現，多囊性卵巢症候群患者的濾泡液 (Agrawal *et al.*, 1998a) 、卵巢組織 (Kamat *et al.*, 1995; Ferrara *et al.*, 2003) 和血清 (Agrawal *et al.*, 1998a; 1998b) 的 VEGF 濃度均顯著增加，這個發現可以解釋為何多囊性卵巢症候群病患其卵巢基質(stroma)的血管密度上升 (Peitsidis and Agrawal, 2010)。除了 VEGF 以外，少數他種血管生成素(angiopoietin) 的表現也曾在文獻中報告過，例如在多囊性卵巢症候群病患的濾泡液中，血小板衍生生長因子(platelet-derived growth factor, PDGF)濃度較低而 angiopoietin 1 的濃度較高 (Scotti *et al.*, 2014)，然而，血管生成以及濾泡滲透壓或通透性與多囊性卵巢症候群的確切相關性仍欠缺完整的實驗研究。

(4) 卵巢顆粒細胞功能異常

卵巢顆粒細胞 (granulosa cell) 的表現異常，也被認為是多囊性卵巢症候群致病機轉重要的一環。構成卵巢濾泡的主要細胞型態就是顆粒細胞，其形態和功能表現會隨著濾泡的生長而變動，顆粒細胞的發育和功能可說是卵巢濾泡生長和荷爾蒙分泌最重要的調節機制 (Hutt and Albertini, 2007)，它們會接受腦下垂體前葉所分泌的濾泡刺激素，在芳香環轉化酶 (aromatase) 的作用下將雄性荷爾蒙轉換為雌性素(estrogen)，在黃體期的時候便產生黃體化現象 (luteinization)，轉換為顆粒黃體細胞 (granulosa lutein cell) 並分泌大量黃體素(progesterone)，因此卵巢最重要的荷爾蒙分泌就是來自於顆粒細胞。除了荷爾蒙分泌，顆粒細胞對於卵子的生長和成熟也非常重要 (Fragouli *et al.*, 2014)，過去的研究顯示，多囊性卵巢症候群病患的卵巢顆粒細胞功能表現與正常女性顯著不同，包括：較顯著的細胞凋亡反應、增生功能缺陷、對於濾泡刺激素反應異常增加、不正常的荷爾蒙生成……等等(Das *et al.*, 2008; Chang and Cook-Andersen, 2013)。然而大多數研究都是透過試管嬰兒療程中的取卵手術來取得多囊性卵巢症候群病患的卵巢顆粒細胞，這些細胞會受到試管嬰兒療程中所注射大量的人工合成濾泡刺

doi:10.6342/NTU202000313

激素 (recombinant FSH, rFSH) 刺激，其功能與特徵不一定能夠反應一般生理情形，要在人體取得未受過人工合成濾泡刺激素藥物刺激的卵巢顆粒細胞，是很困難的事，畢竟在試管嬰兒療程的取卵手術前使用大量藥物是普遍醫療常規。至於多囊性卵巢症候群的模式生物研究之代表性也是讓人有所疑慮的，目前大多數的做法是在小鼠出生前 (針對懷孕母鼠給藥) 或者在剛出生的小鼠給予雄性素治療，使其產生類似多囊性卵巢症候群的徵狀，例如卵巢出現多囊型態，胰島素敏感度下降，排卵功能異常，雄性素表現上升.....等等 (Chen *et al.*, 2015; Hsueh *et al.*, 1994; Wu *et al.*, 2015)，然而一般婦女或嬰幼兒並不會接收到高劑量的雄性素荷爾蒙，因此這類模式生物是否能夠代表多囊性卵巢症候群仍然存在爭議。因此，究竟多囊性卵巢症候群病患的卵巢顆粒細胞在普通生理情況下的功能與特徵如何，與此疾病直接或間接的致病機轉為何，目前仍未明。

(5) 基因調控之影響

目前認為多囊性卵巢症候群是一個複雜的多基因疾病，也與基因和環境交互作用有關。早期的一些家庭群集研究和雙胞胎研究顯示，這個疾病具有高度遺傳性。荷蘭的 Vink 等人 (2006) 分析了共 1332 個同卵雙胞胎，其中多囊性卵巢症候群的共同發病率高達 70%，而同一個家庭的母親或姊妹同時罹患疾病的機率達 20-40%。過去也有許多研究試圖找出致病基因的來源，從較早期的基因連鎖分析 (linkage analysis)或運用病例-對照模式的關聯性研究 (associated study)，這些早期的基因研究受限於樣本數不足、多囊性卵巢症候群診斷方式並未統一、不同族群的疾病盛行率不同等因素，而往往出現歧異的結果。目前已經有超過一百個候選基因被提出可能跟多囊性卵巢症候群的致病機轉有關，並牽涉到多個相關的調控路徑，例如：與雄性荷爾蒙合成和代謝相關的 *LH, LHR, AR, CYP17α, SHBG* 等基因；與胰島素分泌和功能相關的 *IGF1, IGF2, INSR, IRS1* 等基因；與肥胖和胰島素阻抗相關的 *PPARG, SORBS1, PON1* 基因；與慢性發炎有關的 *TNFα, PAI-1, IL-6*；與促性腺激素的功能有關的 *FST* 基因等等 (Diamanti-Kandarakis and Piperi, 2005)。總結來說，這些早期的基因研究提供了很多寶貴的知識，特別是在致病機轉相關的了解，然而這些基因的影響程度和作用方式，特別是在不同族群或者不同臨床表徵的患者中如何造成影響，都還未知。

doi:10.6342/NTU202000313

近年來數個大型全基因組關聯研究 (Genome-Wide Association Studies, GWAS) 也嘗試更大規模的找出多囊性卵巢症候群的致病位點。2011 年中國的陳子江教授發表在 Nature genetics 期刊的一個大型全基因組關聯研究，總共收集 744 個病患及 895 個對照組，結果發現了三個單核苷酸多態性 (single nucleotide polymorphism, SNP) 可能與疾病相關：2p16.3 (rs13405728); 2p21 (rs13429458); 9q33.3 (rs2479106) (Chen *et al.*, 2011)，但另一個澳洲學者針對高加索裔多囊性卵巢症候群病患，進行了同樣這三個單核苷酸多態性的分析，卻沒有統計顯著性 (Lerchbaum *et al.*, 2011)，可見不同地區或者種族的致病基因位點可能不完全相同，尚需更多研究來證實。

(6) 超基因調控之影響

除了基因序列的變異可能導致多囊性卵巢症候群之外，超基因調控 (epigenetic regulation) 亦可能為潛在的致病機轉之一。超基因調控的定義為未改變基因序列的情況下，可遺傳的基因調控方式。常見的超基因調控途徑包括：DNA 甲基化 (DNA methylation)、組蛋白修飾 (histone modification)、染色質重塑 (chromatin remodeling)、核組織重組 (nuclear architecture rearrangements) 以及非編碼 RNA (non-coding RNA) 等等 (Kirchner *et al.*, 2013)。目前已知超基因調控異常與癌症、許多慢性疾病如糖尿病、高血壓等等的發生，具有相關聯性 (Portela and Esteller, 2010)。而超基因調控與多囊性卵巢症候群之關聯性，目前相關文獻仍極少。之所以推測多囊性卵巢症候群與超基因調控有關的理由如下：

1. 此疾病具有高度遺傳性 (Vink *et al.*, 2006)，然而到目前為止所找出的潛在致病基因卻不足以解釋其遺傳性，也許有部分的遺傳性是來自於基因位點之外的改變，也就是超基因調控。

2. 此疾病與新陳代謝疾病如糖尿病、高血壓和心血管疾病息息相關(Bajuk Studen *et al.*, 2013)，而這些新陳代謝疾病已經被發現其部分致病機轉是來自於超基因調控的異常(Johnstone and Baylin, 2010)。

doi:10.6342/NTU202000313

3. 此疾病還有另一個重要特色是其臨床表徵會受到年齡、飲食、運動、體重等許多因素影響而改變，減糖飲食與規則運動都可減輕症狀嚴重程度(Norman *et al.*, 2002)，而外在環境及個人行為是如何造成表現型的改變？此外，過去在哺乳動物實驗中發現，胎兒若在子宮內環境受到高量雄性荷爾蒙刺激，出生後亦會產生多囊性卵巢症候群的表徵，包括卵巢呈現多囊狀，血清雄性荷爾蒙過高，胰島素分泌與血糖代謝異常等症狀(Abbott *et al.*, 2005)。而環境的改變 (包括子宮內環境) 究竟是如何造成疾病呢? 目前有一派理論認為可能就是超基因調控的異常所導致(Feil and Fraga, 2012)。

(五) 多囊性卵巢症候群與 DNA 甲基化相關研究

綜合以上理由，顯示出多囊性卵巢症候群的致病機轉可能與超基因調控有關，然而在過去文獻中，對於多囊性卵巢症候群與超基因調控的探討相當少。以多囊性卵巢症候群的 DNA 甲基化相關研究來說，Xu 等人 (2011) 使用甲基化基因晶片分析以雄性荷爾蒙刺激產生多囊性卵巢徵狀之獼猴的內臟脂肪細胞，與對照組相較發現，兩者 DNA 甲基化的程度與分佈有顯著差異。Qu 等人(2012)針對 *PPARG1* (peroxisome proliferator-activated receptor gamma 1) 基因進行亞硫酸鹽定序 (bisulfite sequencing) 以分析該基因甲基化胞嘧啶 (cytosine) 的位點所在，解析度可高達單一核甘酸序列，其基因產物為細胞核接受器 (nuclear receptor)，與細胞內的脂肪酸儲存和葡萄糖代謝有關。研究結果發現，具有高雄性荷爾蒙表徵的多囊性卵巢症候群患者，在 *PPARG1* 的啟動子 (promoter) 位置的胞嘧啶甲基化比例上升，同時基因表現下降，這個結果顯示多囊性卵巢症候群與新陳代謝異常之間相關聯性，亦可能透過 DNA 甲基化的改變來調控。

(六) 多囊性卵巢症候群與微小核醣核酸相關研究

doi:10.6342/NTU202000313

除了 DNA 甲基化之外，非編碼 RNA 調控也是超基因調控重要的一種機轉，而其中又以微小核醣核酸 (microRNA, miRNA) 的相關研究最多。微小核醣核酸是一種長度約 22 個核甘酸的核醣核酸，在基因轉譯後的調控扮演極為重要的角色 (Haider *et al.*, 2014)，除了位於一般細胞質和細胞核中，微小核醣核酸也存在於一些特殊胞器 (Faruq and Vecchione, 2015)，例如：粒線體、外吐小體 (exosome)、和其他微泡 (microvesicles)，甚至可在各種體液中測量到微小核醣核酸的存在，包括乳汁、羊水、眼淚、腦脊髓液、腹腔積液、血漿、唾液、尿液……等等。自從 2008 年微小核醣核酸被發現至今，已有大量研究在探討其作為診斷疾病或預測預後之生物指標功能(Moreno-Moya *et al.*, 2014)，而其能夠不受到核醣核酸分解脢破壞並且長時間穩定存在體液中的特性，使其具有作為生物指標的良好潛能。

關於微小核醣核酸究竟是如何影響多囊性卵巢症候群的致病機轉，特別是濾泡生長和荷爾蒙分泌調控，目前所知仍不多。對於血清微小核醣核酸濃度是否可以作為多囊性卵巢症候群的診斷指標，Long 等人 (2014) 曾利用微小核醣核酸晶片分析五個多囊性卵巢症候群病患和五個對照組的血清，找出 miR-222, miR-146a, miR-30c 這三者的表現量在多囊性卵巢症候群病患顯著上升，並進一步在 68 個多囊性卵巢症候群病患和 68 個對照組以聚合酶連鎖反應驗證這個發現，結論是利用這三個微小核醣核酸進行多變項迴歸分析區別是否為多囊性卵巢症候群，其接收者操作特徵 (receiver operating characteristic, ROC) 曲線下面積 (area under the curve, AUC) 可達 0.852，鑑別效果還不錯。Sathyapalan (2015) 根據文獻選擇了兩個與胰島素阻抗和第二型糖尿病有關的微小核醣核酸 miR-93 和 miR-223，在 25 個多囊性卵巢症候群病患和 24 個年齡和體重相符的對照組女性檢測其血清濃度，發現這兩個微小核醣核酸在多囊性卵巢症候群病患的血清濃度顯著較高，而 miR-93 和 miR-223 作為診斷多囊性卵巢症候群有無的接收者操作特徵曲線下面積各別為 0.66 和 0.72。以上兩個關於多囊性卵巢症候群病患血清微小核醣核酸研究的個案人數都不多，且並未在一個未經挑選的族群進行驗證，亦缺乏進一步關於微小核醣核酸調控機轉方面的功能性研究，而且兩個研究針對的都是高加索人，由於多囊性卵巢症候群的臨床表現也被認為跟地

doi:10.6342/NTU202000313

區和人種有很大的關聯性，因此華人甚至是臺灣地區的相關研究還非常欠缺。

(1) 微小核醣核酸和胰島素抗性

大約 60-70％的多囊性卵巢症候群女性會出現內生性的胰島素阻抗和高胰島素血症 (Azziz *et al.*, 2009)。在一個關於多囊性卵巢症候群病患皮下脂肪組織的研究中，發現 GLUT4（主要的胰島素依賴性葡萄糖運輸蛋白）表現與胰島素敏感性呈正相關性。此外，在這些患者中，miR-93 活性與 GLUT4 的表現呈現負相關性，顯示出同時罹患胰島素阻抗的多囊性卵巢症候群病患，其胰島素刺激葡萄糖吸收的機轉可能是透過 miR-93 的調節 (Chen *et al.*, 2013) 。目前治療多囊性卵巢症候群的常用藥物包含了二甲雙胍類藥物 metformin，一種常用來治療第二型糖尿病的口服藥物，機制上是一種胰島素敏感劑，不僅可降低胰島素阻抗，而且對降低雄性荷爾蒙濃度、促進排卵甚至生育能力均有顯著療效 (Lord *et al.*, 2003)。metformin 治療也曾被報告可改變某些微小核醣核酸的表現量，Coleman 等人發現在第二型糖尿病病患的血清 miR-221 和 miR-222 表現量顯著上升，而在給予 metformin 治療後，這兩種微小核醣核酸的表現量就降到與健康人無顯著差異 (Coleman *et al.*, 2013)。而 metformin 對多囊性卵巢症候群的療效究竟是透過甚麼潛在機制則尚不明確，這也將成為我們研究的主題之一。

(2) 微小核醣核酸和類固醇荷爾蒙生成

多囊性卵巢症候群已知與類固醇類荷爾蒙生成 (steroidogenesis) 的異常調節有關，特別是與卵巢分泌雄性荷爾蒙的調控息息相關 (Gilling-Smith *et al.*, 1994)，而過去也有部分研究顯示，微小核醣核酸調控則很可能與荷爾蒙生成相關，因此可以通過微小核醣核酸表現量的差異，來解釋異常的卵泡發育和相關表徵的潛在關聯性。許多生物機制都曾被報告過受到微小核醣核酸調控，但只有少數研究分析了微小核醣核酸在多囊性卵巢症候群中的作用。過去文獻中，曾經有數個動物研究探討特定微小核醣核酸的表現與類固醇類荷爾蒙釋放的相關性，結果顯示，在轉殖某些微小核醣核酸模擬物 (mimics) 時，可以改變 KGN 細胞株 (一種類卵巢顆粒細胞瘤的細胞株) 的雌激素分泌 (Blandino *et al.*,

doi:10.6342/NTU202000313

2012)。KGN 細胞株在轉殖 miR-24 模擬物之後，雌激素的分泌顯著下降；反之在轉殖了 miR-132、miR-320、miR-520c-3p 和 miR-222 等模擬物之後，雌激素的分泌顯著增加。另一個小鼠研究中，微陣列晶片分析顯示，在注射人絨毛膜促性腺激素 (human chorionic gonadotropin, hCG) 誘發排卵之前和之後，有 13 種微小核醣核酸的表現量顯著不同。其中，miR-21、miR-132 和 miR-212 的表現量在接受人絨毛膜促性腺激素注射後顯著上升，而可能與排卵調節有關 (Fiedler *et al.*, 2008)。在《Science》期刊發表的另一項研究顯示 (Hasuwa *et al.*, 2013)，缺乏微小核醣核酸 miR-200b 和 miR-429 的母鼠表現出無排卵和不孕的症狀，這個研究進一步剔除了這些微小核醣核酸在母鼠的基因表現，發現黃體生成素的合成顯著受到抑制，導致血清黃體生成素濃度降低，無法產生黃體生成素高峰 (LH surge)，以及後續的排卵失敗。因此，微小核醣核酸可能在下視丘-腦下垂體-卵巢軸的調節中，扮演重要角色。

在人體研究中，最近有兩項研究都針對了多囊性卵巢症候群患者卵巢濾泡液中的微小核醣核酸進行分析 (Sang *et al.*, 2013; Roth *et al.*, 2014)。與對照組相比，兩個研究都發現多囊性卵巢症候群組的微小核醣核酸表現量出現顯著差異。第一個研究分析了七個微小核醣核酸的表現量（miR-132，miR-320，miR-24，miR-520c-3p，miR-193b，miR-483-5p 和 miR-222），這些 miRNA 是由於它們與類固醇類荷爾蒙生成有關而被挑選出來 (Sang *et al.*, 2013)。miR-132，miR-320，miR-520c-3p 和 miR-222 曾被報告可調節雌二醇 (estradiol) 的濃度，而其他則可調節黃體素濃度，結果顯示，兩個微小核醣核酸（miR-132 和 miR-320）在多囊性卵巢症候群組中的表現量顯著降低，進一步以生物資訊學路徑進行分析，發現這些表現量顯著增加的微小核醣核酸，其所調控的標的基因與生殖、內分泌和代謝過程有關。第二個研究則是發現多囊性卵巢症候群組有 5 種微小核醣核酸（miR-9，miR-18b，miR-32，miR-34c 和 miR-135a）的表現量顯著上升 (Roth *et al.*, 2014)， 有三個潛在的微小核醣核酸標的基因在多囊性卵巢症候群女性中表現量顯著下降：胰島素受體基質 2（insulin receptor substrate 2） 、突觸結合蛋白 1 (synaptogamin 1) 和白細胞介素-8 (interleukin-8)，這些基因都被報告與多囊性卵巢症候群的臨床症狀有關，包括排卵，胰島素阻抗和碳水化合物代謝。

doi:10.6342/NTU202000313

總之，在多囊性卵巢症候群患者中，分析表現量具有顯著差異的微小核醣核酸以及其特定標的基因及調控路徑，可以使我們更瞭解這種複雜疾病的病理生理學。分析微小核醣核酸不同時序下的獨特表現模式，將有機會成為一個具有良好敏感度的生物指標，針對多囊性卵巢症候群此一常見疾病提供診斷及預後的相關預測，甚至也可能用來研究與多囊性卵巢症候群相關之生物機轉，例如：排卵功能和類固醇類荷爾蒙生成。由於微小核醣核酸在基因轉錄後表現扮演著關鍵的調控功能，瞭解這些微小核醣核酸的潛在調節機制，將有機會更加透徹研究與多囊性卵巢症候群相關的標的基因，進一步找出更好的診斷方法、預防方式、甚至治療策略。

(七) 多囊性卵巢症候群之誘導性多功能幹細胞模型

雖然多囊性卵巢症候群的臨床症狀通常在青春期下視丘-腦下垂體-卵巢軸成熟後才出現，但許多臨床和基礎研究都顯示，這種疾病具有強大的遺傳性(Kosova *et al.*, 2013)，而其異常基因表現和/或超基因調控亦有可能從早期子宮內胎兒時期(Franks *et al.*, 2006) 即開始出現。然而，由於胚胎研究中的倫理和法律問題，關於多囊性卵巢症候群早期發育起源 (early developmental origin) 的理論難以獲得證實 (King and Perrin, 2014)。

一個解決胚胎實驗中倫理和法律疑慮的方法是使用誘導性多功能幹細胞（induced pluripotent stem cell, iPSC）技術。誘導性多功能幹細胞技術是運用帶有重編程基因 (reprogramming gene) 之載體，將細胞轉化為永生 (immortality) 狀態(Takahashi *et al.*, 2006)，這可以保留原始細胞的基因和遺傳特質，並用來作為一個疾病模型、新藥開發和潛在細胞替代療法的取代方案 (Brandao *et al.*, 2017; Kumar *et al.*, 2017)。將體細胞重編程為誘導性多功能幹細胞，可將體細胞之特性重置回到胚胎階段 (Roessler *et al.*, 2014)，特別是能夠為成年發病之疾病的早期發展，提供寶貴的的病理生理機轉資訊。然而，誘導性多功能幹細胞技術仍存在相當大的挑戰，至今只有一項研究成功建立了多囊性卵巢症候群特異之誘導性多功能幹細

doi:10.6342/NTU202000313

胞。Yang 等人 (2016) 使用帶有重編程因子的反轉錄病毒轉導法，將多囊性卵巢症候群患者尿液中的上皮細胞，轉化為誘導性多功能幹細胞，並將它們分化成脂肪細胞。該研究顯示，從多囊性卵巢症候群組患者之誘導性多功能幹細胞所衍生出的脂肪細胞，與對照組相比，其消耗葡萄糖的能力顯著增加。

除脂肪細胞功能異常外，顆粒細胞功能異常在多囊性卵巢症候群的發病機制中也扮演重要角色。卵巢顆粒細胞的發育和功能是卵巢濾泡生成和類固醇荷爾蒙生成的最關鍵的調控者之一。顆粒細胞是構成卵巢濾泡的主要細胞類型，其功能和構造上的轉換和卵巢濾泡生成的過程相互調控而息息相關 (Hutt *et al.*, 2007)。它們不僅在濾泡刺激素的刺激下產生雌激素，而且還可促進發育中的原始卵母細胞的功能和型態成熟 (Fragouli *et al.*, 2014)。根據先前的研究，在多囊性卵巢症候群病患中可觀察到顆粒細胞的種種功能失調，包括：顆粒細胞過度凋亡、增生缺陷 (Das *et al.*, 2008)、對濾泡刺激素刺激的異常過度反應和類固醇荷爾蒙生成的改變 (Chang *et al.*, 2013)。然而，大多數的研究是利用試管嬰兒療程的取卵手術來取得人類卵巢顆粒細胞，這些細胞往往已經在試管嬰兒療程中，接受了高劑量促性腺激素刺激才被取出，且已經開始出現黃體化，並非一般自然生理狀態下的顆粒細胞 (Catteau-Jonard *et al.*, 2008; Kaur *et al.*, 2012; Lan *et al.*, 2015; Nouri *et al.*, 2016)。另一個取得顆粒細胞的方式，是從接受類固醇荷爾蒙注射後 (Chen *et al.*, 2015; Hsueh *et al.*, 1994) 或飲食誘導產生之多囊性卵巢症候群動物模型來取得其他動物的卵巢顆粒細胞 (Wu *et al.*, 2015)。未受藥物刺激的人類卵巢顆粒細胞幾乎不可能取得到，而人為建立的模式動物也非常可能無法代表實際的病患表徵。總之，多囊性卵巢症候群病患其顆粒細胞的功能異常是否存在，與其致病機轉究竟扮演甚麼樣的角色，其表現異常與疾病之因果關係和出現異常之時間點為何，都還沒有明確的答案。

doi:10.6342/NTU202000313

第二節 欲研究的問題及研究假說

綜合以上所述，可知多囊性卵巢症候群對婦女健康影響之深遠及其重要性，且仍有許多尚待解答之疑問，因此博士班期間之研究目標，將針對此疾病之臨床表徵、病理機轉、治療方針等多方面進行解析，主要包含以下幾個次主題：

一、臨床表徵分組及相關預後因子分析

我們希望找出一個適當的分群模式，透過不同的生殖內分泌表徵進行分組，分出的不同組別將能反應出不同的臨床表現和預後，特別是與新陳代謝異常相關之表徵。在這項研究中，我們和中央研究院統計科學研究所陳君厚研究員 (現為所長) 合作，運用了一種強大且創新的統計學圖表分析法，名為廣義相關圖（generalized association plots，GAP），來分析多囊性卵巢症候群病患的症狀模式和特徵分群。廣義相關圖(GAP)是一個電腦軟體環境，它應用了許多傳統的統計工具，包括矩陣視覺化（matrix visualization, MV）和各種分群演算法，例如：階層式分群 (hierarchical clustering)、k 均值 (k-means) 和二維橢圓體序列化 (rank-two elliptical seriation）等等，進行資料矩陣的互動式探索分析。它可以在人為預設或猜測任何統計模式之前(可能不一定是正確的)，更加直覺地同時探索多達數千個個體和變數之間的數據結構和關係 (Chen, 2002; Tien *et al.*, 2008; Wu *et al.*, 2008, 2010)。該工具已被成功應用於其他異質性高之複雜疾病的研究，如精神分裂症的症狀結構 (Hwu *et al.*, 2002)。而多囊性卵巢症候群也同樣是異質性高之複雜疾病，因此在博士班研究的第一階段，我們將運用此統計方法，探索與新陳代謝異常相關的的風險因子，並找尋能夠預測新陳代謝異常嚴重程度的潛在內分泌特徵，再進一步根據患者的內分泌特徵，針對不同程度的新陳代謝風險對病患進行分組，期待能夠更加瞭解多囊性卵巢症候群病患的

doi:10.6342/NTU202000313

臨床表徵和新陳代謝預後因子。

二、卵巢濾泡液通透性與血管生成因子之相關致病機轉

我們的假說是，多囊性卵巢症候群病患的濾泡液生成過程和卵巢中的血管生成因子的表現，與健康對照組表現可能有所不同，進而可能導致其濾泡成長失調甚至排卵過程異常。因此我們將進行一個病例-對照研究，針對進行試管嬰兒療程之多囊性卵巢症候群病患和非多囊性卵巢症候群之對照組女性，在取卵手術過程抽取其卵巢濾泡液，分析兩組病患之卵巢濾泡液是否會影響相鄰內皮細胞之通透性，倘若濾泡液的滲透壓或通透性不同，則可能影響濾泡液在卵巢之生成。此外由於血管生成因子會影響內皮細胞通透性，我們進一步以蛋白質晶片分析濾泡液內的血管生成因子濃度，並比較疾病組和對照組的表現是否有顯著差異，以及這些血管生成因子和濾泡液通透性之相關聯性，希望可以進一步瞭解卵巢濾泡液對於多囊性卵巢症候群致病機轉所可能扮演的角色。

三、超基因調控之相關致病機轉研究

我們的假說是多囊性卵巢症候群致病機轉與超基因調控異常有關，將分為兩部分來進行研究。

第一部分 DNA 甲基化

第一部分的研究將進行全基因體 DNA 甲基化分析，由於卵巢是多囊性卵巢症候群的一個主要表現病徵的器官，因此本研究計畫收集接受試管嬰兒技術治療的多囊性卵巢症候群病患，取其濾泡液中的顆粒細胞，並以年齡、身體質量指數相對應且無其他新陳代謝疾病之婦女的濾泡液中的顆粒細胞作為對照組，分析兩者之基因表現與超基因調控之間的差異，期能進一步了解超基因調控在致病機轉所扮演角色為何。

doi:10.6342/NTU202000313

除了取得婦女濾泡液中的顆粒細胞之外，我們也將製造具有多囊性卵巢症候群特異性且病患專一性的誘導性多功能幹細胞，並將它們重新分化為卵巢顆粒細胞，進而比較疾病組和對照組之差異。從誘導性多功能幹細胞衍生分化出的顆粒細胞，不會像試管嬰兒取卵手術所取得的顆粒細胞那樣受到大量藥物刺激的影響，且另一個極大的價值是可以作為研究在顆粒細胞在早期分化發育時期，多囊性卵巢症候群相關致病機轉究竟是如何調控的寶貴工具。這也同時是文獻中，首次同時分析「誘導性多功能幹細胞再分化之原始顆粒細胞」和「成熟顆粒細胞」之間的 DNA 甲基化差異的研究，我們期待找出與多囊性卵巢症候群致病相關之 DNA 甲基化調控異常機轉，並將可對多囊性卵巢症候群與環境交互作用相關的遺傳特質和表徵可塑性提供一個良好的解釋。

第二部分 微小核醣核酸

由於微小核醣核酸調控也是超基因調控十分重要的一個途徑，因此第二部分的研究將同時分析多囊性卵巢症候群與微小核醣核酸之相關聯性，我們將分析血液中不同的微小核醣核酸表現是否可以作為診斷多囊性卵巢症候群的生物標記，並比較多囊性卵巢症候群患者的微小核醣核酸與健康人之差異，希望能夠進一步釐清微小核醣核酸調控對其致病機轉的潛在影響。此外，我們將探討微小核醣核酸是否可作為 metformin 治療作用有效與否的預測生物指標，這將可進一步對這種疾病的治療策略和潛在病理生理機轉有所貢獻。最後，我們將進行生物路徑分析，以探索與多囊性卵巢症候群致病相關之特定微小核醣核酸的相關調節基因和生物路徑。

doi:10.6342/NTU202000313

第二章 研究方法與材料

第一節 臨床表徵分組及相關預後因子分析

Symptom patterns and phenotypic subgrouping of women with polycystic ovary syndrome: association between endocrine characteristics and metabolic aberrations. (Huang *et al.*, 2015)

(一) 研究族群

我們進行了一個單一大學醫院中心的前瞻性橫斷性研究，此研究已通過台大醫院研究倫理委員會核准進行。總共從本院婦產部門診招募了 460 名臨床診斷為多囊性卵巢症候群之女性病患，並從所有成年患者或未成年患者之父母取得了知情同意書。患者一開始來門診就醫的主訴多為了評估月經不規則和/或高雄性荷爾蒙症的臨床症狀，例如多毛症或落髮。患者在參與研究前三個月內並未接受荷爾蒙類相關藥物治療，包括口服避孕藥，胰島素增敏劑，抗雄性荷爾蒙藥，排卵誘導劑和中草藥。多囊性卵巢症候群的診斷標準是根據 2003 年制定之鹿特丹標準，以下三項標準中至少有兩項符合：(1) 無月經或月經過少（參與研究前每年少於 9 次自發月經週期，持續至少 3 年）; (2)生化上檢測到高雄性荷爾蒙血症（血清總睪固酮濃度≥0.8ng/ ml）和/或臨床高雄性荷爾蒙表徵，包括多毛症和落髮（由於文獻報告中，痤瘡與高雄性荷爾蒙症的臨床相關性較不顯著，故我們的研究排除僅有出現痤瘡之患者）; 以及 (3) 超音波影像檢查上顯示多囊性卵巢形態（至少一個卵巢出現超過 12 個 2-9 毫米的濾泡或卵巢體積> 10 毫升）。此外，診斷時會先排除其他可能造成排卵異常或雄性荷爾蒙過高之內分泌和器質性異常，如：高泌乳激素血症，甲狀腺失調，庫欣氏症候群，先天性腎上腺增生和腎上腺或卵巢腫瘤。多毛症被定義為 Ferriman-Gallwey 評分> 8 分。

doi:10.6342/NTU202000313

(二) 研究方法

所有受試者均接受抽血、人體測量、婦產科超音波掃描檢查和血壓測量。抽血的時間點是在有自發性排卵週期患者的早期濾泡期 (early follicular phase) ，而在完全無月經的患者則是隨機的，進行隔夜空腹靜脈血採樣。如果採集的血清黃體素濃度大於 2 ng / ml 或血清雌二醇濃度大於 150 pg / ml，則表示病患並非處於早期濾泡期，而必須請患者在下一次月經後第 2-5 天再次進行血液採樣。在抽血後 30 分鐘內處理血液檢體，並在同一天測量血清葡萄糖和胰島素的濃度，之後將剩餘的血清和血漿冷凍保存在-80℃直至進一步化驗。婦產科超音波掃描檢查是由兩位經驗豐富的婦科醫生使用經陰道或者經腹部 (在無性經驗之患者) 的方法進行，計算兩側卵巢所內含直徑為 2-9 mm 的濾泡數量，並用簡單的公式（0.5×長度×寬度×厚度）計算卵巢體積 (Balen *et al.*, 2003; Chen *et al.*, 2008)。肥胖的定義為身體質量指數≥ 25 kg/m^2，這是依據亞洲成年女性的標準（WHO Expert Consultation，2004）。代謝症候群的定義為下列 5 項標準中至少有 3 項符合：收縮壓（systolic blood pressure, SBP） ≥ 130 mmHg 和/或舒張壓（diastolic blood pressure, DBP）≥ 85 mmHg; 空腹血糖值 ≥ 100 mg/dl; 空腹三酸甘油脂值（triglyceride, TG）≥ 150 mg/dl; 高密度脂蛋白膽固醇（high-density lipoprotein, HDL-C）< 50 mg/dl; 和腹部肥胖 (腰圍 > 80 厘米)（Tan *et al.*, 2004）。

(三) 生化檢定方法

血漿葡萄糖濃度（mg/dl，可檢測範圍：10-800），血清胰島素（IU/ml，可檢測範圍：2-140），濾泡刺激素（FSH，mIU/ml，可檢測範圍：0.1-120），黃體刺激素（LH，mIU/ml，可檢測範圍：0.1-100），雌二醇（estradiol，pg/ml，可檢測範圍：20-900），黃體素（progesterone，ng/ml，可檢測範圍：0.2-40），性荷爾蒙結合球蛋白（SHBG，nmol/l，可檢測範圍：0.35-200）， 肝功能指數（丙胺酸轉胺酶[ALT，IU/l，可檢測範圍：3-500]和天門冬胺酸轉胺酶 [AST，IU/l，

doi:10.6342/NTU202000313

可檢測範圍：3-1000]）和血脂肪指數（總膽固醇[total cholesterol，mg/dl，可檢測範圍：25-700]，三酸甘油脂 [TG，mg/dl，可檢測範圍：10-1000]，低密度脂蛋白膽固醇[LDL-C，mg/dl，可檢測範圍：7-450] 和高密度脂蛋白膽固醇[HDL-C，mg/dl，可檢測範圍：3-150]）等，如之前研究所述進行測量（Chen *et al.*, 2006, 2010, 2012）。藉由放射免疫測定法（Diagnostic Systems Laboratories）測量血清總睾固酮（total testosterone，ng/ml，可檢測範圍：0.03-14.4）和硫酸去氫表睾固酮(DHEA-S，μg/dl，可檢測範圍：2.5-800）。並且以游離雄性荷爾蒙指標（Free androgen index, FAI）[FAI（％）= testosterone（ng / ml）×3.47×100 / SHBG（nmol / l）]評估睾固酮的生體利用率（Chen *et al.*,2007）。先前台大陳美州教授的另一個研究中，分析 37 名非多囊性卵巢症候群之健康女性的總睾固酮濃度平均值（標準偏差）為 0.4（0.12）ng / ml（Chen *et al.*, 2009）。評估胰島素阻抗 (insulin resistance，IR) 的程度是用 HOMA-IR 公式 [HOMA-IR =（葡萄糖（mg / dl）×0.05551）×胰島素（IU / ml）/ 22.5]。上述測定的組內和組間檢測變異值均為<10％。

(四) 統計分析

我們和中央研究院統計科學研究所陳君厚研究員合作，運用其所開發之廣義相關圖 (GAP) 進行了矩陣視覺化 (MV) 和叢聚樹分析(clustering tree)(Chen, 2002; Tien *et al.*, 2008; Wu *et al.*, 2008, 2010)，用來解析多囊性卵巢症候群女性的症狀模式和臨床表徵分組。廣義相關圖是一種電腦圖形技術，可以同時探索多達數千個受試者、變數及其交互作用的關聯性，無需首先縮小維度，也不須針對欲分析之資料來預設統計學上的假說。我們分析了五個面向的數據，包括：每個患者與症狀的原始分數、每個患者在所有症狀的分數向量以及每個症狀在所有患者的分數向量、每個患者與患者之間和症狀與症狀之間的關聯性分數、患者的分組結構和分群效應、患者分組與症狀分群的交互作用模式。矩陣視覺化透過適當的重新排序算法以及相應的距離矩陣來置換原始數據矩陣的行和列，然後運用合適的色譜將置換的原始數據矩陣和兩個距離矩陣顯示為新的矩

doi:10.6342/NTU202000313

陣圖，可以在視覺上一目瞭然地觀察到患者群聚分組情形、症狀群集分組情形、和兩者之交互作用。

我們也使用 SPSS（版本 17.0）進行一些其他的統計分析。除非另有說明，否則數值變量以平均值（標準偏差 standard deviation）的形式顯示。根據廣義相關圖分析產生的分組，不同組別的病患特徵差異性是使用單因子變異數分析（Analysis of variance, ANOVA）進行連續變項評估，並對適用的類別變項進行卡方(chi-square)或費雪精準檢定(Fisher's exact tests)。當單因子變異數分析顯示出統計上顯著差異時，則以 Bonferroni 法進行事後比較檢定。我們用"MASS"軟體（Venables and Ripley, 2002）進行兩階段線性判別函數分析 （Two-stage linear discriminant analysis, LDA），來確定由四個選定的內分泌測量組成的模型是否足以預測新陳代謝症候群之發生。驗證評估使用的是 leave-one-out cross-validation（Burman, 1989）。所有統計檢驗均為雙尾，信賴區間為 95%（P = 0.05）。

doi:10.6342/NTU202000313

第二節 卵巢濾泡液通透性與血管生成因子之相關致病機轉

Increased platelet factor 4 and aberrant permeability of follicular fluid in PCOS. (Huang *et al.*, 2019)

(一) 受試者招募

這是一個病例對照研究，從 2014 年 9 月至 2015 年 12 月，招募了在台大醫院接受試管嬰兒療程的多囊性卵巢症候群患者作為試驗組，此研究得到台大醫院倫理委員會的核准。多囊性卵巢症候群的診斷是根據 2003 年鹿特丹標準，如前所述。對照組受試者則是招募因男性因素和/或輸卵管因素不孕症而接受試管嬰兒療程的非多囊性卵巢症候群女性，而非因卵巢因素或排卵功能所造成之不孕。在我們的研究中，每位多囊性卵巢症候群患者均符合慢性無排卵的標準，也就是每年自發性月經少於九次，而對照組受試者則一律符合月經週期規則的標準 (月經週期間距為正常的 25-40 天)，並且僅挑選對試管嬰兒療程的排卵藥物刺激有良好反應（取卵前，直徑大於 10mm 的成熟卵泡超過 20 顆）的患者作為對照組。選擇排卵功能正常且對排卵藥物刺激反應良好的對照組受試者的原因，是要確保多囊性卵巢症候群組和對照組之間的卵子庫存量 (ovarian reserve) 或者卵巢功能沒有顯著差異。如果我們選擇卵巢功能不同的女性作為對照組，則很難判斷我們所欲分析的變項差異，究竟是與卵巢功能較相關或者是與多囊性卵巢症候群致病機制較相關。因此，我們將卵巢功能設定為欲控制的干擾因子，選擇具有相同卵巢功能且排卵正常的女性作為對照組。

(二) 排卵刺激、取卵手術和濾泡液收集

經過一段時間的排卵藥物刺激（controlled ovarian stimulation, COS）之後，

doi:10.6342/NTU202000313

在取卵手術過程中取得受試者之卵巢濾泡液。排卵刺激的給藥方式是根據先前已發表之研究 (Lee *et al.*, 2006; Ho *et al.*, 2008; Huang *et al.*, 2012) 中所述之標準促性腺激素釋放激素拮抗劑療程（gonadotripin releasing hormone antagonist, GnRH antagnoist：cetrorelix acetate®；Merck-Serono，瑞士日內瓦），簡單說明如下，首先從患者月經第二天開始，每天皮下注射重組濾泡刺激素（recombinant FSH，Gonal-F®；Merck-Serono，瑞士日內瓦）或高度純化的人類更年期促性腺激素（highly-purified human menopausal gonadotropin, hp-hMG，Menopur®；Ferring Pharmaceuticals，瑞士日內瓦）進行排卵刺激，從拮抗劑療程的第 6 天開始，每 1-3 天連續以經陰道超音波監測濾泡成長狀況，並評估血清雌激素，黃體素和黃體生成素濃度，一直持續到注射人絨毛膜促性腺激素促使卵子成熟為止。當兩個或兩個以上的濾泡直徑達到 18 毫米時，注射 6500IU 人絨毛膜促性腺激素（hCG，Ovidrel®; Merck-Serono）或兩劑 3.75mg triptorelin（Decapeptyl®; Ferring Pharmaceuticals，瑞士日內瓦）促使卵子成熟，取卵手術安排在 34–36 小時後進行。為了取得乾淨的卵巢濾泡液並避免在取卵手術中沾染到病患血液或胚胎培養液的污染，每個受試者僅從第一個抽吸的濾泡（平均直徑為 18–20 mm）中取得濾泡液，並透過目視檢查判定是否存在血液污染，若外觀上有血液污染的濾泡液則丟棄。取得的濾泡液以 350g 離心 5 分鐘去除細胞雜質，並在 -80°C 冰箱冷凍保存以用於後續實驗。

(三) 人類臍靜脈內皮細胞

人類臍靜脈內皮細胞（human umbilical vein endothelial cells, HUVEC）購自 American Type Culture Collection（美國馬里蘭州羅克維爾）。人類臍靜脈內皮細胞在 M199 培養基中培養，該培養基添加了 20%的胎牛血清、內皮細胞生長補充劑（endothelial cell growth supplement, Intracel，Rockville，MD，美國），肝素，L-glutamine，青黴素和鏈黴素，在 37°C、95%O2 和 5%CO2 的加濕空氣中培養。實驗使用的人類臍靜脈內皮細胞培養不超過 5 代。

doi:10.6342/NTU202000313

(四) 單層細胞滲透性測定

將人類臍靜脈內皮細胞在穿透小室 Transwell chambers （0.4 μm 多孔聚碳酸酯過濾器； Costar，劍橋，MS，美國）中培養，達到細胞匯合後，將培養基替換為卵巢濾泡液（用生理鹽水稀釋成 1/10；上層隔室加入 0.3 ml，下層隔室加入 1 ml），並將濃度為 0.126 μM 的 Horseradish peroxidase (HRP) 分子（VI-A 型，44 kDa； Sigma-Aldrich，美國密蘇里州聖路易斯）添加到上層隔室中，接著如先前文獻描述的方式(Essler *et al.*, 1999)，測量 HRP 分子擴散穿過單層人類臍靜脈內皮細胞進入到下層隔室的濃度。通透性 (permeability) 的計算方式，是將濾泡液和 HRP 分子添加到上層隔室中一小時後，在下層隔室中測得之 HRP 分子濃度，除以初始添加之 HRP 濃度來計算通透性。添加濃度為 50 ng / ml 的血管內皮生長因子 (vascular endothelial growth factor, VEGF) 到卵巢濾泡液時，所得到的通透性定義為 100％，並據此計算相對通透性 (relative permeability) 。

(五) 重組蛋白和抗體

重組人類 platelet factor 4 (rhPF4)蛋白（795-P4-025 / CF）購自 R＆D Systems（Minneapolis，明尼蘇達州，美國）。Anti-interleukin-8（anti-IL-8，sc-8427），anti-PF4（ sc-374195 ）和 anti-albumin 抗體（ sc-271605 ）購自 Santa Cruz Biotechnology, Inc.（Santa Cruz, 加利福尼亞州，美國）。

(六) 人類血管生成抗體晶片(Human angiogenesis antibody array)

人類血管生成抗體晶片（Proteome Profiler™；R＆D Systems）用於分析濾泡液當中的血管生成相關分子濃度。簡而言之，首先將濾泡液檢體（用生理鹽

doi:10.6342/NTU202000313

水稀釋 1/10） 與生物素標定抗體混合溶液 (biotinylated detection antibody cocktail)在室溫下混合 1 小時，同時用製造商提供的阻斷溶液 (blocking solution) 阻攔微陣列晶片膜 (array membrane)。然後將晶片膜與檢體在振盪器上以 2-8°C 反應至隔天。經洗滌後，在室溫下將 HRP-conjugated streptavidin 添加到晶片膜中反應 30 分鐘，接著添加化學螢光偵測試劑 (chemiluminescent detection reagents) 便會呈現訊號，訊號的檢測是使用數位成像系統（美國加利福尼亞州聖地亞哥的 Biopioneer 公司），並使用 ImageJ® program 進一步分析訊號。

(七) 酵素免疫分析法（Enzyme immunoassay, EIA）

濾泡液中 PF4 蛋白的濃度，是使用 PF4 EIA kit（DPF40 for PF4； R&D Systems）進行測量。此方法的分析內及分析間變異係數分別為 7.0%和 11.2%。

(八) 免疫沉澱法和西方墨點法(Immunoprecipitation and Western blot)

為了分析 IL-8 和 PF4 之間的交互作用，我們將 50uL 的濾泡液與 Mammalian Protein Extraction Reagent（Pierce，Rockford，IL，USA）混合，接著用抗 IL-8 或抗 PF4 抗體進行免疫沉澱 4 小時。然後將免疫複合物與 protein A-Sepharose 一起進行反應，接著進行膠體電泳反應 (sodium dodecyl sulfate-polyacrylamide gel electrophoresis, SDS-PAGE)，添加抗 PF4 和抗 IL-8 抗體探針置放過夜。每個檢體經 protein A-Sepharose 純化後取 20μl 上清液進行膠體電泳反應，並用抗白蛋白抗體探測，然後將膜與二抗反應 30 分鐘，再進行特定蛋白之檢測。下一步添加化學螢光偵測試劑使訊號顯影，再使用數位成像系統（Biopioneer Inc.）檢測訊號，並使用 ImageJ 圖像處理系統分析西方墨點法圖像上蛋白質色帶的亮度。

doi:10.6342/NTU202000313

(九) 絲狀肌動蛋白（Filamentous actin, F-actin）免疫螢光染色

人類臍靜脈內皮細胞用 3.7% paraformaldehyde 固定 20 分鐘，並用 0.1% Triton-X-100 滲透。然後將在 PBS（2 U / ml）中稀釋的 Fluorescence isothiocyanate-conjugated phalloidin（Invitrogen，卡爾斯巴德，加利福尼亞州，美國）在黑暗中加入樣品反應 1 小時。樣品亦加入 10%甘油。之後使用螢光顯微鏡（Nikon，東京，日本）觀察圖像。

(十) 統計分析

在這項研究中，每個實驗均進行了三次重複。數值變項表示為平均值±標準偏差。由於樣本數小，我們進行了無母數分析之 Mann-Whitney U 檢驗。所有統計檢驗均為雙尾測試，信賴區間為 95%（P <0.05）。所有統計檢定均使用版本 17 的 SPSS 軟體 (SPSS. Inc.，美國伊利諾伊州芝加哥）。

doi:10.6342/NTU202000313

第三節 超基因調控之相關致病機轉研究

第三節之第一部 多囊性卵巢症候群之 DNA 甲基化研究

Hyperactive CREB signaling pathway involved in the pathogenesis of polycystic ovarian syndrome revealed by patient-specific induced pluripotent stem cell modeling. (Huang *et al.*, 2019)

(一)患者招募和倫理審查

我們進行了在單一大學醫院的臨床病例對照研究和相關基礎實驗，人體試驗內容已通過台大醫院研究倫理委員會核准，從 2014 年 6 月至 2016 年 3 月，總共招募了 18 名多囊性卵巢症候群患者和 10 名非多囊性卵巢症候群對照組，並獲得了所有人的知情同意書。在多囊性卵巢症候群組中，16 名病患藉由試管嬰兒取卵手術取得卵巢顆粒細胞（其中 11 個病患檢體進行了全基因體 DNA 甲基化分析，另外 5 個病患檢體進行了後續的西方墨點法驗證），2 名多囊性卵巢症候群病患接受了皮膚切片以取得皮膚纖維母細胞來進行誘導性多功能幹細胞實驗。在對照組中，其中有 8 名受試者藉由試管嬰兒取卵手術取得卵巢顆粒細胞（4 個病患檢體進行了全基因體 DNA 甲基化分析，另外 4 個病患檢體則進行了西方墨點法驗證），另有 2 名對照組受試者進行了皮膚切片以進行誘導性多功能幹細胞實驗。多囊性卵巢症候群之診斷依據，是根據 2003 年所制定的鹿特丹標準（Rotterdam ESHRE/ASRM–Sponsored PCOS Consensus Workshop Group, 2004）。診斷前亦先排除其他內分泌和器質性異常，如高乳促素血症，甲狀腺失調，庫欣氏症候群，先天性腎上腺增生和腎上腺或卵巢腫瘤等等。多毛症被定義為 Ferriman-Gallwey 評分> 8。所有的對照組受試者都有規律的月經週期（月經間距：25-35 天），沒有符合鹿特丹標準的任何一個診斷條件，也沒有已知的內分泌疾病。

doi:10.6342/NTU202000313

(二) 收集成人卵巢顆粒細胞

在常規試管嬰兒療程的取卵手術當中，卵巢濾泡液會被抽吸出來並從中取得卵子，剩餘之濾泡液一般沒有臨床用途而作為醫療廢棄物丟棄，從這些濾泡液當中便可分離得到實驗所需之成人卵巢顆粒細胞。而對照組受試者雖然不是完全健康，畢竟必然有不孕症診斷才會接受試管嬰兒取卵手術，然而其不孕因素主要是因男性因素不孕和/或輸卵管阻塞因素，其卵巢功能和排卵周期均正常，且未罹患多囊性卵巢症候群或其他內分泌疾患。

試管嬰兒療程中，在取卵手術取得顆粒細胞之前，病患均會先進行一段時間的排卵藥物刺激後，才接受取卵手術。排卵藥物刺激的給予方式，可參考先前研究中 (Huang *et al.*, 2012) 所描述的標準促性腺釋素拮抗劑療程（GnRH antagonist protocol：Cetrotide®，cetrorelix acetate; Merck-Serono，Geneva，Switzerland)。簡言之，排卵藥物刺激是使用人工合成濾泡刺激素（recombinant FSH, rFSH，Gonal-F®; Merck-Serono，Geneva，Switzerland）或是含有 75 IU/ampules FSH 和 LH 活性的高度純化人類停經後促性腺激素（hp-hMG，Menopur®; Ferring Pharmaceuticals，Saint-Prex，Switzerland)。療程開始後，每 1 至 3 天測量血清荷爾蒙數值和濾泡超音波檢查，持續至誘發排卵的那天。當超過 2 個濾泡直徑達到 18mm 時，給予兩劑 3.75mg triptorelin (Decapeptyl®; Ferring Pharmaceuticals)，並在 34-36 小時後安排取卵手術，手術抽取之濾泡液分離出卵子後，剩餘濾泡液體當日即在實驗室進行顆粒細胞之分離萃取。首先，濾泡液以 2000rpm 轉速進行 5 分鐘的離心，將顆粒細胞從濾泡液中分離出來，接著將細胞沉澱物重新懸浮於 Dulbecco phosphate-buffered saline（DPBS; Invitrogen Life Technologies，MA，USA）中，在 50% Ficoll-Paque density gradient media（GE Healthcare，Waukesha，WI，USA）上分層， 然後以 2000rpm 離心 5 分鐘以除去紅血球細胞。接著再收集界面處的卵巢顆粒細胞並將其轉移到 matrix-coated gel（Matrigel; Corning Incorporated，Corning，NY，USA）中培養 2-3 天，將可去除更多的雜質、組織碎片和紅血球細胞。最後，從培養基中收集卵巢顆粒細胞用於進一步的 DNA，RNA 和蛋白質萃取。

doi:10.6342/NTU202000313

(三) 誘導性多功能幹細胞之生成和分化為顆粒細胞

(1) 分離皮膚纖維母細胞和細胞培養

針對非卵巢疾病而須進行良性婦科手術(如子宮肌瘤切除手術)的 2 名多囊性卵巢症候群患者和 2 名非多囊性卵巢症候群病患，取得其同意後，我們在婦科手術過程中進行皮膚切片以取得皮膚纖維母細胞，每位受試者均從前腹壁取出一片 1 平方公分大小的皮膚組織，並從中分離出皮膚纖維母細胞在 DMEM 中培養，加入 10%胎牛血清、非必需氨基酸、L-glutamine 和青黴素/鏈黴素(penicillin/streptomycin)。人類皮膚纖維母細胞衍生之誘導性多功能幹細胞，則培養在含有 mitomycin C-inactivated mouse embryo fibroblast (MEF) 之無血清培養基中（ReproCELL，Shin-Yokohama，Japan），並添加了 10ng / ml basic fibroblast growth factor。

(2) 病患專一性誘導性多功能幹細胞之生成

多囊性卵巢症候群和對照組之誘導性多功能幹細胞重編程是依照廠商說明書之步驟進行（System Biosciences，Palo Alto，CA，USA）。簡而言之，首先使用 ECM 830 Square Wave Electroporation System（BTX，Holliston，MA）進行電穿孔 (electroporation)，將人類 *OCT4，SOX2，LIN28，KLF4，c-MYC* 等基因、p53shRNA 和 miR-302/367 以游離載體 (episomal plasmids) 導入至受試者皮膚纖維母細胞中。接著，將細胞接種到含有纖維母細胞生長培養基的 gelatin-coated 6-well 細胞培養分隔盤上。細胞匯合率(confluency)達到 80%後，將細胞重新接種在含有 mitomycin C-inactivated mouse embryo fibroblast (MEF)之纖維母細胞生長培養基。16 小時後，用添加了 PSGen Reprogramming Supplement 的誘導性多功能幹細胞生長培養基來替換原培養基。一般而言胚胎幹細胞（embryonic stem cell, ESC）樣細胞群出現在 15-20 天後，並可在 20 天後取得。Episomal reprogramming vectors 的表現是使用 SYBR Green qPCR 進行測定。鹼性磷酸酵素染色 (Alkaline phosphatase staining) 和多能性標記物 (pluripotency markers) 的免疫染色則是使用 Complete Antibody 和 AP staining Kit SAB-KIT-1（SBI，System

doi:10.6342/NTU202000313

Biosciences）來進行。 兩個胚胎幹細胞細胞群，NTU1 (Lan *et al.*, 2013) 和 H9 (Thomson *et al.*, 1998; WiCell, Madison, WI, USA) 在本研究中作為陽性對照組 (positive control)。

(3) 顆粒細胞分化

先前台大研究團隊已成功將人類胚胎幹細胞分化成卵巢顆粒細胞(Lan *et al.*, 2013)，因此本研究中也依循相同流程，試圖將衍生自皮膚纖維母細胞之誘導性多功能幹細胞分化成卵巢顆粒細胞。簡單來說，先將誘導性多功能幹細胞聚落以手動方法分成小團塊，並鋪在培養皿上，以形成胚狀體（embryoid body; EB）。接著將胚狀體在 DMEM / F12 培養基中培養 2 天，此種特殊培養基添加了 20％血清替代物、非必需氨基酸，GlutaMAX 和 β-巰基乙醇 (β-mercaptoethanol)。2 天後，再將胚狀體移至添加了 BMP4 的維持培養基中培養 1 天，在接下來的 3 天裡，在添加了 BMP4，WNT3A 和活化素 A (activin A)之培養基中繼續培養。為了進一步誘導成顆粒細胞，胚狀體被轉移到明膠塗層細胞培養皿中再培養六天，培養皿中添加了對於顆粒細胞分化極為重要的 BMP4 和 follistatin。

(四) 驗證 iPSC 多能性

(1) 體外分化 In vitro differentiation

體外分化的步驟是根據製造商的說明書來進行（R＆D Systems，Minneapolis，MN，USA）。簡單地說，細胞使用細胞分離試劑 (accutase) 分離，將其置於 RGF/BME 塗層蓋玻片上，再移至小鼠胚胎纖維母細胞維持培養基中，並輔以 4ng /ml 基本型纖維母細胞生長因子。在細胞達到 50％匯合率後，用分化培養基替換原培養基。在 4 天後收集細胞並用抗 Otx2，Brachyury 和 Sox17 抗體進行染色。

(2) 畸胎瘤形成測定 (Teratoma formation assay)

doi:10.6342/NTU202000313

將 1×10^7 個誘導性多功能幹細胞進行皮下注射到 6-8 週齡免疫缺陷小鼠 (NOD-SCID) 的背側軀幹中。在 8-12 週後生成畸胎瘤，將之切除並使用 hematoxylin and eosin staining 進行組織染色分析。對於涉及小鼠的實驗，所有程序均符合台大實驗動物倫理委員會所核准的指引。

(五) 誘導性多功能幹細胞所衍生顆粒細胞之功能驗證

(1) 萃取 DNA，RNA 和蛋白質

顆粒細胞 DNA 和 RNA 的萃取是使用 AllPrep DNA / RNA Mini Kit（Qiagen，Hilden，Germany），並使用 Nanodrop ASP-2680 （ACTGene，Piscataway，NJ，USA）測量樣品產量和純度。蛋白質的萃取是使用用於培養細胞的 Subcellular Protein Fractionation Kit (Thermo Fisher Scientific，Waltham，MA，USA)，並使用 DTX 800 Multimode Detector（Beckman Coulter，Brea，CA，USA）測量蛋白質產量和純度。

(2) 逆轉錄聚合酶鏈鎖反應和定量即時聚合酶鏈鎖反應

逆轉錄聚合酶鏈式反應的進行是使用 GoTaq Green Master Mix 套裝試劑（Promega，Madison，WI，USA）。定量即時聚合酶鏈鎖反應是使用 Applied Biosystem TagMan（Thermo Fisher Scientific）或 1x EvaGreen 試劑（目錄號 31014; Biotium，Fremont，CA，USA)，並使用 StepOnePlus Real-Time PCR 系統（Thermo Fisher Scientific）進行分析。聚合酶鏈鎖反應所用的引子 (primer) 序列和 TaqMan 探針 ID 列於表一中。GAPDH 作為定量的內部控制 (internal control)。

(3) 免疫組織化學染色分析

將細胞用 PBS 中的 4%多聚甲醛 (paraformaldehyde) 在室溫下固定 30 分鐘。 使用 PBS 洗滌後，在 PBST 中用 0.1%Triton X-100（0.1% TWEEN 20 in PBS）

doi:10.6342/NTU202000313

滲透細胞。接著添加一次抗體(primary antibody) 包括 NANOG、OCT4、SSEA4 和 TRA1-60（SAB-KIT-1），維持在 4°C 下至過夜。所使用的二次抗體為 Alexa Fluor 488 goat anti-rabbit IgG 或 Alexa Fluor 488 rabbit anti-mouse IgG（Thermo Fisher Scientific），在室溫下培養 30 分鐘。之後用 Hoechst 33342 對細胞進行染色以顯現細胞核。

(4) 流式細胞儀分析

使用細胞分離試劑 accumax 將細胞解離成單個細胞進行染色程序，接著使用 human Fc receptor inhibitor 來阻斷細胞並在 flow cytometry staining buffer（Affymetrix; Thermo Fisher Scientific）進行分離純化。主要的一次抗體包括 rabbit anti-aromatase (CYP11A1) PE-conjugated antibody (Bioss, Woburn, MA, USA)，rabbit anti-AMHR2 488-conjugated antibody (Bioss)，和 mouse anti-FSHR APC-conjugated antibody (R&D Systems)。蛋白質表現量是使用 FACSCalibur 流式細胞儀（BD Biosciences，Franklin Lakes，NJ，USA）進行分析。之後則透過 AMHR2 和 FSHR 的結合表現，來分離純化分化第 12 天的誘導性多功能幹細胞衍生之卵巢顆粒細胞，並用於後續的 DNA 甲基化分析。

(5) 芳香酶活性測定和雌激素濃度的測量

芳香酶 (aromatase) 活性的測定方式為，先添加雄性荷爾蒙至細胞培養皿，接著測量培養基中的雌二醇濃度，每次實驗至少複製 3 次。所測量的細胞包括：多囊性卵巢症候群和對照組的誘導性多功能幹細胞衍生之分化第 12 天的卵巢顆粒細胞、人類胚胎幹細胞（H9）和試管嬰兒所取得之成人卵巢顆粒細胞。這些細胞以 4×10^5 個細胞/孔的密度接種，並在 6-well 細胞培養分隔盤上培養 24 小時。接著將細胞在添加有 50ng / mL 睾固酮（Sigma-Aldrich，St. Louis，MO，USA）的培養基中再培養 24 小時後，收集培養基用 estradiol enzyme immunoassay (EIA) kits（Cayman Chemical，Ann Arbor，MI，USA）測量雌二醇濃度。

(六) 甲基化晶片分析的亞硫酸氫鹽轉化、DNA 放大、片段化和雜合

doi:10.6342/NTU202000313

(hybridization)

我們取成人卵巢顆粒細胞和分化第 12 天的誘導性多功能幹細胞衍生之卵巢顆粒細胞來測定全基因體 DNA 甲基化表現。細胞 DNA 的分離萃取是使用 0.5％SDS 和 200μg/ ml proteinase K 進行 K-phenol-chloroform extraction。將 DNA 濃度標準化至 50ng /μl 之後，取 500ng genomic DNA 用 EZ DNA Methylation kit（Zymo Research，Irvine，CA，USA）進行 DNA 亞硫酸氫鹽轉化 (bisulfate conversion)，再將 200ng 經過亞硫酸氫鹽轉化的 DNA 用於 Infinium MethylationEPIC BeadChip 分析（Illumina，San Diego，CA，USA）。EPIC BeadChip 晶片涵蓋超過 850,000 個 CpG 位點，包含超過 90％的前一代 Illumina Infinium Methylation450 BeadChip 所涵蓋之 CpG 位點，並增加額外 350,000 個 CpG 在增強子 (enhancer) 區域。其執行步驟簡單如下，先在 Illumina Hybridization Oven 中以 DNA 聚合酶將亞硫酸氫鹽轉化的 DNA 擴增 1000 倍，條件為 37℃下 20-24 小時，然後將擴增的 DNA 產物切成 300-600 個鹼基對的小片段，以酒精沉澱並重新懸浮片段化的 DNA 後，在 capillary flow-through chamber 中進行雜合以製備 BeadChip。在 Illumina 雜合爐中，經過 48°C 16 小時的雜合步驟後，已擴增和碎片化的 DNA 會黏合到具位點特異性的 50-mers 上。接著使用 biotin-ddNTP 或 dinitrophenol-ddNTP 進行螢光染色並透用 Illumina HiScan 儀器檢測螢光強度。

(七) 全基因體 DNA 甲基化晶片數據品質控制和常態化

DNA 甲基化晶片分析得到的原始數據使用 Illumina GenomeStudio（v2010.1）進行品質控制和校正，包含了色偏校正(color bias correction)和背景調整(background adjustment)。接著在 R 統計環境（v.3.1.1）下進一步過濾探針，並進行 quantile normalization 和 β 值到 M 值轉換。每個 CpG 位點都計算出一個相對應的 β 值(數值分佈從 0 到 1，代表 DNA 甲基化程度從 0％至 100％)。β 值計算方式為甲基化信號強度除以甲基化和未甲基化信號強度總和的比例，來表示各個 CpG 位點的甲基化值。M 值則是計算甲基化探針強度除以未甲基化探針

doi:10.6342/NTU202000313

強度所得比例的 log2 值。在多囊性卵巢症候群組和對照組之間具有顯著甲基化差異基因的相關生物路徑分析，則是使用 MetaCore（Thomson Reuters，New York，NY，USA）和 Ingenuity Pathway Analysis（IPA，Qiagen，Hilden，Germany）。

(八) 基因表現量分析

成人卵巢顆粒細胞的全基因體基因表現量是使用 Affymetrix GeneChip Human Genome Gene 1.0 ST microarray chips (Thermo Fisher Scientific)晶片進行分析。步驟簡述如下，每個檢體均取 100ng 之 total RNA 進行反轉錄生成雙股互補 DNA (cDNA)，透過包含 T7 RNA 合成酶促進子的引子 (oligo primer)。單股互補 DNA 再以生物素化核甘酸 (biotinylated nucleotides)進行標記並進一步使用於晶片雜交，接著晶片再以 Affymetrix® Fluidics Station 450 儀器進行清洗和染色 (stained)並以 Affymetrix® GeneArray 3000 7 G scanner 進行掃描產生螢光訊號，其後的分析則是以 Affymetrix® GeneChip® Command Console®軟體產生細胞訊號數值檔案 (Cell intensity data, CEL files)。數據的標準化 (normalization)是使用分位數標準化方法(quantile normalization methods)，基因表現量則以 R 語言的 Limma 套件分析得到具有顯著差異性表現的基因清單，並以 Benjamini–Hochberg 方法計算其 P 值，再以 IPA 進行後續的生物路徑分析。

(九) 西方墨點法分析

從多囊性卵巢症候群組和對照組取得的卵巢顆粒細胞中萃取蛋白質進行西方墨點法。每個槽中加入 30 微克蛋白質以 SDS-PAGE 分離並轉印到 polyvinylidene difluoride membranes 上。將轉漬膜取出以去離子水清洗，接著加入 3%BSA（Bovogen，Keilor East，Australia）在 Tris-buffered saline TWEEN 20 (Gibco)中封閉，並在 4℃下與下列一次抗體各別作用至隔天：人類 CREB 抗體

doi:10.6342/NTU202000313

（1：1000; Cell Signaling Technology. Danvers，MA，USA），人類 CBP 抗體（1：1000; R＆D Systems），或人類 GAPDH 抗體（1：5000; R＆D Systems）。將聚偏二氟乙烯膜在室溫下與以下二抗作用 60 分鐘：驢抗小鼠抗體（donkey anti-mouse antibody；R＆D Systems）或山羊抗兔抗體（goat anti-rabbit antibody；Cell Signaling）。使用 MGIS-21 蛋白質印跡分析系統（TOPBIO CO.，New Taipei City，Taiwan）通過化學發光檢測免疫複合物。

(十) 統計分析

所有實驗結果均來自三重複實驗，結果表示為平均值±標準偏差，Mann-Whitney U 檢驗用於檢驗組間差異的顯著性，除了圖十八所使用信賴區間為 90%以外，所有其他統計檢定均為雙尾測試，可信度為 95％（P <0.05）。所有統計計算均使用 SPSS version 17 (SPSS, Inc., Chicago, IL, USA) 軟體。

doi:10.6342/NTU202000313

第三節之第二部 多囊性卵巢症候群之微小核醣核酸研究

(一) 受試者召募與研究方法

受試者的召募總共分為兩個階段，第一階段召募了 75 名多囊性卵巢症候群患者和 20 名對照組受試者進行血漿微小核醣核酸之定量即時聚合酶鏈鎖反應測量，多囊性卵巢症候群患者的診斷標準是根據鹿特丹標準，而此部分研究所召募的所有患者均符合慢性無排卵的診斷標準，即每年的自發性月經小於九次，對照組的挑選方式則如前第一節研究方法所述。所有的多囊性卵巢症候群患者均在台大婦產科門診接受至少六個月以上的口服 metformin (loditon 500mg/tab, 生達, 台南)藥物治療，所有受試者在開始口服 metformin 治療前，均會先抽取空腹八小時的靜脈血，人體測量，骨盆超音波掃描檢查和血壓心跳測量。執行細節如前第一節研究方法所述。肥胖和代謝症候群 (metabolic syndrome, MS) 的診斷依據亦如前述。metformin 劑量為每日 1000-1500mg，依病患之容忍度和療效進行劑量調整，後續每三個月安排回診追蹤病患之月經週期、體重變化、血清荷爾蒙和新陳代謝數值 (血糖、血脂肪、肝功能、尿酸) 變化。此部分研究已通過台大醫院倫理委員會核准執行。評估 metformin 有效改善排卵的定義為六個月內出現四次以上的自發性月經，若少於四次則評估為 metformin 在改善排卵方面無效。

第二階段的受試者召募是為了驗證預測 metformin 療效模型之有效性，第二階段總共召募 71 位接受 metformin 治療至少六個月以上的多囊性卵巢症候群患者 (與第一階段之受試者無重疊)，全部都有符合慢性無排卵之診斷條件，其中 40 位在接受 metformin 治療六個月後排卵功能出現顯著改善，其中 31 位在接受 metformin 治療六個月後仍未能改善排卵功能。這 71 位病患在開始 metformin 治療前同樣接受了空腹八小時的靜脈血採樣，人體測量，骨盆超音波掃描檢查和血壓心跳測量。追蹤方式亦如同第一階段之受試者。

doi:10.6342/NTU202000313

(二) 檢體處理及血漿核醣核酸萃取

每個受試者均以促凝劑乾燥管(procoagulant drying tube)收集 5ml 靜脈血，以 4,000rpm 離心 10 分鐘將全血分離成血漿和細胞碎片，然後以 12000rpm 離心 15 分鐘以完全除去細胞碎片。接著進行血漿 RNA 的分離，先用 Trizol Reagent 進行血漿 denaturization 並用 Qiagen miRNeasy Mini Kit（Qiagen，Valencia，CA）進行 RNA 收集和純化。此外，每個實驗步驟中皆取相等的體積處理樣品，以控制潛在的偏差。

(三) 定量即時聚合酶鏈鎖反應

定量即時聚合酶鏈鎖反應是使用 TaqMan MicroRNA Reverse Transcription Kit（Life Technologies，Paisley，UK），每個實驗均進行三重複。擴增 (Amplification)是使用 StepOnePlus PCR 系統（Life Technologies），再以 StepOne software (Life Technologies)和 comparative Ct Method (ΔCT Method)分析擴增曲線。我們從文獻中選擇最可能與致病機轉相關之 14 種微小核醣核酸，包括與血糖代謝或糖尿病有關的七個微小核醣核酸（miR-21，miR-93，miR-132，miR-193，miR-221，miR-222，miR-223）和另外七個曾經被提出與卵巢和腦下垂體功能有關的微小核醣核酸（miR-27a，miR-125b，miR-200b，miR-212，miR-320a，miR-429，miR-483）。所有微小核醣核酸的定量均以 miR-423 作為內部控制 (internal control)。

(四) 微小核醣核酸標的基因的生物資訊學分析和分子路徑預測

微小核醣核酸標的基因的預測是使用 TargetScan 線上軟體 (http://www.targetscan.org/vert_72/) 進行分析，微小核醣核酸標的基因所影響之

doi:10.6342/NTU202000313

生物路徑則是以 Panther 線上軟體 (http://www.pantherdb.org/geneListAnalysis.do) 進行分析。

(五) 統計分析

所有實驗結果均來自三重複，結果表示為平均值±標準偏差，以 Student's T test 分析兩組連續變項數值的差異，以 Chi square 分析兩組類別變項的差異，所有其他統計檢定均為雙尾測試，可信度為 95%（P <0.05）。ROC 曲線分析是以 R 語言進行，其餘統計計算均使用 SPSS version 17 (SPSS, Inc., Chicago, IL, USA) 軟體。

doi:10.6342/NTU202000313

第三章 結果

第一節 臨床表徵分組及相關預後因子分析

Symptom patterns and phenotypic subgrouping of women with polycystic ovary syndrome: association between endocrine characteristics and metabolic aberrations. (Huang *et al.*, 2015)

從 2008 年至 2011 年，我們共招募了 460 名多囊性卵巢症候群的患者。所有患者均符合鹿特丹診斷標準，各個診斷標準符合的百分比如下：符合月經過少/無月經的比例為 92.4%（425/460），符合超音波影像檢查上顯示多囊性卵巢形態者為 94.3%（434/460），符合臨床或生化檢驗上的高雄性荷爾蒙症者為 80.9% (372/460)，臨床高雄性荷爾蒙表徵和高雄性荷爾蒙血症的的百分比分別為 62.8%（289/460）和 52.8%（243/460）。另外兩個文獻常用的多囊性卵巢症候群診斷標準，AE-PCOS 標準和美國 NIH 標準的符合比例，分別為 85.9%（395/460）和 78.3%（360/460）。多囊性卵巢症候群受試者平均年齡為 24.7 歲（標準差 5 歲，分布範圍從 13 至 41 歲），肥胖 （身體質量指數 ≥ 25 mg/m^2）的符合比例為 40.2%（185/460）。

我們用不同的尺度 (Scales) 標準化了總共 21 個臨床表徵之變項，包括 17 個新陳代謝變項和 4 個內分泌變項。廣義相關圖 (GAP) 分析產生了兩個彩色圖形（圖一），包括所有變項之間的相關圖（圖一 A），還有 460 個病患的分群模式，以及每一個臨床表徵變項與病患次族群之間的相關性（圖一 B）。圖一 A 中顯示了 21 個臨床表徵變項之間的相關係數的接近矩陣 (proximity matrix)。極深紅色表示相關係數為 1（完全正相關），白色表示為 0（無相關），極深藍色表示為 -1（完全負相關）。臨床表徵的維度被分為兩大類（內分泌和新陳代謝

doi:10.6342/NTU202000313

之測量)。由矩陣圖十分直觀地可看出，HOMA-IR、血壓、人體測量和血脂肪測量值之間存在強烈的正相關（暗紅色)，而高密度脂蛋白 (HDL-C) 除了和總膽固醇有中度正相關（紅色）之外，高密度脂蛋白和所有其他新陳代謝變項均呈現負相關（藍色)。另一個有趣的發現是，血清黃體化激素 (LH) 濃度與人體測量值 (包括：體重、BMI、臀圍、腰圍) 有強烈的負相關（深藍色)。

在圖一 B 中，根據 21 個臨床表徵變項在 460 名患者的表現值相對高低進行了分析，並據以分組，進一步繪製成矩陣圖。每一個橫紋就代表一個患者，顏色則代表該臨床表徵變項在整個多囊性卵巢症候群病患群組中的相對表現值，白色橫紋表示該變項在特定病患的表現是等於平均值的，紅色橫紋表示該變項在特定病患的表現是高於平均值的，藍色橫紋則表示低於平均值。為瞭解是否存在特定內分泌或代謝特徵可以對應到多囊性卵巢症候群的不同次族群，我們進行了叢聚樹分析，根據四個內分泌變項（濾泡刺激素 FSH、黃體化激素 LH、游離雄性荷爾蒙指標 free androgen index (FAI) 和硫酸去氫表睪固酮 DHEA-S）的相關性，可將患者分成四個不同的次族群，這四個內分泌變數之間具有較高相關性的患者，在叢聚樹上的位置是更相近的。例如，第 1 組中的患者表現出較高的濾泡刺激素和/或黃體化激素濃度（FSH 和/或 LH 欄上顯示為紅色橫紋）和較低的游離雄性荷爾蒙指標（FAI 欄上的藍色橫紋)，因而被聚集而分組在一起，而其相對應之新陳代謝變數的橫紋多為藍色，表示這組病患的新陳代謝表現值在所有病患的相對表現是較低的。相比之下，第 4 組中的患者表現出較高的雄性荷爾蒙活性指標，也就是 FAI 欄上的紅色橫紋)，因此被分組在一起。而且可觀察到其相對應的新陳代謝表現值明顯較高，代謝變項的大多數橫紋都是紅色。此外，每個次族群彼此之間表現出顯著不同的新陳代謝異常之風險率（圖一 B 和圖二)。

表二中列出了來自廣義相關圖分析所分出的四個不同次族群，其各次族群的人體測量特徵，荷爾蒙和新陳代謝數值。四個次族群之間的平均年齡、身高和總膽固醇濃度沒有顯著差異。第 4 組（個案數 = 57）的平均游離雄性荷爾蒙指標和總睪固酮濃度最高，並且呈現最嚴重的新陳代謝異常，包括胰島素阻抗，肝功能指數升高，血脂異常和血壓升高。第 1 組（個案數 = 204）的內分泌特

doi:10.6342/NTU202000313

徵為較低的游離雄性荷爾蒙指標，但平均黃體化激素濃度則相對較高，這組的新陳代謝指標是最良好的，其平均血糖、胰島素、HOMA-IR、尿酸和三酸甘油脂濃度顯著較低，而高密度脂蛋白濃度則較高。

圖二顯示了廣義相關圖四個次族群中，罹患新陳代謝症候群的比率，以及其符合新陳代謝症候群的診斷標準數量。我們的研究群組中，新陳代謝症候群的盛行率為 19.3%（89/460），而四個次族群之間的盛行率有顯著差異（P <0.0001）。第 1 組的新陳代謝症候群盛行率顯著較低（7%），而第 2 組和第 4 組的新陳代謝症候群盛行率較高。儘管第 2 組具有相對較低的平均總睪固酮濃度和游離雄性荷爾蒙指標，但新陳代謝症候群的盛行率仍然很高（高達 30%）。

表三顯示了在廣義相關圖四個次族群中，鹿特丹標準的三個診斷條件各自符合的比率，和鹿特丹診斷標準四個子群的盛行率。鹿特丹標準的四個子群包括：(1) 完全表現型 full-blown phenotype: HA + AO + PCOM; (2) 非多囊性卵巢型 non-PCO phenotype: HA + AO; (3) 排卵型 ovulatory phenotype: HA + PCOM; (4) 非高雄性荷爾蒙型 non-hyperandrogenic phenotype: AO + PCOM。由於我們研究族群中的大多數患者是鹿特丹標準完全表現型（67.6%），因此鹿特丹標準完全表現型仍然在我們的廣義相關圖四個次族群中都佔了最大的比例。然而，第 4 組不僅有最高比例的新陳代謝症候群 (47%) ，也同時具有顯著最高比例的鹿特丹標準完全表現型（94.7%），並且其中沒有任何非高雄性荷爾蒙型。

圖三顯示了廣義相關圖四個次族群，分別在鹿特丹診斷標準四個子群中所佔的比例。雖然在鹿特丹標準的完全表現型中，第 4 組病患明顯較多，但第 4 組僅有 17.4 %為完全表現型之病例。而第 1 組至 3 組平均分佈在四個鹿特丹子群內，顯示出廣義相關圖次族群和鹿特丹子群之間並沒有很好的對應性。

圖四顯示了不同臨床表徵分布在廣義相關圖四個次族群的比例。在高雄性素血症和肥胖症患者中，第 4 組的比例較高。此外，第 1 組最顯著獨特的臨床特徵是較高的黃體化激素濃度。黃體化激素濃度高於 15mIU/ml（在我們研究族群中的第 75 個百分位數）的患者中，95%是第 1 組，而其所對應的新陳代謝症

doi:10.6342/NTU202000313

候群盛行率是最低的 (7%)。

而新陳代謝症候群盛行率在鹿特丹標準中的四個不同子群之間沒有顯著差異（P=0.317），在三個不同診斷標準（P=0.981）之間的盛行率亦無顯著差異 (表四)。此外，進一步以 two-stage LDA 函數分析運用四個內分泌特徵計算得到的預測模型，對於患者是否罹患新陳代謝症候群，顯示出良好的預測力。靈敏度、特異性和準確性分別為 61.8%、85.7%和 81.0%。

doi:10.6342/NTU202000313

第二節 卵巢濾泡液通透性與血管生成因子之相關致病機轉

Increased platelet factor 4 and aberrant permeability of follicular fluid in PCOS. (Huang *et al.*, 2019)

病患和療程特徵

從 2014 年至 2015 年，共招募了 13 位無排卵多囊性卵巢症候群患者和 11 位對照組受試者。幾乎每個參與者都使用拮抗劑療程，只有一名對照組患者使用長療程。試管嬰兒療程的病患特徵和治療情形見表五。兩組的年齡、身體質量指標、未曾生產女性的比例和基礎濾泡刺激素濃度沒有顯著差異。與對照組的正常月經週期相反，多囊性卵巢症候群組的每位患者均符合慢性無排卵之條件，平均月經間隔將近三個月。多囊性卵巢症候群組中大約一半的患者（7/13）具有生化和/或臨床高雄性荷爾蒙症。其中，三位多囊性卵巢症候群患者僅表現出生化上高雄性荷爾蒙血症，兩位患者同時表現出生化和臨床高雄性荷爾蒙症，兩位患者僅表現出臨床高雄性荷爾蒙症。多囊性卵巢症候群組的平均血清黃體化激素濃度明顯較高。而在促性腺激素藥物的總劑量，排卵藥物的使用持續時間，誘發排卵當天的血清雌激素和黃體素濃度，取得卵子的數量，已完成第一次減數分裂的成熟卵子 (metaphase II) 數量、受精率等各變項，兩組均無顯著差異。

人類臍靜脈內皮細胞之通透性測量

為了分析多囊性卵巢症候群組和對照組的卵巢濾泡液對內皮細胞通透性的影響，我們將添加了 HRP 分子的受試者濾泡液加入培養有單層人類臍靜脈內皮細胞的上層隔室（圖五），並測量 HRP 分子穿透內皮細胞到下層隔室的濃度以

doi:10.6342/NTU202000313

計算相對通透性。結果顯示，加入多囊性卵巢症候群病患濾泡液所測量到的相對通透性，比起加入對照組受試者濾泡液時顯著降低（多囊性卵巢症候群組[共 11 人]為 46％ ± 12％，而對照組[共 9 人]為 58％ ± 9％，P = 0.023）。

人類血管生成晶片分析

我們進行了人類血管生成晶片分析來偵測濾泡液中的哪個成分可能導致通透性變化（表六和圖六）。在晶片所能測試的 55 種人類血管生成相關蛋白中，只有一種蛋白第四血小板因子（Platelet factor 4, PF4）在兩組之間具有顯著差異的訊號值（P = 0.004；圖六 A）。 多囊性卵巢症候群患者的濾泡液中存在顯著較高的 PF4 濃度。接著進一步以酵素免疫法驗證，仍然顯示多囊性卵巢症候群組濾泡液中的 PF4 濃度顯著較高 （多囊性卵巢症候群組為 51.6 ± 14.3 ng / ml，而對照組為 35.7 ± 3.8 ng / ml，P = 0.013；圖六 B）。

PF4 與內皮細胞通透性

為了進一步釐清 PF4 與內皮細胞通透性之間的因果關係，我們在人類臍靜脈內皮細胞實驗中將 rhPF4 添加到了對照組受試者的濾泡液中，發現所測量到之內皮細胞通透性顯著降低 （圖七 A）。免疫組織化學染色顯示在濾泡液中添加 rhPF4 後，內皮細胞之間的細胞間隙數量顯著減少（圖七 B）。這個實驗結果亦佐證了 PF4 可能是多囊性卵巢症候群患者濾泡液導致內皮細胞通透性下降的原因。

doi:10.6342/NTU202000313

濾泡液中的 IL-8 / PF4 蛋白複合體

台大先前的研究 (Chen *et al.*, 2010) 已經證實，卵巢濾泡內含有血管生成相關因子，例如 IL-8 和 VEGF，可以增加內皮細胞通透性，並可能在卵巢過度刺激症候群的致病機轉中扮演重要角色。Dudek 等人 (2003) 曾報告，PF4 和 IL-8 之間有高度親和力，會彼此結合並阻斷 IL-8 調控的造血功能。為了釐清這兩種蛋白在卵巢濾泡液的交互作用，我們將對照組和多囊性卵巢症候群組的濾泡液藉由免疫沉澱和西方墨點法中進行 PF4 和 IL-8 蛋白的分析，結果顯示 PF4 / IL-8 蛋白複合體在多囊性卵巢症候群和對照組的卵巢濾泡液中都可被偵測到（圖八 A）。進一步定量顯示，多囊性卵巢症候群組濾泡液中的 IL-8 和 PF4 含量均顯著高於對照組（圖八 B）。由於細胞間隙的形成是內皮細胞通透性的關鍵決定因素之一，所以我們透過人類臍靜脈內皮細胞裝置，在濾泡液添加了 rhPF4 或 rhPF4+rhIL-8，藉由 phalloidin 染色觀察內皮細胞之細胞間隙的形成。結果顯示，添加了 rhIL-8 之後內皮細胞間的細胞間隙數量增加，然而同時添加 rhPF4 和 rhIL-8 時則會使內皮細胞間的細胞間隙數量再次減少（圖八 C）。在單層人類臍靜脈內皮細胞之相對通透性測定中，rhIL-8 引起內皮細胞的相對通透性增加，假如同時添加 rhPF4 則會再次使相對通透性下降（圖八 D）。

綜合以上所述，我們的實驗結果顯示，人類卵巢濾泡液中存在 PF-4 / IL-8 蛋白複合體，而多囊性卵巢症候群組的濾泡液中 PF-4 / IL-8 蛋白複合體的含量顯著高於對照組。此外，PF-4 的存在會抑制細胞間隙的形成，並與 IL-8 相結合而拮抗了 IL-8 促進細胞間隙形成的效果，從而對內皮細胞產生抑制通透性的作用（圖九）。

doi:10.6342/NTU202000313

第三節 超基因調控之相關致病機轉研究

第三節之第一部 多囊性卵巢症候群之 DNA 甲基化研究

Hyperactive CREB signaling pathway involved in the pathogenesis of polycystic ovarian syndrome revealed by patient-specific induced pluripotent stem cell modeling. (Huang *et al.*, 2019)

病患專一性誘導性多功能幹細胞之生成和特徵

從多囊性卵巢症候群組和對照組女性受試者取得的真皮纖維母細胞，藉由攜帶 *OCT4*，*SOX2*，*LIN28*，*KLF4* 和 *c-MYC* 基因的游離載體(origin of replication/Epstein-Barr virus nuclear antigen-1 (ori/EBNA-1)-based episomal vectors)重新編程。載體還帶有 p53shRNA、miR302 和 miR367 等其他附加因子用來克服與重編程相關的障礙，並提高重編程效率。誘導性多功能幹細胞生成實驗的時間表和培養條件如圖十 A 所示。誘導性多功能幹細胞聚落是根據其形態特徵在第 20-25 天左右形成和選擇的，即可見小圓形細胞 (small round cells) 生長在具有與胚胎幹細胞聚落相似的細胞團中（圖十 B）。 我們從 2 名多囊性卵巢症候群患者和 2 名對照組受試者的真皮纖維母細胞中總共培養出 11 株誘導性多功能幹細胞細胞聚落，從每個患者選擇了在培養期間最穩定的一個細胞株用於後續的分化研究（iNFB1-1 和 iNFB3-3 是對照組，iPFB1- 3 和 iPFB3-1 是多囊性卵巢症候群）。透過染色體基因晶片分析顯示，所挑選出這四株誘導性多功能幹細胞均具有 44 + XX 的正常染色體模式（圖十一）。

病患專一性誘導性多功能幹細胞之多能性和分化驗證

我們對這 4 個已建立的誘導性多功能幹細胞株進行了鹼性磷酸酶活性分析

doi:10.6342/NTU202000313

(alkaline phosphatase activity)，證明這些誘導性多功能幹細胞之未分化和多能潛力（圖十二）。在免疫螢光染色下，多囊性卵巢症候群-誘導性多功能幹細胞（iPFB）和對照組-誘導性多功能幹細胞（iNFB）均確定具有多能性相關轉錄因子的存在，包括 *NANOG*，*OCT-4*，*SSEA-4* 和 *TRA-1-60* 基因之表現(圖十三)。所有建立的誘導性多功能幹細胞均進行逆轉錄聚合酶鏈式反應驗證自我更新相關基因(self-renewal genetic markers)的表現，包括 *DNMT3B*，*LCK*，*NANOG*，*OCT4*，*SOX2*，*GDF3*，*c-MYC*，*DPPA5* 和 *TERT* 等基因（圖十四）。人類胚胎幹細胞株 NTU1 用作實驗的陽性控制。在這四株誘導性多功能幹細胞株中，多能性相關基因的表現量沒有顯著差異。

為了驗證這些誘導性多功能幹細胞株的體外 (in vitro) 分化潛能，我們將誘導性多功能幹細胞重新懸浮培養成胚胎體（EB），結果所有 4 個細胞株均能形成形狀良好的胚胎體（圖十五 A）。將胚胎體重新接種到培養皿上並在胚胎幹細胞培養基中培養後，細胞可分化成具有不同形態的細胞。進一步以逆轉錄聚合酶鏈式反應對細胞進行分析，可驗證三個胚層的指標基因均有表現。包括： 外胚層分化標記 zinc finger and BTB domain containing 16 (*ZBTB16*) ；內胚層分化標記 alpha-fetoprotein (*AFP*)，以及中胚層分化標記 cadherin 5 (*CDH5*)（圖十五 B）。為了測試誘導性多功能幹細胞株體內 (in vivo) 的分化潛能，我們將未分化的多囊性卵巢症候群-誘導性多功能幹細胞株和對照組-誘導性多功能幹細胞株注射到 NOD-SCID 免疫缺陷鼠中，檢查畸胎瘤的生成和所有三個胚層的細胞形成（圖十六）。透過 HE 染色從誘導性多功能幹細胞所生成之畸胎瘤的組織切片，顯示外胚層，中胚層和內胚層細胞均有被成功分化出來，例如：外胚層的神經上皮、色素上皮、視網膜樣結構和鱗狀上皮；中胚層的脂肪組織、透明軟骨和粘液樣結締組織(myxoid connective tissue)；內胚層的腺體上皮 (glandular epithelium)（圖十六）。比較多囊性卵巢症候群和對照組的誘導性多功能幹細胞在形成畸胎瘤的能力方面，沒有明顯差異。這些結果顯示，這 2 個多囊性卵巢症候群-誘導性多功能幹細胞株和 2 個對照組-誘導性多功能幹細胞株已被重編程為多能狀態並具有分化能力。

doi:10.6342/NTU202000313

病患專一性誘導性多功能幹細胞衍生之卵巢顆粒細胞特徵

我們將上述四株成功建立之誘導性多功能幹細胞 (2 株多囊性卵巢症候群，2 株對照組) 再進一步分化為具有卵巢顆粒細胞功能和特徵的細胞。在第 0 天（未分化），和分化第 6, 9 和 12 天收集細胞，以檢查這些細胞是否有成功分化並表現出顆粒細胞相關基因，包括 *FOXL2*，*AMH*、*FSHR*、*LHR*、*AMHR2* 和 *CYP19A*（圖十七 A-F）。*FOXL2*，*AMH*，*FSHR*，*AMHR2* 和 *CYP19A* 的表現，在第 0 天（尚未開始分化）時是較低或完全未表現的；但在培養的第 6 天之後，可見多能性基因 *OCT4* 的表現下降，其他顆粒細胞相關基因的表現變得越來越顯著（圖十七 G）。雖然在不同分化天數時，多囊性卵巢症候群和對照組之間的顆粒細胞相關基因表現量沒有顯著差異（圖十七 A-G），然而，多囊性卵巢症候群組仍存在 *AMH*、*AMHR2*、*OCT4*、*FSHR* 和 *LHR* 表現量較高以及 *FOXL2* 表現較低的趨勢。我們在成人卵巢顆粒細胞也分析這些顆粒細胞相關基因的表現，結果顯示多囊性卵巢症候群和對照組之間並無顯著差異。然而，與對照組相比，多囊性卵巢症候群組的 *AMHR2* 基因表現倍數變化（fold change, FC）為 2.7，*LHR* 為 1.87，*CYP19A1* 為 11.27，*FOXL2* 為 2.4，以上基因均有表現增加的趨勢（圖十八）。

接著我們針對誘導性多功能幹細胞衍生之顆粒細胞，在分化第十二天時進行分析，透過顆粒細胞特異性標記（包括 *CYP19A1*，*FSHR* 和 *AMHR*） 進行流式細胞儀分析以鑑定成功分化出的顆粒細胞數量。結果顯示，多囊性卵巢症候群組和對照組的誘導性多功能幹細胞所衍生之顆粒細胞，其分化效率沒有顯著差異（圖十九）。此外，我們以芳香酶（CYP19A1）活性測定來分析這些誘導性多功能幹細胞所衍生之顆粒細胞，是否具備將睪固酮轉化為雌激素的能力（圖二十）。在這項功能性驗證中，多囊性卵巢症候群和對照組的誘導性多功能幹細胞衍生的顆粒細胞，在添加睪固酮後，雌激素濃度均顯著增加，顯示這些衍生顆粒細胞均具備正常芳香酶酵素功能，並與我們先前建立的胚胎幹細胞所衍生的顆粒細胞（H9）（Lan *et al.*, 2013）以及從取卵手術過程取到的成人顆粒細胞的芳香酶功能表現一致。後兩種細胞在這個實驗中作為陽性控制。

doi:10.6342/NTU202000313

DNA 甲基化分析顯示多囊性卵巢症候群的成人顆粒細胞和誘導性多功能幹細胞衍生顆粒細胞均顯現過度活化的 CREB 訊息傳導途徑

我們針對誘導性多功能幹細胞衍生之顆粒細胞 (分化第 12 天) 和透過取卵手術取得之成人卵巢顆粒細胞，均進行了全基因體 DNA 甲基化晶片分析，比較多囊性卵巢症候群和對照組之間是否有 DNA 甲基化差異。總共有 11 名多囊性卵巢症候群患者和 4 名對照組女性的卵巢顆粒細胞接受了 DNA 甲基化分析(這些病患的人體測量和生化特徵顯示在表七中)，總共有 13,326 個訊號不足的探針（1.5%，13,326 / 866,895）被刪除，留下 853,569 個探針用於後續分析。而誘導性多功能幹細胞衍生之顆粒細胞則是有 2 株多囊性卵巢症候群和 2 株對照組進行了 DNA 甲基化分析，總共有 3,703 個探針（0.4%）因訊號不足而被刪除，留下 863,192 個探針用於後續分析。

差異性甲基化區域（differentially methylated region, DMR）的定義是當多囊性卵巢症候群組和對照組的訊號值 M 值差異大於 2.5 倍時，則表示兩者的 DNA 甲基化表現在該位點上有顯著差異。而差異性甲基化區域所對應到的基因組之富集途徑分析 (enrichment pathway analysis) 則是使用 MetaCore 線上軟體進行。在成人卵巢顆粒細胞中，共找出了 472 個差異性甲基化基因（來自 796 個探針）用於生物途徑分析；在誘導性多功能幹細胞衍生顆粒細胞中則找出了 3682 個差異性甲基化基因（來自 10038 個探針）進行分析。表八中列出了差異性甲基化基因的排名前 10 顯著的富集途徑。在誘導性多功能幹細胞衍生顆粒細胞之分析中，其富集途徑的類別包括細胞骨架重塑 (cytoskeletal remodeling)、細胞粘附 (cell adhesion)、神經生理過程 (neurophysiologic processes)、信號轉導 (signal transduction)、轉錄 (transcription)，和發育 (development)。在成人卵巢顆粒細胞的富集途徑分析中，最常出現的差異性甲基化基因是蛋白激酶 C（protein kinase C ，PKC)，蛋白激酶 A（protein kinase A ，PKA）和磷脂酰肌醇-3 激酶（phosphatidylinositol-3 kinase ，PI3K)，它們與 MetaCore 分析數據庫中的許多調節途徑相關聯，例如血栓素 A2 (thromboxane A2)信號傳導途徑，CREB 信號傳導途徑，痛敏素受體(nociceptin receptor)信號傳導途徑，氧化壓力和前胰島–C

doi:10.6342/NTU202000313

胜肽(proinsulin C-peptide)信號傳導。當我們比較成人卵巢顆粒細胞和誘導性多功能幹細胞衍生顆粒細胞的 DNA 甲基化分析結果時，兩種細胞的前 10 名富集途徑都出現了 CREB 信號傳導途徑，這顯示了 CREB 信號傳導途徑在多囊性卵巢症候群病患的表現可能具有特殊功能意義，因此我們針對了 CREB 信號傳導途徑的相關分子進行了進一步驗證。這些差異性甲基化基因也進行了 IPA 分析（表九），IPA 的差異性甲基化定義是 β 值大於 0.25。在 IPA 分析當中，成人卵巢顆粒細胞的多囊性卵巢症候群組和對照組，以及誘導性多功能幹細胞衍生顆粒細胞的多囊性卵巢症候群組和對照組，也出現了相同的差異性甲基化基因富集途徑，包括 NRF2-mediated oxidative stress 和 PPAR / RXR 活化。

圖二十一 A 為 DNA 甲基化差異性表現的主成分分析 (principal component analysis)，顯示出在多囊性卵巢症候群組和對照組之間的 DNA 甲基化表現分佈有明顯區分（圖二十一 A）。圖二十一 B 顯示了 115 個差異性甲基化基因的階層式分群法分析（hierarchical clustering analysis; heatmap）。整體而言，與對照組相比，在多囊性卵巢症候群組的差異性甲基化基因更傾向於低度甲基化 (hypomethylated)（黃色）。

第 12 天誘導性多功能幹細胞衍生顆粒細胞與成人顆粒細胞之間的差異性甲基化基因的維恩圖 (Venn diagram)，顯示出總共有 37 個差異性甲基化基因在兩種不同顆粒細胞的分析是重疊的（圖二十一 C），也就是在多囊性卵巢症候群和對照組都有顯著甲基化差異。表十中記載了這些重疊基因的名稱列表，成人顆粒細胞和誘導性多功能幹細胞衍生之顆粒細胞的多囊性卵巢症候群組，在其中 10 個基因均呈現高度甲基化(hypermethylated)，在其中 8 個基因呈現低度甲基化，在剩餘的 19 個基因中則是一個高度甲基化，一個低度甲基化。

圖二十二中說明了差異性甲基化區域在基因結構上的分布位置，包括了 3' 非轉譯區 (3’ untranslated region, 3’UTR)、基因體(body)、第一個外顯子(1^{st} Exon)、5'非轉譯區 (5’ untranslated region, 3’UTR)、轉錄起始位點上游 200bp (TSS200, 代表較靠近 TSS 的 promotor 區域)、轉錄起始位點上游 1500bp (TSS1500, 代表較遠離 TSS 的 promotor 區域)和基因間 (intergenic) 區域。在成

doi:10.6342/NTU202000313

人顆粒細胞中，位於 TSS200（TSS 至 TSS 上游 200nt，P <0.0001）和 5'UTR（非轉錄區，P = 0.025）的高度甲基化基因區域之富集性明顯高於低度甲基化基因區域。

在成人顆粒細胞和誘導性多功能幹細胞衍生顆粒細胞中的 CREB/CBP 表現驗證

接下來針對成人卵巢顆粒細胞，對 CREB 和 CREB 結合蛋白（CREB binding protein, CBP）進行進一步的定量驗證，共在 5 個多囊性卵巢症候群患者和 4 個對照受試者檢體進行（圖二十三 A 和圖二十三 B）。多囊性卵巢症候群患者在卵巢顆粒細胞顯著地表現更高量的之 CBP 蛋白（P=0.027），同時也表現較高量的 CREB 蛋白，雖然可能是因為病例數量有限而沒有達到統計學的意義。未切碎的原始凝膠如圖二十四所示。誘導性多功能幹細胞衍生顆粒細胞中的 CBP mRNA 表現，也是多囊性卵巢症候群組患者顯著較高（圖二十三 C）。

doi:10.6342/NTU202000313

第三節之第二部 多囊性卵巢症候群之微小核醣核酸研究

（一）多囊性卵巢症候群與對照組比較

在第一階段，我們總共分析了 95 個受試者的血漿微小核醣核酸，包括 75 個多囊性卵巢症候群患者和 20 個對照組受試者，多囊性卵巢症候群患者和對照組受試者的臨床特徵列於表十一。正如預期地，多囊性卵巢症候群和對照組之間有許多內分泌和新陳代謝檢驗存在顯著差異。多囊性卵巢症候群組的身體質量指標、腰圍和臀圍數值顯著較高，血清睾固酮、黃體化激素、低密度脂蛋白和尿酸濃度顯著較高。而兩組的平均年齡，基礎濾泡刺激素濃度，胰島素和葡萄糖濃度則無顯著差異。

接著我們以即時聚合酶連鎖反應定量血漿中的游離微小核醣核酸表現量。最初，我們原想以微小核醣核酸晶片一次檢測數百種已知人類微小核醣核酸。然而基於成本考量，我們決定從文獻中選擇最可能與致病機轉相關之 14 種微小核醣核酸進行即時聚合酶連鎖反應測量，包括與血糖代謝或糖尿病有關的七個微小核醣核酸（miR-21，miR-93，miR-132，miR-193，miR-221，miR-222，miR-223）和另外七個曾經被提出與卵巢和腦下垂體功能有關的微小核醣核酸（miR-27a，miR-125b，miR-200b，miR-212，miR-320a，miR-429，miR-483）。表十二顯示了多囊性卵巢症候群和對照組中這些血液循環的游離微小核醣核酸濃度。總共十四個挑選出來的微小核醣核酸中，共有八個在多囊性卵巢症候群和對照組之間出現顯著濃度差異。其中，在多囊性卵巢症候群組中血漿濃度顯著較高的是 miR-93，miR-132，mR-221，miR-223，miR-27a 和 miR-212，而在多囊性卵巢症候群組中濃度顯著較低是 miR-222 和 miR-320a。

（二）Metformin 治療有效組和無效組

第二部分則是比較 metformin 在排卵和月經週期方面治療有效組和無效組之

doi:10.6342/NTU202000313

間的微小核醣核酸表現差異。有效治療的定義為 metformin 治療後每 3 個月出現超過兩次自發月經週期，每個病患至少追蹤六個月，意即六個月總共出現超過四次月經週期。表十三顯示了對 metformin 治療有效組 (n=37) 和無效組 (n=38) 的人體測量和生化特徵，如表中所示，metformin 治療有效組和無效組的身體測量和生化特徵幾乎沒有顯著差異，兩組有相同的平均年齡、體重、身體質量指標、腰圍和臀圍，唯一一個不同的變項在於治療有效組原本的平均月經週期比無效組的週期還要短，前者為六個月，後者為八個月，雖然治療有效組的週期規律性原本就比無效組顯著較佳，然而兩組的平均月經間隔都比正常月經週期還要長很多。此外在所有內分泌指標，包括高雄性荷爾蒙症的罹患率和平均血清睪固酮和 DHEA-S 濃度都沒有顯著差異。新陳代謝方面，除了在總膽固醇有輕微差異以外，其餘指標包括胰島素阻抗程度、空腹血糖、血脂肪、尿酸、肝功能等各方面指數都沒有顯著不同，換句話說，沒有任何的指標可以幫助我們預測 metformin 治療對多囊性卵巢症候群患者排卵功能的治療效果。因此，我們下一步分析 metformin 有效組和無效組之間血漿微小核醣核酸表現模式的差異。結果如表十四所示，metformin 治療有效組的 miR-27a, miR-93 和 miR-222 平均表現值都比無效組顯著上升。

（三）預測模型之建立

下一步我們想要瞭解是否可以透過血漿微小核醣核酸的表現模式來做為多囊性卵巢症候群的診斷和療效預測指標，故嘗試藉由 ROC 曲線分析來建立預測模型。

微小核糖核酸表現對於多囊性卵巢症候群診斷之預測模型

首先透過ROC曲線分析個別微小核醣核酸表現對於多囊性卵巢症候群診斷是否具有顯著鑑別力，結果顯示 miR-93、miR-132、miR-222、miR-27a、miR-125b、miR-212 這六個微小核醣核酸表現值的 ROC 曲線均出現顯著鑑別力

doi:10.6342/NTU202000313

(統計顯著的標準是 ROC 曲線下面積(area under curve, AUC)的 95%信賴區間 >0.5) (表十五)，因此我們便進一步用這六個微小核醣核酸建立預測模型，得到以下公式 Y = log (p/(1-p)) = 0.00148 – 10.8903 * **miR-93** + 28.6881 * **miR-132** - 48.8523 * **miR-222** + 2.4562 * **miR-27a** + 2.1320 * **miR-125b** + 18.2793 * **miR-212**。此預測模型的曲線下面積可達 0.959 (95%信賴區間 0.924-0.995)，對於有無符合多囊性卵巢症候群診斷的鑑別力非常高。而這六個微小核醣核酸個別的 ROC 曲線圖和預測模型的 ROC 曲線圖如圖二十五所示。

微小核糖核酸表現對於 metformin 改善排卵療效之預測模型

接著我們透過 ROC 曲線分析個別微小核醣核酸表現對於 metformin 有無療效是否具有顯著鑑別力，結果顯示 miR-93、miR-222、miR-223、miR-429 這四個微小核醣核酸表現值的 ROC 曲線均出現顯著鑑別力(表十六)，進一步用這四個微小核醣核酸建立預測模型得到以下公式 Y = log (p/(1-p)) = -1.8255 + 4.1106 * **miR-93** + 18.0284 * **miR-222** - 0.1152 * **miR-223** + 145.8 * **miR-429**。此預測模型的曲線下面積為 0.722 (95%信賴區間 0.602-0.841)。由於多囊性卵巢症候群患者的排卵功能也與其他臨床條件如：患者年齡、BMI、高雄性荷爾蒙症的有無有關，故我們將這三項臨床指標加入模型中，分析校正後的 ROC 曲線是否有更好的表現。此外從先前表十三的 metformin 治療有效和無效組的病患特徵分析得知，病患治療前的月經週期在治療無效和有效組織間有顯著差異，因此我們也將患者治療前的月經週期加入校正後的預測模型進行分析。所得到的校正後預測模型公式為：Y = log (p/(1-p)) = -2.0454 + 0.0242 * **年齡** (歲) + 0.0219 * **BMI** (kg/m^2)+ 0.1168 * **高雄性荷爾蒙症** (0 或 1) - 0.00689 * **月經週期** (天) + 3.6416 * **miR-93** + 25.4973 * **miR-222** - 0.1253 * **miR-223** + 163.0 * **miR-429**。校正後的預測模型曲線下面積為 0.807 (95%信賴區間為 0.704-0.909)，雖然加上臨床指標後的校正後預測模型之曲線下面積有增加趨勢，然而預測效果與未加上臨床指標的預測模型相比並沒有統計上顯著性差異 (P 值為 0.063)。而這四個微小核醣核酸個別的 ROC 曲線圖和校正前後預測模型的 ROC 曲線圖如圖二十六所示。

doi:10.6342/NTU202000313

（四）metformin 療效預測模型之驗證

為了驗證 metformin 療效預測模型之有效性，我們召募了另一個獨立的多囊性卵巢症候群病患族群，所有患者均符合鹿特丹標準並且都出現慢性無排卵之表徵，且均接受超過六個月的 metformin 治療，總共召募了 71 名多囊性卵巢症候群患者，包含了 40 名 metformin 治療有效和 31 名治療無效者，分析其治療前血漿中 miR-93、miR-222、miR-223、miR-429 這四項微小核醣核酸數值，並帶入預測模型進行計算。根據四個微小核醣核酸所建立預測模型進行計算的結果，預測為有效人數為 40 人，預測為無效人數為 31 人，算得敏感度為 70%，特異度為 61%，偽陽性為 30%，偽陰性為 29%。而根據四個微小核醣核酸以及四個臨床指標之校正後預測模型來計算，預測為有效人數為 59，預測為無效人數為 12，算得敏感度為 98%，特異度為 35%，偽陽性為 34%，偽陰性為 8%。相較之下，加上四個臨床指標後，預測為有效的人數增加，偽陰性下降，能夠更準確地找出治療無效的患者。

（五） Metformin 治療六個月後之臨床表徵與微小核醣核酸變化

所有接受 metformin 治療的患者均在開始治療之六個月後接受了空腹抽血檢驗，追蹤其微小核醣核酸和生化數值之變化，並追蹤其月經週期與身體質量特徵之改變如表十七。Metformin 治療有效亦即能夠顯著改善排卵功能和月經週期，無效組則反之。在 metformin 治療無效組，所檢測的 14 種微小核醣核酸血漿濃度在治療前和治療後沒有顯著差別，然而在治療有效阻，則有五種微小核醣核酸在前後側的數值出現顯著差異，包括：miR-21, miR-93, miR-222, miR-223, miR-27a。此處的統計學顯著標準為 P 值小於 0.0035，為了降低多重檢定之偽陽性而進行了最嚴格的 P 值校正，直接將 0.05 除以 14，也就是檢測的變相數目。而無論 metformin 是否有效改善排卵，在治療有效組和無效組兩組的體重、BMI、腰圍、臀圍、總睪固酮和游離雄性荷爾蒙指標，在接受 metfromin 治療六個月後都有顯著下降，顯示 metformin 對這些臨床表徵的改善效果與病患排卵功

doi:10.6342/NTU202000313

能的改善並無直接相關，然而在治療有效組的空腹血糖和胰島素濃度，在 metformin 治療六個月後有顯著下降，在治療無效組則在 metformin 治療前後沒有顯著差異，顯示兩組病患的胰島素和血糖變化與其排卵功能的改善很可能有顯著相關。

（六）關鍵微小核糖核酸之調控基因以及其富集途徑分析

(1) 多囊性卵巢症候群 v.s. 對照組

根據表十五，對於區分多囊性卵巢症候群和對照組兩組，總共有六個微小核醣核酸具有顯著的鑑別能力，包括：miR-93, miR-132, miR-222, miR-27a, miR-125b, miR-212，個別來看，以 miR-132 具有最高的曲線下面積，因此我們進一步以 TargetScan 線上軟體分析 miR-132 的標的基因，總共找出了 474 個可能的標的基因，再以 Panther 資料庫根據這些基因進行基因本體分析(gene ontology analysis, GO analysis) 結果如表十八，其中排名前十顯著的 GO 生物途徑 (biological process) 包括：regulation of nitrogen compound metabolic process, regulation of primary metabolic process, regulation of macromolecule metabolic process, regulation of cellular metabolic process, regulation of metabolic process, regulation of RNA metabolic process, regulation of nucleobase-containing compound metabolic process, regulation of gene expression, regulation of macromolecule biosynthetic process, regulation of cellular macromolecule biosynthetic process (以上依照錯誤發現率 (false discovery rate, FDR) 由低至高排列)，其中可見大多數為細胞代謝相關路徑。

而曲線下面積第二高的微小核醣核酸為 miR-27a，總共預測有 1421 個可能的標的基因，進行 GO 分析結果如表十九，而其所影響之排名前十顯著的 GO 生物途徑包括：regulation of primary metabolic process, regulation of metabolic process, regulation of nitrogen compound metabolic process, regulation of macromolecule metabolic process, regulation of cellular metabolic process, positive

doi:10.6342/NTU202000313

regulation of cellular process, positive regulation of metabolic process, positive regulation of macromolecule metabolic process, positive regulation of biological process, positive regulation of cellular metabolic process (以上依照錯誤發現率由低至高排列), 亦可見大多數的生物路徑為細胞代謝相關路徑。

(2) metformin 有效 v.s. metformin 無效

根據表十六，對於區分 metformin 有效改善排卵和無效兩組，總共有四個微小核醣核酸具有顯著鑑別力，其個別曲線下面積最高者為 miR-222，其以 TargetScan 預測之標的基因共 504 個，GO 分析結果如表二十，其所影響之排名前十顯著的 GO 生物途徑包括：regulation of cellular metabolic process, regulation of nitrogen compound metabolic process, regulation of macromolecule metabolic process, regulation of primary metabolic process, regulation of metabolic process, negative regulation of cellular process, negative regulation of metabolic process, negative regulation of macromolecule metabolic process, positive regulation of cellular process, negative regulation of biological process，仍可見排名前幾名者均為細胞代謝相關路徑。

而曲線下面積第二高的微小核醣核酸為 miR-93，其以 TargetScan 預測之標的基因共 1385 個，GO 分析結果如表二十一，其所影響之排名前十顯著的 GO biological process 包括：regulation of cellular metabolic process, regulation of metabolic process, regulation of primary metabolic process, regulation of nitrogen compound metabolic process, regulation of cellular process, regulation of macromolecule metabolic process, biological regulation, negative regulation of cellular process, regulation of cellular biosynthetic process, regulation of biosynthetic process，可見其所影響之生物路徑以細胞代謝以及生物合成為主。

doi:10.6342/NTU202000313

第四章 討論

第一節 臨床表徵分組及相關預後因子分析

Symptom patterns and phenotypic subgrouping of women with polycystic ovary syndrome: association between endocrine characteristics and metabolic aberrations. (Huang *et al.*, 2015)

在第一節的研究中，我們應用了一個強大的圖形分析統計工具（廣義相關圖）來直接從數據中解析各種臨床表徵相關性。廣義相關圖分析是一種不同於傳統圖形工具的無維度統計視覺化方法，所有訊息都能保存在最終輸出的結果圖像中。廣義相關圖分析還具有提供直接視覺感知的優勢，適合用於探索龐大而複雜的資料集中的資訊結構 (Wu *et al.*, 2008)。由於多囊性卵巢症候群病患的臨床表徵個體差異性相當高，因此，個別化分析其綜合臨床特徵來評估患者，篩選出高風險病患並擬定適當治療策略來改善其長期預後，是非常重要的（Orio and Palomba, 2014）。

過去有一些文獻曾提及了臨床高雄性荷爾蒙症徵狀的重要性，如多毛症和落髮(Legro *et al.*, 2013)，而另一些文獻則提到了肥胖對代謝異常的影響 (Azziz *et al.*, 2009)。過去有些研究指出，同時出現無排卵表徵和高雄性荷爾蒙表徵的鹿特丹完全表現型子群 (phenotype A) 和非多囊性卵巢型子群 (phenotype B)，相較於排卵型子群 (phenotype C) 和非高雄性荷爾蒙症子群 (phenotype D) 的患者，其胰島素阻抗 (Carmina *et al.*, 2005; Diamanti-Kandarakis and Panidis, 2007; Moghetti *et al.*, 2013) 或新陳代謝症候群 (Moran and Teede, 2009; Wild *et al.*, 2010) 的盛行率較高。然而，在我們的研究中，以鹿特丹標準所區分出的四個子群之間，其新陳代謝症候群的盛行率卻沒有顯著差異。原因之一可能為，我們研究的多囊性卵巢症

doi:10.6342/NTU202000313

候群病患為亞洲族群，新陳代謝症候群盛行率（19.3%）與其他在高加索人種的多囊性卵巢症候群病患進行的其他研究相比 (33% ~ 47%; Wild *et al.*, 2010)，相對較低，新陳代謝症候群在不同種族的差異性表現可能是其中一個解釋，此外在亞洲人種，高雄性荷爾蒙症的症狀嚴重度通常較為輕微，可能因此與新陳代謝異常的單獨相關性沒有高加索人種那麼高，同時，也可能需要更多案例來顯示出不同子群之間的差異。此外，不同研究對於高雄性荷爾蒙症的定義並不同，有的研究測量血清總睪固酮濃度，有的研究測量血清游離睪固酮，有的研究以游離雄性荷爾蒙指標作為標準，甚至於不同研究設定的標準數值也不一樣，有的研究有納入嚴重痤瘡作為診斷高雄性荷爾蒙症的臨床表徵，有的沒有。總之，臨床診斷標準的歧異，無可避免地造成了不同研究的結果難以彼此分析比較。當然，還有另一種可能的潛在解釋可能是，傳統的鹿特丹診斷標準所採用的多囊性卵巢症候群表徵，對於病患究竟是屬於新陳代謝上較健康還是較不健康者，鑑別的效果有限。因此，在我們研究中決定囊括更多的指標來進行分組，將四種內分泌特徵（FAI、DHEA-S、FSH、LH）組合應用在病患的分組中。結果顯示，藉由不同內分泌表徵所進行的分組，不僅個別具有其顯著臨床表現的差異性，其相應的新陳代謝症候群風險也存在顯著差異。

許多研究顯示，雄性荷爾蒙過高是導致新陳代謝異常的關鍵因素，其中包括中央性肥胖，胰島素阻抗和血脂異常……等等 (Kauffman *et al.*, 2002; Lerchbaum *et al.*, 2012; Barber and Franks, 2013)。在動物研究中，睪固酮可透過直接改變在脂肪和骨骼肌組織中的胰島素作用，或提高內臟脂肪量及其功能來誘發胰島素阻抗 (Mannerås *et al.*, 2007)。相比之下，在患有多囊性卵巢症候群的女性中，用抗雄性荷爾蒙藥物或促性腺激素釋放激素（GnRH）抑制雄性荷爾蒙濃度，可導致胰島素敏感性出現顯著性的改善 (Elkind-Hirsch *et al.*, 1993; Moghetti *et al.*, 1996)。然而，在我們的分組中，高雄性荷爾蒙和新陳代謝異常的正相關並沒有完全存在。儘管具有最高新陳代謝症候群盛行率的第 4 組，確實具有最高的游離雄性荷爾蒙指標 (Free androgen index, FAI)，但具有較低游離雄性荷爾蒙指標的另一群（第 2 組）也呈現出上升的新陳代謝症候群盛行率，由此可知，多囊性卵巢症候群的新陳代謝異常風險不能只透過雄性荷爾蒙之活性來進行預測。新陳代謝症候群盛行率較高

doi:10.6342/NTU202000313

的第 2 組和第 4 組，其共同的內分泌特徵是血清 LH 濃度顯著降低。此外，在我們研究分群的第 1 組中，新陳代謝症候群的盛行率僅為 7%，顯著低於我們研究中的平均盛行率（19%），並且也低於先前其他多囊性卵巢症候群研究中報告的盛行率（7.1%~41.6%的多囊性卵巢症候群患者）(Goverde *et al.*, 2009)。在一個中國的流行病學研究中，其新陳代謝症候群在一般非多囊性卵巢症候群女性的盛行率與我們研究中的第 1 組相似（5.2%[182/3470]）(Li *et al.*, 2010)，顯示出第 1 組的病患雖然診斷上符合多囊性卵巢症候群，但是其新陳代謝表徵是相對較健康的，與同齡未罹病女性無顯著差異，這些女性可能不一定需要遵循現行多囊性卵巢症候群治療導引那般強調規律性的新陳代謝檢查，而在我們研究中，近一半的研究病患（204/460）被分類到第 1 組，減少對這群病患的新陳代謝篩檢，不僅可節省不必要的醫療花費，降低健保支出，更可以讓病患放心，減少其對未來健康的焦慮不安。我們的研究還發現高 LH 濃度（超過 15 mIU/ml）是代謝健康的第 1 組的最相關指標，其中 95%的高 LH 濃度患者分佈於第 1 組（圖四），因此倘若病患的血清 LH 較高，亦可作為其新陳代謝表徵較為健康的預測因子。

腦下垂體促性腺激素的分泌改變，包括 LH 血清濃度上升、LH/FSH 比率增加、LH 脈衝頻率增加、以及 LH 對促性腺激素釋放激素的反應增加，都被認為是多囊性卵巢症候群的特徵。雖然過去曾有學者提議，將腦下垂體促性腺激素的分泌改變視為多囊性卵巢症候群發病機轉的一部分(Ehrmann, 2005)，但訂定鹿特丹診斷標準的共識小組，乃未建議將血清 LH 濃度絕對值或 LH/FSH 比率納入多囊性卵巢症候群的診斷標準。主要是由於血清 LH 濃度改變，可能會受到許多因素的影響，例如：排卵前的 LH surge、BMI、甚至所使用的檢驗試劑 (Rotterdam ESHRE / ASRM-Sponsored PCOS Consensus Workshop Group, 2004)，都會導致 LH 數值改變。然而，一些日本的研究顯示，患有多囊性卵巢症候群的婦女中，LH 濃度異常上升的表徵比雄性荷爾蒙上升更加普遍和顯著。因此，內分泌異常在多囊性卵巢症候群表現很可能具有種族或地理差異。事實上，自 2006 年以來，日本婦產科學會建議將高 LH 濃度或高 LH/FSH 比率納入日本多囊性卵巢症候群診斷標準的一部分（Kubota, 2013）。

雖然 LH 分泌異常在多囊性卵巢症候群的病理生理學中十分重要，但高血

doi:10.6342/NTU202000313

清 LH 濃度對於代謝的影響仍不甚清楚。先前有研究指出，當病患接受胰島素輸注後期基礎 LH 濃度下降，且 LH 對 GnRH 反應也會減少，顯示出了 LH 和胰島素濃度之間的負相關性 (Taylor *et al.*, 1997)。然而，這一發現在另一項研究中未得到證實(Tosi *et al.*, 2012)。另一個研究則是提出了 BMI 和 LH 濃度之間呈現負相關性 (Pagán *et al.*, 2006; Lawson *et al.*, 2008) 。然而，在我們的研究中，排除了 BMI 的干擾因子後，LH 與新陳代謝症候群盛行率之間的負相關性仍然達到統計學顯著性，因此還需要更多的研究來釐清 LH 濃度如何影響多囊性卵巢症候群患者的新陳代謝症狀。

此外，應該應用哪一個標準來診斷多囊性卵巢症候群仍是一個持續不斷的爭論。目前文獻中最常用來診斷多囊性卵巢症候群的標準除了本研究所使用的鹿特丹標準，還包括較為嚴格的 AE-PCOS 標準和更嚴格的 NIH 標準。過去就曾有一些研究指出，鹿特丹診斷標準的非高雄性荷爾蒙子群 (僅符合慢性無排卵和超音波多囊性卵巢表徵，沒有高雄性荷爾蒙症) 的新陳代謝較為良好 (Wild *et al.*, 2010)，將這些婦女與其他多囊性卵巢症候群子群之患者歸在一起追蹤治療，可能會不必要地增加其焦慮和健康支出。我們的研究則是顯示，這三個常用診斷標準之間的新陳代謝症候群盛行率沒有顯著差異。此外，假如我們研究所使用的是更嚴格的 NIH 和 AE-PCOS 診斷標準，會有部分患者不符合多囊性卵巢症候群標準，而這些未被診斷成多囊性卵巢症候群的病患仍然有 19%（17/89）和 12%（11/89）的比例罹患新陳代謝症候群。因此，採用更嚴格的 NIH 或者 AE-PCOS 診斷標準到底是否對病患更加有利，仍存在爭議。

我們研究的一個主要限制是缺乏非多囊性卵巢症候群女性作為正常對照組，來驗證分群模式的臨床診斷效用，並驗證廣義相關圖分析所顯示的相關內分泌特徵在非多囊性卵巢症候群女性是否仍存在關聯性。另一個限制是我們的結果之可類推性，很可能會受到不同種族或不同地域的影響。種族差異對多囊性卵巢症候群表徵的差異性在文獻中經常被提及(Zhao *et al*,. 2013)。Legro 等人（2006）指出，與美國高加索裔患者相比，亞洲裔多囊性卵巢症候群患者的多囊性卵巢症候群表徵較輕，包括：高雄性荷爾蒙症程度較低，卵巢體積較小，多囊情形較輕微。不過在他們的研究中，參與研究期間的亞洲患者（只有 2.7%，17/626 例）的

doi:10.6342/NTU202000313

病例數量相對較少，因此也可能導致他們的結果有所偏差。另一項比較研究報告了一個相反的結果，認為中國人的多囊性卵巢症候群患者，其高雄性荷爾蒙症的發生率高於荷蘭白人女性的多囊性卵巢症候群患者，然而這兩個族群中所使用的荷爾蒙測定方法實際上是不同的(Guo *et al.*, 2012)。此外，過去研究報告亦指出，患有多囊性卵巢症候群的亞洲女性比其他種族的多囊性卵巢症候群患者更瘦(Legro *et al.*, 2006; Welt *et al.*, 2006)，並且需使用較為寬鬆的標準來定義肥胖（亞洲人 BMI≥25; 在非亞洲人則是 BMI≥30）和亞洲女性的新陳代謝症候群（亞洲人腰圍≥80cm; 在非亞洲人腰圍≥88cm）(Tan *et al.*, 2004)。然而，種族差異究竟多大程度地影響多囊性卵巢症候群的臨床表徵和新陳代謝預後，而這些診斷標準的調整能否平衡種族差異的影響，仍然是未知數。

總結來說，在第一部分的研究中，我們我們首先運用關聯性分析，找出與多囊性卵巢症候群新陳代謝異常較為相關的四個內分泌指標 (FSH, LH, FAI, DHEA-S)，接著依照這四個內分泌指標表現值相近度，將多囊性卵巢症候群患者分為四個次族群，每個次族群中的個體即這四個內分泌指標表現最相近的一群病患。有趣的是，所分出的四個次族群，不僅各自具有獨特的內分泌表徵，也同時具有顯著不同的新陳代謝異常風險。這對於我們臨床上面對多囊性卵巢症候群病患的追蹤治療和預後說明有很大的幫助，當病患出現高 FAI 指標且低 LH 濃度時，可更加頻繁更密集的追蹤病患的新陳代謝指標，同時在衛教上更加強調運動、飲食等日常生活保養和注意體重控制的重要性。倘若病患出現低 FAI 指標且高 LH 濃度時，則可告知病患日後得到新陳代謝異常風險與同齡女性無異，應可降低不必要的追蹤檢測和健保花費，也可降低病患之焦慮不安。多囊性卵巢症候群是一種高異質性和高複雜度之婦女內分泌疾病，透過我們的分析成果，得以更加了解新陳代謝相關的危險因子，並可據以設計並提供更有效的篩選和治療方針。對於日後的相關研究，也提供了很好的流行病學資料。

doi:10.6342/NTU202000313

第二節 卵巢濾泡液通透性與血管生成因子之相關致病機轉

Increased platelet factor 4 and aberrant permeability of follicular fluid in PCOS. (Huang *et al.*, 2019)

我們的研究顯示，多囊性卵巢症候群患者的卵巢濾泡液會導致相鄰之內皮細胞通透性下降，且多囊性卵巢症候群患者的濾泡液中的 PF4 和 PF4 / IL-8 複合物濃度顯著上升，這在過去的文獻報告中從未被發現過。多囊性卵巢症候群患者卵巢濾泡液對於內皮細胞通透性的抑制作用是濾泡內的 PF4 分子所引起的，藉由阻斷 PF4 功能便可使得內皮細胞通透性恢復，我們的發現進一步增加了這個分子在降低內皮細胞通透性方面的直接證據，對於其與卵巢功能相關之細胞生理機轉有了更深一層的認識。

PF4，也稱為 CXC chemokine ligand 4（CXCL4），是一種 CXC 趨化因子，以其抗血管生成作用而聞名(Aidoudi and Bikfalvi, 2010)。最初認為 PF4 主要在巨核細胞 (megakaryocytes) 中合成，並在血小板被活化後釋放出來，例如血管壁損傷的情況之下會促進其釋放(Aidoudi and Bikfalvi, 2010, Eslin *et al.*, 2004) ，與肝素 (heparin) 結合並抑制其抗凝血功能，促進血液凝固以及組織修復。然而，越來越多的證據顯示，不僅是巨核細胞會合成並釋放 PF4，其他類型的細胞也同樣會表現這個蛋白，例如：平滑肌細胞，小神經膠質細胞 (microglia)，巨噬細胞 (macrophages) 或 T 細胞，這些「非血小板之 PF4」的生理功能許多尚待研究 (Kasper *et al.*, 2010)，而其功能很可能與其生成的特定組織有關 (Vandercappellen *et al.*, 2011)。除了抗血管生成的作用外，一些報告指出，PF4 在調控其他幾種細胞生理機轉中也發揮重要作用，例如：巨核細胞生成，血栓形成，免疫調節，慢性炎症和動脈粥樣硬化等等 (Kasper *et al.*, 2010; Vandercappellen *et al.*, 2011; Gonza´lez *et al.*, 2012)。由於我們的卵巢濾泡液檢體僅從第一個卵泡收集而來，在插入針頭的過程中同時吸出了這些濾泡液，因此不太可能是取卵手術過程造成之濾泡壁血管損傷而引起血小板釋放 PF4。另一種可能的解釋是，

doi:10.6342/NTU202000313

慢性低度發炎被認為在多囊性卵巢症候群的致病機轉中也可能扮演重要角色(Gonza´lez *et al.*, 2014)。在多囊性卵巢症候群患者中，胰島素阻抗和雄性荷爾蒙過多都有助於增加單核細胞的敏感性和活性，進一步活化活性氧系統（Reactive oxygen species, ROS）並產生促發炎細胞激素 (pro-inflammatory cytokines)，例如：tumor necrosis factor-α（TNF-α）和 interleukin-6 (IL-6) (Kasper *et al.*, 2011; Gonza´lez *et al.*, 2014)。而另一方面，PF-4 也已經被證實可以誘導單核細胞活化，PF-4 本身即會促使活性氧系統形成和 TNF-α 的表達(Kasper *et al.*, 2011)。因此，從慢性發炎的角度來推論，PF4 可能部分參與了多囊性卵巢症候群的致病機轉，然而以上推論仍需要進一步的研究，才能釐清卵泡內 PF4 的確切來源和其特定的生物學功能。

我們透過人類臍靜脈內皮細胞裝置進行內皮細胞通透性的研究發現，多囊性卵巢症候群患者的卵巢濾泡液會造成其相鄰內皮細胞的通透性下降。雖然這是一個細胞研究，而人體卵巢濾泡內是否具有同樣機轉仍有待進一步釐清，但可以據此推測卵巢濾泡的通透性失調可能對卵泡生成產生負面影響，甚至可能與排卵功能有關，畢竟我們安排取卵手術並取得卵巢濾泡液的時間是在誘導排卵後的 33 至 35 小時，相當靠近實際排出卵子的時間點。卵泡的生長是一個複雜的動態過程，其中包含了許多生理調控機轉，例如：卵子細胞增大，顆粒細胞複製增生，濾泡液累積和中央濾泡腔室擴張 (Rodgers *et al.*, 2010)。過去的文獻指出，生殖器官的生長和分化會受到纖維母細胞生長因子 （fibroblast growth factor, FGF）家族的調節 (Price *et al.*, 2016)。在一些研究顯示，纖維母細胞生長因子家族中被研究最多的成員 FGF-2，可促進卵巢顆粒細胞增殖，減少其凋亡並促進類固醇荷爾蒙生成 (Lavranos *et al.*, 1994; Vernon *et al.*, 1994)。PF4 可以直接結合並且抑制 FGF-2，接著進一步抑制內皮細胞的增殖和遷移(Wang *et al.*, 2013)。因此，PF4 可能通過與 FGF-2 拮抗性結合並抑制顆粒細胞增殖，進而損害濾泡的生長。FGF-2 的抑制也可能促進顆粒細胞的類固醇荷爾蒙生成，即在濾泡刺激素的刺激下雌激素和黃體素的產生較多，這也是多囊性卵巢症候群的曾被提出的病理生理特徵之一 (Franks *et al.*, 2003)。因此，我們的研究結果提供了 PF4 與多囊性卵巢症候群異常卵泡生長和類固醇荷爾蒙生成之間的可能相關

doi:10.6342/NTU202000313

性。

我們透過免疫組織化學染色結果發現，PF4 抑制通透性的作用可能是藉由促進內皮細胞間的粘附所造成的。過去 Abu 等人透過糖尿病模式大鼠的研究發現 (2015)，血小板因子 4 變異體（platelet factor 4 variant, PF4var）顯著增加了視網膜細胞中黏著小帶蛋白 (adherens junction protein)、血管內皮型鈣離子依賴性黏著分子 (vascular endothelial cadherin, VE-cadherin) 和緊密連結蛋白 (tight junction protein) 的表現，並進一步降低了視網膜血管通透性，PF4var 和 PF4 在蛋白鍊羧基端有三個氨基酸與 PF4 不同，但被認為具有相似的生物學功能，例如同樣具有抗血管生成的功能，只是 PF4var 的功能活性更高(Struyf *et al.*, 2004)，因此很可能 PF4 也跟 PF4var 一樣具有促進黏附蛋白表現並抑制細胞通透性的效果。在我們的研究中，還顯示了 PF4 可以減少細胞間隙，並增強內皮細胞的粘附性，這很可能進一步抑制卵巢濾泡中內皮細胞的通透性和卵巢濾泡液的形成，而影響了濾泡生成的關鍵步驟。

有趣的是，我們的研究還發現濾泡液中的血管生成抑制性分子 PF4，會與 IL-8 形成蛋白質複合物。IL-8 是一種強大的血管生成因子，已被證實在血管生成的多個步驟都有促進的效果，例如：內皮細胞遷移，穿透和細胞增殖等等 (Chen *et al.*, 2008)，而過去的研究還顯示 IL-8 在卵巢過度刺激症候群患者的血管內皮通透性上升中扮演著關鍵角色 (Chen *et al.*, 2010)。與正常排卵的對照組相比，多囊性卵巢症候群患者的卵巢濾泡液中 PF4 / IL-8 蛋白複合物的表現量明顯上升，因此，PF4 的抗通透性作用可能來自與 IL-8 的結合，從而抑制了 IL-8 下游對內皮細胞通透性的作用。過去 Dudek 等人 (2003) 的研究指出，PF4 能以高親和力結合 IL-8，並阻斷 CD34 +人類造血母細胞中 IL-8 媒介的訊息傳導途徑，而 IL-8 和 VEGF 與內皮細胞上 VEGF 受體的結合均會受到 PF4 的抑制，進而導致 VEGF 所誘導的內皮細胞增生受到抑制 (Gengrinovitch *et al.*, 1995)。而 PF4 對其他血管生成蛋白的抑制作用也可能在卵巢濾泡液中發生，並導致濾泡內通透性失調和功能障礙，甚至可能造成周圍顆粒細胞的生長失調。

我們的研究與先前研究相比 (Agrawal *et al.*, 2002; Artini *et al.*, 2009) 有個不

doi:10.6342/NTU202000313

同的地方，過去的研究提出多囊性卵巢症候群患者濾泡液的 VEGF 濃度顯著高於對照組，然而在我們研究中，多囊性卵巢症候群和對照組之間的濾泡液的 VEGF 和其他多數與血管生成相關的蛋白質濃度均沒有顯著差異，只有 PF4 在多囊性卵巢症候群組中的濃度較高。一種可能的解釋是對照組的收案標準不同，我們僅招募對卵巢刺激反應良好的正常排卵患者作為我們的對照組。我們訂定此收案標準是因為我們想排除卵巢功能與卵巢血管生成之間的交互作用影響。因此在我們的研究中，多囊性卵巢症候群組和對照組之間的基礎 FSH 濃度，取得的卵子數量，成熟的卵子數量和胚胎受精率都沒有顯著差異。然而，在 Agrawal 等人(2002)的研究中，多囊性卵巢症候群患者平均取得的卵子數量是對照組的兩倍（26.9±4.5 v.s. 13.2±2.3，p = 0.001）。而在 Artini 等人的研究(2009)中，儘管取得的卵子數量沒有差異，但多囊性卵巢症候群組取卵前的卵泡數量顯著高於對照組（37±8 vs. 14±5，p <0.001）。這些研究可能只是顯示了卵巢濾泡內 VEGF 濃度與卵巢功能之間的相關性，而不一定是顯示 VEGF 與多囊性卵巢症候群疾病之間的相關性，因為其實驗組和對照組之間的卵巢功能是顯著不同的，而我們的研究召募了卵巢功能相同的實驗組和對照組，兩組的差異僅在於是否符合多囊性卵巢症候群的診斷，因此應能更精準地反應出血管生成蛋白表現和多囊性卵巢症候群致病機轉的相關聯性。

然而我們的研究仍存在一些限制。首先，我們的研究是生物體外研究，使用人類臍靜脈內皮細胞裝置來模擬測試內皮細胞的通透性，這與實際人體內卵巢濾泡的環境還是不同，人體卵巢濾泡內的內皮細胞通透性可能受到更複雜的機制調控。此外，基於目前的實驗結果，還無法完全證實多囊性卵巢症候群中濾泡內 PF4 的異常表現與濾泡生成之間的因果關係，還需要進一步的體內研究來釐清。其次，濾泡生成過程長達近三個月，可分為數個不同階段，血管生成相關蛋白的濃度和濾泡內通透性很可能是一個動態變化，但在人體研究中，透過試管嬰兒取卵手術所能取得的濾泡液時間僅限於排卵前期 (注射誘導排卵針劑後的 33 到 35 小時之間) ，因此我們的研究無法反應出這些血管生成相關蛋白在不同濾泡生成階段的動態改變。第三，不同病患之間的排卵刺激藥物使用量和藥物種類並不完全相同，而這可能會影響卵巢濾泡內的蛋白表現。不過，

doi:10.6342/NTU202000313

我們進行了敏感性測試以評估排卵刺激過程使用不同藥物的可能效果，我們的研究中幾乎每位患者都使用 rFSH 進行排卵刺激，而多囊性卵巢症候群組中只有一位患者使用 hMG。如果我們排除使用 hMG 的患者，則排除前後 FF 中 PF4 濃度的平均值（51.6 ng / ml v.s. 51.7 ng / ml，排除前和排除後）和濾泡液所誘導之相對內皮細胞通透性（46.3% v.s. 46.8%，排除前和排除後）沒有顯著差異。另外，實驗組和對照組兩組之間，不同誘發排卵藥物的比例也沒有統計學上的顯著差異（Fisher 精確檢驗的 p = 0.408），而兩組的促性腺激素平均總劑量以及在誘發排卵當日的血清雌激素的平均濃度也都沒有顯著差異。因此，排卵刺激藥物的種類和劑量差異應不會對我們的研究產生重大影響。過去 Cerrillo 等人（2011）的研究指出，當使用 hCG 作為誘發排卵藥物時，濾泡內的 VEGF 的濃度顯著增加，並進而為 OHSS 的風險提供了可能的解釋，但是他們的研究並沒有檢查 PF4 的濃度，PF4 表現與不同誘發排卵藥物之間的相關性仍待進一步研究釐清。

總而言之，我們的研究提供了血管抑制蛋白 PF4 對卵巢病理生理機轉有所相關的初步證據。在控制了患者的年齡，BMI 和卵巢功能後，多囊性卵巢症候群與對照組相比，卵巢濾泡液中 PF4 的濃度和其所調控之內皮細胞通透性存在顯著差異，而這個差異性亦可能導致卵巢濾泡液的生成失調和濾泡生長異常。進一步的實驗顯示了在卵巢濾泡液中，PF4 與另一種血管生成蛋白 IL-8 之間的結合作用，並顯示 PF4 的調節機制可能是透過與 IL-8 的拮抗性結合效果。這些結果不僅提供了多囊性卵巢症候群致病機轉的另一種新解釋，而且也讓我們對於卵巢濾泡液通透性、濾泡液生成和濾泡生長的正常卵巢生理機制有更進一步的了解。然而還需要更多的研究以釐清 PF4 表現增加的源頭為何，其所調控的細胞種類為何，以及其下游的詳細訊息傳導途徑。在累積了更多研究證據之後，調節卵巢滲透性或者調節血管生成過程也可能成為日後多囊性卵巢症候群的另一種新治療方法。

doi:10.6342/NTU202000313

第三節 超基因調控之相關致病機轉研究

第三節之第一部 多囊性卵巢症候群之 DNA 甲基化研究

Hyperactive CREB signaling pathway involved in the pathogenesis of polycystic ovarian syndrome revealed by patient-specific induced pluripotent stem cell modeling. (Huang *et al.*, 2019)

我們這部份的研究應用了非病毒載體重編程方法，成功地從成人皮膚纖維母細胞衍生出具有病患專一性且具有多囊性卵巢症候群疾病特異性的誘導性多功能幹細胞，這些具有多囊性卵巢症候群特異性的誘導性多功能幹細胞能夠成功表現出多能性相關基因，並在體外細胞實驗和小鼠活體實驗都具有分化成三個胚層的能力。成功分化出多囊性卵巢症候群特異性之誘導性多功能幹細胞後，我們添加與中胚層分化相關以及卵巢顆粒細胞成長相關的重要生長因子混合物，將誘導性多功能幹細胞成功分化為卵巢顆粒細胞，這些誘導性多功能幹細胞所衍生分化出的顆粒細胞能夠成功地表現與卵巢顆粒細胞相關之基因，也成功產生芳香酶活性將雄性荷爾蒙轉換為雌激素，從而證明了我們這一系列研究方法的可靠性。

具多囊性卵巢症候群特異性之誘導性多功能幹細胞可以做為良好的疾病模型，可以分化成各種與多囊性卵巢症候群相關的組織和細胞，改善原本難以達成的組織可及性，例如過去許多學者根據血清所測得下視丘與腦下垂體荷爾蒙的變化，推測多囊性卵巢症候群的致病機轉很可能與這些神經細胞的調控異常有關，然而不可能有任何研究能夠取得多囊性卵巢症候群病患的腦部組織進行分析，此時誘導性多功能幹細胞就是最好的研究工具。再加上目前還沒有足夠好的模式生物能夠代表這個疾病，大多數研究是運用外加注射雄性荷爾蒙的小鼠模型，但仍有許多表徵與多囊性卵巢症候群病患有所不同。我們成功建立的多囊性卵巢症候群特異性誘導性多功能幹細胞，可以更貼近多囊性卵巢症候群在病患細胞上的表現，同時可依據其病患專一性，進一步作為藥物篩選的平台，甚至根據不同的患

doi:10.6342/NTU202000313

者臨床表徵，找出不同的潛在致病機轉，對於基礎治療和臨床研究都有極大的應用價值。而且在誘導性多功能幹細胞的建立過程中，我們還能將細胞引導回到近似於胚胎階段的原始初分化時期，這也對於複雜疾病的早期發展起源 (early developmental origin) ，提供了進一步研究的寶貴途徑。

在重編程和再分化後，誘導性多功能幹細胞衍生的卵巢顆粒細胞保留了許多與成熟卵巢顆粒細胞相關的特徵和功能。我們的研究結果顯示，比較多囊性卵巢症候群和對照組之間的誘導性多功能幹細胞，其多能性和分化潛能沒有明顯差異，雖然病例數不足以進行統計學之顯著性比較，但似乎有一種趨勢顯示來自多囊性卵巢症候群患者之誘導性多功能幹細胞所衍生的卵巢顆粒細胞，相較於對照組，許多與顆粒細胞相關之特異性基因表現是較高的，包括：*AMH*，*AMHR2* 和 *FSHR*。過去的文獻曾經指出，在接受排卵刺激的多囊性卵巢症候群患者，透過取卵手術取得的濾泡液中所收集之顆粒細胞，其 *AMH* 和 *AMHR2* 的基因表現顯著增加，並與濾泡生長異常有關 (Pellatt *et al.*, 2007; Pierre *et al.*, 2017)。此外另一篇文獻還報告了在卵巢顆粒細胞中，多囊性卵巢症候群病患的 *FSHR* 表現顯著增加 (Catteau-Jonard *et al.*, 2008)，此一發現也合理解釋了在多囊性卵巢症候群之顆粒細胞對 FSH 刺激的過度反應性（Coffler *et al.*, 2003）。此外還有一個有趣的現象是，來自多囊性卵巢症候群患者的誘導性多功能幹細胞所衍生之顆粒細胞中，幾個顆粒細胞相關基因（*AMHR2*、*LHR* 和 *CYP19A1*）的表現量，從分化第 6 天到第 12 天有逐漸增加的趨勢（圖十八），而這些基因的表現量也似乎在多囊性卵巢症候群組病患的成人顆粒細胞中較高，這顯示出在多囊性卵巢症候群患者的早期分化顆粒細胞和成人顆粒細胞中，某些顆粒細胞相關基因都具有一致性的較高表現，這也支持了多囊性卵巢症候群早期發育起源的理論，即相關的致病基因表現異常，很可能是從細胞剛開始分化的胚胎時間或者胎兒時期就存在著，並且可能不僅僅是繼發於環境或行為上的改變。不過，由於產生誘導性多功能幹細胞細胞株的困難度極高，我們的病例數量有限而缺乏統計學上之顯著性，因此這方面的發現我們無法得出確切的結論。如何更加穩定的產生病患專一性誘導性多功能幹細胞細胞株，並且提高後續的分化效率和純度以實現更廣泛的臨床應用，仍然是進一步巨大的挑戰。

doi:10.6342/NTU202000313

過去的研究發現，在多囊性卵巢症候群患者的姐妹和同卵雙胞胎身上有高度的共同發病率，顯示此疾病的估計遺傳率可能高達 60％以上(Vink *et al.*, 2006)。過去也有不少使用家族聚集(familial clustering)或病例對照設計的基因關聯性研究，試圖想要找尋多囊性卵巢症候群患者的潛在致病基因，但大多沒有得到顯著的發現。而過去數個全基因組關聯研究（genome-wide association studies ，GWAS）使用高通量遺傳篩選方法，發現了可能與多囊性卵巢症候群相關的幾種遺傳變異(Shi *et al.*, 2012; Day *et al.*, 2015; Hayes *et al.*, 2015)，也僅能解釋非常輕微的遺傳風險，無法解釋多囊性卵巢症候群那麼高的估計遺傳率。超基因調控 (epigenetics) ，又被稱為表觀遺傳，定義為在 DNA 序列不改變的情況下，可遺傳的基因表現變化。超基因調控已被許多研究證實參與相當多複雜性疾病的致病機轉 (Kirchner *et al.*, 2013)，如：癌症發展，神經發育障礙 (Portela *et al.*, 2010)，自體免疫疾病，和新陳代謝疾病包括第 2 型糖尿病和肥胖症等等 (Drong *et al.*, 2012; Kirchner *et al.*, 2013)。新陳代謝疾病有許多與超基因調控相關的特徵，與多囊性卵巢症候群的疾病性質是一致的，包括了 DNA 變異無法完全解釋的高遺傳性，可改變性 (flexibility) 和動態變化性 (dynamic)，且同樣可能受到子宮內環境以及出生後早期發育環境變化的影響 (Drong *et al.*, 2012; Kirchner *et al.*, 2013; Li *et al.*, 2016)。過去曾經有數個針對多囊性卵巢症候群患者不同組織的全基因體 DNA 甲基化研究，包括：周邊血液 (Xu *et al.*, 2010; Shen *et al.*, 2013)，脂肪組織 (Kokosar *et al.*, 2016) 和卵巢組織 (Yu *et al.*, 2015)，結果顯示多囊性卵巢症候群患者的這些組織可能出現 DNA 甲基化表現異常。由於 DNA 甲基化表現具有細胞和組織特異性，上述這些研究結果彼此不一致，且難以直接進行比較。此外，不同研究使用了不同的 DNA 甲基化分析方法，且其差異性甲基化表現區域 (DMR) 的定義在各研究之間也有所不同，因此很難證明在多囊性卵巢症候群這個複雜疾病中，其基因和環境相互作用中所涉及的超基因調控變化究竟為何。

我們同時對成人顆粒細胞和誘導性多功能幹細胞所衍生的顆粒細胞進行了全基因體 DNA 甲基化分析，結合了成熟疾病細胞和分化初期細胞的分析結果以釐清致病機轉。在我們的實驗中，使用了新一代高密度 DNA 甲基化晶片-Illumina 850K Infinium MethylationEPIC 晶片進行檢測，其偵測範圍涵蓋了先前 Illumina

doi:10.6342/NTU202000313

450K 甲基化陣列中未包括的另外 413,745 個新 CpG 位點(Moran *et al.*, 2016)，是目前全基因體 DNA 甲基化研究在考量性價比之下最佳的分析工具之一。誘導性多功能幹細胞所衍生的顆粒細胞的出現的相關病徵，可為症狀出現之前的早期細胞病變提供一些線索，過去的文獻也曾提到這可能是多因素遺傳性疾病的致病關鍵(Devine *et al.*, 2017)，而成人卵巢顆粒細胞的病徵則可以代表疾病發作之後的較晚期病變。有趣的是，透過成人顆粒細胞和誘導性多功能幹細胞衍生之顆粒細胞的 DNA 甲基化分析，我們發現在多囊性卵巢症候群的兩種顆粒細胞都同樣表現了過度活化的 CREB 訊息傳遞途徑，進一步以西方墨點法和即時聚合酶連鎖反應驗證，同樣證實了多囊性卵巢症候群在成人顆粒細胞和誘導性多功能幹細胞衍生之顆粒細胞均出現較高表現的 CBP 蛋白和 mRNA。

過去已經有大量文獻證實，CREB 及其共同活化因子 (coactivator) 的家族成員（例如 CBP），在調節能量恆定效應（如葡萄糖和脂質代謝）中扮演了關鍵角色 (Altarejos *et al.*, 2011)。然而，從未有文獻提及 CREB 訊息傳導途徑的失調與多囊性卵巢症候群有何相關。在過去一個小鼠研究中發現，CREB 蛋白的過度磷酸化活化，會進一步導致濾泡鞘間質細胞 (theca-interstitial cell) 增生，並表現較高濃度的血清睾固酮以及嚴重的卵巢囊腫 (Restuccia *et al.*, 2012)。此外，過去文獻也曾經報告過，生殖荷爾蒙的許多訊號傳導途徑會受到 CREB 的密切調控，包括濾泡鞘間質細胞受到 LH / hCG 刺激後所產生膽固醇攝取和雄性荷爾蒙生成的作用，可以通過抑制 CREB 活性來達到抑制的效果 (Towns *et al.*, 2005; Restuccia *et al.*, 2012)。與野生型對照組相比，CBP 基因剔除小鼠會表現出動情週期中斷、對 GnRH 的反應性降低和生育能力受損等表徵 (Miller *et al.*, 2012)。而 CREB 路徑也是卵巢顆粒細胞之芳香酶酵素作用的關鍵訊息傳導途徑 (Lai *et al.*, 2014)，有趣的是，過去曾有報告指出 metformin 對 FSH 誘發之 CREB 活化和芳香酶酵素均具有抑制的作用 (Rice *et al.*, 2013)，而這也可以做為 metformin 對於多囊性卵巢症候群具有臨床療效的合理機轉解釋之一。綜合上述數個文獻的研究結果，CREB 途徑的慢性活化，很可能與多囊性卵巢症候群的多種致病機制相關，包括：高血糖、胰島素阻抗、代償性高胰島素血症、脂肪組織炎症、LH 功能和雄性荷爾蒙過高等等。由於多囊性卵巢症候群具有高度異質性，且廣泛涵蓋了各種生殖內分泌和新陳代謝方

doi:10.6342/NTU202000313

面的臨床表徵，因此很可能其致病機轉是發生在同時涉及荷爾蒙調控和能量調節的共同上游訊息傳導途徑中。我們的結果初步顯示，DNA 甲基化的調控異常可能參與了 CREB 傳導途徑的過度活化，並且可能在多囊性卵巢症候群病徵的早期和晚期發展階段期間都存在，這些結果也都還需要進行更多的研究來予以證實。

過去只有一個研究針對了多囊性卵巢症候群和對照組受試者的成人卵巢顆粒細胞，進行了全基因體 DNA 甲基化表現的比較分析 (Xu *et al.*, 2016)，然而，CREB 傳導途徑未出現在該研究的前十項顯著的調控途徑中。分析其原因之一可能是由於該研究在排卵刺激過程使用的是 GnRH 長療程，與我們研究使用的 GnRH 拮抗劑療程相比，會導致顆粒細胞中的 protein kinase C 活性和 aromatase 活性顯著下降 (Khalaf *et al.*, 2010)。而在我們研究中，不僅是多囊性卵巢症候群成人顆粒細胞中出現 CREB 路徑調控異常，誘導性多功能幹細胞所衍生之顆粒細胞的全基因體 DNA 甲基化分析也同樣出現了 CREB 路徑調控異常，這可以作為一個良好的疾病模型，以進一步探索具有患者特異性之顆粒細胞的功能，同時避免所研究的顆粒細胞受到於卵巢刺激藥物的影響。此外在我們研究中，多囊性卵巢症候群和對照組受試者的年齡和體重都沒有顯著差異，故也排除了這些因子對 DNA 甲基化表現的干擾作用。

小結

總之，我們的研究成功地建立了具病患特異性和多囊性卵巢症候群特異性的誘導性多功能幹細胞，並且成功將之重新分化為卵巢顆粒細胞，這可以作為評估多囊性卵巢症候群在早期細胞分化和發育狀態之相關病徵之生物模型。我們同時分析成人顆粒細胞和誘導性多功能幹細胞衍生之顆粒細胞中的 DNA 甲基化表現，發現了在多囊性卵巢症候群和對照組之間，有數個差異性甲基化基因的相關調控路徑在兩種顆粒細胞都有出現，而 CREB 訊息傳導途徑的過度活化可能與多囊性卵巢症候群的致病機轉相關，已知 CREB 及其 coactivator 是荷爾蒙和新陳代謝相關路徑的重要調控因子，而 CREB 信號傳導途徑的異常可為多囊性卵巢症候群複雜的荷爾蒙和新陳代謝異常提供了嶄新而合理的解釋，以上結果仍需要在更進一步的研究中進行驗證。這些研究成果可以對多囊性卵巢症候群的早期發育起源、

doi:10.6342/NTU202000313

家族群聚性質、高度遺傳性和易與環境相互作用等特性提供了機制上的說明，也有機會成為將來新的治療標的。

doi:10.6342/NTU202000313

第三節之第二部 多囊性卵巢症候群之微小核醣核酸研究

我們這個部分的研究從文獻中選擇了 14 種可能與多囊性卵巢症候群致病機轉相關的標的微小核醣核酸，所選擇的相關調控機轉包括：葡萄糖代謝，胰島素阻抗，糖尿病，卵巢或腦下垂體功能。第一個階段的標的微小核醣核酸檢測中，我們發現多囊性卵巢症候群患者與非多囊性卵巢症候群受試者的血液游離微小核醣核酸表現模式確實有顯著不同。這些微小核醣核酸在基因本體分析 (GO analysis) 中顯示與葡萄糖代謝和糖尿病前期狀態有關。這些微小核醣核酸可以用作多囊性卵巢症候群的診斷標記，甚至可以用作多囊性卵巢症候群代謝異常的預測標記。此外，metformin 針對排卵和月經週期治療的效果，在有效和無效兩組之間的微小核醣核酸表現也有顯著的差異。第二個階段則是成功的建立了針對多囊性卵巢症候群診斷鑑別的預測模型，透過 miR-93、miR-132、miR-222、miR-27a、miR-125b、miR-212 這六個微小核醣核酸的表現值，對於受試者是否符合多囊性卵巢症候群臨床診斷有極佳的預測性，此外我們針對 metformin 療效的預測模型，也成功在另一個獨立病患族群中驗證其效果，藉由臨床指標和四個微小核醣核酸的血液表現值，可以幫忙預測患者是否可以在接受 metformin 治療後，出現排卵功能及月經週期上的改善，對於臨床治療的療效預測和藥物選擇有顯著幫忙。

在多囊性卵巢症候群患者的周邊血液中表現量顯著較高的微小核醣核酸包括 miR-93, miR-132, miR-221, miR-223, miR-27a, miR-212，而表現量顯著較低的為 miR-222 和 miR-320a，以上之顯著標準為 P 值小於 0.05，若以多重比較修正 P 值，採取較嚴格的修正方式為 P 值除以變項數目，則修正後的 P 值為 0.0035，在兩組之間表現差異達到統計學顯著的微小核醣核酸有 miR-93，miR-132 和 miR-27a。miR-93 在過去已有數篇與多囊性卵巢症候群相關的研究，包括其在多囊性卵巢症候群病患不同器官組織的表現。Wu 等人(2014)報告了多囊性卵巢症候群病患的脂肪細胞表現顯著較多的 miR-93，而 miR-93 表現增加會抑制 glucose transporter isoform 4 (*GLUT4*) 的基因表現，並進而抑制了血糖代謝和胰島素敏感性。而在卵巢組織切片的研究中，則發現多囊性卵巢症候群病患的顆

doi:10.6342/NTU202000313

粒細胞會表現顯著較高量的 miR-93，miR-93 會透過抑制 *CDKN1A* 基因去促進顆粒細胞增生和細胞週期演進，而胰島素也會促進 miR-93 在顆粒細胞的表現 (Jiang *et al.*, 2015)，可見 miR-93 在胰島素阻抗和卵巢顆粒細胞的功能均扮演重要角色。而另一個英國的研究也嘗試以血液 miR-93 的表現量來鑑別患者是否符合多囊性卵巢症候群之診斷 (Sathyapalan *et al.*, 2015)，發現其存活曲線下的面積為 0.72，與我們研究結果所得到的 0.74 十分接近，顯見其在多囊性卵巢症候群患者的血液表現量與對照組顯著不同，在不同國家及族群的研究都有一致的結果，更說明了 miR-93 與此疾病之重要相關。而另一個有趣的是，在我們預測 metformin 療效的模型中，miR-93 也具有顯著的鑑別能力，在 metformin 治療可以改善排卵的多囊性卵巢症候群病患中，miR-93 的血液濃度顯著較高，雖然 miR-93 表現在 metformin 治療多囊性卵巢症候群的確切因果關係為何仍不明，但其顯著的差異性表現和過去多項研究的一致性結果，均支持著 miR-93 與多囊性卵巢症候群致病機轉顯著相關的假說，並值得進一步研究以其作為診斷輔助及療效預測，甚至將來作為治療標的的可能性。

過去在小鼠腦下垂體分泌促性腺激素的細胞株實驗中，發現給予 GnRH 刺激後，miR-132 的分泌顯著增加 (Yuen *et al.*, 2009)。而進一步大鼠的活體實驗亦顯示，剔除 miR-132 的基因表現後，GnRH 刺激產生的 FSH 濃度顯著下降 (Lannes *et al.*, 2015)，顯示出 miR-132 在 FSH 荷爾蒙的分泌調控上扮演重要角色，然而過去並沒有相關文獻研究其分泌過高與多囊性卵巢症候群致病機轉的相關性，仍待後續進一步研究釐清。此外，在胰島素和血糖代謝方面，miR-132 也扮演著重要的調控角色，在數個大鼠實驗中，無論是高血糖狀態、糖尿病前期、或者是糖尿病疾病狀態的大鼠，其 miR-132 在胰臟 β 細胞的分泌均顯著上升，並與血糖誘發之胰島素分泌有關(Malm *et al.*, 2016)，而血糖代謝、胰島素阻抗以及高胰島素血症也都是多囊性卵巢症候群關鍵病理機轉的一部分，為 miRNA-132 的差異性表現提供了合理的解釋。

miR-27a 在過去曾經被報告與卵巢類固醇荷爾蒙的生成有關 (Sirotkin *et al.*, 2009)，進一步的小鼠活體實驗和小鼠體外卵巢顆粒細胞實驗則顯示，miR-27a 過度表現會促使卵巢顆粒細胞凋亡並導致雌激素的分泌受到抑制，此外雄性荷

doi:10.6342/NTU202000313

爾蒙亦會促進 miR-27a 的表現 (Wang *et al.*, 2017)。而在多囊性卵巢症候群病患的卵巢顆粒細胞研究中，則發現多囊性卵巢症候群患者的 miR-27a 表現量在整個卵巢或顆粒細胞中均顯著上升 (Wang *et al.*, 2018)，與我們在多囊性卵巢症候群患者血液中觀察到顯著表現增加的情形是一致的。

除了比較多囊性卵巢症候群和對照組之間的微小核醣核酸表現，我們也比較了 metformin 治療排卵有效和無效組之間的微小核醣核酸表現模式。metformin 是一種胰島素增敏劑，經常被使用在多囊性卵巢症候群的治療以改善胰島素抵抗之徵狀。去年，台大陳美州教授研究團隊在《Journal of Clinical Endocrinology and Metabolism》期刊上發表了一篇研究，顯示 metformin 可以有效改善排卵和月經週期，無論病患是否罹患胰島素阻抗都有效 (Yang *et al.*, 2018)，該研究對排卵和月經週期有效治療的定義為 metformin 治療後每 3 個月出現超過兩次自發月經週期，觀察期為兩年，在研究結束時，metformin 改善多囊性卵巢症候群患者排卵及月經週期的有效性約為 50%。根據先前的治療指引，metformin 僅推薦使用於同時罹患胰島素抵抗的多囊性卵巢症候群患者。然而陳醫師的研究結果卻顯示，即使是沒有罹患胰島素阻抗的多囊性卵巢症候群患者，接受 metformin 治療也有 50%的患者能夠出現自發排卵而達到臨床症狀的改善。到目前為止，還沒有有效的方法來選擇哪一部分多囊性卵巢症候群患者在接受 metformin 治療後會改善排卵和月經週期。我們的結果顯示，在 metformin 有效和無效的兩組患者之間，有三個微小核醣核酸的表現值有差異性，但若是考量多重比較下進行 P 值校正，則缺乏統計學上的顯著性。不過以 ROC 曲線分析微小核醣核酸對於 metformin 療效鑑別力的曲線下面積，則可找出 miR-93, miR-222, miR-223, miR-429 有顯著鑑別力。其中特別引起興趣的是 miR-429 這個微小核醣核酸，近年來有許多文獻報告指出 miR-429 調控可能與癌細胞的生長和凋亡相關 (Shen *et al.*, 2019)，然而與排卵功能可能相關的文獻，則是 2013 年發表在 Science 期刊的一個小鼠研究 (Hasuwa *et al.*, 2013)，顯示在小鼠的腦下垂體可以偵測到 miR-429 的大量表現，一旦剔除了 miR-429 的基因表現，小鼠的 LH 生成受到抑制，無法產生 LH surge 也無法排卵，我們無法測量 miR-429 在病患腦下垂體組織的表現，而血液游離 miR-429 的表現量在病患組和對照組並無顯著差異，究

doi:10.6342/NTU202000313

竟 miR-429 是否在特定組織或細胞參與了多囊性卵巢症候群的的致病機轉調控，仍需進一步研究。總之，這些微小核醣核酸不僅可作為治療反應的預測性生物指標，而且也可以對 metformin 究竟是透過甚麼機轉改善排卵提供進一步研究的方向。

在相關標的基因和調控生物路徑的分析中，我們分析了四個在預測模型當中出現顯著鑑別力的微小核醣核酸，包括：miR-132, miR-27a, miR-222, miR-93，有趣的是這四個微小核醣核酸參與調控的排行前幾名顯著 GO biological process 大部分都與細胞代謝有關，包括 regulation of cellular metabolic process, regulation of nitrogen compound metabolic process, regulation of macromolecule metabolic process, regulation of RNA metabolic process, regulation of nucleobase-containing compound metabolic process, 顯示出微小核醣核酸在多囊性卵巢症候群潛在的致病機轉可能是透過對於細胞代謝功能的調控改變，而出現了與相關病徵，不管是在生殖內分泌或是血糖血脂肪等新陳代謝功能上，都與此習習相關，我們也將進一步規劃動物實驗和細胞實驗，驗證這些微小核醣核酸究竟是透過何種機轉影響了多囊性卵巢症候群的致病機轉和疾病表徵，並且將進一步收集一個未經診斷篩選的女性族群，驗證我們的多囊性卵巢症候群診斷模型是否能夠在無選擇偏差的另一個族群中，確實達到鑑別多囊性卵巢症候群診斷的效果。

doi:10.6342/NTU202000313

第四節 總結

這些年來進行了一系列多囊性卵巢症候群相關之臨床與基礎研究，在臨床症狀、疾病診斷、疾病預後、致病機轉以及臨床治療上都有了新的發現。

在臨床症狀和疾病預後危險因子分析方面，重新分析了與新陳代謝症候群最相關的荷爾蒙指標，發現當病患出現高 FAI 指標且低 LH 濃度時，將會是罹患新陳代謝症候群的高風險群，這些患者可更密集地接受新陳代謝相關追蹤檢查，倘若病患出現低 FAI 指標且高 LH 濃度時，則可告知病患日後得到新陳代謝異常風險與同齡女性無異，應可降低不必要的追蹤檢測和健保花費，也可降低病患之焦慮不安。

在致病機轉方面，從濾泡液中影響內皮細胞通透性的血管生成或抑制因子著手，發現多囊性卵巢症候群病患的濾泡液表現較高量的 PF4，進而會抑制相鄰內皮細胞的通透性，而這可能對於卵巢濾泡生長有負面影響。此外在超基因調控方面也有新的發現，透過多囊性卵巢症候群特異性和病患專一性之誘導性多功能幹細胞建立並且重分化為卵巢顆粒細胞，這些誘導性多功能幹細胞可以做為良好的疾病模型，提供多囊性卵巢症候群相關研究珍貴的工具，而我們進一步針對誘導性多功能幹細胞衍生之顆粒細胞和成人顆粒細胞的全基因體 DNA 甲基化分析結果，顯示出多囊性卵巢症候群患者出現 CREB 訊息傳導路徑過度活化的情形，此發現可為多囊性卵巢症候群的致病機轉和複雜臨床表徵提供嶄新而合理的解釋。

在疾病診斷和療效預測方面，分析了血液微小核醣核酸濃度，在多囊性卵巢症候群診斷和 metformin 療效預測上，建立了效果良好的預測模型。而這個部分的研究也呼應了 DNA 甲基化研究所找出的 CREB 調控路徑的活化，我們發現多囊性卵巢症候群患者的血液游離 miR-132 表現量顯著較對照組高，而一個瑞典的研究指出 (Malm *et al.*, 2016)，在胰島的 β 細胞中，PKA 會促進 CREB 分子活化並進入細胞核中，結合在 miR-132 基因上並促進 miR-132 基因的轉錄，而 miR-132 生成後則會進一步促進胰島素的釋放，我們的研究結果顯示多囊性卵巢症候群的致病機轉很可能與此調控途徑相關，也可據此解釋多囊性卵巢症候

doi:10.6342/NTU202000313

群患者與胰島素阻抗/高胰島素血症的相關性。此外，miR-132 也會促進 TGF-β 訊息調控路徑的活化 (Ucar *et al.*, 2010)，而 TGF-β 家族分子會大量表現於卵巢，並與卵巢濾泡生長和雄性荷爾蒙的分泌有著密不可分的關係 (Raja-Khan *et al.*, 2014)，而 TGF-β 也會大量表現在細胞外基質 (extracellular matrix, ECM)，其訊息調控亦可能與患者卵巢出現纖維組織和膠原蛋白沉積以及多囊型態有關 (Raja-Khan *et al.*, 2014)。

綜合以上數個研究的成果，我們確立了多囊性卵巢症候群的臨床表徵和新陳代謝危險因子，也驗證了此複雜疾病與超基因調控的相關致病機轉，不但有助於其臨床診斷和治療，也可提供相關研究許多新的材料與方向。

doi:10.6342/NTU202000313

第五章 展望

第一節 臨床表徵分組及相關預後因子分析

Symptom patterns and phenotypic subgrouping of women with polycystic ovary syndrome: association between endocrine characteristics and metabolic aberrations. (Huang *et al.*, 2015)

雖然過去有許多研究證據指出，多囊性卵巢症候群不僅表現出內分泌調控異常，而且還與新陳代謝異常密切相關，而，在鹿特丹標準中，哪一個表型子群與新陳代謝症候群風險最相關，用那一種診斷標準最能準確找出高風險患者並給予適當的追蹤治療和衛教說明以改善其長期預後，則始終沒有定論。而我們研究所召募的 460 名多囊性卵巢症候群病患，若以 2003 鹿特丹標準分成四個表型子群，則其新陳代謝症候群盛行率在四個鹿特丹子群沒有統計上顯著差異，這顯示了以傳統的鹿特丹診斷標準和分群，確實在我們的病患族群之新陳代謝相關風險上，無法有良好的預測和評估。

因此，在這個研究中，我們使用了強大且創新的圖表分析法--廣義相關圖（generalized association plots，GAP），來分析多囊性卵巢症候群病患的症狀模式和特徵分群。我們首先運用關聯性分析，找出與多囊性卵巢症候群新陳代謝異常找出較為相關的四個內分泌指標 (FSH, LH, FAI, DHEA-S)，接著依照這四個內分泌指標表現值相近度，將多囊性卵巢症候群患者分為四個次族群，每個次族群中的個體即這四個內分泌指標表現最相近的一群病患。結果可發現，所分出的四個次族群，不僅各自具有獨特的內分泌表徵，也同時具有顯著不同的新陳代謝異常風險。與新陳代謝症候群盛行率呈現正相關的內分泌參數為游離雄性荷爾蒙指標，而高血清 LH 濃度則被發現是被納入新陳代謝健康群組的最佳指標。這對於

doi:10.6342/NTU202000313

我們臨床上面對多囊性卵巢症候群病患的追蹤治療和預後說明有很大的幫助，當病患出現高 FAI 指標且低 LH 濃度時，可更加頻繁更密集的追蹤病患的新陳代謝指標，包括血糖、血脂肪、肝功能、血壓、體重和腰圍變化，同時在衛教上更加強調運動、飲食等日常生活保養和注意體重控制的重要性。倘若病患出現低 FAI 指標且高 LH 濃度時，則可告知病患日後得到新陳代謝異常風險並不會像一般多囊性卵巢症候群病患那般高，而是與同齡女性無異，應可降低不必要的追蹤檢測和健保花費，也可降低病患之焦慮不安。

多囊性卵巢症候群是一種高異質性和高複雜度之婦女內分泌疾病，我們的研究成功的將患者進行了良好分組，也找出了與新陳代謝表徵嚴重度相關的內分泌因子，透過我們的分析成果，得以更加了解新陳代謝相關的危險因子，並可據以設計並提供更有效的篩選和治療方針。對於日後的相關研究，也提供了很好的流行病學資料，對於 LH 是如何與多囊性卵巢症候群病患的新陳代謝風險呈現負相關，LH 對於新陳代謝異常的調控是否有直接或間接的影響，究竟是因還是果，都值得我們進一步設計相關實驗去證實。

doi:10.6342/NTU202000313

第二節 卵巢濾泡液通透性與血管生成因子之相關致病機轉

Increased platelet factor 4 and aberrant permeability of follicular fluid in PCOS. (Huang *et al.*, 2019)

在這個階段的研究中，我們發現多囊性卵巢症候群患者的卵巢濾泡液會導致相鄰之內皮細胞通透性下降，且多囊性卵巢症候群患者的濾泡液中的 PF4 和 PF4 / IL-8 複合物濃度顯著上升，這些結果提供了血管抑制蛋白 PF4 對卵巢病理生理機轉有所相關的初步證據，而這個差異性亦可能導致卵巢濾泡液的生成失調和濾泡生長異常。進一步的實驗顯示了在卵巢濾泡液中，PF4 與另一種血管生成蛋白 IL-8 之間的結合作用，並顯示 PF4 的調節機制可能是透過與 IL-8 的拮抗性結合效果。多囊性卵巢症候群的致病機轉十分複雜，然而過去文獻從未提及其在濾泡生長過程的內皮細胞通透性變化，事實上是對於卵巢正常的濾泡成長機制都尚有許多未明之處，包括在濾泡生長過程中血管生成因子和血管抑制因子的表現。而我們的研究結果不僅提供了多囊性卵巢症候群致病機轉的另一種新解釋，而且也讓我們對於卵巢濾泡液通透性、濾泡液生成和濾泡生長的正常卵巢生理機制有更進一步的了解。

此外，這部分的成果也開啟了一個新的研究領域，我們將進一步設計細胞實驗與動物實驗，以釐清究竟是哪些細胞過度分泌 PF4 導致其在卵巢濾泡液濃度增加，而濾泡液中的 PF4 所調控的細胞種類為何，是否涉及顆粒細胞的功能以及排卵功能，以及其所參與的下游訊息傳導途徑為何等等。若能更進一步釐清相關致病機轉，調節卵巢滲透性或者調節血管生成過程也可能成為日後多囊性卵巢症候群另一種新治療方法。

doi:10.6342/NTU202000313

第三節 超基因調控之相關致病機轉研究

第三節之第一部 多囊性卵巢症候群之 DNA 甲基化研究

Hyperactive CREB signaling pathway involved in the pathogenesis of polycystic ovarian syndrome revealed by patient-specific induced pluripotent stem cell modeling. (Huang *et al.*, 2019)

我們的研究成功地從成人皮膚纖維母細胞衍生出具有病患專一性且具有多囊性卵巢症候群疾病特異性的誘導性多功能幹細胞，並且將誘導性多功能幹細胞成功分化為卵巢顆粒細胞，這些誘導性多功能幹細胞所衍生分化的顆粒細胞能夠表現與卵巢顆粒細胞相關之基因，也可出現芳香酶活性將雄性荷爾蒙轉換為雌激素，從而證明了我們這一系列研究方法的可靠性。具多囊性卵巢症候群特異性之誘導性多功能幹細胞可以做為良好的疾病模型，可以分化成各種與多囊性卵巢症候群相關的組織和細胞，特別是那些原本難以取得的組織，例如可以進一步分化為腦部神經細胞，以進一步釐清多囊性卵巢症候群病患之下視丘和腦下垂體分泌 GnRH 和促性腺激素的功能是否失調，另外也可分化成胰臟的胰島細胞，以分析其分泌胰島素的功能是否異常，以上都是難以在多囊性卵巢症候群病患身上取得的細胞組織，此外，有些組織雖然可以取得但會增加病患的疼痛不適，例如先前文獻中進行的脂肪組織切片或肌肉組織切片，為了研究多囊性卵巢症候群患者是否在這些周邊組織出現胰島素阻抗，透過誘導性多功能幹細胞再分化，我們便能更容易得到多囊性卵巢症候群特異性之脂肪組織和肌肉組織，對於難以取得的疾病特異性器官組織提供良好的可及性。再加上目前還沒有足夠好的多囊性卵巢症候群模式生物能夠代表這個疾病，透過外加注射雄性荷爾蒙的小鼠模型仍有許多表徵與多囊性卵巢症候群病患有所不同，我們成功建立的多囊性卵巢症候群特異性誘導性多功能幹細胞可以更貼近多囊性卵巢症候群在病患細胞上的表現，同時可依據其病患專一性，進一步作為藥物篩選的平台，甚至根據不同的患者臨床表徵，找出不同的潛在致病機轉，對於基礎治療和臨床研究都有極大的應用價值。

doi:10.6342/NTU202000313

我們的研究成功地建立了具病患特異性和多囊性卵巢症候群特異性的誘導性多功能幹細胞，並且成功將之重新分化為卵巢顆粒細胞，這可以作為評估多囊性卵巢症候群在早期細胞分化和發育狀態之相關病徵之生物模型。我們同時分析成人顆粒細胞和誘導性多功能幹細胞衍生之顆粒細胞中的 DNA 甲基化表現，發現了在多囊性卵巢症候群和對照組之間，有數個差異性甲基化基因表現途徑在兩種顆粒細胞都有出現，包括：CREB 訊息傳導途徑的過度活化、NRF2-mediated oxidative stress、PPAR / RXR 過度活化等等，這些都可能與多囊性卵巢症候群的致病機轉相關，而我們目前只有針對 CREB 訊息傳導途徑進行西方墨點法和 PCR 的驗證，還有許多發掘出來的潛在致病機轉尚待進一步驗證和釐清。而我們所驗證的 CREB/CBP 是荷爾蒙和新陳代謝相關路徑的重要調控因子，而多囊性卵巢症候群最重要的病徵即為荷爾蒙和新陳代謝調控異常，因此 CREB 訊息傳導途徑的異常可能與多囊性卵巢症候群機轉相關。我們的初步研究成果可以對多囊性卵巢症候群的致病機轉提供了一個嶄新的解釋，也開啟了許多新的研究方向，而目前臨床上已經有 CREB 路徑的調控試驗藥物被嘗試用來治療第二型糖尿病，亦有可能成為多囊性卵巢症候群新的治療選擇藥物而對臨床醫療有所貢獻。

doi:10.6342/NTU202000313

第三節之第二部 多囊性卵巢症候群之微小核醣核酸研究

我們這個部分的研究分為兩個階段，第一個階段是特定微小核醣核酸測量，第二個階段是預測模式建立與臨床驗證。

在第一個階段的特定微小核醣核酸測量中，我們發現多囊性卵巢症候群患者與非多囊性卵巢症候群受試者的血液游離微小核醣核酸表現模式確實有顯著不同，這些微小核醣核酸可以用作多囊性卵巢症候群的診斷標記，此外，metformin 針對排卵和月經週期治療的效果，在有效和無效兩組之間的微小核醣核酸表現也有顯著的差異。metformin 是一種胰島素增敏劑，經常被使用在多囊性卵巢症候群的治療以改善胰島素抵抗之徵狀。根據過去的治療指引建議，metformin 僅推薦使用於同時罹患胰島素抵抗的多囊性卵巢症候群患者。然而台大團隊先前的研究顯示 (Yang *et al.*, 2018)，即使是沒有罹患胰島素阻抗的多囊性卵巢症候群患者，接受 metformin 治療也有 50%的患者能夠出現自發排卵而達到臨床症狀的改善，因此假如能夠預測哪些多囊性卵巢症候群病患可以對 metformin 治療產生臨床排卵功能的改善，那我們就能減少病患接受不必要的藥物治療及其所產生的副作用。我們的結果確實顯示出有趣的發現，即在 metformin 有效和無效的兩組多囊性卵巢症候群患者之間，有幾種微小核醣核酸的表現量具有顯著差異。這些微小核醣核酸不僅可作為治療反應的預測性生物指標，而且也可以對 metformin 究竟是透過甚麼機轉改善排卵提供另一個可能的解釋。

第二個階段我們成功的建立了針對多囊性卵巢症候群診斷鑑別的預測模型，透過 miR-93、miR-132、miR-222、miR-27a、miR-125b、miR-212 這六個微小核醣核酸的表現值，對於受試者是否符合多囊性卵巢症候群臨床診斷有極佳的預測性，此外我們也針對 metformin 療效建立了預測模型，藉由臨床指標和四個微小核醣核酸的血液表現值，可以幫忙預測患者是否可以在接受 metformin 治療後，出現排卵功能及月經週期上的改善，並也成功在另一個病患族群中驗證此預測模型的效果，對於多囊性卵巢症候群臨床治療的療效預測和藥物選擇

doi:10.6342/NTU202000313

有顯著的幫忙。

在相關標的基因和調控生物路徑的分析中，我們分析了四個在預測模型當中出現顯著鑑別力的微小核醣核酸，包括：miR-132, miR-27a, miR-222, miR-93，發現這四個微小核醣核酸參與調控的排行前幾名顯著 GO biological process 大部分都與細胞代謝有關，顯示出微小核醣核酸在多囊性卵巢症候群潛在的致病機轉可能是透過對於細胞代謝功能的調控改變，這些發現對於多囊性卵巢症候群在微小核醣核酸相關致病機轉上提供了良好的材料，可據以規劃進一步之動物實驗和細胞實驗，驗證這些微小核醣核酸究竟是透過何種機轉影響了多囊性卵巢症候群的致病機轉和疾病表徵，對於多囊性卵巢症候群之相關基礎與臨床研究均有所貢獻。

doi:10.6342/NTU202000313

第四節 總結

這些年來針對多囊性卵巢症候群這個疾病進行了一系列相關研究，從病患卵巢濾泡液、卵巢顆粒細胞、血液檢體、到病患專一性誘導性多功能幹細胞株的建立，透過各種分析方法，在臨床症狀、疾病診斷、疾病預後、致病機轉以及臨床治療上都有許多新的發現，包括：臨床症狀的分組解析和新陳代謝症候群危險因子的探尋、濾泡液中血管生成因子與其潛在影響內皮細胞通透性之機轉解析、病患專一性及多囊性卵巢症候群特異性誘導性多功能幹細胞之建立與再分化研究、全基因體 DNA 甲基化分析所發現之 CREB 訊息調控路徑異常對於致病機轉之可能影響、以血液游離微小核醣核酸建立之良好多囊性卵巢症候群診斷模型和 metformin 療效預測模型，無論是研究過程所積累的經驗，或者是所獲得的種種研究成果，都為日後多囊性卵巢症候群相關基礎或臨床研究提供了大量的工具和材料，在臨床醫療的診斷和治療也有所貢獻。

根據目前已經獲得的初步成果，我們正在進行或者準備下一步進行的各種多囊性卵巢症候群相關研究，將包括以下主題：

(1) 多囊性卵巢症候群之神經內分泌起源 (neuroendocrine origin) -- 以疾病專一誘導性多功能幹細胞分化出腦神經元細胞及其相關致病機轉探討

近年來越來越受到矚目的是神經內分泌調控在多囊性卵巢症候群的致病機轉研究，過去許多文獻都曾經報告過，罹患多囊性卵巢症候群婦女的腦下垂體所分泌之黃體化激素分泌頻率增快，且黃體化激素和促濾泡激素的比例 (LH/FSH ratio) 上升，而這樣的表徵與促性腺激素釋放荷爾蒙 GnRH 在下視丘神經元的活性上升和分泌頻率增快有關 (Dumesic *et al.*, 2015)。一般而言，下視丘神經元上帶有雌激素受體 (estrogen receptor) ，可接受血清雌激素的負回饋刺激而使下視丘的 GnRH 分泌受到抑制，然而證據顯示，在多囊性卵巢症候群病患往往需要外在給予更高濃度的雌激素才能抑制下視丘分泌 GnRH，可知此負回饋調控機轉之異常表現也是多囊性卵巢症候群病患之神經內分泌調控異常之一環 (Pastor *et al.*, 1998) 。總歸來說，下視丘的 GnRH 和腦下垂體的 LH 分泌增加究竟是因還是果目前仍未明，

doi:10.6342/NTU202000313

然其結果則會造成多囊性卵巢症候群最重要的臨床症狀—高雄性荷爾蒙症，GnRH-LH 分泌增加則會刺激下游的卵巢濾泡鞘細胞將黃體素轉換為雄性素，進而導致病患出現高雄性荷爾蒙血症和高雄性荷爾蒙症狀，包括：多毛、嚴重痤瘡、雄性禿……等等，而高雄性荷爾蒙又會加重其他新陳代謝方面的異常，包括：高胰島素血症、中央型肥胖、高血壓、肝功能異常……等等。

此外，在以雄性素誘導產生多囊性卵巢表徵之小鼠實驗中，發現下視丘 arcuate nucleus 的神經傳導和 GABA 分泌，會受到雄性素的刺激而增加，並進一步增加 GnRH 神經元的活性及分泌(Sullivan and Moenter, 2004; Roland and Moenter, 2011)。而 2017 年一篇研究亦發現多囊性卵巢症候群病患的腦脊髓液中 GABA 濃度較對照組顯著上升 (Kawwass *et al.*)。除了 GABA 神經元，另一個被認為與多囊性卵巢症候群致病機轉可能相關的是 kisspeptin-/neurokinin B-/dynorphin-expressing 'KNDy'神經元的調控。KNDy 神經元同樣位在下視丘，負責接受卵巢荷爾蒙的刺激並調控 GnRH 分泌的頻率，在給予雄性素誘發多囊性卵巢表徵的大鼠，會產生較高濃度的 LH 並在下視丘表現出較多的 KNDy 神經元(Osuka *et al.*, 2017)。此外，在一個小規模的多囊性卵巢症候群病患之病例對照研究中，發現病患血清中的 Kisspeptin 濃度與 LH 濃度有顯著正相關，且 KISS1 基因上面的 rs2889 位點多型性，也與在多囊性卵巢症候群和對照組出現顯著差異(Albalawi *et al.*, 2018)。可以說多囊性卵巢症候群病患的神經內分泌調控異常，與其致病機轉和臨床表徵有著密不可分的關聯性。然而，臨床上要取得多囊性卵巢症候群病患的下視丘或腦下垂體細胞進行研究是極為困難的事，因此根基於我們成功建立多囊性卵巢症候群特異性誘導性多功能幹細胞以及再分化為卵巢顆粒細胞的經驗，我們下一步將嘗試將誘導性多功能幹細胞分化為更不易取得的腦神經細胞，希望能夠更加釐清此複雜疾病之神經內分泌相關致病機轉。

(2) 微小核醣核酸調控對於多囊性卵巢症候群致病機轉之進一步解析

我們將利用卵巢顆粒細胞、卵巢濾泡鞘細胞、腦下垂體、下視丘等各種與排卵機轉相關之細胞株進行實驗，針對初步研究成果所找出的在多囊性卵巢症候群具有顯著差異性表現的數個標的微小核醣核酸，包括 miR-93，miR-132 和

doi:10.6342/NTU202000313

miR-27a，進一步驗證這些微小核醣核酸對於荷爾蒙調控以及排卵相關基因表現之影響，並分析其與排卵異常致病機轉之相關性。

(3) 透過血液微小核醣核酸表現所建立之多囊性卵巢症候群診斷模型之驗證

我們將另外召募一群未經診斷或篩選，且尚未接受過任何相關治療的一般育齡年齡女性受試者，徵求其同意之後，測量其血液微小核醣核酸濃度，並為其進行檢查以確認是否在臨床上符合多囊性卵巢症候群之診斷，以確認我們診斷模型之適用性和準確度。

(4) 卵巢顆粒細胞之 DNA 甲基化差異性表現之富集路徑機轉驗證

在病患卵巢顆粒細胞和誘導性多功能幹細胞衍生顆粒細胞的DNA甲基化分析研究中，我們找出了數個在兩種細胞都共同出現的多囊性卵巢症候群組差異性表現，包括：CREB 訊息傳導途徑的過度活化、NRF2-mediated oxidative stress、PPAR / RXR 過度活化等等，我們將逐一分析這些訊息傳導路徑與多囊性卵巢症候群致病機轉的相關性。

綜合上述彙整，期待日後積累更豐盛的研究成果，對於多囊性卵巢症候群此一重要而複雜的內分泌疾病能夠有更多的瞭解與貢獻。

doi:10.6342/NTU202000313

第六章 論文英文簡述(summary)

INTRODUCTION

Polycystic ovary syndrome (PCOS) is one of the most common endocrine disorders, affecting 5%-10% of reproductive age women (Diamanti-Kandarakis *et al.*, 1999; Asuncio´n *et al.*, 2000; Azziz *et al.*, 2004). The characteristic features of PCOS include clinical and/or biochemical hyperandrogenism (HA), chronic anovulation (AO), and polycystic ovaries morphology (PCOM) on ultrasound. One of the most commonly used diagnostic criteria, the Rotterdam criteria, requires the presence of at least two of the above features (Rotterdam ESHRE/ASRM-Sponsored PCOS Consensus Workshop Group, 2004). Therefore implementation of Rotterdam criteria resulted in four different phenotypic subgroups (full-blown phenotype: HA + AO + PCOM; non-PCO phenotype: HA + AO; non-hyperandrogenic phenotype: AO + PCOM; ovulatory phenotype: HA + PCOM) and this further increased the diversity and heterogeneity of the PCOS population.

Meanwhile, there is abundant evidence suggesting that PCOS not only presents with hormonal abnormalities, but it is also strongly associated with metabolic aberrations, including dyslipidemia, insulin resistance (IR), abdominal obesity, type II diabetes mellitus (T2DM), and hypertension (HTN) (Chen *et al.*, 2007; Moran *et al.*, 2010; Diamanti-Kandarakis and Dunaif, 2012; Wild *et al.*, 2012). However which phenotypic subgroup of Rotterdam criteria best correlates women with PCOS and women at risk for metabolic syndrome (MS) is an ongoing debate. While some studies showed that HA might predict an increased risk of metabolic aberrations (Shroff *et al.*, 2007; Chae *et al.*, 2008), others revealed that there was no significant difference in the prevalence of MS between different phenotypic subgroups (Hassa *et al.*, 2006; Kauffman *et al.*, 2008; Wijeyaratne *et al.*, 2011; Li *et al.*, 2013; Hosseinpanah *et al.*, 2014). Besides, other hormones such as dehydroepiandrosterone sulfate (DHEA-S) and luteinizing hormone (LH) level had also been proposed to be correlated to the metabolic presentations of PCOS in separate studies (Chen *et al.*, 2006; Lawson *et al.*, 2008; Lerchbaum *et al.*, 2012). Therefore it is important to evaluate the patients individually with composite endocrine characteristics, instead of evaluating the testosterone level alone.

In the first part of our study we applied a powerful and innovated graphical approach, generalized association plots (GAP), to identify the symptom patterns and phenotypic clustering in women with PCOS. GAP is an innovated computer software

doi:10.6342/NTU202000313

environment that implemented many traditional statistical tools, including matrix visualization (MV) and various clustering algorithms (e.g., hierarchical clustering, k-means, and rank-two elliptical seriation) for interactive exploration of data matrices. It can simultaneously explore the data structure and relationships between up to thousands of subjects and variables before any presumed statistical modeling (Chen, 2002; Tien *et al.*, 2008; Wu *et al.*, 2008, 2010). This tool had been successfully applied in the studies of other complex and heterogeneous disorders, such as the symptom structure of Schizophrenia (Hwu *et al.*, 2009). The aim of this study was to determine the potential endocrine characteristics related to risk and severity of metabolic disturbances. We also attempted to cluster the patients according to their endocrine characteristics regarding the related risk of MS.

Chronic anovulation is one of the most prominent and bothersome symptoms affecting the young PCOS population, with an estimated prevalence of at least 70%-90% (Balen et al., 1995). The impact of menstrual irregularity is even more significant in women of Asian ethnicity, in whom the prevalence of hirsutism and obesity are less frequent (Zhao et al., 2013). The related pathophysiologic abnormalities, such as increased preantral follicle number, mid-antral follicular arrest, failure of selection of the dominant follicle and ovulation, and abnormal survival and steroidogenesis of granulosa-thecal cells, have all been well-described (Franks et al., 2008; Chang et al., 2013; Dumesic et al., 2013). Premature luteinization resulting from overexpression of luteinizing hormone (LH) receptors in granulosa cells and inadequate secretion of gonadotropins have been proposed to cause arrest of follicular development (Jonard and Dewailly, 2004). Moreover, both hyperinsulinemia and hyperandrogenemia might disturb the responsiveness toward gonadotropins and steroidogenesis of granulosa-thecal cells, which could further cause follicular arrest (Franks S 2008; Jonard and Dewailly, 2004).

Another possible explanation for the abnormal follicular development in PCOS is dysregulated ovarian angiogenesis. Vascular endothelial growth factor (VEGF), one of the most important angiogenic proteins mediating the physiologic processes of follicular development, ovulation, corpus luteum formation (Tamanini and De Ambrogi, 2004), and the pathologic process of ovarian hyperstimulation syndrome (OHSS) (Chen et al., 2008, 2010), has been shown to be significantly increased in the follicular fluid (FF) (Agrawal et al., 1998a), ovarian tissues (Kamat et al., 1995; Ferrara et al., 2003), and serum (Agrawal et al., 1998a; 1998b) of PCOS patients. This finding might partially explain the intense vascularity in the ovarian stroma and the abnormal growth of theca interna, which are characteristics of polycystic ovaries (Peitsidis and Agrawal, 2010). In addition to VEGF, other angiogenesis-related proteins, such as platelet-derived growth factor (PDGF) and angiopoietins, have also been observed to be differentially

doi:10.6342/NTU202000313

expressed in the FF of PCOS patients compared with healthy controls (Scotti et al., 2014). A wide range of angiogenic and angiostatic proteins have been discovered; however, a thorough investigation regarding their roles in PCOS is lacking.

These angiogenesis-related proteins are not only essential in angiogenesis, during which new blood vessels grow from the pre-existing vasculature, but are also key regulators of vascular permeability by which the plasma and its solutes cross the vascular barrier (Nagy et al., 2008; Bates, 2010). A change in the relative permeability of the follicular wall might influence the formation of FF and follicular antrum, which are both important processes in folliculogenesis, but are rarely investigated (Rodgers et al., 2010), especially in PCOS research.

Therefore, in the second part of our study, we conducted a case-control study to elucidate the modulating effects of FF on endothelial cell permeability. Then, a comprehensive analysis of intrafollicular proteins which might be involved in the permeability and/or angiogenesis processes was performed. This is the first study to examine whether or not and how the FF from PCOS patients influences the endothelial cell permeability, which might be involved in the pathophysiology of abnormal folliculogenesis.

Although a number of pathophysiologic explanations have been proposed (Baskind and Balen 2016; Huang *et al.*, 2019; Moran *et al.*, 2010), such as a dysregulated hypothalamus-pituitary-ovary (HPO) axis, hyperandrogenism (HA), and insulin resistance, no single etiology can completely explain the full spectrum of this complex disease and the underlying mechanisms remain unclear. Although the clinical symptoms of PCOS usually manifest after maturation of the HPO axis during puberty, numerous clinical and experimental studies have supported that this disease has a strong genetic basis (Kosova and Urbanek, 2013) and its pathogenic genetic expression and/or epigenetic regulation may develop starting in early intra-uterine life (Franks *et al.*, 2006). However, the theory regarding the early developmental origin of PCOS is difficult to confirm due to ethical and legal problems in embryonic research (King and Perrin, 2014).

A possible resolution for the ethical and legal disputes in embryonic experiments is using induced pluripotent stem cell (iPSC) technology. iPSC uses vectors to transform a cell to a state of immortality (Takahashi and Yamanaka, 2006). This could preserve the genetic and inherited nature of the original cell and be used as a method of disease modeling, drug discovery, and potential cell replacement therapy (Brandão *et al.*, 2017; Kumar *et al.*, 2017). Reprogramming of somatic cells to iPSCs resets their identity to an embryonic stage (Roessler *et al.*, 2014) and could provide valuable pathogenic

doi:10.6342/NTU202000313

information on the early development of adult-onset diseases. However, challenges remain with the technique and only one study has successfully established PCOS-specific iPSCs. Yang et al. produced PCOS-specific iPSCs from epithelial cells in the urine using retroviral transduction with defined reprogramming factors and differentiated them into adipogenic cells (Yang *et al.*, 2016). The study showed that the ability of iPSC-derived adipogenic cells to consume glucose increased in the PCOS group compared with the controls.

In addition to adipocyte dysfunction, aberrant granulosa cell (GC) function is critical in the pathogenesis of PCOS. The development and function of ovarian GCs is one of the most critical regulators of ovarian folliculogenesis and steroidogenesis. The GCs constitute the primary cell type within the ovarian follicles and their role in functional and structural modifications synchronizes with the process of folliculogenesis (Hutt and Albertini, 2007). They not only produce estrogen under the stimulation of follicle-stimulating hormone (FSH), but also regulate the maturation and competence acquisition of the developing oocyte (Fragouli *et al.*, 2014). According to previous studies, dysregulated GC function has been observed among women with PCOS, including excessive GC apoptosis, defective proliferation (Das *et al.*, 2008), abnormal hyperresponsiveness to FSH stimulation, and altered steroidogenesis (Chang and Cook-Andersen, 2013). However, most of these studies utilized GCs derived during follicle aspiration after the administration of a high dose of gonadotropin stimulation for an in vitro fertilization (IVF) program in humans (Catteau-Jonard *et al.*, 2008; Kaur *et al.*, 2012; Lan *et al.*, 2015; Nouri *et al.*, 2016) or steroid hormone-treated (Chen *et al.*, 2015; Hsueh *et al.*, 1994) or diet-induced PCOS animal models (Wu *et al.*, 2015). The unstimulated, un-luteinized, human ovarian GCs are seldom available and the manipulated animal models may not be representative of actual human phenotypes. Taken together, it remains unclear whether the different functional expressions of GCs between women with and without PCOS actually exist, and the definite pathogenic contributions are ambiguous. The current research aimed to generate PCOS-specific iPSCs and re-differentiate them into ovarian GCs. The derived differentiated GCs from iPSCs represent the non-luteinized GCs without prior ovarian hyperstimulation and may serve as a valuable tool for discovering the PCOS mechanisms of disease during early development.

Epigenetic modifications, defined as heritable changes in gene expression without changing the underlying DNA sequences, have been proposed as a potential solution for the missing heritability in complex diseases (Kirchner *et al.*, 2013). Only a few studies Kokosar *et al.*, 2016; Shen *et al.*, 2013; Xu *et al.*, 2010; Yu *et al.*, 2015) have focused on the correlation between DNA methylomic aberrations and the pathogenesis of PCOS but without definite conclusions. Therefore in our third part of

doi:10.6342/NTU202000313

the study, we aimed to conduct a genome-wide DNA methylation analysis to compare the methylation profiles between PCOS and non-PCOS controls in both iPSC-derived GCs and primary adult GCs. This is the first study to examine the methylation profiles between disease-specific iPSCs and mature disease cells to evaluate potential contributing factors in the mechanisms of PCOS. The preserved hyperactive CREB pathway, which is related to aberrant DNA methylation, may provide an explanation for the inheritance nature (Kosova and Urbanek, 2013) and phenotypic plasticity associated with environmental interactions of PCOS (Diamanti-Kandarakis *et al.*, 2012).

In the fourth part of our study, we will focus on the correlation between PCOS and microRNA regulation, which is also an important portion of epigenetic regulation. MicroRNAs (miRNAs) are small (~22-nt), stable RNAs that play critical role during post-transcriptional gene regulation (Haider et al., 2014). In addition to cytoplasmic and nuclear locations, microRNAs are located in other cellular and non-cellular compartments, including mitochondria, exosomes, and microvesicles (Faruq and Vecchione, 2015). Besides, they have been detected in virtually all bodily fluids including breast milk, amniotic fluid, tears, cerebrospinal fluid, peritoneal fluid, blood, pleural fluid, saliva, semen, and urine. Ever since the discovery of microRNAs within human blood in 2008, there was enormous interest for the potential use of plasma or serum microRNAs as biomarkers of neoplastic and non-neoplastic disease (Moreno-Moya et al., 2014). MicroRNAs are especially appealing as biomarkers because they are not prone to RNase degradation and remain stable in stored samples (Haider et al., 2014).

Evidence of possible role of miRNAs by GWAS studies

One interesting result from the largest genome-wide association study (GWAS) of PCOS (Chen et al., 2011) showed that, one of the PCOS susceptibility genes, DENND1A, which encodes miR-601(McAllister et al., 2015). Another singlenucleotide polymorphism near the genes of high mobility group AT-hook 2 and the Ras-related protein Rab-5B (Shi et al., 2012) identified by a recent PCOS GWAS study appears to be targeted by miR-132 and -32, respectively (Sang et al., 2013). Further functional analysis will be needed to clarify the association between these genetic factors and epigenetic factors, i.e. miRNA expression in PCOS.

doi:10.6342/NTU202000313

Serum/Plasma miRNA Biomarkers for PCOS

So far, little is known about the roles of miRNAs during follicular development, steroidogenesis and in PCOS. The possible modes of action for miRNA within the pathophysiology of PCOS have only been sparsely investigated, and only a few miRNA-PCOS studies existed in the literature. Only two studies had explored the possible role of serum miRNA as diagnostic biomarkers in PCOS. Long et al. (2014) used the miRNA microarray to explore the expression of serum miRNAs in patients with PCOS compared to age-matched controls. Three miRNAs (miR-222, miR-146a and miR-30c) were significantly increased in PCOS patients with a combination AUC of 0.852. Sathyapalan et al. (2015) selected two miRNAs (miR-93 and miR-223) which were related to insulin resistance and type II diabetes from the literature for analysis. The area under the receiver operator characteristic curve for miR-223 and miR-93 was 0.66 and 0.72 respectively, suggesting miR-93 was a better biomarker for the diagnosis of PCOS. However both studies were inherited with the problems with limited case number, absence of verification in another non-selected cohort, lack of replication in other studies and lack of further functional analysis. Meanwhile, the subjects of both studies were Caucasian. Since there is substantial ethnic and racial difference in the clinical presentation of PCOS (Wang et al., 2013), it is important to establish our own database in Taiwan.

MicroRNAs and Insulin Resistance in PCOS

Approximately 60-70% of women with PCOS have intrinsic insulin resistance (IR) and some degree of hyperinsulinemia (Azziz et al., 2009). In a study of primary subcutaneous adipose tissue from women with PCOS, it was found that the level of GLUT4, the major insulin-dependent glucose transporter, was positively correlated with insulin sensitivity. Furthermore, a negative association between miR-93 activity and GLUT4 expression was noted in these patients, suggesting a novel mechanism for regulating insulin-stimulated glucose uptake via miR-93 in the women with PCOS and IR (Chen et al., 2013). Currently metformin, an insulin-sensitizing agent, is one of the mainstream medical therapies of PCOS. This medication not only decreases insulin resistance but also have several positive effects on androgen levels, ovulation and even fertility (Lord et al., 2003). The administration of metformin may also change the expression pattern of certain miRNAs. In type 2 diabetes, the serum expression level of miR-221 and miR-222 was found to be elevated, while patients on metformin had a similar expression level with non-diabetic patients (Coleman et al., 2013). The underlying mechanism of the therapeutic effect of metformin on the diverse phenotypes

doi:10.6342/NTU202000313

of PCOS is still unclear and this will also become one of our research interests in our study.

MicroRNA and steroidogenesis

It has been proposed that PCOS results from abnormal regulation of steroidogenesis and specifically from androgen secretion by the ovary (Gilling-Smith et al., 1994). The miRNAs in the control of the release of the main ovarian steroids might be dysregulated and therefore pathogenic. The abnormal follicular development and the underlying pathways associated with this phenotype might be explained by the differences in miRNA expression. Many biological mechanisms are regulated by miRNA, but only very few studies have investigated the role of miRNAs in PCOS. The association between the expression pattern of specific miRNAs and the release of steroid hormone has been demonstrated by several studies across a variety of species. It was shown that the estradiol secretion from the steroidogenic human granulosa-like tumor cell line, KGN, could be changed while transfected with certain miRNA mimics. The KGN cells decreased estradiol secretion while transfected with miR-24 mimics and increased estradiol secretion while transfected with miR-132, miR-320, miR-520c-3p and miR-222 mimics (Blandino et al., 2012). In the mice study, the microarray analysis revealed that 13 miRNAs were differently expressed before and after oocyte triggering with hCG injection. Specifically, the expression level of miR-21, miR-132 and miR-212 were shown to be up-regulated by hCG injection during oocyte triggering (Fiedler et al., 2008). In another delicate study published on Science, female mice lacking the microRNAs miR-200b and miR-429 exhibited symptoms of anovulation and infertility. Eliminating these miRNAs inhibits luteinizing hormone (LH) synthesis, which leads to lowered serum LH concentration, an impaired LH surge, and failure to ovulate (Hasuwa et al., 2013). Therefore miRNA might play an important role in the regulation of the hypothalamus-pituitary-ovarian axis.

Two studies identified miRNAs in follicular fluid from patients with PCOS recently (Sang et al., 2013; Roth et al., 2014). Both of them found differences in the expression patterns of miRNAs in the PCOS group compared with a control group. The first group investigated a subset of seven miRNAs (miR-132, -320, -24, -520c-3p, -193b, -483-5p, and -222) which were chosen because of their connection with steroidogenesis (Sang et al., 2013). miR-132, miR-320, miR-520c-3p, and miR-222 regulate the concentration of estradiol while the others regulate progesterone concentrations. Two were found to have significantly decreased expression in the PCOS group (miR-132 and -320). Those highly expressed miRNAs targeted genes were associated with

doi:10.6342/NTU202000313

reproductive, endocrine, and metabolic processes in the bioinformatics analysis. The second group also found that the PCOS group had significant overexpression of five miRNAs (hsa-miR-9, -18b, -32, -34c, and -135a) (Roth et al., 2014). Three potential miRNA target genes had significantly decreased expression in the women with PCOS: insulin receptor substrate 2, synaptogamin 1, and interleukin-8. These factors were found to be associated with the PCOS phenotypes, including ovulation, insulin resistance and carbohydrate metabolism.

In conclusion, identification of differentially expressed miRNAs and their specific target genes in the patients with PCOS might provide us better understanding of the pathophysiology of this complex disease. Discovery of a unique temporal miRNA pattern might provide sensitive new biomarkers for the diagnosis and prognostic prediction of this common disease, and even new biomarkers for important biological processes underlying this disease, such as ovulation function and steriodogenesis. Given the critical regulatory function of miRNAs in posttranscriptional gene expression, understanding the underlying mechanisms of the function of these regulatory miRNAs might lead to the development of better diagnostic methods, preventive or even therapeutic strategies by regulating specific target genes associated with PCOS. Therefore in the fourth part of our study, the aims will include: (1) Analysis of the differentially expressed pattern of miRNAs in the circulation could be diagnostic biomarkers for PCOS, and of the different phenotypic subtypes of PCOS exhibit distinct expression patterns of miRNAs. Comparing the miRNA profiles of PCOS patients to healthy controls might reveals that contribution of regulatory miRNAs to the underlying pathogenesis. (2) Establishment of prediction model for the diagnosis of PCOS and the therapeutic effects of metformin, according to expression level of circulatory miRNAs. (3) Validation of our prediction models by another separate cohort.

MATERIAL AND METHODS

Study 1: Symptom patterns and phenotypic subgrouping of women with polycystic ovary syndrome: association between endocrine characteristics and metabolic aberrations.

Subjects

This was a cross-sectional study in a single university hospital setting with approval by the Research Ethics Committee of the National Taiwan University Hospital.

doi:10.6342/NTU202000313

Four hundred sixty women with PCOS were recruited from our reproductive endocrinology outpatient clinic and informed consent was obtained from all of patients and/or their parents. The patients initially sought evaluation at the clinic for menstrual irregularities and/or clinical symptoms of HA, such as hirsutism and alopecia. The patients did not receive medical treatment, including oral contraceptives, insulin-sensitizing agents, anti-androgenic agents, ovulation-induction agents, and Chinese herbal medicines, within 3 months before enrollment. The diagnosis were made according to the 2003 Rotterdam criteria, and at least 2 of the following 3 criteria were fulfilled: amenorrhea or oligomenorrhea (fewer than nine spontaneous menstrual cycles per year for at least 3 years before enrollment); biochemical hyperandrogenemia (serum total testosterone level ≧ 0.8 ng/ml) and/or clinical HA, including hirsutism and alopecia (acne was excluded due to inconsistency of the correlation with HA in the literature); and PCOM on ultrasound (greater than twelve 2-9 mm follicles or an ovarian volume > 10 ml in at least 1 ovary). Other endocrine and organic abnormalities, such as hyperprolactinemia, thyroid dysfunction, Cushing's syndrome, congenital adrenal hyperplasia, and adrenal or ovarian tumors were excluded. Hirsutism was defined as a Ferriman–Gallwey score > 8.

Protocol

All subjects underwent collection of blood samples, anthropometric measurements, pelvic ultrasonography, and measurements of blood pressure on the same day. Overnight fasting venous blood samples were collected in the early follicular phase in patients with spontaneous ovulation cycles, and randomly in amenorrheic patients. The blood sample was discarded if the serum progesterone level was > 2 ng/ml, or the serum estradiol level was > 150 pg/ml. If the serum progesterone level was higher 2 ng/ml, the patients were invited for blood sampling 2-5 days after menstruation. Blood samples were processed within 30 minutes of collection and the levels of serum glucose and insulin were measured on the same day (Chen *et al.*, 2009). The remaining serum and plasma were frozen at -80℃ until assayed. Pelvic ultrasonography was performed by 1 or 2 experienced gynecologists using a transvaginal approach whenever possible. The number of follicles ranging from 2-9 mm in diameter was counted and the ovarian volume was calculated with a simple formula (0.5 x length x width x thickness) (Balen *et al.*, 2003; Chen *et al.*, 2008). Obesity was defined as a body mass index (BMI) ≧ 25 kg/m^2, which is based on the guidelines for an adult Asian population (WHO Expert Consultation, 2004). The establishment of MS required at least 3 of the following 5 criteria: a systolic blood pressure (SBP) ≥ 130 mmHg and/or a diastolic blood pressure (DBP) ≥ 85 mmHg; a fasting glucose ≥ 100 mg/dl; a fasting triglyceride (TG) ≥ 150

doi:10.6342/NTU202000313

mg/dl; a high-density lipoprotein-cholesterol (HDL-C) < 50 mg/dl; and abdominal obesity (waist circumference (WC) > 80 cm) (Tan *et al.*, 2004).

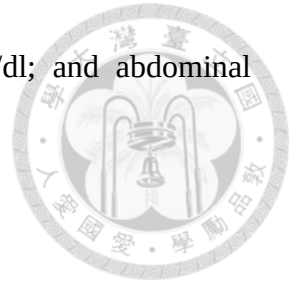

Assays

The concentration of plasma glucose (mg/dl; the detectable range: 10-800), serum insulin (IU/ml, 2-140), hormone profiles (follicle-stimulating hormone [FSH, mIU/ml, 0.1-120], LH [mIU/ml, 0.1-100], estradiol [pg/ml, 20-900], progesterone [ng/ml, 0.2-40], sex hormone-binding globulin [SHBG, nmol/l, 0.35-200], liver enzymes (alanine aminotransferase [ALT, IU/l, 3-500] and aspartate aminotransferase [AST, IU/l, 3-1000]), and lipid profiles (total cholesterol [mg/dl, 25-700], TG [mg/dl, 10-1000], low-density lipoprotein-cholesterol [LDL-C, mg/dl, 7-450], and HDL-C [mg/dl, 3-150]) were measured as described previously (Chen *et al.*, 2006, 2010, 2012). Serum total testosterone (ng/ml, 0.03-14.4) and DHEA-S (μg/dl, 2.5-800) were measured by radioimmunoassay (Diagnostic Systems Laboratories). And the bioavailability of testosterone was assessed by free androgen index (FAI) [FAI (%) = testosterone (ng/ml) x 3.47 x 100 / SHBG (nmol/l)] (Chen *et al.*, 2007). The mean (standard deviation(SD)) value of total testosterone level was 0.4(0.12) ng/ml in a historical control arm with 37 non-PCOS healthy women recruited from previous study (Chen *et al.*, 2009). The degree of IR was evaluated with the homeostasis model assessment (HOMA) [HOMA-IR = (glucose (mg/dl) x 0.05551) x insulin (IU/ml) / 22.5]. The intra- and inter-assay coefficients of variation of the aforementioned assays were all <10%.

Statistical analysis

We adopted a clustering tree with MV in GAP (Chen, 2002; Tien *et al.*, 2008; Wu *et al.*, 2008, 2010) to determine the symptom patterns and phenotypic clustering of women with PCOS. GAP is a graphical technique that can simultaneously explore the associations of up to thousands of subjects, variables, and their interactions, without first reducing dimensions. Five levels of information can be retrieved, as follows: preliminary score for each patient/symptom combination; individual patient score-vector across all symptoms and individual symptom-vector on all patients; association score for each patient-patient and symptom-symptom relationship; grouping structure or symptoms and clustering effect for patients; and interaction pattern of the patient-clusters on symptom-groups. MV permutes the rows and columns of the raw

doi:10.6342/NTU202000313

data matrix by suitable re-ordering algorithms, together with the corresponding proximity matrices. The permuted raw data matrix and two proximity matrices are then displayed as matrix maps through suitable color spectra, and the subject-clusters, variable-groups, and interactions embedded in the data set can be visually extracted.

Some statistical analysis was performed using SPSS (version 17.0). The numeric variables are presented as the mean (SD), unless indicated otherwise. Associations between demographic and clinical characteristics of the patients according to the different clusters from GAP analysis were assessed using one-way analysis of variance (ANOVA) for continuous variables and chi-square or Fisher's exact tests for categorical variables, as appropriate. The Bonferroni *post hoc* test was applied when ANOVA revealed statistical significance. Two-stage linear discriminant analysis (LDA) done by the "MASS" package (Venables and Ripley, 2002) were used to determine if the model composed by the four selected endocrine measurements was adequate to predict MS. The validation was estimated using a leave-one-out cross-validation procedure (Burman, 1989). All tests were two-tailed with a confidence level of 95% ($P < 0.05$).

Study 2: Increased platelet factor 4 and aberrant permeability of follicular fluid in PCOS.

Patient recruitment

This was a tertiary center-based case-control study. From September 2014 to December 2015, patients with PCOS who underwent *in vitro* fertilization-embryo transfer (IVF-ET) at our hospital were enrolled. This study was approved by the Ethics Committee of the National Taiwan University Hospital (No.: 201302062RIND). The diagnosis were made according to the 2003 Rotterdam criteria, and at least 2 of the following 3 criteria were fulfilled: (1) amenorrhea or oligomenorrhea (fewer than 9 spontaneous menstrual cycles per year for at least 3 years before enrollment); (2) biochemical hyperandrogenemia (serum total testosterone level $\geqq$ 0.8 ng/ml) and/or clinical HA, including hirsutism and alopecia; and (3) polycystic ovaries on ultrasound (>twelve 2-9 mm follicles or an ovarian volume > 10 ml in at least 1 ovary). Other endocrine and organic abnormalities, such as hyperprolactinemia, thyroid dysfunction, Cushing's syndrome, congenital adrenal hyperplasia, and adrenal or ovarian tumors, were excluded. Hirsutism was defined as a Ferriman–Gallwey score > 8. Patients without PCOS who underwent IVF-ET for male factor and/or tubal factor infertility were selected as the control group. In our study, the criteria of

doi:10.6342/NTU202000313

amenorrhea/oligomenorrhea was fulfilled in every PCOS patients. Only the patients who had regular menstrual cycles and showed good response to ovarian simulation (more than 20 follicles larger than 10mm before oocyte triggering) were enrolled as the control group. The reason of choosing good responders with normal ovulatory function was to make sure the ovarian reserve was comparable between the PCOS and control group. If we chose the women with different ovarian reserves as the control group, it would be difficult to tell whether the differences of ovarian angiogenetic cytokines were related to the ovarian reserve per se or to the mechanism of PCOS. Therefore we determined the ovarian reserve as a controllable confounding factor and we chose ovulatory women with comparable retrieved oocyte numbers as the control group.

Controlled ovarian stimulation, oocyte retrieval and follicular fluid collection

After a period of controlled ovarian stimulation (COS), FF was collected during oocyte retrieval. COS was performed according to the standard gonadotropin-releasing hormone (GnRH) antagonist protocols described in our previous publications (Lee et al., 2006; Ho et al., 2008; Huang et al., 2012) (GnRH antagonist: Cetrotide®, cetrorelix acetate; Merck-Serono, Geneva, Switzerland). Ovarian stimulation was achieved with recombinant follicle-stimulating hormone (rFSH, Gonal-F®; Merck-Serono, Geneva, Switzerland) or highly-purified human menopausal gonadotropin (hp-hMG, Menopur®; Ferring Pharmaceuticals, Geneva, Switzerland), containing 75 IU/ampules of FSH and LH activity. IVF/ICSI cycles were monitored by serial folliculometry and assessment of serum estradiol, progesterone and LH levels every 1–2 days, starting from Day 6 in GnRH antagonist protocol and continued until the day of hCG injection for the final oocyte maturation. A dose of 6500IU hCG (Ovidrel®; Merck-Serono) or two doses of 3.75mg triptorelin (Decapeptyl®; Ferring Pharmaceuticals, Switzerland) was administered when two or more than two follicles reached 18 mm in diameter. Oocyte retrieval was scheduled 34–36 h later. To obtain the FF and avoid contamination from blood and flush medium during oocyte retrieval, only the FF from the first retrieved follicle (mean diameter = 18–20 mm) was collected. The presence or absence of blood contamination was determined by visual inspection, and samples with blood staining were discarded. The obtained fluid was centrifuged at 350g for 5 min to remove cells and frozen at −80°C for subsequent assays.

Human umbilical vein endothelial cells (HUVECs)

Human umbilical vein endothelial cells (HUVECs) were purchased from the American Type Culture Collection (Rockville, MD, USA). HUVECs are cultured in M199 medium supplemented with 20% fetal bovine serum, endothelial cell growth supplement (Intracel, Rockville, MD, USA), heparin, L-glutamine, penicillin, and

doi:10.6342/NTU202000313

streptomycin in a humidified atmosphere of 95% air and 5% CO_2 at 37°C. The following experiments were performed using HUVECs at $\leq$ 5 passages.

HUVEC monolayer permeability assay

HUVECs were cultured in Transwell chambers (0.4-μm pore polycarbonate filters; Costar, Cambridge, MS, USA). After reaching confluence, the medium was replaced with the FF (1/10 dilution with normal saline; 0.3 ml in the upper chamber and 1 ml in the lower chamber). Horseradish peroxidase (HRP) molecules (type VI-A, 44 kDa; Sigma-Aldrich, St. Louis, MO, USA) at a concentration of 0.126 μM was added to the upper compartment. HRP diffusion through the HUVEC monolayer was measured as previously described (Essler et al., 1999), with some modifications. After incubation for 1 h, the medium in the lower compartment was assayed for enzymatic activity using a photometric guaiacol substrate assay (Sigma-Aldrich). The permeability was calculated by dividing the concentration of HRP molecules in the lower compartment measured 1 h after adding the FF and HRP molecules into the upper compartment by the initial HRP concentration. The induced permeability of FF when adding VEGF with a concentration of 50 ng/ml was defined as 100% and the relative permeability was calculated accordingly.

Recombinant protein and antibody

Recombinant human platelet factor 4 (rhPF4) protein (795-P4-025/CF) was purchased from R and D Systems (Minneapolis, MN, USA). Anti-interleukin-8 (anti-IL-8, sc-8427), anti-PF4 (sc-374195), and anti-albumin antibodies (sc-271605) were purchased from Santa Cruz Biotechnology, Inc. (Santa Cruz, CA, USA).

Human angiogenesis antibody array

A human angiogenesis antibody array (Proteome Profiler™; R&D Systems) was used to analyze the protein profiles. Briefly, FF samples (1/10 dilution with normal saline) were first mixed with the biotinylated detection antibody cocktail at room temperature for 1 h, while the array membrane was blocked with the blocking solution provided by the manufacturer. Then, the membrane was incubated with the samples overnight at 2-8 °C on a shaker. After washing, HRP-conjugated streptavidin was added to the membrane for 30 min at room temperature, and signal development was achieved by addition of the commercial chemiluminescent detection reagents. A digital imaging system (Biopioneer, Inc., San Diego, CA, USA) was used to detect the signals, which were further analyzed using the ImageJ® program.

doi:10.6342/NTU202000313

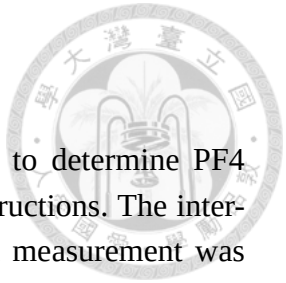

Enzyme immunoassay (EIA)

A PF4 EIA kit (DPF40 for PF4; R&D Systems) was used to determine PF4 concentrations in the human FF according to the manufacturer's instructions. The inter- and intra-assay coefficients of variation are 7.0% and 11.2%. Each measurement was performed in duplicate.

Immunoprecipitation and Western blot

To determine the interaction between IL-8 and PF4, 50 uL of FF was mixed with the Mammalian Protein Extraction Reagent (Pierce, Rockford, IL, USA). Immunoprecipitation with anti-IL-8 or with anti-PF4 antibodies was performed for 4 h; the immune complexes were incubated with protein A-Sepharose. The samples were then subjected to sodium dodecyl sulfate-polyacrylamide gel electrophoresis (SDS-PAGE) and probed with anti-PF4 and anti-IL-8 antibodies overnight. The supernatants of each sample after protein A-Sepharose purification (20 µl) was subjected to SDS-PAGE and probed with anti-albumin antibody. The membranes were then incubated with secondary antibody for 30 min and processed for detection of the specific proteins. Signal development was achieved by addition of the commercial chemiluminescent detection reagents. A digital imaging system (Biopioneer Inc.) was used to detect the signals. The density of the protein bands on the Western blot image was analyzed with the ImageJ image processing program.

Filamentous actin (F-actin) fluorescence staining

HUVECs were fixed with 3.7% paraformaldehyde for 20 min and permeabilized with 0.1% Triton-X-100. Fluorescence isothiocyanate-conjugated phalloidin (Invitrogen, Carlsbad, CA, USA), diluted in PBS (2 U/ml) was then applied to the specimens in the dark for 1 h. The specimens were mounted with 10% glycerol. The images were viewed using a fluorescence microscope (Nikon, Tokyo, Japan).

Statistical analysis

In this study, each experiment was repeated at least three times on different occasions. The numeric variables were presented as the mean ± standard deviation. The Mann–Whitney U test was performed for non-parametric analysis due to the small sample size. All tests were two-tailed with a confidence level of 95% ($P < 0.05$). The Statistical Program for Social Sciences (SPSS version 17; SPSS, Inc., Chicago, IL, USA) was used for all calculations.

doi:10.6342/NTU202000313

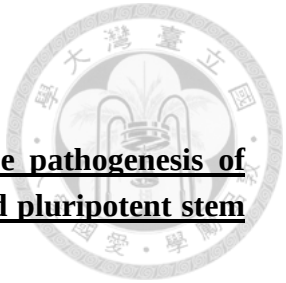

Study 3: Hyperactive CREB signaling pathway involved in the pathogenesis of polycystic ovarian syndrome revealed by patient-specific induced pluripotent stem cell modeling.

Patient recruitment and ethical approval

The current study was a case-controlled clinical and experimental study in a single university hospital setting with approval by the Research Ethics Committee of the National Taiwan University Hospital. From June 2014 to March 2016, 18 patients with PCOS and 10 non-PCOS controls were enrolled and informed consent was obtained from all. In the PCOS group, 16 patients had primary GC retrieval during IVF (genomic DNA methylation analysis was conducted in 11 cases and Western blotting validation was performed later in an additional 5 cases) and 2 patients had skin biopsy for iPSC experiments. In the control group, 8 subjects had primary GC retrieval during IVF (genomic DNA methylation analysis was conducted in 4 cases and Western blotting validation was performed later in an additional 4 cases) and 2 patients had skin biopsy. PCOS was diagnosed according to the 2003 Rotterdam criteria, and at least 2 of the following 3 criteria were fulfilled: (1) amenorrhea or oligomenorrhea (fewer than 8 spontaneous menstrual cycles per year for at least 3 years before enrollment); (2) biochemical hyperandrogenemia (serum total testosterone level $\geqq$0.8 ng/ml) and/or clinical HA, including hirsutism and alopecia; and (3) polycystic ovaries on ultrasound. Patients with other endocrine and organic abnormalities, such as hyperprolactinemia, thyroid dysfunction, Cushing's syndrome, congenital adrenal hyperplasia, and adrenal or ovarian tumors, were excluded. Hirsutism was defined as having a Ferriman-Gallwey score >8. A total of 10 PCOS subjects (including 2 subjects with skin biopsy) were full-blown phenotype (Type A) and 8 PCOS subjects were non-hyperandrogenic phenotype (Type D). The control subjects had regular menstruation cycles (interval: 25-35 days). They did not have all three features of the Rotterdam criteria and had no known endocrinopathies.

Collection of primary adult granulosa cells

Primary adult GCs were collected during IVF treatment and transvaginal oocyte retrieval. The patients without PCOS but with regular menstrual cycles who underwent IVF for male factor and/or tubal factor infertility were selected for the control group in

doi:10.6342/NTU202000313

the analysis of primary adult GCs. After a period of controlled ovarian stimulation (COS), follicular fluid was collected during oocyte retrieval. COS was performed according to the standard gonadotropin-releasing hormone (GnRH) antagonist protocols described in our previous publications (Huang *et al.*, 2012) (GnRH antagonist: Cetrotide, cetrorelix acetate; Merck-Serono, Geneva, Switzerland). Briefly, ovarian stimulation was achieved using recombinant follicle stimulating hormone (rFSH, Gonal-F; Merck-Serono, Geneva, Switzerland) or highly purified human menopausal gonadotropin (hp-hMG, Menopur; Ferring Pharmaceuticals, Saint-Prex, Switzerland) containing 75 IU/ampules of FSH and LH activity. IVF/ICSI cycles were monitored using serial folliculometry, including an assessment of serum estradiol, progesterone, and LH levels every 1-3 days, starting at day 6 in the GnRH antagonist protocol and continuing until the day of oocyte triggering for the final oocyte maturation. Two doses of 3.75 mg triptorelin (Decapeptyl; Ferring Pharmaceuticals) were administered when ≥2 follicles reached 18 mm in diameter and oocyte retrieval was scheduled 34-36 h later. The GCs were isolated and prepared from follicular aspirates after oocyte removal. The samples were then centrifuged at 2000 rpm for 5 min to separate the fluid from the cells. The cell pellets were resuspended in Dulbecco's phosphate-buffered saline (DPBS; Gibco; Invitrogen Life Technologies, Gibco, Waltham, MA, USA), layered on 50% Ficoll-Paque density gradient media (GE Healthcare, Waukesha, WI, USA), and then centrifuged at 2000 rpm for 5 min to remove the red blood cells. To remove debris, tissue, and more red blood cells, the GCs at the interface were collected and transferred to matrix-coated gel (Matrigel; Corning Incorporated, Corning, NY, USA) to culture for 2-3 days. The GCs were ultimately collected from the medium for further DNA, RNA, and protein extraction.

iPSC derivation and differentiation into granulosa cells

Isolation of skin fibroblasts and cell culture

Skin fibroblasts from 2 women with PCOS and 2 non-PCOS controls were obtained by skin biopsy that was performed during benign gynecological surgery. One piece of 1 cm^2 size skin tissue was removed from the abdominal wall. Skin fibroblasts were isolated and cultured in DMEM supplemented with 10% fetal bovine serum, non-essential amino acid, L-glutamine, and penicillin/streptomycin. Human skin fibroblast-derived iPSCs were maintained on mitomycin C-inactivated MEF with ReproCELL serum-free medium (ReproCELL, Shin-Yokohama, Japan) supplemented with 10 ng/ml of basic fibroblast growth factor.

doi:10.6342/NTU202000313

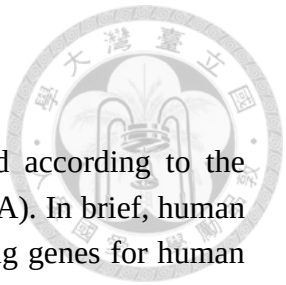

PCOS and non-PCOS iPSC derivation

PCOS and non-PCOS iPSC reprogramming was performed according to the manufacturer's instructions (System Biosciences, Palo Alto, CA, USA). In brief, human skin fibroblasts were electroporated with episomal plasmids encoding genes for human OCT4, SOX2, LIN28, KLF4, c-MYC, p53shRNA, and miR-302/367 clusters using the ECM 830 Square Wave Electroporation System (BTX, Holliston, MA, USA). The cells were plated to gelatin-coated 6-well plates with fibroblast growth medium. After cell confluency reached 80%, the cells were replated on mitomycin C-inactivated MEF with fibroblast growth medium. After 16 h, the medium was replaced with iPSC growth medium supplemented with PSGen Reprogramming Supplement. The embryonic stem cell (ESC)-like cell colonies appeared after 15-20 days and were selected after day 20. The expression of episomal reprogramming vectors was determined using SYBR Green qPCR. Alkaline phosphatase staining and immunostaining of pluripotency markers were performed using a Complete Antibody and AP staining Kit SAB-KIT-1 (SBI, System Biosciences). Two ESC lines, NTU1 (Lan *et al.*, 2013) and H9 (Thomson *et al.*, 1998; WiCell, Madison, WI, USA), were used as positive controls in this study.

Granulosa cell differentiation

GC differentiation was done as previously described in human ESCs (Lan *et al.*, 2013). Briefly, the iPSC colonies were manually split into small clumps and plated onto petri dishes to form embryoid bodies (EBs). The EBs were cultured for 2 days in maintenance medium that contained DMEM/F12 medium supplemented with 20% knockout serum, replacement, non-essential amino acid, GlutaMAX, and β-mercaptoethanol. After 2 days, the EBs were cultured for 1 day in maintenance medium supplemented with BMP4 followed with BMP4, WNT3A, and activin A for the next 3 days. For further induction toward GCs, the EBs were transferred to gelatin-coated cell culture dishes and cultured on maintenance medium supplemented with BMP4 and follistatin for 6 days.

Validation of iPSC pluripotency

In vitro differentiation

In vitro differentiation was performed according the manufacturer's instructions (R&D Systems, Minneapolis, MN, USA). Briefly, the cells were dissociated using

doi:10.6342/NTU202000313

Accutase and plated on RGF/BME-coated coverslips in mouse embryonic fibroblast-conditioned medium supplemented with 4 ng/ml basic fibroblast growth factor. After the cells reached 50% confluency, the medium was replaced with differentiation medium. The samples were collected on day 4 and stained with anti-Otx2, Brachyury, and Sox17 antibody.

Teratoma formation assay

1×10^7 iPSCs were injected subcutaneously into the dorsal trunk of 6- to 8-week-old NOD-SCID mice. Teratomas developed after 8-12 weeks and were excised for histological analysis using hematoxylin and eosin staining. For the experiments involving mice, all of the animal care procedures and experiments were performed according to the Assessment and Accreditation of Laboratory Animal Care-approved guidelines using protocols approved by the Institutional Review Board-Institutional Animal Care and Use Committee of National Taiwan University.

Functional validation of iPSC-derived granulosa cells

Extraction of DNA, RNA, and protein

The DNA and RNA of the GCs were extracted using an AllPrep DNA/RNA Mini Kit (Qiagen, Hilden, Germany) per the manufacturer's instructions. The sample yield and purity was measured after each step using a Nanodrop ASP-2680 (ACTGene, Piscataway, NJ, USA). The proteins were extracted using a Subcellular Protein Fractionation Kit for Cultured Cells (Thermo Fisher Scientific, Waltham, MA, USA) per the manufacturer's instructions. The protein yield and purity was measured using a DTX 800 Multimode Detector (Beckman Coulter, Brea, CA, USA).

RT-PCR and qPCR

PCR was performed using a GoTaq Green Master Mix (Promega, Madison, WI, USA). Quantitative PCR was performed using the Applied Biosystem TagMan (Thermo Fisher Scientific) or 1x EvaGreen reagent (catalog number 31014; Biotium, Fremont, CA, USA) and analyzed using a StepOnePlus Real-Time PCR system (Thermo Fisher Scientific). Primer sequences and TaqMan probe assay IDs for the PCR and qPCR systems used are listed in Table 1. Glyceraldehyde 3-phosphate dehydrogenase (GAPDH) transcript expression was used as an internal control for quantification.

doi:10.6342/NTU202000313

Immunohistochemistry

The cells were fixed using 4% paraformaldehyde in PBS for 30 min at room temperature. After washing with PBS, the cells were permeabilized with 0.1% Triton X-100 in PBST (0.1% TWEEN 20 in PBS) and blocked with 3% BSA in PBST. Primary antibodies, including NANOG, OCT4, SSEA4, and TRA1-60 (SAB-KIT-1), were used and incubated overnight at 4°C. Secondary antibodies included Alexa Fluor 488 goat anti-rabbit IgG or Alexa Fluor 488 rabbit anti-mouse IgG (Thermo Fisher Scientific) and were incubated for 30 min at room temperature. The cells were counterstained with Hoechst 33342 to visualize the nuclei.

Flow cytometry analysis

The cells were dissociated into single cells using Accumax. The staining procedure was performed according to the manufacturer's instructions (Affymetrix; Thermo Fisher Scientific). The cells were blocked using human Fc receptor inhibitor purified in flow cytometry staining buffer (Affymetrix; Thermo Fisher Scientific). The primary antibodies included rabbit anti-aromatase (CYP11A1) PE-conjugated (Bioss, Woburn, MA, USA), rabbit anti-AMHR2 488-conjugated (Bioss), and mouse anti-FSHR APC-conjugated antibody (R&D Systems). Isotype control cells were treated with non-specific isotype-matched antibodies. Before aromatase staining, the cells were fixed and permeabilized. The protein expression level was analyzed using a FACSCalibur flow cytometer (BD Biosciences, Franklin Lakes, NJ, USA). Conjunction of AMHR2 and FSHR was used to sort and purify the twelve-day iPSC-derived GCs for subsequent methylation array analysis.

Aromatase activity assay and measurement of estradiol levels

An aromatase activity assay was conducted by measuring the estradiol levels in the culture medium after treating the cultured cells with testosterone. Each culture treatment was replicated at least 3 times. Differentiated GCs (day 12) of the PCOS and non-PCOS iPSCs, human ESCs (H9), and human GCs were seeded at a density of 4×10^5 cells/well and cultured in 6-well plates. After a 24-h culture, the cells were incubated for 24 h in maintenance medium with 50 ng/mL testosterone (Sigma-Aldrich, St. Louis, MO, USA). The culture media were collected for the measurement of the estradiol levels using estradiol enzyme immunoassay (EIA) kits (Cayman Chemical, Ann Arbor, MI, USA).

Bisulfate conversion, DNA amplification, fragmentation, and hybridization of the

doi:10.6342/NTU202000313

Illumina Infinium methylation array

Whole genomic DNA methylation profiles were assayed in primary adult ovarian GCs and iPSC-derived GCs after 12 days of culture. Genomic DNA was isolated using proteinase K-phenol-chloroform extraction following standard protocols with 0.5% SDS and 200 μg/ml proteinase K. The concentration of DNA was normalized to 50 ng/μl and total genomic DNA (500 ng) was used for DNA bisulfate conversion using an EZ DNA Methylation kit (Zymo Research, Irvine, CA, USA). 200ng of bisulfate-treated DNA was used for Infinium MethylationEPIC BeadChip analysis (Illumina, San Diego, CA, USA). The EPIC BeadChip covers over 850,000 CpG sites and contains greater than 90% of the previous Illumina Infinium Methylation450 BeadChip content plus an additional 350,000 CpGs in the enhancer regions. Briefly, the bisulfate-converted DNA was amplified 1000X by DNA polymerase during the incubation step in an Illumina Hybridization Oven for 20-24 h at 37°C. The amplified DNA products were then fragmented into 300-600 base pairs. After alcohol precipitation and resuspension of the fragmented DNA, the BeadChip was prepared for hybridization in the capillary flow-through chamber. The amplified and fragmented DNA samples annealed to locus-specific 50-mers during the hybridization step at 48°C for 16 h in the Illumina Hybridization Oven. After hybridization, allelic specificity was conferred by enzymatic single base extension. The products were subsequently fluorescently stained using biotin-ddNTP or dinitrophenol-ddNTP. The intensity of the bead fluorescence was detected using an Illumina HiScan.

EPIC BeadChip data quality control and normalization

The resulting raw data (IDATs) from the arrays were preprocessed and corrected using Illumina GenomeStudio (v2010.1) software for an initial quality check that involved color bias correction and background adjustment. Further probe filtering, quantile normalization, and β value to M value transformation were performed under an R statistical environment (v.3.1.1). A beta (β) value of 0-1.0 was reported for each CpG site (methylation ranging from 0% to 100%, respectively). The β value was calculated as the ratio of the methylated signal intensity to the sum of both methylated and unmethylated signals to represent the methylation values for individual CpG sites. The M value was calculated as the log2 ratio of the intensities of the methylated probe versus the unmethylated probe. Analyses of differentially methylated genes between the PCOS and controls of the adult GCs and day 12 iPSC-derived GCs were performed using MetaCore (Thomson Reuters, New York, NY, USA) and Ingenuity Pathway Analysis (IPA) (Qiagen, Hilden, Germany).

Expression array analysis

doi:10.6342/NTU202000313

Affymetrix GeneChip Human Genome Gene 1.0 ST microarray chips (Thermo Fisher Scientific) were performed on the primary adult GCs following the manufacturer's protocol as briefly described in our previous publication (Lan et al., 2015).

Western blotting analyses

Total protein was extracted from the primary adult GCs from the PCOS and non-PCOS women. Thirty micrograms of protein per lane was separated by SDS-PAGE and blotted onto polyvinylidene difluoride membranes. The membranes were then blocked using 3% BSA (Bovogen, Keilor East, Australia) in Tris-buffered saline TWEEN 20 (Gibco) and incubated overnight at 4°C with one of the following primary antibodies: human CREB antibody (1:1000; Cell Signaling Technology. Danvers, MA, USA), human CBP antibody (1:1000; R&D Systems), or human GAPDH antibody (1:5000; R&D Systems). The polyvinylidene difluoride membranes were incubated for 60 min at room temperature with the following secondary antibodies: donkey anti-mouse antibody (R&D Systems) or goat anti-rabbit antibody (Cell Signaling). The immune complexes were detected by chemiluminescence using the MGIS-21 Western blotting analysis system (TOPBIO CO., New Taipei City, Taiwan).

Statistical analysis

All of the results were derived from experiments performed in triplicate. The results were presented as mean±standard deviation. The Mann-Whitney U test was used to examine the significance of the between-group differences. All of the tests were two-tailed with a confidence level of 95% ($P<0.05$), except for the 90% confidence interval used in Supplemental Figure 8. The Statistical Program for Social Sciences (SPSS version 17; SPSS, Inc., Chicago, IL, USA) was used for all of the calculations.

Study 4: Circulatory miRNAs as prediction models for the diagnosis of PCOS and the therapeutic effects of metformin.

Selection of subjects

The patients of PCOS might initially seek evaluation at the clinic for menstrual irregularities and/or clinical symptoms of HA, such as hirsutism and alopecia. The recruited patients cannot receive medical treatment, including oral contraceptives,

doi:10.6342/NTU202000313

insulin-sensitizing agents, anti-androgenic agents, ovulation-induction agents, and Chinese herbal medicines, within 3 months before enrollment. The diagnosis is made according to the 2003 Rotterdam criteria, and at least 2 of the following 3 criteria were fulfilled: amenorrhea or oligomenorrhea (fewer than nine spontaneous menstrual cycles per year for at least 3 years before enrollment); biochemical hyperandrogenemia (serum total testosterone level ≧ 0.8 ng/ml) and/or clinical HA, including hirsutism and alopecia (acne was excluded due to inconsistency of the correlation with HA in the literature); and PCOM on ultrasound (greater than twelve 2-9 mm follicles or an ovarian volume > 10 ml in at least 1 ovary). Other endocrine and organic abnormalities, such as hyperprolactinemia, thyroid dysfunction, Cushing's syndrome, congenital adrenal hyperplasia, and adrenal or ovarian tumors will be excluded. Hirsutism is defined as a Ferriman–Gallwey score > 8. The control group will be selected from healthy women asking for Pap smear or HPV vaccine.

Protocol

All subjects receive collection of blood samples, anthropometric measurements, pelvic ultrasonography, and measurements of blood pressure on the same day. Overnight fasting venous blood samples are collected in the early follicular phase in patients with spontaneous ovulation cycles, and randomly in amenorrheic patients. Blood samples are processed within 30 minutes of collection and the levels of serum glucose and insulin were measured on the same day. The remaining serum and plasma are frozen at -80℃ until assayed. Pelvic ultrasonography is performed by 1 or 2 experienced gynecologists using a transvaginal approach whenever possible. The number of follicles ranging from 2-9 mm in diameter are counted and the ovarian volume is calculated with a simple formula (0.5 x length x width x thickness). Obesity is defined as a body mass index (BMI) ≧ 25 kg/m2, which is based on the guidelines for an adult Asian population (WHO Expert Consultation, 2004). The establishment of MS required at least 3 of the following 5 criteria: a systolic blood pressure (SBP) ≥ 130 mmHg and/or a diastolic blood pressure (DBP) ≥ 85 mmHg; a fasting glucose ≥ 100 mg/dl; a fasting triglyceride (TG) ≥ 150 mg/dl; a high-density lipoprotein-cholesterol (HDL-C) < 50 mg/dl; and abdominal obesity (waist circumference (WC) > 80 cm).

Serum preparation and RNA extraction

doi:10.6342/NTU202000313

Five ml venous blood is collected from each participant using a procoagulant drying tube. The whole blood is separated into serum and cellular fractions by centrifugation at 4,000 rpm for 10 min, followed by 12000 rpm for 15 min to completely remove cell debris. Isolation of serum total RNA is performed with the Trizol Reagent for serum denaturizing and Qiagen miRNeasy Mini kit (Qiagen, Valencia, CA) for RNA collection and purification according to the manufacturer's protocol. Synthetic C elegans miR-39 will be added to a final concentration of 1024pmol/ ml for all samples in order to control variations in RNA extraction and/or purification procedures because of the absence of homologous sequences in humans. Furthermore, all study subjects are recruited during the same period, and the samples are handled in equal volume in each experiment step to control the potential bias.

TLDA chip miRNA microarray

The expression profiles of the miRNAs are determined using the TaqMan Array Human MicroRNA A and B Cards Set version 3.0 (Applied Biosystems). The cards contain assays for 766 mature miRNAs present in the Sanger miRBase version 18.0. RT-PCRs are performed with Megaplex Primers Pool A with preamplification according to the manufacturer's instructions. PCRs are performed using 450 L TaqMan Universal PCR Master Mix, No AmpErase UNG(2X), and 9 uL diluted preamplification product, and the reactions are brought to a final volume of 900 uL. One hundred microliters of the PCR mix are dispensed into each port of the TaqMan miRNA array, and the fluidic card is centrifuged and mechanically sealed. Quantitative RT-PCR was carried out on an Applied Biosystems 7900HT thermocycler using the manufacturer's recommended program. Detailed analysis of the results is performed using the Real-Time Statminer software package (Applied Biosystems).

Reverse transcription (RT) and quantitative PCR (qPCR)

Total RNA is reverse transcribed using the TaqMan MicroRNA Reverse Transcription Kit (Life Technologies, Paisley, UK) following manufacturer's instructions. Mature miRNA TaqMan assays are purchased from Life Technologies and the generated cDNA amplified using the Taqman 2x Universal PCR master mix, No AmpErase UNG (Life Technologies), with each reaction performed in triplicate. The amplification is performed in a StepOnePlus PCR System (Life Technologies) in 96

doi:10.6342/NTU202000313

well plates. The amplification curves are analyszed using the StepOne software (Life Technologies) and the comparative Ct Method (Δ CT Method). Calibration is based on the expression of the C-elegans miR-39 spike-in.

Gene ontology pathway analysis and miRNA target network analysis

Potential miRNA targets were identified from TargetScan (http://www.targetscan.org/vert_72/). Final target lists and relevant miRNAs were uploaded to Panther (http:// www.pantherdb.org/) were applied to annotate the biological functions of the predicted targets. The results were presented as mean±standard deviation. All of the tests were two-tailed with a confidence level of 95% ($P<0.05$) with appropriated statistical methods. The Statistical Program for Social Sciences (SPSS version 17; SPSS, Inc., Chicago, IL, USA) was used for all of the calculations.

RESULTS

Study 1: Symptom patterns and phenotypic subgrouping of women with polycystic ovary syndrome: association between endocrine characteristics and metabolic aberrations.

From 2008-2011, a total of 460 PCOS patients were recruited. All of the patients met the Rotterdam criteria, while the percentage of women with phenotypic oligomenorrhea/amenorrhea, ultrasonographic morphology of PCO, clinical HA and/or hyperandrogenemia was 92.4% (425/460), 94.3% (434/460), and 80.9% (372/460) (62.8% (289/460) and 52.8% (243/460) for clinical HA and hyperandrogenemia, respectively). The percentage of fulfillment of the Androgen Excess and PCOS Society (AE-PCOS) and National Institutes of Health (NIH) criteria was 85.9% (395/460) and 78.3% (360/460), respectively. The mean(SD) age was 24.7(5.0) years (range, 13-41 years) and the percentage of obesity (BMI $\geqq$ 25 mg/m^2) was 40.2% (185/460).

We standardized all the symptomatic variables with different scales. The GAP analysis generated two color graphics (Figure 1), including the correlation among 17 metabolic and 4 endocrine variables (symptom-dimension; Figure 1A), the clustering pattern among 460 patients (patient-subgroup), and the correlation between the

doi:10.6342/NTU202000313

symptom-dimension and the patient-subgroup (Figure 1B). The color map in Figure 1A revealed the proximity matrix of the between-symptom correlation coefficient for 21 symptomatic items. The extreme dark red color represents a correlation coefficient of 1 (positive correlation), white represents 0 (no correlation), and the extreme dark blue color represents -1 (negative correlation). The dimensions of symptoms were designated into two major categories (endocrine and metabolic measurements). As expected, there was a strong positive correlation (dark red) between measurements of HOMA-IR, blood pressure, anthropometric measurements, and lipid profiles, while HDL-C only had a moderate positive relationship (red) with total cholesterol and revealed a negative relationship (blue) with all the other metabolic measurements. The LH level revealed a strong negative correlation (dark blue) with anthropometric measurements.

In Figure 1B, the relationship structure of 460 patients according to the level on the 21 symptomatic measurements was analyzed and plotted in the matrix map. Each patient was shown as a stripe with a color representing the relative severity of symptomatic expression, with red indicating an expression above average, blue indicating an expression less than average, and white representing the mean expression. To ascertain whether or not there is a specific endocrine or metabolic signature corresponding to each subgroup of different PCOS phenotypes, we performed a GAP clustering tree. The patients were clustered into four distinct phenotypic subgroups based on the correlation of four endocrine characteristics (FSH, LH, FAI and DHEA-S levels) that the patients with higher correlation between these four endocrine variables will be located more closely on the clustering tree. For example, the patients in the cluster 1 exhibited a higher FSH and/or LH level (red-color stripes on the FSH and/or LH column) and lower FAI level (blue-color stripes on the FAI column), therefore they were clustered together, and the corresponding stripes of the metabolic variables were blue color, indicating a relative lower value of the metabolic measurements. In contrast, the patients in the cluster 4 exhibited higher FAI level (red stripes on the FAI column) and therefore were grouped together. And the corresponding metabolic measurements obviously had higher values that most of the stripes of the metabolic variables were red-colored. In the end, each resulting subgroup exhibited a different risk of metabolic aberration (Figures 1B and 2).

The anthropometric characteristics, and hormonal and metabolic profiles of the four different clusters derived from the GAP analysis are listed in Table 2. There was no significant difference in the age, height, and total cholesterol level between the clusters. Cluster 4 (N=57) had the highest mean FAI and total testosterone level, and presented with the most severe metabolic aberration, including IR, elevated liver enzymes, dyslipidemia, and elevated blood pressure. Cluster 1 (N=204) was characterized by low FAI, but a relatively high mean LH levels. It also represented the most favorable

doi:10.6342/NTU202000313

metabolic outcomes, which had significantly lower mean glucose, insulin, HOMA-IR, uric acid, and TG levels, and higher HDL-C levels.

The prevalence of MS in the four clusters and the corresponding number of fulfilled criteria items are shown in Figure 2. The mean prevalence of MS in our study population was 19.3% (89/460) and there were significant differences between clusters (P<0.0001). Cluster 1 had a significantly lower prevalence of MS (7%), while cluster 2 and 4 had the higher prevalence of MS. Although cluster 2 had a relatively lower mean total testosterone and FAI level, the risk of MS was still high (30%).

The prevalence of different PCOS features and four phenotypic subgroups of Rotterdam criteria in each cluster were shown in Table 3. Since most of the patients in our study population were full-blown Rotterdam phenotype (67.6%), it remained the largest proportion in each cluster. However, the cluster 4, in which nearly half of the patients had MS, had significantly largest proportion of the full-blown Rotterdam phenotype (94.7%) and no any non-hyperandrogenic Rotterdam phenotype within it.

Figure 3 showed the proportion of each cluster in different phenotypic subgroups of Rotterdam criteria. Although there were significantly more cases of cluster 4 in the full-blown phenotype, only 17.4% of cases with full-blown phenotype were cluster 4. And the cluster 1 to 3 distributed equally within each Rotterdam phenotypes. Therefore the definition of specific Rotterdam subgroup could not be indicative of a specific cluster. Other potential characteristics that might be more indicative of a specific cluster were shown in Figure 4. There was a higher proportion of cluster 4 in the patients with hyperandrogenemia or obesity. Besides, the most indicative phenotype to cluster 1 was higher LH level. Ninety-five percent of the patients who had a serum LH level higher than 15mIU/ml (the 75th percentile of our study population) were cluster 1, which corresponded to the lowest risk of MS.

There was no significant difference in the prevalence of MS amongst different phenotypic subgroups of Rotterdam criteria (P=0.317) and amongst different diagnostic criteria (P=0.981; Table 4).

Study 2: Increased platelet factor 4 and aberrant permeability of follicular fluid in PCOS.

Baseline characteristics of participants

doi:10.6342/NTU202000313

From 2014-2015, a total of 13 patients with anovulatory PCOS and 11 ovulatory controls were recruited. Almost every participant used antagonist protocol and only one patient in the control group used long protocol. The baseline characteristics and the outcomes of IVF therapy are shown in Table 5. The two groups were similar with respect to age, body mass index (BMI), percentage of nulliparas, and baseline FSH concentration. In contrast to the normal mean cycle length in the control group, every patient in the PCOS group was oligomenorrhea and the average interval between menstrual cycles was nearly 3 months. Approximately half of patients (7/13) in the PCOS group had biochemical and/or clinical HA. Among them, 3 patients exhibited biochemical hyperandrogenemia only, 2 patients exhibited both biochemical and clinical HA, and 2 patients exhibited clinical HA only. There was significantly higher serum LH concentration in the PCOS group. There were no significant difference in the characteristics and outcomes of IVF therapy between two groups with respect to the total dose of gonadotropin, the duration of COS, the serum estradiol and progesterone concentration on the day of oocyte triggering, the number of retrieved oocytes, the number of mature metaphase II (MII) oocytes, and the fertilization rate.

HUVEC monolayer permeability assay

To elucidate the influence of FF from the PCOS and control groups on endothelial cell permeability, a HUVEC monolayer was exposed to the FF with the addition of HRP molecules (Figure 5). The relative permeability was significantly less when induced by the FF from the PCOS group (46% ± 12% in the PCOS group [n=11] vs. 58% ± 9% in the control group [n=9], P=0.023).

Human angiogenesis array

Human angiogenesis array analysis was applied to determine which component within the FF might cause permeability changes (Table 6 and Figure 6). Among the 55 proteins tested, there was only 1 protein (PF4) that had significantly different signal values between the two groups (P=0.004; Figure 6A). A significantly higher level of PF4 existed in the FF of patients with PCOS. Further confirmation with an EIA also revealed a significantly higher concentration of PF4 within the FF of the PCOS group (51.6 ± 14.3 ng/ml in the PCOS group vs. 35.7 ± 3.8 ng/ml in the control group, P=0.013; Figure 6B).

doi:10.6342/NTU202000313

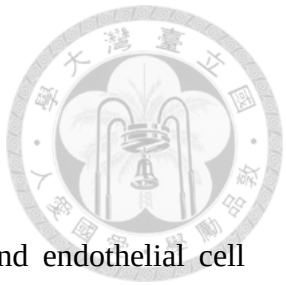

PF4 and endothelial cell permeability

To further elucidate the causal relationship between PF4 and endothelial cell permeability, we added rhPF4 to the control group FF in the HUVEC assay, and the resulting endothelial cell permeability decreased significantly (Figure 7A). Immunohistochemical staining revealed significantly decreased amounts of intercellular gaps between HUVECs after the addition of rhPF4 to the FF (Figure 7B). This finding provided clear and direct evidence that PF4 is responsible for the poor permeabilizing effect of FF from PCOS patients.

Interleukin-8/PF4 protein complex in the FF

Our previous research (Chen et al., 2010) has confirmed that intra-follicular angiogenic chemokines, such as IL-8 and VEGF, can enhance endothelial permeability and might play major roles in the pathogenesis of OHSS. Dudek *et al.*(2003) suggested that PF4 binds IL-8 with high affinity and blocks IL-8-mediated activation of hematopoiesis. To clarify this phenomenon, FF from the control and PCOS groups were subjected to the PF4/IL-8 protein complex in immunoprecipitation and immunoblotting assay, which revealed that the PF4/IL-8 protein complex exists in FF from both the PCOS and control groups (Figure 8A). Quantitative analysis demonstrated that the amount of IL-8 and PF4 in the PCOS group was significantly higher than the control group (Figure 8B). Because intercellular gap formation is one of the critical determinants of endothelial cell permeability, a confluent endothelial monolayer was treated with rhPF4 or rhPF4/rhIL-8 to confirm the anti-permeability effect of PF4 and the intercellular gap formation was determined by phalloidin staining. The results revealed that rhIL-8 induced the formation of intercellular gaps; however, the gaps were alleviated in the rhPF4+rhIL-8 group (Figure 8C). In the HUVEC monolayer permeability assay, rhIL-8-induced relative permeability was indeed blocked by the addition of rhPF4 (Figure 8D).

Taken together, our results proved the presence of the PF-4/IL-8 protein complex within human FF, and there was a higher amount of PF-4/IL-8 protein complex in the FF from the PCOS group than the control group. Furthermore, the presence of PF-4 could induce an anti-permeability effect on the endothelial cells through down-regulating the formation of intercellular gaps and antagonistic binding with IL-8

doi:10.6342/NTU202000313

(Figure 9).

Study 3: Hyperactive CREB signaling pathway involved in the pathogenesis of polycystic ovarian syndrome revealed by patient-specific induced pluripotent stem cell modeling.

Generation and characteristics of iPSC from the women with and without PCOS

Dermal fibroblasts obtained from the women with and without PCOS were reprogrammed using origin of replication/Epstein-Barr virus nuclear antigen-1 (ori/EBNA-1)-based episomal vectors carrying OCT4, SOX2, LIN28, KLF4, and c-MYC. Additional factors such as p53shRNA, miR302, and miR367 in the episomal system were used to overcome barriers associated with reprogramming and enhance reprogramming efficiencies. The timeline and culture conditions of the experiment are shown in Figure 10A. The iPSC colonies were formed and selected over the course of 20-25 days based on their morphological characteristics as small round cells growing in clusters with clear ages similar to ESC colonies (Figure 10B). Among a total of 11 iPSC cell lines derived from 2 PCOS women and 2 control women, we selected a colony that was most stable during culture from each patient for the subsequent differentiation studies (iNFB1-1 and iNFB3-3 for the controls and iPFB1-3 and iPFB3-1 for the PCOS). All of the iPSCs had a normal chromosome pattern of 44+XX by array CGH analysis (Figure 11).

Pluripotency and differentiation validation of iPSC from the women with and without PCOS

A total of 4 established iPSCs were analyzed for alkaline phosphatase activity demonstrating the undifferentiated and pluripotent potential of the iPSCs derived from the women with and without PCOS (Figure 12). Using immunofluorescence staining, both PCOS-iPSC (iPFB) and non-PCOS-iPSC (iNFB) had a positive presence of pluripotency-associated transcription factors and membrane markers including NANOG, OCT-4, SSEA-4, and TRA-1-60 (Figure 13). All of the established iPSCs were tested via RT-PCR for self-renewal genetic markers to determine the expression of DNMT3B, LCK, NANOG, OCT4, SOX2, GDF3, c-MYC, DPPA5, and TERT (Figure 14). Human ESC (hESC) line NTU1 was used as a positive control in the studies. No significant differences were discerned among all of the iPSC lines in terms of their expression of pluripotency markers.

doi:10.6342/NTU202000313

To examine the in vitro differentiation potential, the iPSCs were suspended for embryonic body (EB) formation and all 4 formed well-shaped EBs (Figure 15A). After re-plating the EBs onto culture dishes and culturing in ESC culture medium, the cells appeared to differentiate into cells with varied morphology. The resulting cells were analyzed using RT-PCR for markers characteristic of the three germ layers. A qRT-PCR analysis was performed to detect the expression of zinc finger and BTB domain containing 16 (ZBTB16) to detect the differentiated cells of the ectoderm, the expression of alpha-fetoprotein (AFP) to detect the differentiated cells of the endoderm, and the expression of cadherin 5 (CDH5) as the mesoderm marker (Figure 15B). To test the differentiation potential of the iPSCs' in vivo developmental propensity, we injected undifferentiated PCOS iPSCs and non-PCOS iPSCs into NOD-SCID mice and examined the formation of teratomas and cells containing all three embryonic germ layers (Figure 16). Tissue sections of the teratomas derived from the patients with and without PCOS by HE staining showed differentiated derivatives of ectodermal, mesodermal, and endodermal lineage, such as neuroepithelium, pigmented epithelium, retina-like structure, and squamous epithelium for ectoderm; adipose tissue, hyaline cartilage, and myxoid connective tissue for mesoderm; and glandular epithelium for endoderm (Figure 16). There was no discernible difference between the iPSCs derived from the women with and without PCOS regarding the ability to form teratomas. These findings indicated that the 2 PCOS-iPSCs and 2 non-PCOS iPSCs had been reprogrammed into a pluripotent state and possessed the ability for differentiation.

Characterization of the PCOS- and non-PCOS iPSC-derived granulosa cells

The four established iPSCs were successfully differentiated into cells with the function and characterization of ovarian GCs. The differentiated PCOS and non-PCOS iPSCs were collected on days 0(undifferentiated), 6, 9, and 12 to examine GC-associated genes, including FOXL2, AMH, FSHR, LHR, AMHR2, and CYP19A (Figure 17A-F). The expression of FOXL2, AMH, FSHR, AMHR2, and CYP19A was low or absent on day 0 (undifferentiated iPSCs), but became significantly detectable after day 6 of culture, when the expression of pluripotency gene OCT4 decreased concomitantly (Figure 17G). The expression of LHR was not different among the differentiation time points compared to the undifferentiated iPSCs. Comparisons between the PCOS and control groups at each differentiation time point did not reveal significant differences (Figure 17A-G). However, there were still trends of higher expression of AMH, AMHR2, OCT4, FSHR, and LHR and lower expression of FOXL2 in the PCOS group. The expression of concordant genes in the aspirated adult GCs did not reveal significant differences between the PCOS and control groups (data not shown). However, a trend of higher expression of AMHR2 (fold change (FC): 2.7), LHR (FC: 1.87), CYP19A1 (FC: 11.27), FOXL2 (FC: 2.4) genes was noted in the

doi:10.6342/NTU202000313

PCOS group compared to the control group (Figure 18).

Flow cytometry analyses were performed to identify the differentiated GCs using GC-specific markers including CYP19A1, FSHR, and AMHR in the PCOS and non-PCOS iPSC-derived GCs after 12 days of culture. There was no significant difference in the yield rate of the differentiated GCs between the PCOS- and non-PCOS-derived iPSCs (Figure 19). The aromatase (CYP19A1) activity assay was used to investigate the conversion ability of testosterone to estradiol in the differentiated GCs derived from the iPSCs (Figure 20). In this functional study, the estradiol levels significantly increased after testosterone treatment in both the PCOS and non-PCOS iPSC-derived GCs, consistent with our previously established ESC-derived GCs (H9) (Lan et al., 2013) and GCs derived from oocyte retrieval in women who were receiving IVF treatment. The latter two cells were used as positive controls in this study.

Comparative methylomic analysis revealed a common hyperactive CREB pathway in the primary adult GCs and iPSC-derived GCs

A genome-wide DNA methylation analysis was conducted to compare the methylation profiles between the PCOS and non-PCOS women in the iPSC-derived GCs and primary adult GCs. The adult GCs were retrieved from 11 patients with PCOS and 4 non-PCOS women (anthropometric and biochemical characteristics are shown in Table 7). A total of 13,326 probes (1.5%, 13,326/866,895) with missing beta values were eliminated from the raw data of the patients' GCs and 3,703 probes (0.4%) and were filtered from the day 12 iPSC-derived GC data, leaving a total of 853,569 and 863,192 probes for analysis, respectively.

A change in the signal value by >2.5-fold was the threshold for a differentially methylated region (DMR), and an enrichment pathway analysis was performed using MetaCore. A total of 472 DMR-located genes (from 796 probes) in the primary adult GCs and a total of 3,682 DMR-located genes (from 10,038 probes) in the iPSC-derived GCs were added for pathway analysis. The top 10 enriched canonical pathway maps of the DMR-located genes are listed in Table 8. The categories of these enriched pathways in the methylomic analysis of the iPSC-derived GCs included cytoskeletal remodeling, cell adhesion, neurophysiological processes, signal transduction, transcription, and development. The most commonly appeared network objects in the methylomic analysis of the primary adult GCs were protein kinase C (PKC), protein kinase A (PKA), and phosphatidylinositol-3 kinase (PI3K), which were linked to many regulatory pathways in the MetaCore analytical database, such as the thromboxane A2 signaling pathway, CREB signaling pathway, nociceptin receptor signaling pathway, oxidative stress, and proinsulin C-peptide signaling. When we compared the results of the methylation array

doi:10.6342/NTU202000313

in the primary adult GCs and iPSC-derived GCs, only the CREB signaling pathway was commonly preserved in the top 10 enriched pathway maps in both datasets. This should increase the functional significance of this signaling pathway, and therefore further validation of the involved molecules was performed. The datasets from both experiments also underwent IPA (Table 9), and a beta value >0.25 was indicative of DMRs. The overlapping top toxicological pathways included NRF2-mediated oxidative stress response and PPAR/RXR activation in the two experiments.

A principle component analysis of the entire DNA methylation level revealed distinct distributions between the PCOS and non-PCOS groups (Figure 21A). The hierarchical clustering analysis (heatmap) of the 115 differentially methylated genes is shown in Figure 21B. In general, the DMR-located genes tended to be more hypomethylated (yellow bar) in the PCOS group compared with the control group. A Venn diagram of the DMR-located genes between the day 12 iPSC-derived GCs and the primary adult GCs revealed 37 overlapping genes (Figure 21C). A list of the overlapping genes is documented in Table 10. The differentially methylated probes were both hypermethylated in 10 genes, both hypomethylated in 8 genes, and one hypermethylated and one hypomethylated in the remaining 19 genes. The number of hypermethylated and hypomethylated DMRs in relation to the nearest gene regions between the PCOS and the control group in the primary adult GCs and iPSC-derived GCs is shown in Figure 22. Both the hyper- and hypomethylated gene regions were located in all of the gene regions. There was a significantly higher enrichment of the hypermethylated gene regions located in the TSS200 (the region from the transcription start site [TSS] to 200 nt upstream of the TSS, $P<0.0001$) and the 5'UTR (untranslated region, $P=0.025$) than the hypomethylated gene regions in the primary adult GCs.

Validation of the overexpressed CREB/CBP in both the primary adult GCs and iPSC-derived GCs in the women with PCOS

Further quantitative validation of CREB and CREB binding protein (CBP) among the ovarian GCs was conducted on a separate cohort of five PCOS and four control subjects (Figure 23A and 23B). The expression of CBP proteins was significantly higher in the adult GCs from the PCOS patients ($P=0.027$). Higher expression of CREB protein was also observed in the PCOS group, although statistical significance was not reached, possibly due to a limited case number. The unchopped raw gels are shown in Figure 24. The expression level of CBP mRNA was also significantly higher from the 12-day iPSC-derived GCs in the PCOS group (Figure 23C) .

Study 4: Circulatory miRNAs as prediction models for the diagnosis of PCOS and

doi:10.6342/NTU202000313

the therapeutic effects of metformin.

(1) PCOS v.s. Control group

First, we compare the miRNA expression level between 75 PCOS patients and 20 control subjects. The characteristics of PCOS patients and control subjects were listed in Table 11. As we expected, there were significant differences in many hormonal and metabolic parameters. The PCOS group had a significantly high BMI, larger waist and hip circumference, higher serum testosterone level and LH level, higher LDL and uric acid level. There was no difference in age, baseline FSH level, insulin and glucose level.

The free miRNA expression level in plasma was quantified by qPCR. Initially we aimed to perform the miRNA microarray. However, after considering the cost we decided to choose targeted miRNA from the literatures. Seven miRNAs (miR-21, miR-93, miR-132, miR-193, miR-221, miR-222, miR-223) which had been reported to be related with glucose metabolism or diabetes and another seven miRNAs (miR-27a, miR-125b, miR-200b, miR-212, miR-320a, miR-429, miR-483) which had been reported to be related to ovarian and pituitary function were chosen. The plasma level of these circulating free miRNAs in the PCOS and control group are shown in the Table 12. The expression level of miR-93, miR-132, mR-221, miR-223, miR-27a and miR-212 were significantly higher and the level of miR-222 and miR-320a were significantly lower in the PCOS group.

The next step we established the prediction model for the diagnosis of PCOS according to the ROC curve of individualized miRNA. The diagnostic model of PCOS was as followed: Y = log (p/(1-p)) = 0.00148 – 10.8903 * miR-93 + 28.6881 * miR-132 - 48.8523 * miR-222 + 2.4562 * miR-27a + 2.1320 * miR-125b + 18.2793 * miR- 212. The AUC of our model was as high as 0.959 (95% CI: 0.924-0.995) and this suggested an excellent accurary of our prediction model (Table 15, Figure 25).

(2) Metformin-effective and metformin ineffective group

We recruited and analyzed 37 metformin-effective PCOS patients and 38 metformin ineffective patients in this part of the study. Table 13 showed the characteristics of patients in these two groups. There wasn't significant difference in nearly every characteristic except the interval of menstrual cycle. The interval was significantly longer in the metformin-ineffective group. And then we analyzed and compared the serum level of 14 selected miRNAs between two groups (Table 14). The

doi:10.6342/NTU202000313

expression levels of circulating miR-27a, miR-93 and miR-222 were significantly higher in the metformin-ineffective group.

The next step we established the prediction model for the therapeutic effects of metformin according to the ROC curve of individualized miRNA (Table 16, Figure 26). The prediction model was as followed: Y = log (p/(1-p)) = -1.8255 + 4.1106 * miR-93 + 18.0284 * miR-222 - 0.1152 * miR-223 + 145.8 * miR-429。The AUC of our model was 0.722 (95% CI: 0.602-0.841) and this suggested a good accurary of our model. We added four clinical parameters in our model to see whether the prediction accurary could be improved. The adjusted model was as followed: Y = log (p/(1-p)) = -2.0454 + 0.0242 * age (years) + 0.0219 * BMI (Kg/m^2) + 0.1168 * hyperandrogenism (0 or 1) - 0.00689 * interval of menstrual cycle (days) + 3.6416 * miR-93 + 25.4973 * miR-222 - 0.1253 * miR-223 + 163.0 * miR-429。The AUC of the adjusted model was 0.807 (95% CI: 0.704-0.909). The accurary seemed improved however the difference didn't reach statistical significance. The efficacy of our model was validated on a separate cohort of 71 PCOS patients, including 40 metformin-effective patients and 31 metformin-ineffective patients. The sensitivity and specificity of the first model with only miRNA level was 70% and 61%. The sensitivity and specificity of the second adjusted model with both clinical parameters and miRNA level was 98% and 35%.

(3) Gene ontology pathway analysis and miRNA target network analysis

Go pathway analysis was miRNA target network analysis was performed on the most discrimitive miRNAs in our models, including miR-132, miR-27a, miR-222, miR-93. The targets genes of these miRNAs were enriched mainly in the cellular metabolism pathways (Table 17-20).

DISCUSSION

Study 1: Symptom patterns and phenotypic subgrouping of women with polycystic ovary syndrome: association between endocrine characteristics and metabolic aberrations.

In this study we applied a powerful graphical analytical tool (GAP method) to determine symptoms correlation directly from data. GAP analysis is a dimension-free statistical visualization method which is different from the conventional graphic tools;

doi:10.6342/NTU202000313

specifically, all information is preserved in the final output. GAP analysis also has the advantage of providing direct visual perception for exploring information structures that are embedded within a massive and complex data set (Wu *et al.*, 2008). Since PCOS comprises a population with highly heterogeneous phenotypes, it is important to evaluate the patients individually with composite features and to improve their long-term outcomes with personalized screening and treatment strategy (Orio and Palomba, 2013). Some authors emphasized the phenotypes of clinical HA such as hirsutism and alopecia (Legro *et al.*, 2013), while others highlighted the effect of obesity toward metabolic aberrations (Azziz *et al.*, 2009). Previous studies have suggested that patients with the NIH phenotype (HA and AO, with or without PCOM) have a higher prevalence of IR (Carmina *et al.*, 2005; Diamanti-Kandarakis and Panidis, 2007; Moghetti *et al.*, 2013) or MS (Moran and Teede, 2009; Wild *et al.*, 2012) than the ovulatory and non-hyperandrogenic phenotype. In the current study, however, there was no significant difference in the prevalence of MS between these phenotypic subgroups. One of the reasons might be a lower prevalence of MS in our study population (19.3%), compared with other studies performed in Caucasian PCOS population (33% to 47%; Wild *et al.*, 2012) and more cases might be needed to reveal a between-subgroup difference. Another possible explanation might be the limitation of traditional PCOS features to identity the metabolically unhealthy PCOS patients. Therefore a combination of four endocrine characteristics (FAI, DHEA-S, FSH, LH) was applied in the patient-clustering in our study. And the results showed that not only the endocrine characteristics had a distinct pattern in each cluster, the corresponding metabolic features also had significant difference.

A number of studies have suggested that androgen excess is a key factor resulting in an unfavorable metabolic state, including central obesity, IR, and dyslipidemia (Kauffman *et al.*, 2002; Lerchbaum *et al.*, 2010; Barber and Franks, 2013). In animal studies, testosterone can induce IR by directly altering insulin action in adipose and skeletal muscle tissues, or enhancing visceral adiposity (Mannerås *et al.*, 2007). In contrast, suppression of the androgen level with anti-androgenic medications or gonadotropin-releasing hormone (GnRH) in women with PCOS results in significant improvement in insulin sensitivity (Elkind-Hirsch *et al.*, 1993; Moghetti *et al.*, 1996). However, in our clusters the positive correlation did not exist universally. Although the cluster 4, which had the highest prevalence of MS, did have a high FAI level, another cluster (cluster 2) with a low FAI level also presented with high prevalence of MS. It was in concordance with previous studies that the risk of metabolic aberrations in PCOS could not be predicted solely by androgen bioactivity. A common endocrine characteristic within cluster 2 and 4 was a significantly lower LH level. Besides, a cluster of extremely low metabolic risks was identified. The prevalence of MS in cluster 1 was only 7% which was significantly lower than the average risk (19%) in our study

doi:10.6342/NTU202000313

and was also lower than the prevalence reported in previous studies (7.1~41.6% of PCOS patients) (Goverde *et al.*, 2009). In addition, the prevalence was even similar with the risk of MS in the general Chinese population of comparable gender and age (5.2% [182/3470]) (Li *et al.*, 2010). This result suggested that nearly half of the study population (204/460), who were clustered into cluster 1, might not be necessary to be screened for metabolic aberrations. And a high LH level (≧15 mIU/ml) was found to be a best indicator of this metabolically healthy cluster that 95% of these patients were cluster 1 (Figure 4).

Altered pituitary gonadotropin secretion, including an elevated mean LH serum concentration, increased LH-to-FSH ratio, increased LH pulse frequency, and increased LH response to gonadotropin have all been considered to be characteristics of PCOS (Taylor *et al.*, 1997; Lawson *et al.*, 2008; Diamanti-Kandarakis and Dunaif, 2012). Although altered gonadotropin secretion has been widely proposed to be part of the pathogenesis of PCOS (Ehrmann *et al.*, 2005), neither absolute circulating LH level nor LH-to-FSH ratio was suggested by the Rotterdam consensus panel to constitute the diagnostic criteria. Because the serum LH concentration fluctuated and could be influenced by many factors, such as recent ovulation, BMI, and even the assay system used (Rotterdam ESHRE/ASRM-Sponsored PCOS Consensus Workshop Group, 2004). However, racial or geographic variations of the endocrine anomalies in PCOS were reported by some studies that an abnormally high LH level was more prevalent and significant than HA in Japanese PCOS women. Therefore high LH level or LH to FSH ratio has been proposed to constitute part of the diagnostic criteria in Japan by Japanese Society of Obstetrics and Gynecology since 2006 (Kubota, 2013). Although abnormal LH secretion is important in pathophysiology, the metabolic impact of unusually high serum LH level is still unclear. An inverse correlation between LH and insulin levels has been reported based on the reduction in basal LH and LH responses to GnRH following an insulin infusion (Taylor *et al.*, 1997); however, this finding was not confirmed in another study (Tosi *et al.*, 2012). Prior studies have also proposed a negative relationship between BMI and LH levels (Pagán *et al.*, 2006; Lawson *et al.*, 2008). In the current study, however, the negative correlation between LH and the prevalence of MS still reached statistical significance after excluding the confounding effect of BMI (data not shown). Therefore more researches are needed to clarity how the LH level influences the metabolic outcomes of PCOS patients.

Finally, which diagnostic criteria should be applied is still an ongoing debate. Some researchers suggested that the non-hyperandrogenic phenotype from Rotterdam criteria was metabolically favorable (Wild *et al.*, 2010) and defining these women as diseased individuals might unnecessarily increase their anxiety and health expenditure. In the current study, there were no significant differences in the prevalence of MS

doi:10.6342/NTU202000313

between three major diagnostic criteria. Moreover, 19% (17/89) and 12% (11/89) of PCOS patients with MS might not be diagnosed when applying NIH and AE-PCOS criteria. Therefore, identifying more women at risk for metabolic disturbances with the application of broader criteria, i.e., the Rotterdam criteria, might be beneficial.

The major limitation of our study is a lack of non-PCOS women as normal control to validate the clinical utility of the clustering pattern and the associated endocrine characteristics revealed by GAP analysis. And another possible limitation of the generalizability of our results might be racial differences in the phenotypic expression of PCOS, which had been frequently mentioned in the literatures (Zhao *et al*,. 2013). Legro *et al.* (2006) reported lighter PCOS phenotypes, including less degree of hyperandrogenemia and smaller ovarian volume in Asian PCOS patients, compared with Caucasian patients in the United States. But their results might be biased by a relatively small case number of Asian patients during enrollment (only 2.7%, 17/626 patients). Another comparative study reported an opposite result that the Chinese had a higher incidence of HA than Dutch Caucasian women with PCOS, although the hormone assay applied in these two ethnic populations were actually different (Guo *et al.*, 2012). Besides, many studies reported that the Asian women with PCOS were leaner than other ethnic groups (Legro *et al.*, 2006; Welt *et al.*, 2006) and a looser criteria has been already applied to define obesity (BMI≧25 in Asian; ≧30 in non-Asian) and MS (WC ≧80cm in Asian; ≧88cm in non-Asian) in Asian women (Tan *et al.*, 2004). However, to which extent do the racial or ethnic differences influence the phenotypic expression and metabolic outcome in PCOS population, and whether the adjustment of criteria item can balance the impact of ethnic differences between separate studies, were still unknown.

In conclusion, applying GAP analysis, PCOS patients were sorted into four distinct clusters with significantly different metabolic risks. The endocrine parameter which had strongest positive correlation with MS was FAI, while a high LH level during early follicular phase was found to be the best indicator of the metabolically healthy cluster. PCOS is a heterogeneous and complex disease, especially as defined by the Rotterdam criteria. Stratifying women with PCOS into meaningful subtypes could provide a better understanding of related risk factors and potentially enable the design and delivery of more effective screening and treatment intervention.

Study 2: Increased platelet factor 4 and aberrant permeability of follicular fluid in PCOS.

doi:10.6342/NTU202000313

This is the first work revealing that the FF from patients with PCOS induced poor endothelial cell permeability and there were significantly higher level of PF4 and PF4/IL-8 complex in the FF from PCOS patients. The anti-permeabilizing effect of the FF from PCOS patients was caused by intra-follicular PF4, and could be reversed by blocking the function of PF4, further adding direct evidence of its biological role in reducing endothelial cell permeability.

PF4, also called CXC chemokine ligand 4 (CXCL4), is a CXC-chemokine which is best known for its anti-angiogenic effect (Aidoudi and Bikfalvi, 2010). PF4 was initially thought to be predominantly synthesized in megakaryocytes and released upon platelet activation, such as vessel wall injury (Aidoudi and Bikfalvi, 2010, Eslin et al., 2004). More and more evidence suggested that other cell types, such as smooth muscle cells, microglia, macrophages, or T cells, also expressed PF4 (Kasper et al., 2010). The physiologic function of "non-platelet PF4" is awaiting determination and may be related to the specific tissue where it is localized (Vandercappellen et al., 2011). Besides the angiostatic effect, PF4 was also shown to play an important role in the direct regulation of several other cellular functions, such as megakaryopoiesis, thrombosis, immune modulation, chronic inflammation, and atherosclerosis (Kasper et al., 2010; Vandercappellen et al., 2011; Gonza´lez et al., 2012). Because our FF samples were only collected from the first follicle, which was aspirated nearly simultaneously during needle insertion, it was unlikely that the intra-follicular PF4 was produced secondary to the vessel injury during oocyte retrieval. One possible explanation is that chronic low-grade inflammation has been proposed to play an important role in the pathogenesis of PCOS (Gonza´lez et al., 2014). In patients with PCOS, both insulin resistance and androgen excess contribute to the increased sensitivity and activity of mononuclear cells, further activating the reactive oxygen species (ROS) system and producing pro-inflammatory cytokines, such as tumor necrosis factor-α (TNF-α) and interleukin-6 [IL-6] (Kasper et al., 2011; Gonza´lez et al., 2014). It has been demonstrated that PF-4 can induce monocyte activation, namely PF-4-mediated ROS formation, and the expression of TNF-α(Kasper et al., 2011). Therefore, PF4 might participate, at least in part, in the inflammatory process of PCOS, whether being induced or actively aggravated. Additional studies are needed to confirm the exact origin and specific biological function of intra-follicular PF4.

In the current study, the FF from PCOS patients was shown to induce a significantly poorer permeabilizing effect towards the adjacent endothelial cells. Although the *in vivo* effect remains to be clarified, it is reasonable to assume that dysregulated permeability of the ovarian follicles might exert a negative impact on folliculogenesis, and even ovulation, considering that the timing of FF collection was 33-35 h after oocyte triggering. The growth of follicles is a complex dynamic process

doi:10.6342/NTU202000313

which is constituted by many physiologic and cellular events, such as enlargement of the oocytes, replication of granulosa-theca cells, accumulation of FF, and expansion of the central follicular antrum (Rodgers et al., 2010). The growth and differentiation of reproductive tissues has been shown to be regulated by the fibroblast growth factor (FGF) family (Price et al., 2016). The most studied member of the FGF family, FGF-2, has been shown to promote the proliferation of granulosa cells and to decrease apoptosis and steroidogenesis in several *in vitro* studies (Lavranos et al., 1994; Vernon et al., 1994). PF4 can directly bind and suppress the function of FGF-2 and further inhibit endothelial cell proliferation and migration (Wang et al., 2013). It is therefore possible that PF4 may impair the growth of follicles by antagonistic binding with FGF-2 to inhibit granulosa cell proliferation. The down-regulation of FGF-2 might also promote steroidogenesis of granulosa cells, i.e., increased estradiol and progesterone production under FSH stimulation, which is also an important pathophysiologic feature of PCOS (Franks et al., 2003). Therefore, the results of our study provided a possible link between PF4 and abnormal follicular growth and steroidogenesis in this complex disease.

Based on the results of immunohistochemical staining in the present study, the anti-permeability effect of PF4 might be caused by promoting endothelial cell-cell adhesion. The platelet factor 4 variant (PF4var), which differs from PF4 in three carboxyl terminal amino acids, has been identified to share a similar biological function, such as anti-angiogenesis with even stronger potency (Struyf et al., 2004). In a previous study involving diabetic rats, Abu *et al.*(2015) reported that PF4var significantly increased the expression of the adherens junction protein, VE-cadherin, and the tight junction protein, occluding, in retinal cells, further decreasing retinal vascular permeability. In the current study, administration of PF4 was also shown to eliminate the intercellular gap and to enhance the adhesiveness of endothelial cells, further inducing an inhibitory effect on the permeability within the ovarian follicles and the aberrant formation of FF, which was a critical process in folliculogenesis.

Interestingly, in the current study the angiostatic PF4 in the FF was shown to constitute a protein complex with IL-8, a strong angiogenic factor that has been confirmed to functionally enhance the multi-step processes of angiogenesis, such as migration, permeability, and proliferation of endothelial cells (Chen et al., 2008). IL-8 has also been proposed to play a major role in inducing endothelial hyperpermeability in patients with OHSS (Chen et al., 2010). There was a significantly higher expression of PF4/IL-8 protein complex in the FF of PCOS patients compared with ovulatory controls. Therefore, the anti-permeability effect of PF4 might come from antagonistic binding with IL-8 to inhibit the downstream simulation effect on endothelial cell permeability. Previously, Dudek *et al.* (2003) reported that PF4 can bind IL-8 with high affinity and

doi:10.6342/NTU202000313

block IL-8–dependent signaling in CD34+ human hematopoietic progenitors. Both IL-8 and VEGF have been shown to be inhibited from binding with VEGF receptor on endothelial cell by PF4, therefore causing a down-regulation of VEGF-induced endothelial cell proliferation (Gengrinovitch et al., 1995). The inhibitory effect of PF4 on other angiogenic proteins might also occur in the FF and result in dysregulation of intra-follicular permeability and dysfunction and poor growth of surrounding follicular cells (i.e., granulosa cells).

Unlike previous studies (Agrawal et al., 2002; Artini et al., 2009) that showed a significantly higher level of VEGF in the FF of PCOS patients, there was no difference in the intra-follicular level of VEGF and other angiogenesis-related proteins between the two groups in the current study, except a significantly higher PF4 concentration in the PCOS group. One of the explanations might be the inclusion criteria that only the normo-ovulatory patients with good response to ovarian stimulation were recruited as our control group. We set this inclusion criteria because we wanted to eliminate the confounding effect of the ovarian reserve on the ovarian angiogenesis. Therefore, there was no significant difference in the baseline FSH level, number of retrieved oocytes, number of mature oocytes, and fertilization rate between the PCOS and control groups. In contrast, based on the work by Agrawal *et al.*(2002), the average number of retrieved oocytes in PCOS patients was two-fold greater than the control group (26.9 ± 4.5 vs. 13.2 ± 2.3, p=0.001). In the study by Artini *et al.* (2009), although there was no difference in the number of retrieved oocytes, the antral follicle count was significantly higher in the PCOS group than the control group (37 ± 8 vs. 14 ± 5, $p<0.001$). It might be possible that these studies revealed a correlation between an increased intra-follicular VEGF concentration and a better ovarian reserve instead of the actual mechanism of disease underlying PCOS.

There were several limitations inherent in the current study. First, the permeability test with the usage of HUVECs might not absolutely reflect the intra-follicular environment and the *in vivo* intra-follicular permeability might be regulated by a far more complex pattern. Besides, the causal relationship between the aberration of intrafollicular PF4 and the abnormal folliculogenesis in PCOS is uncertain based on current evidences and further in vivo studies will be needed. Second, although the level of angiogenesis-related proteins and the degree of intra-follicular permeability might change during different stages of folliculogenesis, the timing of FF collection was limited to the pre-ovulatory phase in the current study, which might not reflect a potential temporal change. Third, the regimens of COS and triggering agents were not identical between individuals and this might affect the expression of ovarian cytokines. However, a sensitivity test was performed to evaluate the possible effects of COS. Almost every patient in our study used rFSH for COS and only one patient in the PCOS

doi:10.6342/NTU202000313

group used hMG. If we excluded the patient who used hMG for COS, the mean value of PF4 concentration in FF (51.6 ng/ml v.s. 51.7 ng/ml, before and after exclusion) and the relative permeability of FF (46.3% v.s. 46.8%, before and after exclusion) didn't change significantly. Also, there wasn't statistically significant difference in the proportion of the different triggering agents between two groups (p=0.408 by Fisher's exact test). Meanwhile, there weren't significant differences in the average total dose of gonadotropin and the mean serum level of estradiol on the triggering day between two groups. Therefore the difference in the regimens of COS might not have significant impact in our study. Interestingly, Cerrillo *et al* (2011) had proposed that the intrafollicular VEGF concentration was significantly higher when using hCG as triggering agent, thus provided a possible explanation of the risk of OHSS. However they didn't check PF4 concentration and the correlation between the PF4 with different triggering agents merits further study.

In conclusion, our study provides the first evidence of the pathophysiologic contribution of the well-known angiostatic protein, PF4, on human reproductive biology. After controlling for patient age, BMI, and ovarian reserve, there was a significant difference in the concentration of PF4 within the FF and the inducing permeability between PCOS and control groups, possibly contributing to dysregulation of the formation of FF and folliculogenesis. Further functional assays revealed a binding effect between PF4 and another angiogenic protein, IL-8, inside the FF, suggesting that the regulatory mechanism of PF4 might be the antagonistic combination with IL-8, at least in part. These results not only reflect the pathologic condition in PCOS, but also delineate the normal ovarian physiology involving intra-follicular permeability, the formation of FF, and follicular growth. Further studies will be necessary to elucidate the origin of increased PF4, the responsive cell types, and the downstream signaling pathway. After accumulation of evidence from more studies, modulating ovarian permeability and/or angiogenesis process might be another new therapeutic approach for PCOS in the future.

Study 3: Hyperactive CREB signaling pathway involved in the pathogenesis of polycystic ovarian syndrome revealed by patient-specific induced pluripotent stem cell modeling.

The present study demonstrated the successful derivation of PCOS-specific iPSCs from skin fibroblasts by applying non-viral episomal reprogramming and differentiating the cells into ovarian GCs using a cocktail of growth factors as well as transient enrichment of the intermediate plate mesodermal stage populations. The established

doi:10.6342/NTU202000313

PCOS-specific iPSCs expressed pluripotency markers and possessed the ability of in vitro and in vivo differentiation into three germ layers. We also successfully differentiated iPSCs into GCs that could successfully express GC-associated genes and aromatase activity after differentiation, thus demonstrating the reliability of the study methodology. The PCOS-specific iPSCs may provide promising progress in the field of disease modeling. This revolutionary technique was not only able to enable valuable accessibility to various kinds of PCOS-relevant tissues and cells, but also directed the cells back to their embryonic stage. This offers a significant opportunity to elucidate the developmental origin of early onset complex diseases.

After reprogramming and re-differentiation, the iPSC-derived GCs retained many characteristics and functions associated with ovarian GCs. There was no difference in the pluripotency and differentiation potential between the iPSCs from the PCOS and control groups. Although the case number was not large enough for a statistical comparison, there seemed to be a trend showing that the iPSC-derived GCs from the PCOS patients expressed higher levels of many GC-specific markers, such as AMH, AMHR2, and FSHR, compared with the controls. Overexpression of AMH and AMHR2 in the GCs retrieved from stimulated follicles in the patients with PCOS was reported and was thought to be related to abnormal folliculogenesis (Pellatt et al., 2007; Pierre et al., 2017). The upregulation of FSHR expression in GCs was also reported (Catteau-Jonard et al., 2008) and might explain the hyper-responsiveness of GC to FSH stimulation in vivo in PCOS (Coffler et al., 2003). A trend of gradually increased expression of several GC-associated genes (AMHR2, LHR, and CYP19A1) from differentiation day 6 to day 12 in the iPSC-derived GCs from PCOS patients was noted (Figure 18), and these genes also appeared to express higher in the PCOS group in the aspirated adult GCs. This might reflect the concordant higher expression of certain GC-associated genes in the PCOS patients both in the early differentiated cells and adult cells, supporting the theory of early developmental origin of PCOS. The commonly overexpressed genes that appeared in both the iPSC-derived GCs and adult GCs could suggest that the GCs in PCOS might cause hormonal dysregulation during an early embryonic stage and may not only be secondary to environmental or behavioral changes. However, we cannot draw solid conclusions due to the absence of significance, which might be due to the limited case number. Improving the yield rate and purity of the iPSC-derived differentiated cells to achieve wider clinical application remains a further challenge.

The etiology of PCOS remains unclear, and the iPSC model could be a valuable tool in the discovery of disease mechanisms. The high occurrence rate among sisters and monozygotic twins in women with PCOS implies the estimated heritability could be as high as over 60% (Vink et al., 2006). Several genetic association studies have

doi:10.6342/NTU202000313

examined potential candidate genes in women with PCOS using familial clustering or case-control designs but have not resulted in significant findings. Even genome-wide association studies (GWAS) using a strong high throughput genetic screening method have identified several genetic variants associated with PCOS (Shi et al., 2012; Day et al., 2015; Hayes et al., 2015). These identified variants conferred only a relatively slight incremental risk and explained a small proportion of familial clustering and were not able to explain the strong heritability trait associated with PCOS. Epigenetics, defined as heritable changes in gene expression without changing the underlying DNA sequences, has been shown to be involved in the mechanism of a broad spectrum of human diseases (Kirchner et al., 2013), such as cancer development, neurodevelopmental disorders (Portela et al., 2010), autoimmune diseases, and metabolic diseases including type 2 DM and obesity (Drong et al., 2012; Kirchner et al., 2013). Many characteristics of epigenetic modifications in metabolic diseases are aligned with the nature of PCOS that is not fully explained by DNA variants, including the high heritability, flexibility, and dynamic nature, vulnerability to in-utero reprogramming, and postnatal environmental changes (Drong et al., 2012; Kirchner et al., 2013; Li et al., 2016). Several genome-side DNA methylomic studies have shown aberrant DNA methylation on different tissues, such as peripheral blood (Xu et al., 2010; Shen et al., 2013), adipose tissue (Kokosar et al., 2016), and ovarian tissue (Yu et al., 2015) in patients with PCOS. The results were inconsistent and it was difficult to make direct comparisons since the DNA methylation profiles are cell- and tissue-specific. Furthermore, the methodologies for DNA methylomic analysis and the definition of DMRs were different between studies making it difficult to prove the causal relationship of epigenetic aberration involved in the gene-environment interactions of complex diseases.

We applied whole-genomic methylation analysis on the iPSC-derived and adult GCs to assist in the discovery of disease mechanisms. A new generation high-density methylation array, the Illumina 850K Infinium MethylationEPIC array, which covers an additional 413,745 new CpG sites not included in the previous Illumina 450K methylation array, was utilized (Moran et al., 2016). The disease-relevant phenotypes of iPSC-derived GCs may provide some clues to the early pathogenic events during the pre-symptomatic phase, which may be critical in multifactorial hereditary diseases (Devine et al., 2017), while the phenotypes of adult ovarian GCs may represent late pathogenic events. Interestingly, a commonly overexpressed CREB pathway in the PCOS group was revealed by the DNA methylation array analysis in both the adult GCs and iPSCs-derived GCs. Further validation via Western blotting and qRT-PCR also confirmed the overexpressed CBP protein and mRNA in the primary adult GCs and iPSC-derived GCs.

doi:10.6342/NTU202000313

CREB and its coactivator family members (for example, CBP) are well-known for their critical roles in mediating the effects of energy homeostasis, such as glucose and lipid metabolism (Altarejos et al., 2011). However, the contribution of a dysregulated CREB pathway to the mechanism of PCOS has seldom been reported. Severe ovarian cysts with hyperplastic theca-interstitial cells and higher levels of serum testosterone were associated with the activating phosphorylation of CREB protein in a mouse study (Restuccia et al., 2012). Various signaling pathways of major reproductive hormones have also been found to be closely modulated by CREB activity. The stimulatory action of LH/hCG on the theca-interstitial cells associated with cholesterol uptake and androgen production could be inhibited by inhibiting CREB activity in vitro (Towns et al., 2005; Restuccia et al., 2012). CBP knockout mice demonstrated disrupted estrous cyclicity, reduced responsiveness to GnRH, and impaired fertility compared with wild type controls (Miller et al., 2012). The CREB pathway is also a critical signaling pathway for aromatase function (Lai et al., 2014) and interestingly, metformin has been shown to have inhibitory effects on FSH-induced CREB activation and downstream aromatase expression and activity in vitro (Rice et al., 2013). In summary, the chronic activation of the CREB pathway could be involved in multiple pathogenic mechanisms associated with PCOS, including hyperglycemia, insulin resistance and compensatory hyperinsulinemia, adipose tissue inflammation, excess LH function, and androgen production. Since PCOS has a heterogeneous and broad spectrum of various reproductive and metabolic phenotypes, it is possible that pathogenic dysregulation happens in a common upstream signaling pathway that involves both hormonal and energy regulation. Our results demonstrated that dysregulation of DNA methylation may be involved in the activation of the CREB pathway and may be present during both the early and late developmental stages of PCOS phenotypes. Additional research will be necessary to confirm the novelty of these preliminary results.

One previous study reported the genome-wide DNA methylation profiles in GCs from PCOS and control subjects (Xu et al., 2016). However, the CREB pathway did not appear in the top 10 canonical pathways in the study. This may be due to the GnRH long protocol used, which has been shown to cause significantly lower protein kinase C activity and aromatase activity in GCs than the GnRH antagonist protocol used in the current study (Khalaf et al., 2010). The DNA methylation profiles of the iPSC-derived GCs also demonstrated the dysregulated CREB pathway in the current study, which could serve as an excellent model to further explore the function of patient-specific GCs while avoiding the influence of controlled ovarian stimulation. There was no significant difference in the age and BMI in the current PCOS and control subjects, which eliminated the confounding effect of obesity or aging on the DNA methylation profiles.

In conclusion, the current study successfully established patient-specific iPSCs and

doi:10.6342/NTU202000313

re-differentiated GCs for the first time in the published literature. This could serve as a valuable model to evaluate the pre-symptomatic pathogenic events in early cellular differentiation and developmental status. The combination of DNA methylomic analysis in the adult GCs and iPSC-derived GCs revealed several differentially methylated genes and differentially expressed pathways between the PCOS and control groups, and a preserved persistent hyperactivation of the CREB signaling pathway might be involved in the pathogenesis of PCOS. However, further validation in a larger cohort is necessary. CREB and its co-activators are known to be critical sensors for both hormonal and metabolic signals, and it is possible that the aberration of the CREB signaling pathway could be related to complex hormonal and metabolic disorders such as PCOS. These results could have implications on the early developmental origin, familial nature, and environmental interaction effects of this disease, providing possible therapeutic targets in the future.

Study 4: Circulatory miRNAs as prediction models for the diagnosis of PCOS and the therapeutic effects of metformin.

We successfully recruited 75 PCOS and 20 control patients for plasma free miRNA analysis. Totally 14 targeted miRNA which were reported to be associated with glucose metabolism, insulin resistance, diabetes, ovarian or pituitary function were selected from literatures. The expression level of several miRNAs was statistically different between PCOS and control. And we also established a diagnostic model for the prediction of PCOS with excellent accurary. This could help clinical diagnosis and further valiated on a separate cohort is necessary.

Later, we compared the pattern of plasma free miRNA expression between the metformin-effective and metformin-ineffective PCOS patients. According to previous researches, metformin was only recommended for PCOS patients with insulin resistance. However 50% of PCOS patients did recover spontaneous ovulation after metformin treatment even though they didn't show insulin resistance. And so far there was no effective method to select which subgroup of PCOS patients will respond to metformin treatment. About 50% of PCOS patients might receive two years of ineffective metformin treatment and suffered from the frequent gastrointestinal side effects unnecessarily. Our results did showed exciting finding that several miRNAs expressed differentially between metformin-effective and metformin-ineffective PCOS patients. We also established a prediction model for the therapeutic response of metformin and the model were successfully validated on another separate PCOS cohort. Our result might also be served as one of the missing puzzles that what's the underlying pathophysiology that metformin could improve ovulation.

doi:10.6342/NTU202000313

參考文獻

Abbott DH, Barnett DK, Bruns CM, Dumesic DA. Androgen excess fetal programming of female reproduction: a developmental aetiology for polycystic ovary syndrome? Hum Reprod Update 2005;11(4):357-74.

Abu El-Asrar AM, Mohammad G, Nawaz MI, Abdelsaid M, Siddiquei MM, Alam K, et al. The chemokine platelet Factor-4 variant (PF-4var)/CXCL4L1 inhibits diabetes-induced bloodretinal barrier breakdown. Invest Ophthalmol Vis Sci 2015;56:1956e64.

Agrawal R, Conway G, Sladkevicius P, Tan SL, Engmann L, Payne N, et al. Serum vascular endothelial growth factor and Doppler blood flow velocities in in vitro fertilization: relevance to ovarian hyperstimulation syndrome and polycystic ovaries. Fertil Steril 1998a Oct;70(4):651-8.

Agrawal R, Sladkevicius P, Engmann L, Conway GS, Payne NN, Bekis J, et al. Serum vascular endothelial growth factor concentrations and ovarian stromal blood flow are increased in women with polycystic ovaries. Hum Reprod 1998b Mar;13(3):651-5.

Agrawal R, Jacobs H, Payne N, Conway G. Concentration of vascular endothelial growth factor released by cultured human luteinized granulosa cells is higher in women with polycystic ovaries than in women with normal ovaries. Fertil Steril 2002;78:1164e9.

Aidoudi S, Bikfalvi A. Interaction of PF4 (CXCL4) with the vasculature: a role in atherosclerosis and angiogenesis. Thromb Haemost 2010;104:941e8.

Albalawi FS, Daghestani MH, Daghestani MH3, Eldali A4, Warsy AS. rs4889 polymorphism in KISS1 gene, its effect on polycystic ovary syndrome development and anthropometric and hormonal parameters in Saudi women. J Biomed Sci. 2018 May 30;25(1):50.

Altarejos JY, Montminy M. CREB and the CRTC co-activators: sensors for hormonal and metabolic signals. Nat Rev Mol Cell Biol 2011;12:141–51.

Alvarez‐Blasco, F., Botella‐Carretero, J. I., San Millan, J. L. & Escobar‐Morreale, H. F. Prevalence and characteristics of the polycystic ovary syndrome in overweight and obese women. Arch. Intern. Med. 166, 2081–2086 (2006).

Artini PG, Ruggiero M, Parisen Toldin MR, Monteleone P, Monti M, Cela V, et al. Vascular endothelial growth factor and its soluble receptor in patients with

doi:10.6342/NTU202000313

polycystic ovary syndrome undergoing IVF. Hum Fertil (Camb) 2009;12:40e4.

Azziz R, Carmina E, Dewailly D, Diamanti-Kandarakis E, Escobar-Morreale HF, FutterweitW, Janssen OE, Legro RS, Norman RJ, Taylor AE et al. Positions statement: criteria for definingpolycystic ovary syndromeas a predominantly hyperandrogenic syndrome: an Androgen Excess Society guideline. J Clin Endocrinol Metab 2006 Nov;91(11):4237–4245.

Azziz, R. et al. The Androgen Excess and PCOS Society criteria for the polycystic ovary syndrome: the complete task force report. Fertil. Steril. 2009;91:456–488.

Azziz R, Dumesic DA, Goodarzi MO. Polycystic ovary syndrome: an ancient disorder? Fertil Steril. 2011 Apr;95(5):1544-8.

Azziz R, Carmina E, Chen Z, Dunaif A, Laven JS, Legro RS, Lizneva D, Natterson-Horowtiz B, Teede HJ, Yildiz BO. Polycystic ovary syndrome. Nat Rev Dis Primers. 2016 Aug;11(2):16057.

Bairey Merz, C. N. et al. Cardiovascular disease and 10‐year mortality in postmenopausal women with clinical features of PCOS. J Womens Health (Larchmt). 2016 Sep 1; 25(9): 875–881.

Bajuk Studen K, Jensterle Sever M, Pfeifer M. Cardiovascular risk and subclinical cardiovascular disease in polycystic ovary syndrome. Front Horm Res. 2013;40:64-82.

Balen A, Conway G, Kaltsas G. Polycystic ovary syndrome: the spectrum of the disorder in 1741 patients. Hum Reprod 1995 Aug;10(8):2107–11.

Balen AH, Laven JS, Tan SL, Dewailly D. Ultrasound assessment of the polycystic ovary: international consensus definitions. Hum Reprod Update 2003;9:505–514.

Barber TM, Franks S. Adipocyte biology in polycystic ovary syndrome. Mol Cell Endocrinol 2013;373:68–76.

Baskind NE, Balen AH. Hypothalamic-pituitary, ovarian and adrenal contributions to polycystic ovary syndrome. Best Pract Res Clin Obstet Gynaecol 2016;37:80–97.

Bates DO. Vascular endothelial growth factors and vascular permeability. Cardiovasc Res 2010;87:262e71.

Blandino, G.; Valerio, M.; Cioce, M.; Mori, F.; Casadei, L.; Pulito, C.; Sacconi, A.; Biagioni, F.; Cortese, G.; Galanti, S.; et al. Metformin elicits anticancer effects through the sequential modulation of DICER and c-MYC. Nat. Commun. 2012, 3, 865.

doi:10.6342/NTU202000313

Brand~ao KO, Tabel VA, Atsma DE, Mummery CL, Davis RP. Human pluripotent stem cell models of cardiac disease: from mechanisms to therapies. Dis Model Mech 2017;10:1039–59.

Burman P. A comparative study of ordinary cross-validation, v-fold cross-validation and the repeated learning-testing methods. Biometrika 1989;76:503–514.

Cai, X., Liu, C. & Mou, S. Association between fat mass- and obesity-associated (FTO) gene polymorphism and polycystic ovary syndrome: a meta-analysis. PLoS ONE 9, e86972 (2014).

Carmina, E., Campagna, A. M. & Lobo, R. A. Emergence of ovulatory cycles with aging in women with polycystic ovary syndrome (PCOS) alters the trajectory of cardiovascular and metabolic risk factors. Hum. Reprod. 28, 2245–2252 (2013).

Carmina, E. Polycystic ovary syndrome: metabolic consequences and long-term management. Scand. J. Clin. Lab. Invest. Suppl. 244, 23–26; discussion 26 (2014).

Carmina E, Chu MC, Longo RA, Rini GB, Lobo RA. Phenotypic variation in hyperandrogenic women influences the findings of abnormal metabolic and cardiovascular risk parameters. J Clin Endocrinol Metab 2005; 90:2545–2549.

Catteau-Jonard S, Jamin SP, Leclerc A, Gonzales J, Dewailly D, di Clemente N. Anti-m€ullerian hormone, its receptor, FSH receptor, and androgen receptor genes are overexpressed by granulosa cells from stimulated follicles in women with polycystic ovary syndrome. J Clin Endocrinol Metab 2008;93:4456–61.

Cerrillo M, Pacheco A, Rodrı´guez S, Go´mez R, Delgado F, Pellicer A, et al. Effect of GnRH agonist and hCG treatment on VEGF, angiopoietin-2, and VE-cadherin: trying to explain the link to ovarian hyperstimulation syndrome. Fertil Steril 2011;95:2517e9.

Chae SJ, Kim JJ, Choi YM, Hwang KR, Jee BC, Ku SY, Suh CS, Kim SH, Kim JG, Moon SY. Clinical and biochemical characteristics of polycystic ovary syndrome in Korean women. Hum Reprod. 2008 Aug;23(8):1924-31.

Chang RJ, Cook-Andersen H. Disordered follicle development. Mol Cell Endocrinol 2013 Jul 5;373(1-2):51-60.

Chen CH. Generalized association plots: information visualization via iteratively generated correlation matrices. Stat Sin 2002;12:7–29.

Chen MJ, Yang WS, Yang JH, Hsiao CK, Yang YS, Ho HN. Low sex hormone-binding globulin is associated with low high-density lipoprotein cholesterol and metabolic syndrome in women with PCOS. Hum Reprod. 2006 Sep;21(9):2266-71.

doi:10.6342/NTU202000313

Chen MJ, Yang WS, Yang JH, Chen CL, Ho HN, Yang YS. Relationship between androgen levels and blood pressure in young women with polycystic ovary syndrome. Hypertension. 2007 Jun;49(6):1442-7.

Chen MJ, Yang WS, Chen CL, Wu MY, Yang YS, Ho HN. The relationship between anti-Mullerian hormone, androgen and insulin resistance on the number of antral follicles in women with polycystic ovary syndrome. Hum Reprod 2008;23:952–957.

Chen MJ, Chen HF, Chen SU, Ho HN, Yang YS, Yang WS. The relationship between follistatin and chronic low-grade inflammation in women with polycystic ovary syndrome. Fertil Steril 2009;92:2041–2044.

Chen MJ, Chiu HM, Chen CL, Yang WS, Yang YS, Ho HN. Hyperandrogenemia is independently associated with elevated alanine aminotransferase activity in young women with polycystic ovary syndrome. J Clin Endocrinol Metab 2010;95:3332–3341.

Chen MJ, Han DS, Yang JH, Yang YS, Ho HN, Yang WS. Myostatin and its association with abdominal obesity, androgen and follistatin levels in women with polycystic ovary syndrome. Hum Reprod 2012;27:2476–2483.

Chen MJ, Chou CH, Chen SU, Yang WS, Yang YS, Ho HN. The effect of androgens on ovarian follicle maturation: Dihydrotestosterone suppress FSH-stimulated granulosa cell proliferation by upregulating PPARgamma-dependent PTEN expression. Sci Rep. 2015 Dec 17;5:18319.

Chen SU, Chen CD, & Yang YS. Ovarian hyperstimulation syndrome (OHSS): new strategies of prevention and treatment. J Formos Med Assoc. 2008 Jul;107(7):509-12.

Chen SU, Chou CH, Lee H, Ho CH, Lin CW, Yang YS. Lysophosphatidic acid up-regulates expression of interleukin-8 and -6 in granulosa-lutein cells through its receptors and nuclear factorkappaB dependent pathways: implications for angiogenesis of corpus luteum and ovarian hyperstimulation syndrome. J Clin Endocrinol Metab 2008;93:935e43.

Chen SU, Chou CH, Lin CW, Lee H, Wu JC, Lu HF, et al. Signal mechanisms of vascular endothelial growth factor and interleukin-8 in ovarian hyperstimulation syndrome: dopamine targets their common pathways. Hum Reprod. 2010 Mar;25(3):757-67.

Chen YH, Heneidi S, Lee JM, Layman LC, Stepp DW, Gamboa GM, Chen BS, Chazenbalk G, Azziz R. miRNA-93 inhibits GLUT4 and is overexpressed in

doi:10.6342/NTU202000313

adipose tissue of polycystic ovary syndrome patients and women with insulin resistance. Diabetes. 2013 Jul;62(7):2278-86.

Chen ZJ, Zhao H, He L, Shi Y, Qin Y, Li Z, You L, et al. Genome-wide association study identifies susceptibility loci for polycystic ovary syndrome on chromosome 2p16.3, 2p21 and 9q33.3. Nat Genet 2011;43:55–59

Christian, R. C. et al. Prevalence and predictors of coronary artery calcification in women with polycystic ovary syndrome. J. Clin. Endocrinol. Metab. 88, 2562–2568 (2003).

Cinar, N. et al. Depression, anxiety and cardiometabolic risk in polycystic ovary syndrome. Hum. Reprod. 26, 3339–3345 (2011).

Coffler MS, Patel K, Dahan MH, Malcom PJ, Kawashima T, Deutsch R, et al. Evidence for abnormal granulosa cell responsiveness to follicle-stimulating hormone in women with polycystic ovary syndrome. J Clin Endocrinol Metab 2003;88:1742–7.

Coleman, C.B.; Lightell, D.J.; Moss, S.C.; Bates, M.; Parrino, P.E.; Woods, T.C. Elevation of miR-221 and -222 in the internal mammary arteries of diabetic subjects and normalization with metformin. Mol. Cell. Endocrinol. 2013, 374, 125–129.

Das M, Djahanbakhch O, Hacihanefioglu B, Saridogan E, Ikram M, Ghali L, Raveendran M, Storey A. Granulosa cell survival and proliferation are altered in polycystic ovary syndrome. J Clin Endocrinol Metab. 2008 Mar;93(3):881-7.

Day FR, Hinds DA, Tung JY, Stolk L, Styrkarsdottir U, Saxena R, et al. Causal mechanisms and balancing selection inferred from genetic associations with polycystic ovary syndrome. Nat Commun 2015;6:8464.

DeUgarte, C. M., Woods, K. S., Bartolucci, A. A. & Azziz, R. Degree of facial and body terminal hair growth in unselected black and white women: toward a populational definition of hirsutism. J. Clin. Endocrinol. Metab. 91, 1345–1350 (2006).

Devine H, Patani R. The translational potential of human induced pluripotent stem cells for clinical neurology: the translational potential of hiPSCs in neurology. Cell Biol Toxicol 2017;33:129–44.

Diamanti-Kandarakis E, Piperi C. Genetics of polycystic ovary syndrome: searching for the way out of the labyrinth. Hum Reprod Update. 2005 Nov-Dec;11(6):631-43.

Diamanti-Kandarakis E, Papavassiliou AG. Molecular mechanisms of insulin resistance in polycystic ovary syndrome. Trends Mol Med 2006 Jul;12(7):324-32.

doi:10.6342/NTU202000313

Diamanti-Kandarakis E, Panidis D. Unravelling the phenotypic map of polycystic ovary syndrome (PCOS): a prospective study of 634 women with PCOS. Clin Endocrinol 2007;67:735–742.

Diamanti‐Kandarakis E, Dunaif A. Insulin resistance and the polycystic ovary syndrome revisited: an update on mechanisms and implications. Endocr Rev 2012 Dec;33(6):981–1030.

Dokras, A., Clifton, S., Futterweit, W. & Wild, R. Increased risk for abnormal depression scores in women with polycystic ovary syndrome: a systematic review and meta-analysis. Obstetr. Gynecol. 117, 145–152 (2011).

Drong AW, Lindgren CM, McCarthyMI. The genetic and epigenetic basis of type 2 diabetes and obesity. Clin Pharmacol Ther 2012;92:707–15.

Dudek AZ, Nesmelova I, Mayo K, Verfaillie CM, Pitchford S, Slungaard A. Platelet factor 4 promotes adhesion of hematopoietic progenitor cells and binds IL-8: novel mechanisms for modulation of hematopoiesis. Blood 2003;101:4687e94.

Dumesic DA & Lobo RA Cancer risk and PCOS. Steroids 2013;78:782–785.

Dumesic DA, Richards JS. Ontogeny of the ovary in polycystic ovary syndrome. Fertil Steril 2013 Jul;100(1):23-38.

Dumesic DA et al. Scientific statement on the diagnostic criteria, epidemiology, pathophysiology, and molecular genetics of polycystic ovary syndrome. Endocr. Rev. 2015;36:487–525

Ehrmann DA. Polycystic ovary syndrome. N Engl J Med 2005;352:1223–1236.

Elkind-Hirsch KE, Valdes CT, Malinak LR. Insulin resistance improves in hyperandrogenic women treated with Lupron. Fertil Steril 1993; 60:634–641.

Eslin DE, Zhang C, Samuels KJ, Rauova L, Zhai L, Niewiarowski S, et al. Transgenic mice studies demonstrate a role for platelet factor 4 in thrombosis: dissociation between anticoagulant and antithrombotic effect of heparin. Blood 2004;104:3173e80.

Essler M, Retzer M, Bauer M, Heemskerk JW, Aepfelbacher M, Siess W. Mildly oxidized low density lipoprotein induces contraction of human endothelial cells through activation of Rho/Rho kinase and inhibition of myosin light chain phosphatase. J Biol Chem 1999;274:30361e4.

Ezeh, U., Yildiz, B. O. & Azziz, R. Referral bias in defining the phenotype and prevalence of obesity in polycystic ovary syndrome. J. Clin. Endocrinol. Metab. 98,

doi:10.6342/NTU202000313

E1088–E1096 (2013).

Faruq O, Vecchione A. microRNA: Diagnostic Perspective. Front Med (Lausanne) 2015;3:2:51.

Feil R, Fraga MF. Epigenetics and the environment: emerging patterns and implications. Nat Rev Genet 2012;13(2):97-109.

Ferrara N, Frantz G, LeCouter J, Dillard-Telm L, Pham T, Draksharapu A, et al. Differential expression of the angiogenic factor genes vascular endothelial growth factor (VEGF) and endocrine gland-derived VEGF in normal and polycystic human ovaries. Am J Pathol 2003 Jun;162(6):1881-93.

Fiedler, S.D.; Carletti, M.Z.; Hong, X.; Christenson, L.K. Hormonal regulation of microRNA expression in periovulatory mouse mural granulosa cells. Biol. Reprod. 2008, 79, 1030–1037.

Fragouli E, Lalioti MD, Wells D. The transcriptome of follicular cells: biological insights and clinical implications for the treatment of infertility. Hum Reprod Update 2014 Jan-Feb;20(1):1-11.

Franks S, McCarthy MI, Hardy K. Development of polycystic ovary syndrome: involvement of genetic and environmental factors. Int J Androl 2006;29: 278–85.

Franks S, Stark J, Hardy K. Follicle dynamics and anovulation in polycystic ovary syndrome. Hum Reprod Update 2008 Jul-Aug;14(4):367-78.

Gengrinovitch S, Greenberg SM, Cohen T, Gitay-Goren H, Rockwell P, Maione TE, et al. Platelet factor-4 inhibits the mitogenic activity of VEGF121 and VEGF165 using several concurrent mechanisms. J Biol Chem 1995;270:15059e65.

Gilling-Smith C, Willis DS, Beard RW, Franks S. Hypersecretion of androstenedione by isolated thecal cells from polycystic ovaries. J Clin Endocrinol Metab 1994;79:1158–65.

Gonza´lez F. Inflammation in polycystic ovary syndrome: underpinning of insulin resistance and ovarian dysfunction. Steroids 2012;77:300e5.

Gonza´lez F, Sia CL, Shepard MK, Rote NS, Minium J. The altered mononuclear cell-derived cytokine response to glucose ingestion is not regulated by excess adiposity in polycystic ovary syndrome. J Clin Endocrinol Metab 2014;99:E2244e51.

Goverde AJ, van Koert AJ, Eijkemans MJ, Knauff EA, Westerveld HE, Fauser BC, Broekmans FJ. Indicators for metabolic disturbances in anovulatory women with

doi:10.6342/NTU202000313

polycystic ovary syndrome diagnosed according to the Rotterdam consensus criteria. Hum Reprod 2009;24:710–717.

Guo M, Chen ZJ, Eijkemans MJ, Goverde AJ, Fauser BC, Macklon NS. Comparison of the phenotype of Chinese versus Dutch Caucasian women presenting with polycystic ovary syndrome and oligo/amenorrhoea. Hum Reprod 2012;27:1481–1488.

Haider BA, Baras AS, McCall MN, Hertel JA, Cornish TC, Halushka MK. A critical evaluation of microRNA biomarkers in non-neoplastic disease. PLoS One 2014;26:9:e89565.

Hassa H, Tanir HM, Yildiz Z. Comparison of clinical and laboratory characteristics of cases with polycystic ovarian syndrome based on Rotterdam's criteria and women whose only clinical signs are oligo/anovulation or hirsutism. Arch Gynecol Obstet. 2006 Jul;274(4):227-32.

Hasuwa H, Ueda J, Ikawa M, Okabe M. miR-200b and miR-429 function in mouse ovulation and are essential for female fertility. Science. 2013 Jul 5;341(6141):71-3.

Hayes MG, Urbanek M, Ehrmann DA, Armstrong LL, Lee JY, Sisk R, et al. Genome-wide association of polycystic ovary syndrome implicates alterations in gonadotropin secretion in European ancestry populations. Nat Commun 2015;6:7502.

Ho CH, Chen SU, Peng FS, Chang CY, Lien YR, Yang YS. Prospective comparison of short and long GnRH agonist protocols using recombinant gonadotrophins for IVF/ICSI treatments. Reprod Biomed Online 2008;16:632e9.

Hosseinpanah F, Barzin M, Keihani S, Ramezani Tehrani F, Azizi F. Metabolic aspects of different phenotypes of polycystic ovary syndrome: Iranian PCOS Prevalence Study. Clin Endocrinol (Oxf). 2014 Jul;81(1):93-9.

Hsueh AJ, Billig H, Tsafriri A. Ovarian follicle atresia: a hormonally controlled apoptotic process. Endocr Rev. 1994 Dec;15(6):707-24.

Huang CC, Lien YR, Chen HF, Chen MJ, Shieh CJ, Yao YL, et al. The duration of pre-ovulatory serum progesterone elevation before hCG administration affects the outcome of IVF/ICSI cycles. Hum Reprod 2012;27:2036e45.

Huang CC, Tien YJ, Chen MJ, Chen CH, Ho HN, Yang YS. Symptom patterns and phenotypic subgrouping of women with polycystic ovary syndrome: association between endocrine characteristics and metabolic aberrations. Hum Reprod 2015;30(4):937-46.

doi:10.6342/NTU202000313

Huang CC, Chou CH, Chen SU, Ho HN, Yang YS, Chen MJ. Increased platelet factor 4 and aberrant permeability of follicular fluid in PCOS. J Formos Med Assoc. 2019 Jan;118:249-259.

Huang CC, Chen MJ, Lan CW, Wu CE, Huang MC, Kuo HC, Ho HN*. Hyperactive CREB signaling pathway involved in the pathogenesis of polycystic ovarian syndrome revealed by patient-specific induced pluripotent stem cell modeling. Fertil Steril. 2019 Sep;112(3):594-607.

Hutt KJ, Albertini DF. An oocentric view of folliculogenesis and embryogenesis. Reprod Biomed Online. 2007 Jun;14(6):758-64.

Hwu HG, Chen CH, Hwang TJ, Liu CM, Cheng JJ, Lin SK, Liu SK, Chen CH, Chi YY, Ou-Young CW et al. Symptom patterns and subgrouping of schizophrenic patients: significance of negative symptoms assessed on admission. Schizophr Res 2002;56:105–119.

Jiang L, Huang J, Li L, Chen Y, Chen X, Zhao X, Yang D. MicroRNA-93 promotes ovarian granulosa cells proliferation through targeting CDKN1A in polycystic ovarian syndrome. J Clin Endocrinol Metab. 2015 May;100(5):E729-38.

Joham, A. E., Teede, H. J., Ranasinha, S., Zoungas, S. & Boyle, J. Prevalence of infertility and use of fertility treatment in women with polycystic ovary syndrome: data from a large community-based cohort study. J. Womens Health (Larchmt) 24, 299–307 (2015).

Jonard S, Dewailly D. The follicular excess in polycystic ovaries, due to intra-ovarian hyperandrogenism, may be the main culprit for the follicular arrest. Hum Reprod Update 2004 Mar-Apr;10(2):107-17.

Johnstone SE, Baylin SB. Stress and the epigenetic landscape: a link to the pathobiology of human diseases? Nat Rev Genet 2010;11(11):806-12.

Kamat BR, Brown LF, Manseau EJ, Senger DR, Dvorak HF. Expression of vascular permeability factor/vascular endothelial growth factor by human granulosa and theca lutein cells. Role in corpus luteum development. Am J Pathol. 1995 Jan;146(1):157-65.

Kasper B, Winoto-Morbach S, Mittelsta¨dt J, Brandt E, Schu¨tze S, Petersen F. CXCL4-induced monocyte survival, cytokine expression, and oxygen radical formation is regulated by sphingosine kinase 1. Eur J Immunol 2010;40:1162e73.

Kasper B, Petersen F. Molecular pathways of platelet factor 4/CXCL4 signaling. Eur J Cell Biol 2011;90:521e6.

doi:10.6342/NTU202000313

Kauffman RP, Baker VM, Dimarino P, Gimpel T, Castracane VD. Polycystic ovarian syndrome and insulin resistance in white and Mexican American women: a comparison of two distinct populations. Am J Obstet Gynecol 2002;187:1362–1369.

Kauffman RP, Baker TE, Baker VM, DiMarino P, Castracane VD. Endocrine and metabolic differences among phenotypic expressions of polycystic ovary syndrome according to the 2003 Rotterdam consensus criteria. Am J Obstet Gynecol. 2015 Nov;213(5):670.e1-7.

Kaur S, Archer KJ, Devi MG, Kriplani A, Strauss JF, Singh R. Differential gene expression in granulosa cells from polycystic ovary syndrome patients with and without insulin resistance: identification of susceptibility gene sets through network analysis. J Clin Endocrinol Metab 2012;97:E2016–21.

Kawwass JF, Sanders KM, Loucks TL, Rohan LC, Berga SL. Increased cerebrospinal fluid levels of GABA, testosterone and estradiol in women with polycystic ovary syndrome. Hum Reprod. 2017 Jul 1;32(7):1450-1456.

Khalaf M, Mittre H, Levallet J, Hanoux V, Denoual C, Herlicoviez M, et al. GnRH agonist and GnRH antagonist protocols in ovarian stimulation: differential regulation pathway of aromatase expression in human granulosa cells. Reprod Biomed Online 2010;21:56–65.

King NM, Perrin J. Ethical issues in stem cell research and therapy. Stem Cell Res Ther 2014;5:85.

Kirchner H, Osler ME, Krook A, Zierath JR. Epigenetic flexibility in metabolic regulation: disease cause and prevention? Trends Cell Biol. 2013;23(5):203-9.

Kokosar M, Benrick A, Perfilyev A, Fornes R, Nilsson E, Maliqueo M, et al. Epigenetic and transcriptional alterations in human adipose tissue of polycystic ovary syndrome. Sci Rep 2016;6:22883.

Kosova G, Urbanek M. Genetics of the polycystic ovary syndrome. Mol Cell Endocrinol 2013;373:29–38.

Kubota T. Update in polycystic ovary syndrome: new criteria of diagnosis and treatment in Japan. Reprod Med Biol 2013;12:71–77.

Kumar D, Anand T, Kues WA. Clinical potential of human-induced pluripotent stem cells: perspectives of induced pluripotent stem cells. Cell Biol Toxicol 2017;33:99–112.

Lai WA, Yeh YT, Fang WL, Wu LS, Harada N, Wang PH, et al. Calcineurin and CRTC2

doi:10.6342/NTU202000313

mediate FSH and TGFb1 upregulation of Cyp19a1 and Nr5a in ovary granulosa cells. J Mol Endocrinol 2014;53:259–70.

Lan CW, Chen MJ, Jan PS, Chen HF, Ho HN. Differentiation of human embryonic stem cells into functional ovarian granulosa-like cells. J Clin Endocrinol Metab 2013;98:3713–23.

Lan CW, Chen MJ, Tai KY, Yu DC, Yang YC, Jan PS, et al. Functional microarray analysis of differentially expressed genes in granulosa cells from women with polycystic ovary syndrome related to MAPK/ERK signaling. Sci Rep 2015;5:14994.

Lannes J, L'Hôte D, Garrel G, Laverrière JN, Cohen-Tannoudji J, Quérat B. Rapid communication: A microRNA-132/212 pathway mediates GnRH activation of FSH expression. Mol Endocrinol. 2015 Mar;29(3):364-72.

Lass, N., Kleber, M., Winkel, K., Wunsch, R. & Reinehr, T. Effect of lifestyle intervention on features of polycystic ovarian syndrome, metabolic syndrome, and intima–media thickness in obese adolescent girls. J. Clin. Endocrinol. Metab. 96, 3533–3540 (2011).

Lavranos TC, Rodgers HF, Bertoncello I, Rodgers RJ. Anchorage independent culture of bovine granulosa cells: the effects of basic fibroblast growth factor and dibutyryl cAMP on cell division and differentiation. Exp Cell Res 1994;211:245e51.

Lawson MA, Jain S, Sun S, Patel K, Malcolm PJ, Chang RJ. Evidence for insulin suppression of baseline luteinizing hormone in women with polycystic ovarian syndrome and normal women. J Clin Endocrinol Metab. 2008 Jun;93(6):2089-96.

Lee TH, Wu MY, Chen HF, Chen SU, Ho HN, Yang YS. Association of a single dose of gonadotropin-releasing hormone antagonist with nitric oxide and embryo quality in in vitro fertilization cycles. Fertil Steril 2006;86:1020e2.

Legro RS, Myers ER, Barnhart HX, Carson SA, Diamond MP, Carr BR, Schlaff WD, Coutifaris C, McGovern PG, Cataldo NA et al.; Reproductive Medicine Network. The Pregnancy in Polycystic Ovary Syndrome study: baseline characteristics of the randomized cohort including racial effects. Fertil Steril 2006;86:914–933.

Legro RS, Arslanian SA, Ehrmann DA, Hoeger KM, Murad MH, Pasquali R, Welt CK; Endocrine Society. Diagnosis and treatment of polycystic ovary syndrome: an Endocrine Society clinical practice guideline. J Clin Endocrinol Metab 2013;98:4565–4592.

Lerchbaum E, Trummer O, Giuliani A, Gruber HJ, Pieber TR, Obermayer-Pietsch B.

doi:10.6342/NTU202000313

Susceptibility loci for polycystic ovary syndrome on chromosome 2p16.3, 2p21, and 9q33.3 in a cohort of Caucasian women. Horm Metab Res 2011;43:743-7

Lerchbaum E, Schwetz V, Giuliani A, Pieber TR, Obermayer-Pietsch B. Opposing effects of dehydroepiandrosterone sulfate and free testosterone on metabolic phenotype in women with polycystic ovary syndrome. Fertil Steril. 2012 Nov;98(5):1318-25.

Li G, de Courten M, Jiao S, Wang Y. Prevalence and characteristics of the metabolic syndrome among adults in Beijing, China. Asia Pac J Clin Nutr 2010;19:98–102.

Li R, Zhang Q, Yang D, Li S, Lu S, Wu X, Wei Z, Song X, Wang X, Fu S, Lin J, Zhu Y, Jiang Y, Feng HL, Qiao J. Prevalence of polycystic ovary syndrome in women in China: a large community-based study. Hum Reprod. 2013 Sep;28(9):2562-9.

Li S, Zhu D, Duan H, Tan Q. The epigenomics of polycystic ovarian syndrome: from pathogenesis to clinical manifestations. Gynecol Endocrinol 2016;32:942–6.

Lim, S. S., Davies, M. J., Norman, R. J. & Moran, L. J. Overweight, obesity and central obesity in women with polycystic ovary syndrome: a systematic review and meta-analysis. Hum. Reprod. Update 18, 618–637 (2012).

Lizneva, D. et al. The criteria, prevalence and phenotypes of PCOS. Fertil. Steril. 106, 6–15 (2016).

Long W, Zhao C, Ji C, Ding H, Cui Y, Guo X, Shen R, Liu J. Characterization of serum microRNAs profile of PCOS and identification of novel non-invasive biomarkers. Cell Physiol Biochem 2014;33(5):1304-15

Lord, J.M.; Flight, I.H.K.; Norman, R.J. Metformin in polycystic ovary syndrome: Systematic review and meta-analysis. BMJ 2003, 327, 951–953.

Luque‐Ramirez, M., Mendieta‐Azcona, C., Alvarez‐Blasco, F. & Escobar‐Morreale, H. F. Androgen excess is associated with the increased carotid intima–media thickness observed in young women with polycystic ovary syndrome. Hum. Reprod. 22, 3197–3203 (2007).

Luque‐Ramirez, M. et al. Referral bias in female functional hyperandrogenism and polycystic ovary syndrome. Eur. J. Endocrinol. 173, 603–610 (2015).

Malm HA, Mollet IG, Berggreen C, Orho-Melander M, Esguerra JL, Göransson O, Eliasson L. Transcriptional regulation of the miR-212/miR-132 cluster in insulin-secreting β-cells by cAMP-regulated transcriptional co-activator 1 and salt-inducible kinases. Mol Cell Endocrinol. 2016 Mar 15;424:23-33.

doi:10.6342/NTU202000313

Mannera˚s L, Cajander S, Holma¨ng A, Seleskovic Z, Lystig T, Lo¨nn M, Stener-Victorin E. A new rat model exhibiting both ovarian and metabolic characteristics of polycystic ovary syndrome. Endocrinology 2007;148:3781–3791.

McAllister JM, Legro RS, Modi BP, Strauss JF. Functional genomics of PCOS: from GWAS to molecular mechanisms. Trends Endocrinol Metab 2015 Mar;26(3):118–124.

Miller RS, Wolfe A, He L, Radovick S, Wondisford FE. CREB binding protein (CBP) activation is required for luteinizing hormone beta expression and normal fertility in mice. Mol Cell Biol 2012;32:2349–58.

Moghetti P, Tosi F, Castello R, Magnani CM, Negri C, Brun E, Furlani L, Caputo M, Muggeo M. The insulin resistance in women with hyperandrogenism is partially reversed by antiandrogen treatment: evidence that androgens impair insulin action in women. J Clin Endocrinol Metab 1996;81:952–960.

Moghetti P, Tosi F, Bonin C, Di Sarra D, Fiers T, Kaufman JM, Giagulli VA, Signori C, Zambotti F, Dall'Alda M et al. Divergences in insulin resistance between the different phenotypes of the polycystic ovary syndrome. J Clin Endocrinol Metab 2013;98:E628–E637.

Moran L, Teede H. Metabolic features of the reproductive phenotypes of polycystic ovary syndrome. Hum Reprod Update 2009;15:477–488.

Moran LJ, Misso ML, Wild RA, Norman RJ. Impaired glucose tolerance, type 2 diabetes and metabolic syndrome in polycystic ovary syndrome: a systematic review and meta-analysis. Hum Reprod Update. 2010 Jul-Aug;16(4):347-63.

Moran LJ, Deeks AA, Gibson‐Helm ME & Teede HJ. Psychological parameters in the reproductive phenotypes of polycystic ovary syndrome. Hum. Reprod. 27, 2082–2088 (2012).

Moran LJ, Norman RJ, Teede HJ. Metabolic risk in PCOS: phenotype and adiposity impact. Trends Endocrinol Metab. 2015 Mar;26(3):136-43.

Moran S, Arribas C, Esteller M. Validation of a DNA methylation microarray for 850,000 CpG sites of the human genome enriched in enhancer sequences. Epigenomics 2016;8:389–99.

Moreno-Moya JM, Vilella F, Simón C. MicroRNA: key gene expression regulators. Fertil Steril 2014 Jun;101(6):1516-23.

Nagy JA, Benjamin L, Zeng H, Dvorak AM, Dvorak HF. Vascular permeability, vascular hyperpermeability and angiogenesis. Angiogenesis 2008;11:109e19.

doi:10.6342/NTU202000313

Nestler JE, Jakubowicz DJ, de Vargas AF, Brik C, Quintero N, Medina F. Insulin stimulates testosterone biosynthesis by human thecal cells from women with polycystic ovary syndrome by activating its own receptor and using inositolglycan mediators as the signal transduction system. J Clin Endocrinol Metab 1998 Jun;83(6): 2001-5.

Nicholson F, Rolland C, Broom J, Love J. Effectiveness of long-term (twelve months) nonsurgical weight loss interventions for obese women with polycystic ovary syndrome: a systematic review. Int J Womens Health. 2010 Nov 10;2:393-9.

Norman RJ, Davies MJ, Lord J, Moran LJ. The role of lifestyle modification in polycystic ovary syndrome. Trends Endocrinol Metab 2002;13(6):251-7.

Nouri M, Aghadavod E, Khani S, Jamilian M, Amiri Siavashani M, Ahmadi S, et al. Association between BMI and gene expression of anti-m€ullerian hormone and androgen receptor in human granulosa cells in women with and without polycystic ovary syndrome. Clin Endocrinol (Oxf) 2016;85:590–5.

Orio F, Palomba S. Reproductive endocrinology: new guidelines for the diagnosis and treatment of PCOS. Nat Rev Endocrinol 2014;10:130–132.

Osuka S et al. Kisspeptin in the hypothalamus of 2 rat models of polycystic ovary syndrome. Endocrinology 2017;158:367–377

Paga´n YL, Srouji SS, Jimenez Y, Emerson A, Gill S, Hall JE. Inverse relationship between luteinizing hormone and body mass index in polycystic ovarian syndrome: investigation of hypothalamic and pituitary contributions. J Clin Endocrinol Metab 2006;91:1309–1316.

Palomba, S. et al. Pregnancy complications in women with polycystic ovary syndrome. Hum. Reprod. Update 21, 575–592 (2015).

Pan, M. L., Chen, L. R., Tsao, H. M. & Chen, K. H. Relationship between polycystic ovarian syndrome and subsequent gestational diabetes mellitus: a nationwide population-based study. PLoS ONE 10, e0140544 (2015).

Pastor CL et al. Polycystic ovary syndrome: evidence for reduced sensitivity of the gonadotropin-releasing hormone pulse generator to inhibition by estradiol and progesterone. J. Clin. Endocrinol. Metab. 1998;83:582–590

Peitsidis P and Agrawal R. Role of vascular endothelial growth factor in women with PCO and PCOS: a systematic review. Reprod Biomed Online 2010;20:444e52.

Pellatt L, Hanna L, Brincat M, Galea R, Brain H, Whitehead S, et al. Granulosa cell production of anti-m€ullerian hormone is increased in polycystic ovaries. J Clin

doi:10.6342/NTU202000313

Endocrinol Metab 2007;92:240–5.

Pierre A, Taieb J, Giton F, Grynberg M, Touleimat S, el Hachem H, et al. Dysregulation of the anti-m€ullerian hormone system by steroids in women with polycystic ovary syndrome. J Clin Endocrinol Metab 2017;102:3970–8.

Portela A, Esteller M. Epigenetic modifications and human disease. Nat Biotechnol. 2010 Oct;28(10):1057-68.

Price CA. Mechanisms of fibroblast growth factor signaling in the ovarian follicle. J Endocrinol 2016;228:R31e43.

Qu F, Wang FF, Yin R, Ding GL, El-Prince M, Gao Q, Shi BW, Pan HH, Huang YT, Jin M, Leung PC, Sheng JZ, Huang HF. A molecular mechanism underlying ovarian dysfunction of polycystic ovary syndrome: hyperandrogenism induces epigenetic alterations in the granulosa cells. J Mol Med 2012;90(8):911-23.

Ramezani Tehrani, F. et al. Trend of cardio-metabolic risk factors in polycystic ovary syndrome: a population‐based prospective cohort study. PLoS ONE 10, e0137609 (2015).

Raja-Khan N, Urbanek M, Rodgers RJ, Legro RS. The role of TGF-β in polycystic ovary syndrome. Reprod Sci. 2014 Jan;21(1):20-31.

Randeva HS, Tan BK, Weickert MO, Lois K, Nestler JE, Sattar N, Lehnert H. Cardiometabolic aspects of the polycystic ovary syndrome. Endocr Rev 2012 Oct;33(5):812-41.

Restuccia DF, Hynx D, Hemmings BA. Loss of PKBb/Akt2 predisposes mice to ovarian cyst formation and increases the severity of polycystic ovary formation in vivo. Dis Model Mech 2012;5:403–11.

Rice S, Elia A, Jawad Z, Pellatt L, Mason HD. Metformin inhibits folliclestimulating hormone (FSH) action in human granulosa cells: relevance to polycystic ovary syndrome. J Clin Endocrinol Metab 2013;98: E1491–500.

Rodgers RJ, Irving-Rodgers HF. Formation of the ovarian follicular antrum and follicular fluid. Biol Reprod 2010;82: 1021e9.

Roessler R, Smallwood SA, Veenvliet JV, Pechlivanoglou P, Peng SP, Chakrabarty K, et al. Detailed analysis of the genetic and epigenetic signatures of iPSC-derived mesodiencephalic dopaminergic neurons. Stem Cell Reports 2014;2:520–33.

Roland AV and Moenter SM. Prenatal androgenization of female mice programs an increase in firing activity of gonadotropin-releasing hormone (GnRH) neurons that

doi:10.6342/NTU202000313

is reversed by metformin treatment in adulthood. Endocrinology 2011;152:618–628

Roos, N. et al. Risk of adverse pregnancy outcomes in women with polycystic ovary syndrome: population based cohort study. BMJ 343, d6309 (2011).

Rosenfield RL, Ehrmann DA. The pathogenesis of Polycystic Ovary Syndrome (PCOS): the hypothesis of PCOS as functional ovarian hyperandrogenism revisited. Endocr Rev. 2016 Oct;37(5):467-520.

Roth LW, McCallie B, Alvero R, Schoolcraft WB, Minjarez D, Katz-Jaffe MG. Altered microRNA and gene expression in the follicular fluid of women with polycystic ovary syndrome. J Assist Reprod Genet 2014;31:355–62.

Rotterdam ESHRE/ASRM-Sponsored PCOS Consensus Workshop Group. Revised 2003 consensus on diagnostic criteria and long-term health risks related to polycystic ovary syndrome (PCOS). Hum Reprod 2004 Jan;19(1):41–47.

Sang, Q.; Yao, Z.; Wang, H.; Feng, R.; Wang, H.; Zhao, X.; Xing, Q.; Jin, L.; He, L.; Wu, L.; et al. Identification of microRNAs in human follicular fluid: Characterization of microRNAs that govern steroidogenesis in vitro and are associated with polycystic ovary syndrome in vivo. J. Clin. Endocrinol. Metab. 2013, 98, 3068–3079.

Sathyapalan T, David R, Gooderham NJ, Atkin SL. Increased expression of circulating miRNA-93 in women with polycystic ovary syndrome may represent a novel, non-invasive biomarker for diagnosis. Sci Rep. 2015 Nov 19;5:16890.

Scotti L, Parborell F, Irusta G, De Zuñiga I, Bisioli C, Pettorossi H, et al. Platelet-derived growth factor BB and DD and angiopoietin1 are altered in follicular fluid from polycystic ovary syndrome patients. Mol Reprod Dev 2014 Aug;81(8):748-56.

Shen F, Zheng H, Zhou L, Li W, Xu X. Overexpression of MALAT1 contributes to cervical cancer progression by acting as a sponge of miR-429. J Cell Physiol. 2019 Jul;234(7):11219-11226.

Shen HR, Qiu LH, Zhang ZQ, Qin YY, Cao C, Di W. Genome-wide methylated DNA immunoprecipitation analysis of patients with polycystic ovary syndrome. PLoS One 2013;8:e64801.

Shi Y, Zhao H, Shi Y, Cao Y, Yang D, Li Z, et al. Genome-wide association study identifies eight new risk loci for polycystic ovary syndrome. Nat Genet 2012;44:1020–5.

doi:10.6342/NTU202000313

Shroff R, Syrop CH, Davis W, Van Voorhis BJ, Dokras A. Risk of metabolic complications in the new PCOS phenotypes based on the Rotterdam criteria. Fertil Steril. 2007 Nov;88(5):1389-95.

Sirotkin AV, Ovcharenko D, Grossmann R, Laukova M, Mlyncek M. Identification of microRNAs controlling human ovarian cell steroidogenesis via a genome-scale screen. J Cell Physiol 2009;219:415–20.

Souter, I., Sanchez, L. A., Perez, M., Bartolucci, A. A. & Azziz, R. The prevalence of androgen excess among patients with minimal unwanted hair growth. Am. J. Obstet. Gynecol. 191, 1914–1920 (2004).

Stein IF, Leventhal ML. Amenorrhea associated with bilateral polycystic ovaries. Am J Obstet Gynecol 1935;29(2):181-91.

Stepto NK, Cassar S, Joham AE, Hutchison SK, Harrison CL, Goldstein RF, Teede HJ. Women with polycystic ovary syndrome have intrinsic insulin resistance on euglycaemic-hyperinsulaemic clamp. Hum Reprod. 2013 Mar;28(3):777-84.

Sterling, L. et al. Pregnancy outcomes in women with polycystic ovary syndrome undergoing in vitro fertilization. Fertil. Steril. 105, 791–797.e2 (2016).

Struyf S, Burdick MD, Proost P, Van Damme J, Strieter RM. Platelets release CXCL4L1, a nonallelic variant of the chemokine platelet factor-4/CXCL4 and potent inhibitor of angiogenesis. Circ Res 2004;95:855e7.

Sullivan SD and Moenter SM. Prenatal androgens alter GABAergic drive to gonadotropin-releasing hormone neurons: implications for a common fertility disorder. Proc. Natl. Acad. Sci. U. S. A. 2004;101:7129–7134

Takahashi K, Yamanaka S. Induction of pluripotent stem cells from mouse embryonic and adult fibroblast cultures by defined factors. Cell 2006;126: 663–76.

Talbott, E. O. et al. Evidence for an association between metabolic cardiovascular syndrome and coronary and aortic calcification among women with polycystic ovary syndrome. J. Clin. Endocrinol. Metab. 89, 5454–5461 (2004).

Tamanini C, De Ambrogi M. Angiogenesis in developing follicle and corpus luteum. Reprod Domest Anim 2004 Aug;39(4):206-16.

Tan CE, Ma S, Wai D, Chew SK, Tai ES. Can we apply the National Cholesterol Education Program Adult Treatment Panel definition of the metabolic syndrome to Asians? Diabetes Care 2004;27:1182–1186.

Taylor AE, McCourt B, Martin KA, Anderson EJ, Adams JM, Schoenfeld D, Hall JE.

doi:10.6342/NTU202000313

Determinants of abnormal gonadotropin secretion in clinically defined women with polycystic ovary syndrome. J Clin Endocrinol Metab 1997;82:2248–2256.

Teede HJ, Misso ML, Deeks AA, Moran LJ, Stuckey BG, Wong JL, Norman RJ, Costello MF; Guideline Development Groups. Assessment and management of polycystic ovary syndrome: summary of an evidence based guideline. Med J Aust 2011; 195:S65–112.

Teede HJ, Joham AE, Paul E, Moran LJ, Loxton D, Jolley D, Lombard C. Longitudinal weight gain in women identified with polycystic ovary syndrome: results of an observational study in young women. Obesity (Silver Spring) 2013;21:1526–1532.

Thomson JA, Itskovitz-Eldor J, Shapiro SS, Waknitz MA, Swiergiel JJ, Marshall VS, et al. Embryonic stem cell lines derived from human blastocysts. Science 1998;282:1145–7.

Tien YJ, Lee YS, Wu HM, Chen CH. Methods for simultaneously identifying coherent local clusters with smooth global patterns in gene expression profiles. BMC Bioinformatics 2008;9:155–170.

Tosi F, Negri C, Perrone F, Dorizzi R, Castello R, Bonora E, Moghetti P. Hyperinsulinemia amplifies GnRH agonist stimulated ovarian steroid secretion in women with polycystic ovary syndrome. J Clin Endocrinol Metab 2012;97:1712–1719.

Towns R, Azhar S, Peegel H, Menon KM. LH/hCG-stimulated androgen production and selective HDL-cholesterol transport are inhibited by a dominantnegative CREB construct in primary cultures of rat theca-interstitial cells. Endocrine 2005;27:269–77.

Ucar A, Vafaizadeh V, Jarry H, Fiedler J, Klemmt PA, Thum T, Groner B, Chowdhury K. miR-212 and miR-132 are required for epithelial stromal interactions necessary for mouse mammary gland development. Nat Genet. 2010 Dec;42(12):1101-8.

Vandercappellen J, Van Damme J, Struyf S. The role of the CXC chemokines platelet factor-4 (CXCL4/PF-4) and its variant (CXCL4L1/PF-4var) in inflammation, angiogenesis and cancer. Cytokine Growth Factor Rev 2011;22:1e18.

Veltman‐Verhulst, S. M., Boivin, J., Eijkemans, M. J. & Fauser, B. J. Emotional distress is a common risk in women with polycystic ovary syndrome: a systematic review and meta-analysis of 28 studies. Hum. Reprod. Update 18, 638–651 (2012).

Venables WN, Ripley BD. Modern Applied Statistics with S, 4th edn. NewYork: Springer-Verlag, 2002, 331–338.

doi:10.6342/NTU202000313

Vernon RK, Spicer LJ. Effects of basic fibroblast growth factor and heparin on follicle-stimulating hormone-induced steroidogenesis by bovine granulosa cells. J Anim Sci 1994;72: 2696e702.

Vink JM, Sadrzadeh S, Lambalk CB, Boomsma DI. Heritability of polycystic ovary syndrome in a Dutch twin-family study. J Clin Endocrinol Metab 2006;91:2100–2104.

Wang ET, Calderon-Margalit R, Cedars MI, Daviglus ML, Merkin SS, Schreiner PJ, Sternfeld B, Wellons M, Schwartz SM, Lewis CE, Williams OD, Siscovick DS, Bibbins-Domingo K. Polycystic ovary syndrome and risk for long-term diabetes and dyslipidemia. Obstet Gynecol. 2011 Jan;117(1):6-13.

Wang M, Liu M, Sun J, Jia L, Ma S, Gao J, Xu Y, Zhang H, Tsang SY, Li X. MicroRNA-27a-3p affects estradiol and androgen imbalance by targeting Creb1 in the granulosa cells in mouse polycytic ovary syndrome model. Reprod Biol. 2017 Dec;17(4):295-304.

Wang M, Sun J, Xu B, Chrusciel M, Gao J, Bazert M, Stelmaszewska J, Xu Y, Zhang H, Pawelczyk L, Sun F, Tsang SY, Rahman N, Wolczynski S, Li X. Functional Characterization of MicroRNA-27a-3p Expression in Human Polycystic Ovary Syndrome. Endocrinology. 2018 Jan 1;159(1):297-309.

Wang S, Alvero R. Racial and ethnic differences in physiology and clinical symptoms of polycystic ovary syndrome. Semin Reprod Med. 2013 Sep;31(5):365-9.

Wang Z, Huang H. Platelet factor-4 (CXCL4/PF-4): an angiostatic chemokine for cancer therapy. Cancer Lett 2013;331: 147e53.

Welt CK, Arason G, Gudmundsson JA, Adams J, Palsdo´ ttir H, Gudlaugsdo´ ttir G, Ingado´ ttir G, Crowley WF. Defining constant versus variable phenotypic features of women with polycystic ovary syndrome using different ethnic groups and populations. J Clin Endocrinol Metab 2006;91:4361–4368.

WHO Expert Consultation. Appropriate body-mass index for Asian populations and its implications for policy and intervention strategies. Lancet 2004;363:157–163.

Wijeyaratne CN, Seneviratne Rde A, Dahanayake S, Kumarapeli V, Palipane E, Kuruppu N, Yapa C, Seneviratne Rde A, Balen AH. Phenotype and metabolic profile of South Asian women with polycystic ovary syndrome (PCOS): results of a large database from a specialist Endocrine Clinic. Hum Reprod. 2011 Jan;26(1):202-13.

Wild RA, Carmina E, Diamanti-Kandarakis E, Dokras A, Escobar-Morreale HF,

doi:10.6342/NTU202000313

Futterweit W, Lobo R, Norman RJ, Talbott E, Dumesic DA. Assessment of cardiovascular risk and prevention of cardiovascular disease in women with the polycystic ovary syndrome: A consensus statement by the Androgen Excess and Polycystic Ovary Syndrome (AE-PCOS) Society. J Clin Endocrinol Metab. 2010 May;95(5):2038-49.

Wild, S., Pierpoint, T., Jacobs, H. & McKeigue, P. Long-term consequences of polycystic ovary syndrome: results of a 31 year follow‐up study. Hum. Fertil. (Camb.) 3, 101–105 (2000).

Wu HL, Heneidi S, Chuang TY, Diamond MP, Layman LC, Azziz R, Chen YH. The expression of the miR-25/93/106b family of micro-RNAs in the adipose tissue of women with polycystic ovary syndrome. J Clin Endocrinol Metab. 2014 Dec;99(12):E2754-61.

Wu HM, Tzeng S, Chen CH. Matrix visualization. In: Chen CH, Ha¨rdle W, Unwin A. (eds) Handbook of Computational Statistics (volume III): Data Visualization. Berlin: Springer-Verlag, 2008, 681–708.

Wu HM, Tien YJ, Chen CH. GAP: a graphical environment for matrix visualization and cluster analysis. Comput Stat Data Anal 2010; 54:767–778.

Wu Y, Zhang Z, Liao X, Wang Z. High fat diet triggers cell cycle arrest and excessive apoptosis of granulosa cells during the follicular development. Biochem Biophys Res Commun. 2015 Oct 23;466(3):599-605.

Xu J, Bao X, Peng Z, Wang L, Du L, Niu W, et al. Comprehensive analysis of genome-wide DNA methylation across human polycystic ovary syndrome ovary granulosa cell. Oncotarget 2016;7:27899–909.

Xu N, Azziz R, Goodarzi MO. Epigenetics in polycystic ovary syndrome: a pilot study of global DNA methylation. Fertil Steril 2010;94:781–3.

Xu N, Kwon S, Abbott DH, Geller DH, Dumesic DA, Azziz R, Guo X, Goodarzi MO. Epigenetic mechanism underlying the development of polycystic ovary syndrome (PCOS)-like phenotypes in prenatally androgenized rhesus monkeys. PLoS One 2011;6(11):e27286.

Yang PK, Hsu CY, Chen MJ, Lai MY, Li ZR, Chen CH, Chen SU, Ho HN. The Efficacy of 24-Month Metformin for Improving Menses, Hormones, and Metabolic Profiles in Polycystic Ovary Syndrome. J Clin Endocrinol Metab. 2018 Mar 1;103(3):890-899.

Yang S, Ding S, Jiang X, Sun B, Xu Q. Establishment and adipocyte differentiation of

doi:10.6342/NTU202000313

polycystic ovary syndrome–derived induced pluripotent stem cells. Cell Prolif 2016;49:352–61.

Yildiz, B. O., Knochenhauer, E. S. & Azziz, R. Impact of obesity on the risk for polycystic ovary syndrome. J. Clin. Endocrinol. Metab. 93, 162–168 (2008).

Yildiz, B. O., Bozdag, G., Yapici, Z., Esinler, I. & Yarali, H. Prevalence, phenotype and cardiometabolic risk of polycystic ovary syndrome under different diagnostic criteria. Hum. Reprod. 27, 3067–3073 (2012).

Yu YY, Sun CX, Liu YK, Li Y, Wang L, Zhang W. Genome-wide screen of ovary specific DNA methylation in polycystic ovary syndrome. Fertil Steril 2015;104:145–53.

Yuen T, Ruf F, Chu T, Sealfon SC. Microtranscriptome regulation by gonadotropin-releasing hormone. Mol Cell Endocrinol. 2009 Apr 10;302(1):12-7.

Zawadzki JK, Dunaif A. Diagnostic criteria for polycystic ovary syndrome: towards a rational approach. In: Dunaif AGJ, Haseltine F (eds) Polycystic Ovary Syndrome. Boston: Blackwell Scientific, 1992, 377–384.

Zhao Y, Qiao J. Ethnic differences in the phenotypic expression of polycystic ovary syndrome. Steroids 2013;78:755–760.

doi:10.6342/NTU202000313

圖一.

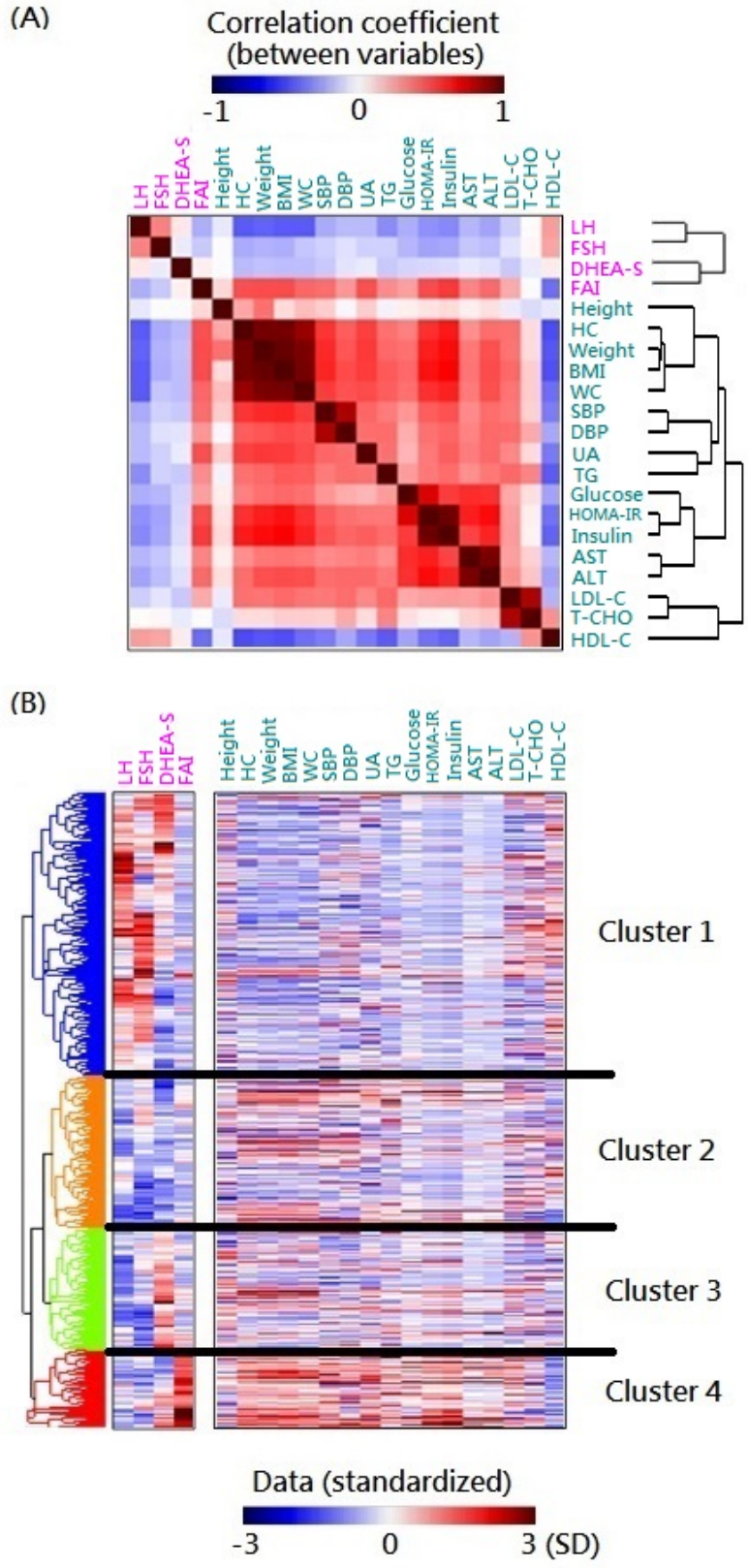

doi:10.6342/NTU202000313

圖一：廣義相關圖分析

圖一 A：此彩圖顯示 23 個症狀項目間的相關係數之接近矩陣。極端深紅色表示相關係數為 1（正相關），白色表示 0（無相關性），極端深藍色表示 -1（負相關）。例如，SHBG 濃度與幾乎每種新陳代謝指標都呈現負相關（藍色），而 SHBG 與 HDL-C 呈現正相關（暗紅色），並與總膽固醇濃度幾乎沒有相關性（淺紅色）。

圖一 B：此彩圖說明了 460 名患者之間的關係結構，根據 23 個症狀項目的相對數值表現和相近程度，進行了群組分組，並以矩陣圖顯示。每個患者顯示為一個橫紋，某一個橫紋的顏色，代表某病患之特定症狀在整個病患族群的相對嚴重程度; 紅色表示高於平均值的表現，藍色表示低於平均值的表現，白色表示等於平均表現。使用 GAP 分群樹，根據四種內分泌測量值 (包括 FSH，LH，FAI 和 DHEA-S) 的相關性，將患者進一步分成四個不同的次族群。每個次族群都表現出獨特的內分泌和代謝特徵。第 2 組和第 4 組都顯示最嚴重的新陳代謝異常（新陳代謝指標多呈現暗紅色），而第 1 組顯示了較良好的新陳代謝指標（多呈現藍色）。

doi:10.6342/NTU202000313

圖二.

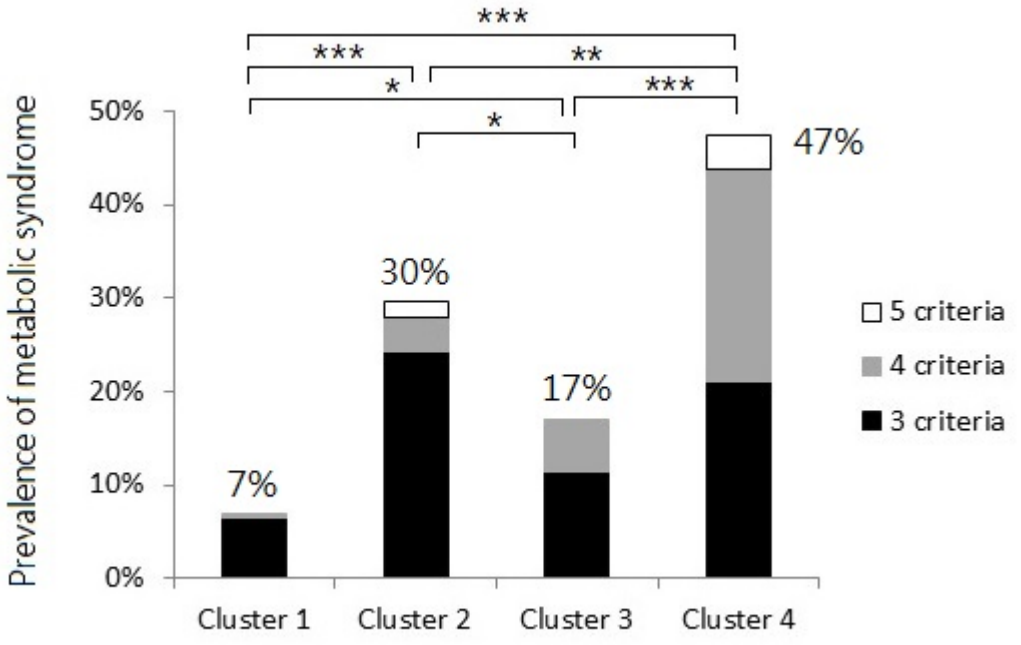

圖二：新陳代謝症候群在廣義相關圖四個次組群之盛行率。所符合之新陳代謝症候群的診斷標準數目以不同的灰階顏色顯示，白色表示五個診斷標準全符合，灰色表示符合四個診斷標準，黑色表示符合三個診斷標準。第二組和第四組的新陳代謝症候群盛行率顯著性地較高。第一組的新陳代謝症候群盛行率顯著性地較低。事後比較檢定是透過 LSD 方法。*P , 0.05; **P , 0.01; ***P , 0.001.

doi:10.6342/NTU202000313

圖三.

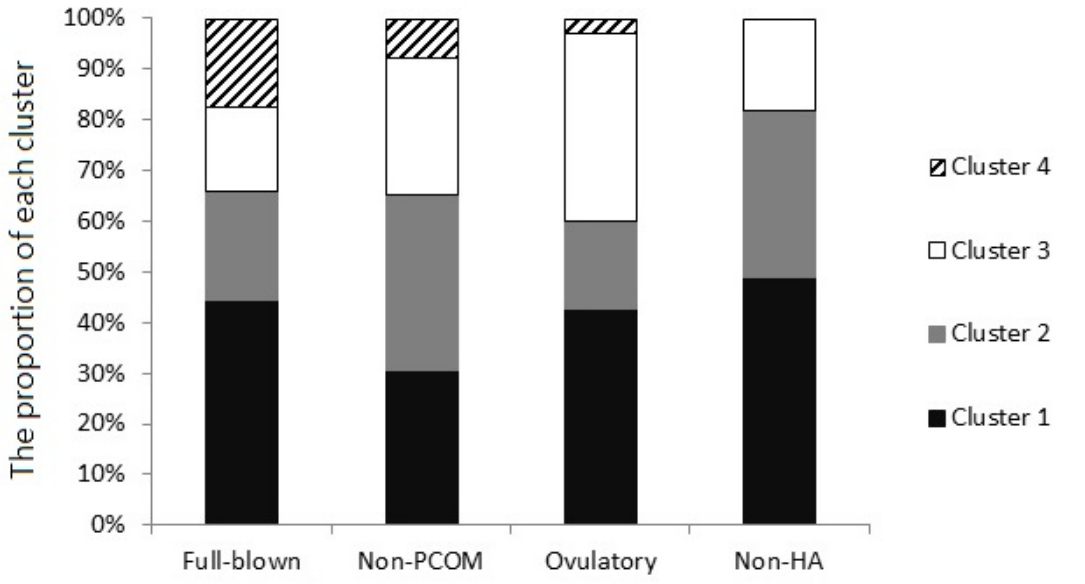

圖三：廣義相關圖四個次族群在鹿特丹標準不同表型子群的分佈情形。第四組的分佈在鹿特丹完全表型子群 (full-blown phenotype) 中的比例，顯著較其他鹿特丹表型子群更高，相較之下，第一到三組在不同鹿特丹表型子群的分佈比例沒有顯著差異。(PCOM, polycystic ovaries morphology; HA, hyperandrogenism.)

doi:10.6342/NTU202000313

圖四.

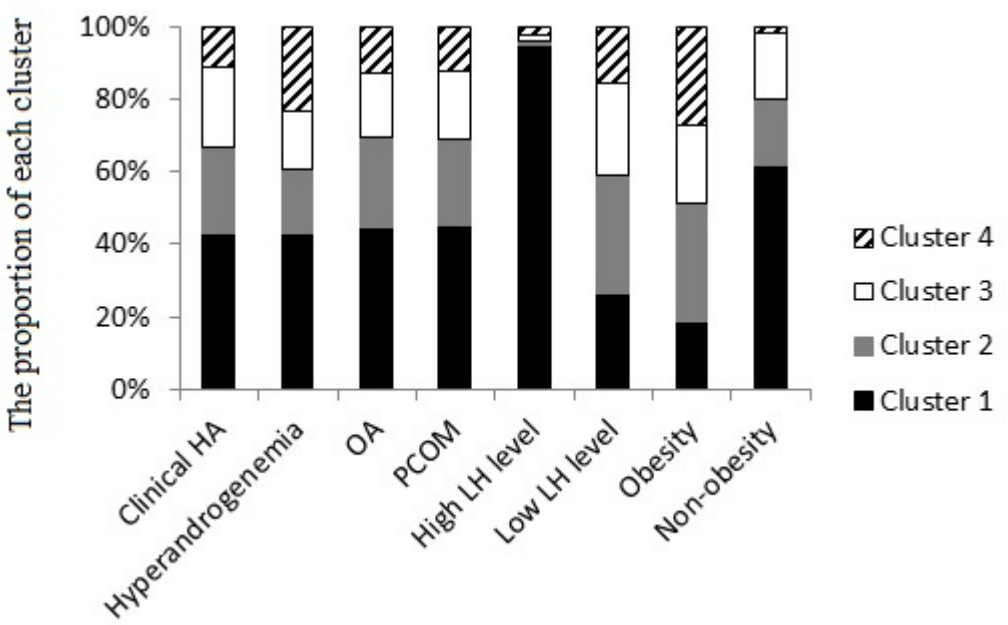

圖四：不同臨床表徵分佈在廣義相關圖四個次族群的比例。在高雄性荷爾蒙症和肥胖症患者中，第 4 組的比例較高。此外，第 1 組最顯著獨特的臨床特徵是較高的 LH 濃度。(HA, hyperandrogenism; OA, chronic anovulation; PCOM, polycystic ovaries morphology; LH, luteinizing hormone.)

doi:10.6342/NTU202000313

圖五.

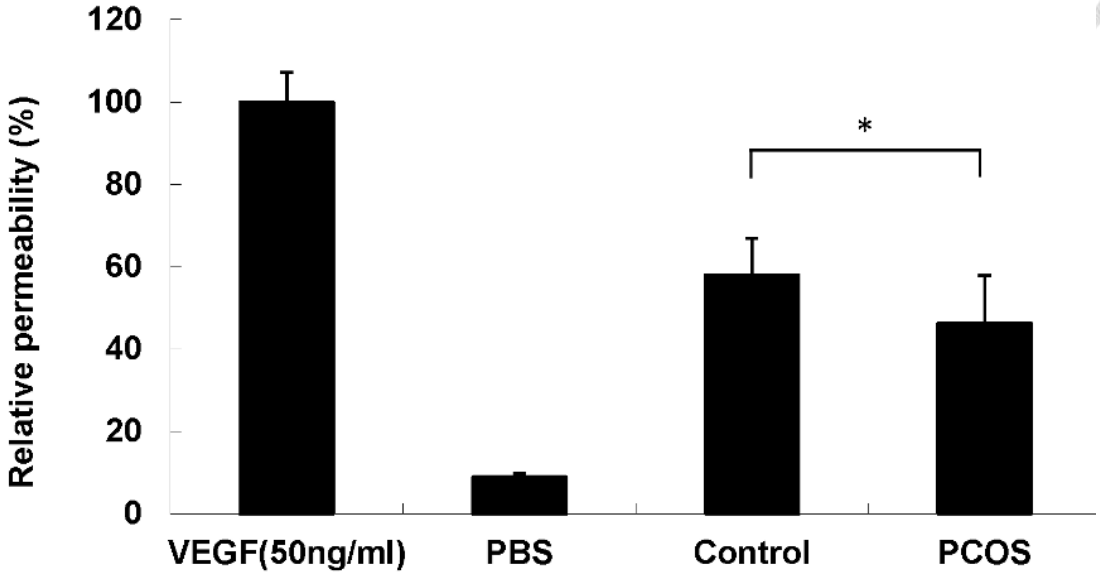

圖五：不同病患濾泡液對內皮細胞相對通透性之影響。顯示添加不同濾泡液於人類臍靜脈內皮細胞裝置時測到的相對通透性，相對通透性(relative permeability)的計算，是以加入 VEGF 到卵巢濾泡液中時(50ng/ml)的通透性定義為 100%，並據此計算其他情況的相對比率。添加 PCOS 病患濾泡液至人類臍靜脈內皮細胞裝置時，與對照組相比會產生顯著下降的內皮細胞通透性（多囊性卵巢症候群組[n = 11]為 46%±12%，而對照組[n = 9]為 58%±9%，P = 0.023）。*P < 0.05.

doi:10.6342/NTU202000313

圖六.

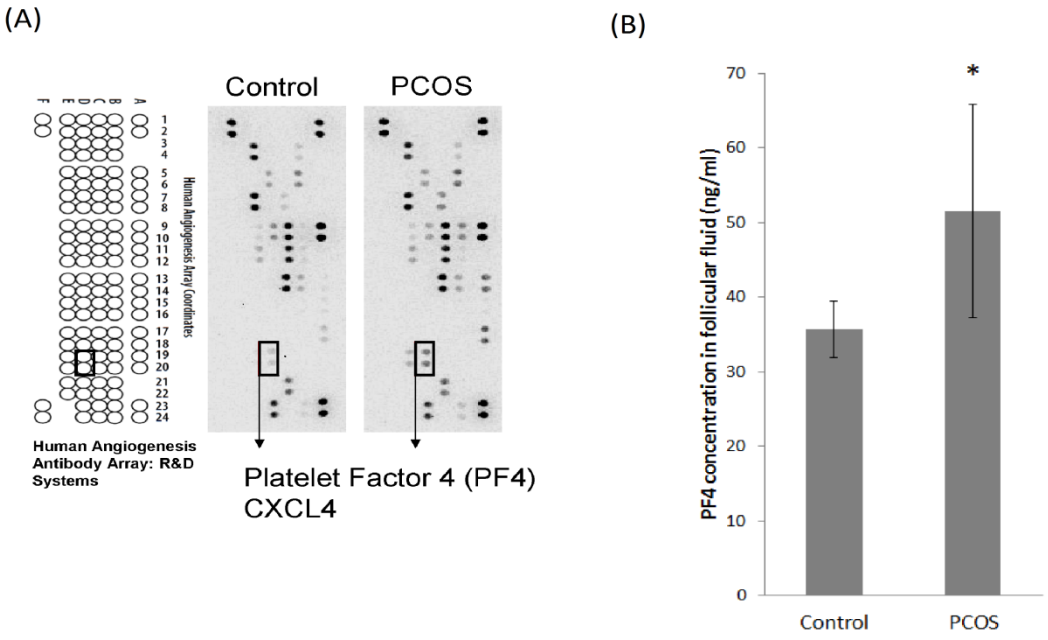

圖六：多囊性卵巢症候群病患濾泡液中的 PF4 蛋白表現。Platelet factor 4 (PF4) 在多囊性卵巢症候群病患之卵巢濾泡液中的濃度比起對照組顯著增加。

圖六 A：我們針對了 11 個對照組和 13 個多囊性卵巢症候群患者的濾泡液，進行了人類血管生成晶片分析，來偵測濾泡液中的哪個成分可能導致通透性變化。在晶片所能測試的 55 種人類血管生成相關蛋白質中，只有一種蛋白質（PF4）在兩組之間具有顯著差異的訊號值，多囊性卵巢症候群組表現顯著增加。圖例中的方框顯示 PF4 測量在晶片上的相對位置。

圖六 B：以酵素免疫法測量濾泡液中的 PF4 濃度。總共有 11 個對照組和 13 個多囊性卵巢症候群組病患的檢體進行比較。*$P < 0.05$.

doi:10.6342/NTU202000313

圖七.

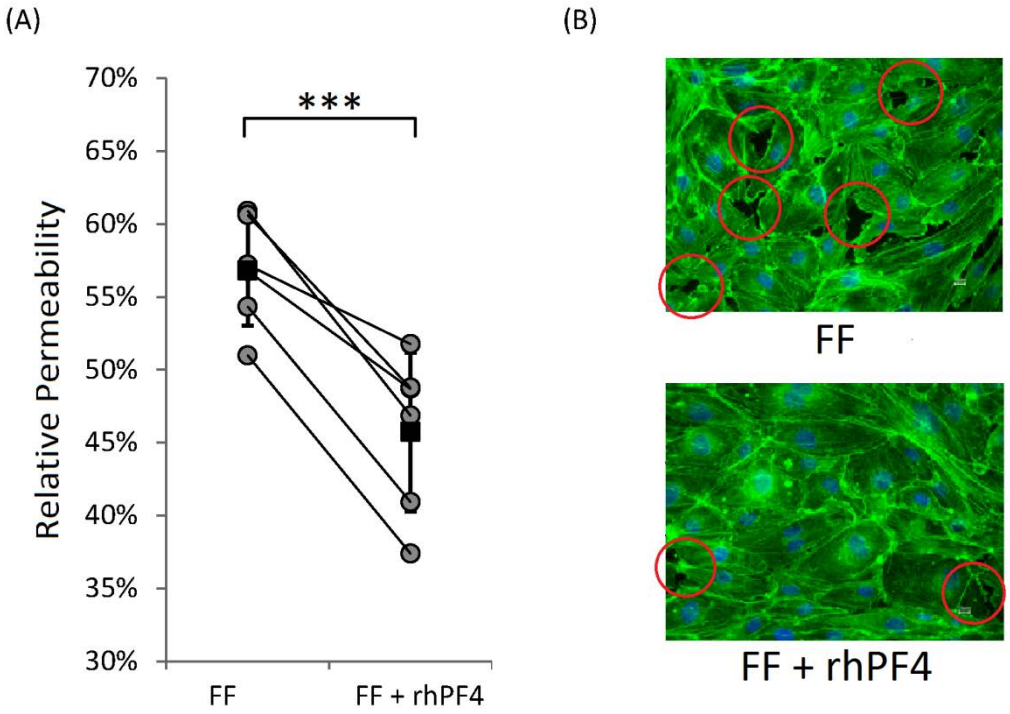

圖七：添加 PF4 對於內皮細胞相對通透性和內皮細胞間隙之影響。

圖七 A：我們在 HUVEC 實驗中將 rhPF4 添加到了對照組受試者 (n=6) 的濾泡液中，發現所測量到之內皮細胞通透性顯著降低。所添加之 rhPF4 濃度為(100 ng/ml)，並以添加 VEGF (50 ng/ml)時的通透性定義為 100% ，然後計算其他情況之相對通透性 (***P < 0.001).。

圖七 B：在人類臍靜脈內皮細胞裝置實驗中，進一步的免疫組織化學染色顯示在對照組 (n=6) 濾泡液中添加 rhPF4 後，內皮細胞之間的細胞間隙數量顯著減少。細胞間隙之位置以紅色圓圈顯示。

doi:10.6342/NTU202000313

圖八.

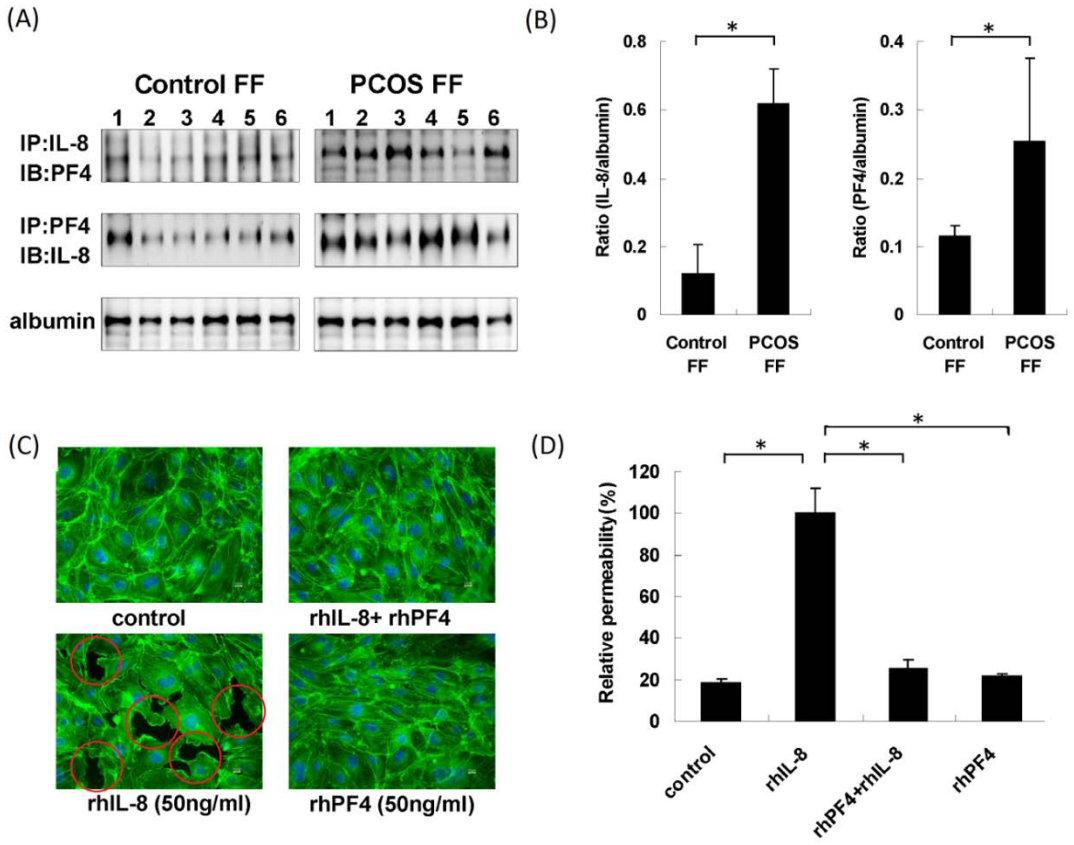

圖八：PF4 / IL-8 蛋白複合物在卵巢濾泡液的表現。

圖八 A：我們將對照組 (n=6) 和多囊性卵巢症候群組 (n=6) 的濾泡液藉由免疫沉澱和西方墨點法中進行 PF4 / IL-8 蛋白的分析。藉由 anti-IL-8 抗體所沉澱下來的蛋白質可以進一步在西方墨點法中被 anti-PF4 抗體所偵測到，反過來亦然。顯示 PF4 和 IL-8 兩個蛋白質是以結合的方式存在於多囊性卵巢症候群和對照組的卵巢濾泡液體中。白蛋白作為是對照組 (loading control)。 (IP, immunoprecipitation; IB, immunoblot)

圖八 B：濾泡液中 IL-8 和 PF4 蛋白的定量分析。是將圖八 A 電泳圖的色帶密度量化成數據，以白蛋白作為對照組 (loading control)。多囊性卵巢症候群病患濾泡液有顯著較高的 PF4 和 IL-8 蛋白質濃度(*P < 0.05)。

doi:10.6342/NTU202000313

圖八 C：以 FITC-labeled phalloidin (green) 染色分析不同情形下的 HUVEC 細胞間隙，包含了(a) control (M199 培養液) 、(b) rhIL-8 (50 ng/ml)、(c) rhIL-8 (50 ng/ml) + rhPF4 (50 ng/ml) (d) rhPF4 (50 ng/ml) 四個組別，治療後一小時後進行觀察。每組實驗均進行三重複。紅色圓圈代表細胞間隙處。

圖八 D：以長條圖顯示圖八 C 中四個組別其相對通透性的數值。此處是以 rhIL-8 組定義為 100%的通透率，並計算其他組的相對比率。結果顯示添加了 rhIL-8 可顯著增加內皮細胞通透性，而這個效果會受到 rhPF4 抑制。*$P < 0.05$.

doi:10.6342/NTU202000313

圖九.

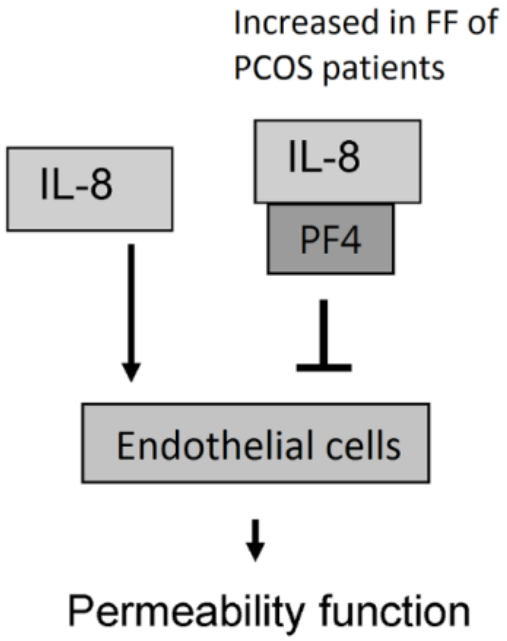

圖九：以流程圖說明 PF4/IL-8 蛋白影響內皮細胞通透性之交互調控機轉。濾泡液中原本就存在 PF4 和 IL-8 這兩種蛋白質且會彼此結合的方式存在。IL-8 的作用是會增加內皮細胞通透性，而 PF4 則會拮抗 IL-8 的作用，而抑制內皮細胞之通透性。

doi:10.6342/NTU202000313

圖十.

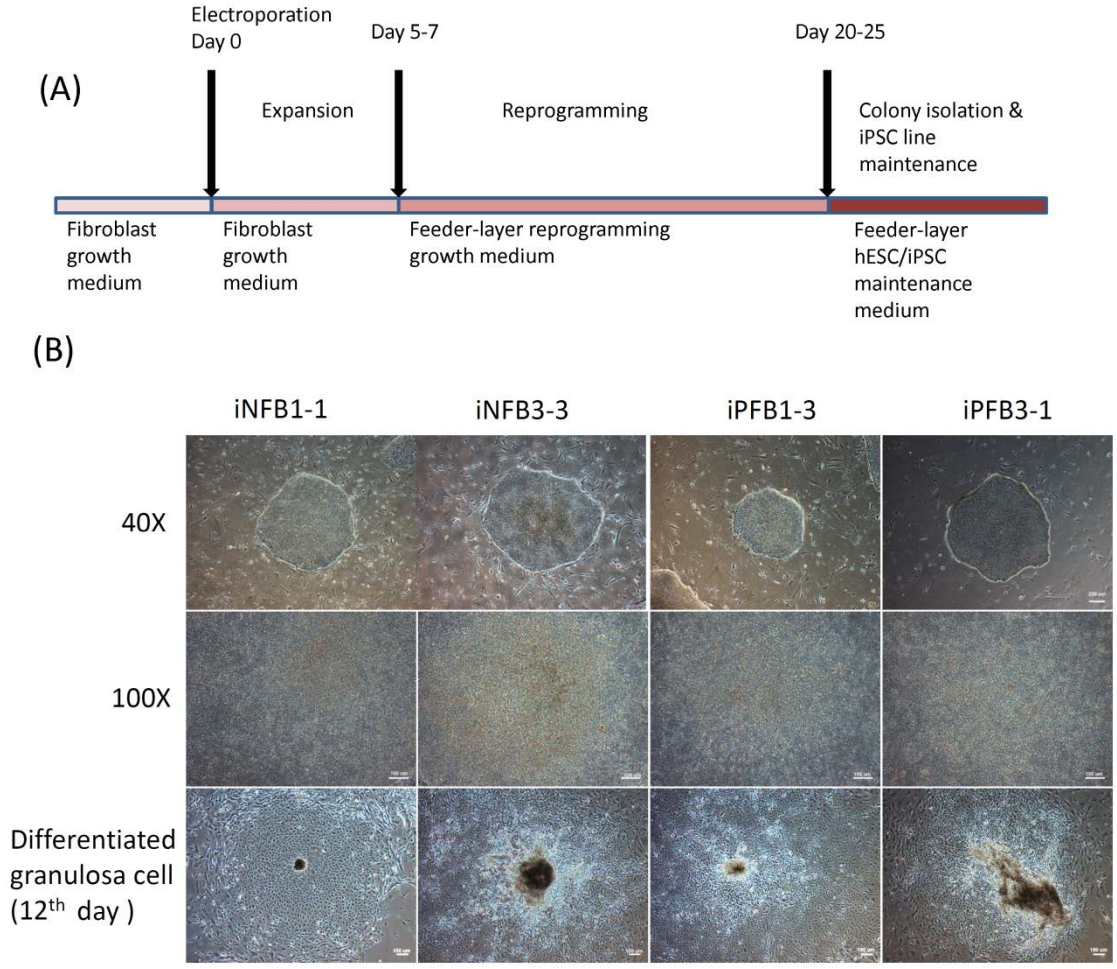

圖十：多囊性卵巢症候群病患特異性之 iPSC 細胞株的產生流程和細胞表徵。

圖十 A：將皮膚纖維母細胞以非病毒載體傳遞重編程相關基因，進行 iPSC 生成實驗的時間表和培養條件。

圖十 B：可藉由顯微鏡觀察細胞外形之變化，從最上方放大 40 倍時的紡錘形皮膚纖維母細胞，漸漸轉變為最下方分化第 12 天之圓形顆粒細胞 （非多囊性卵巢症候群之對照組 iPSC 株：iNFB1-1 和 iNFB3-3; 多囊性卵巢症候群組 iPSC 株：iPFB1-3 和 iPFB3-1）。

doi:10.6342/NTU202000313

圖十一.

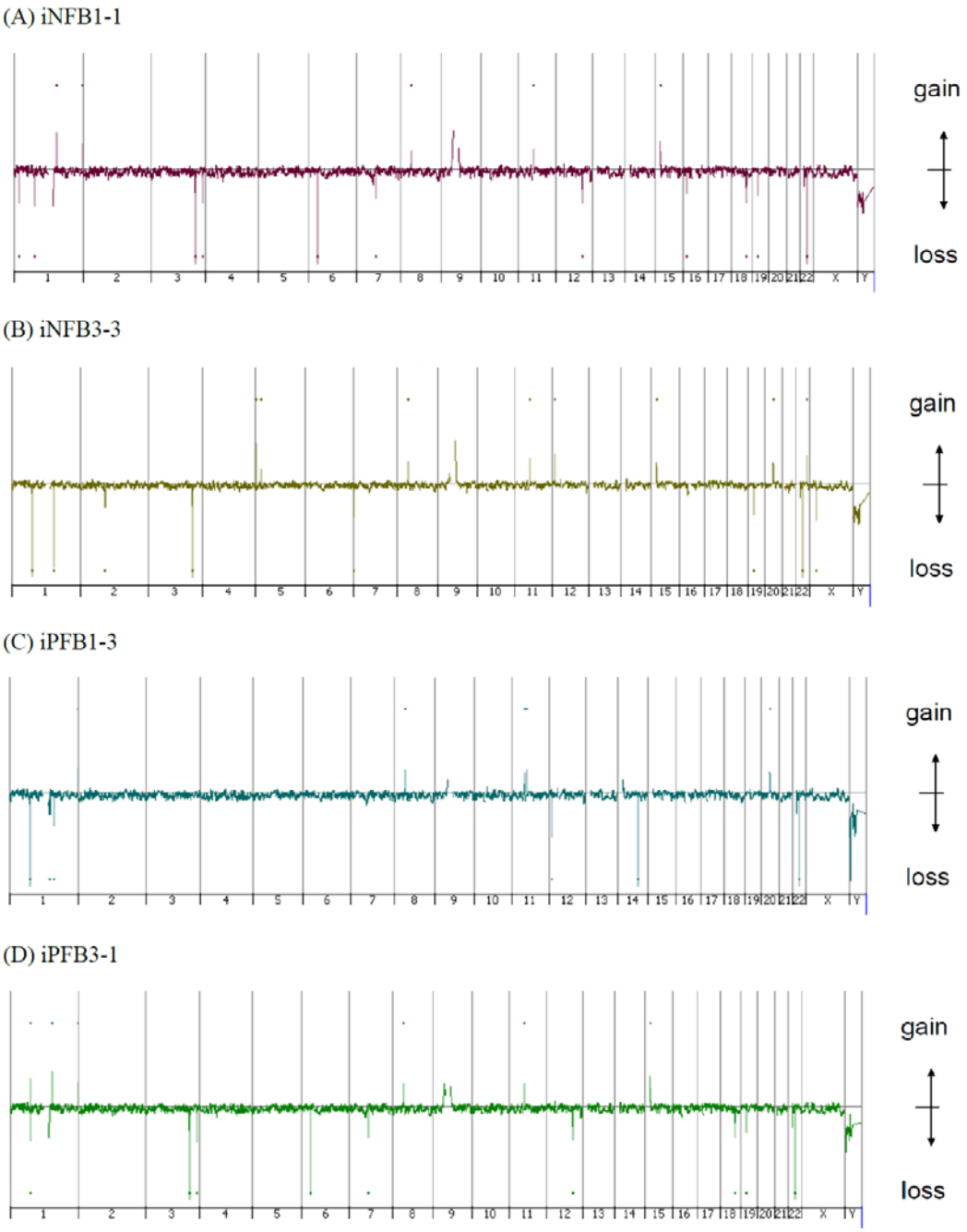

圖十一：iPSC 細胞株的染色體核型分析。顯示所有 iPSC 皆具有 44 + XX 的正常染色體模式。(非多囊性卵巢症候群之對照組 iPSC 株：iNFB1-1 和 iNFB3-3; 多囊性卵巢症候群組 iPSC 株：iPFB1-3 和 iPFB3-1)

doi:10.6342/NTU202000313

圖十二.

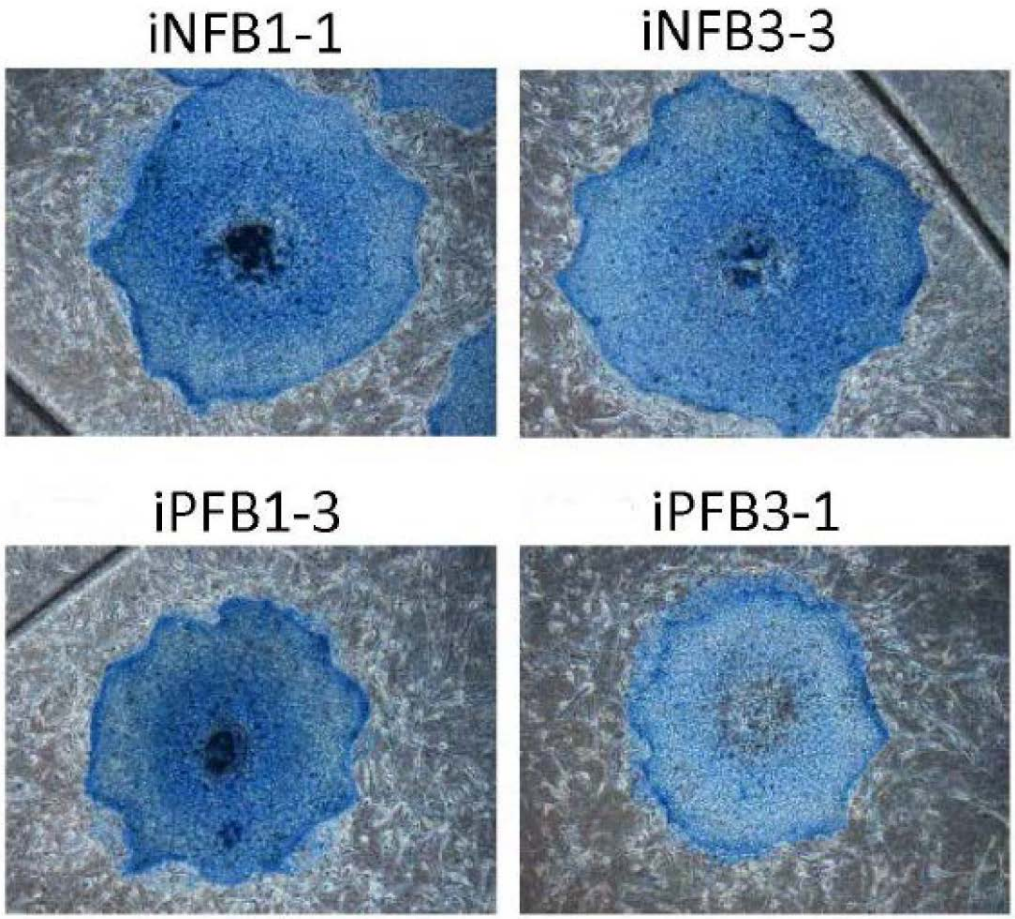

圖十二：iPSC 細胞株中的鹼性磷酸酶活性。在所有四個 iPSC 細胞株中，都可染色到陽性的鹼性磷酸酶活性，顯示其未分化和多能潛力。（非多囊性卵巢症候群之對照組 iPSC 株：iNFB1-1 和 iNFB3-3; 多囊性卵巢症候群組 iPSC 株：iPFB1-3 和 iPFB3-1）

doi:10.6342/NTU202000313

圖十三.

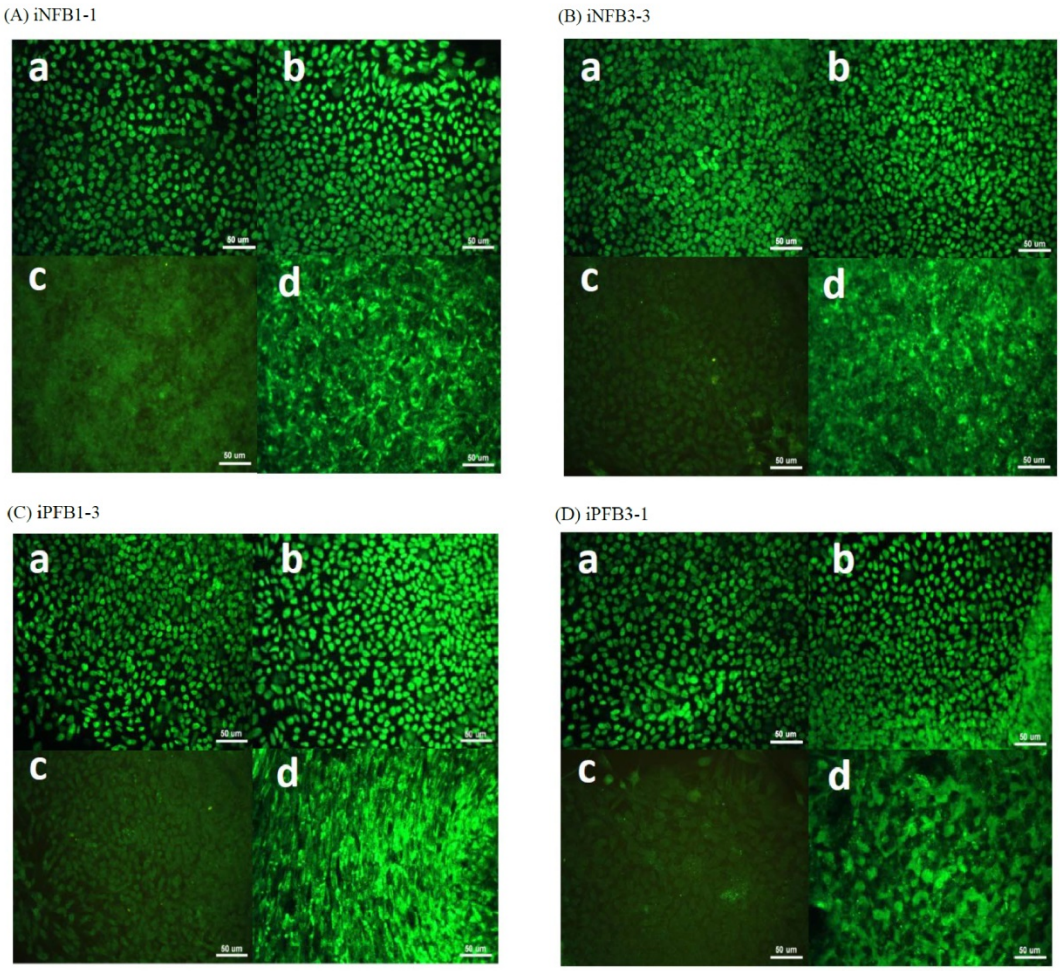

圖十三：iPSC 細胞株中多能性相關轉錄因子的免疫螢光染色。每個 iPSC 細胞株均成功表現多能性相關轉錄因子之標記，包括（a）NANOG、（b）OCT-4、（c）SSEA-4 和（d）TRA-1-60。 比例尺：50μm。（非多囊性卵巢症候群之對照組 iPSC 株：iNFB1-1 和 iNFB3-3; 多囊性卵巢症候群組 iPSC 株：iPFB1-3 和 iPFB3-1）

doi:10.6342/NTU202000313

圖十四.

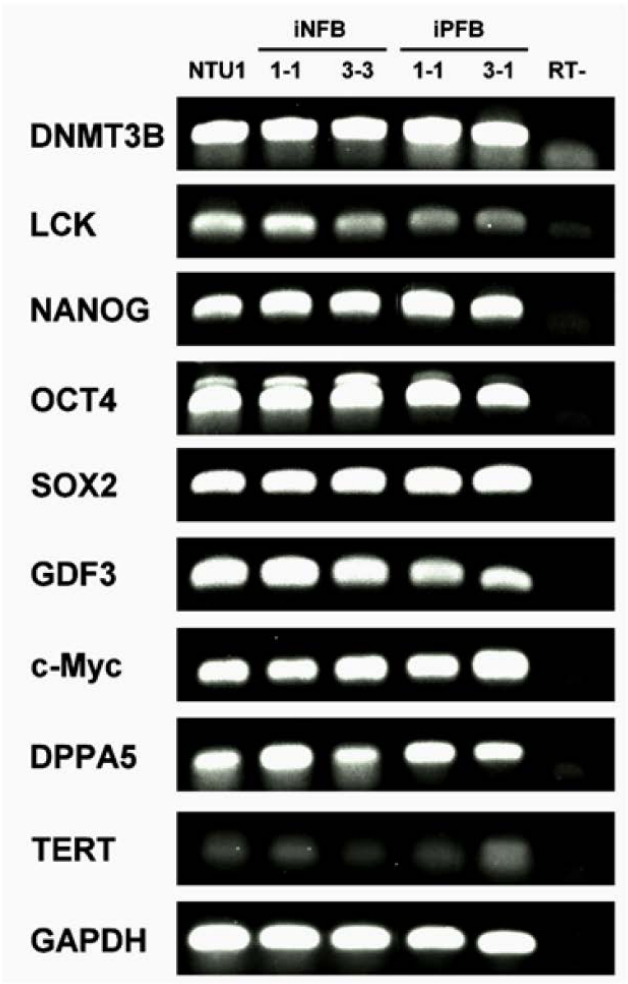

圖十四：iPSC 細胞株的自我更新相關基因表現。以逆轉錄聚合酶鏈式反應驗證自我更新基因標記之表現，包括 *DNMT3B*、*LCK*、*NANOG*、*OCT4*、*SOX2*、*GDF3*、*cMyc*、*DPPA5* 和 *TERT*。NTU1 是人類胚胎幹細胞株，在研究中用作陽性控制 (positive control)。每一株 iPSC 的自我更新基因表現均沒有顯著差異。（非多囊性卵巢症候群對照組：iNFB；多囊性卵巢症候群組：iPFB。）

doi:10.6342/NTU202000313

圖十五.

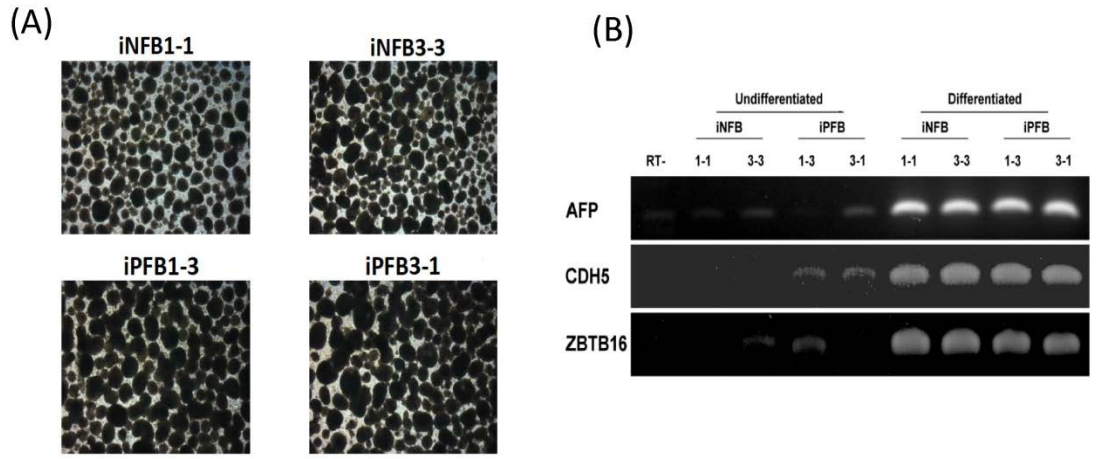

圖十五：以細胞實驗驗證 iPSC 的體外分化潛能。

圖十五 A:所有四株 iPSC 均成功形成胚胎體。(非多囊性卵巢症候群之對照組 iPSC 株：iNFB1-1 和 iNFB3-3; 多囊性卵巢症候群組 iPSC 株：iPFB1-3 和 iPFB3-1)。

圖十五 B：所有四株 iPSC 均成功表現三個胚層的指標基因。包括：外胚層分化標記 zinc finger and BTB domain containing 16 (ZBTB16) ；alpha-fetoprotein (AFP) 內胚層分化標記，以及中胚層分化標記 cadherin 5 (CDH5)。

doi:10.6342/NTU202000313

圖十六.

(A) iNFB1-1

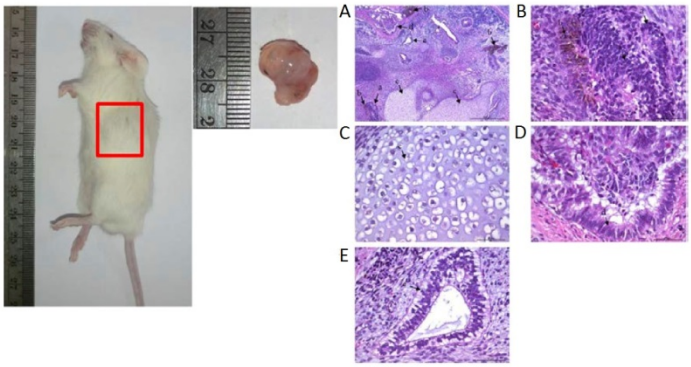

(B) iNFB3-3

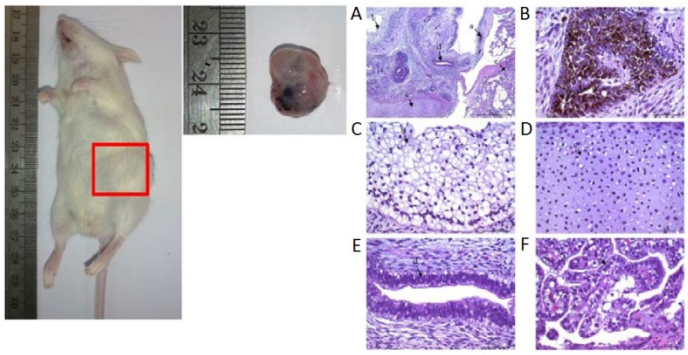

(C) iPFB1-3

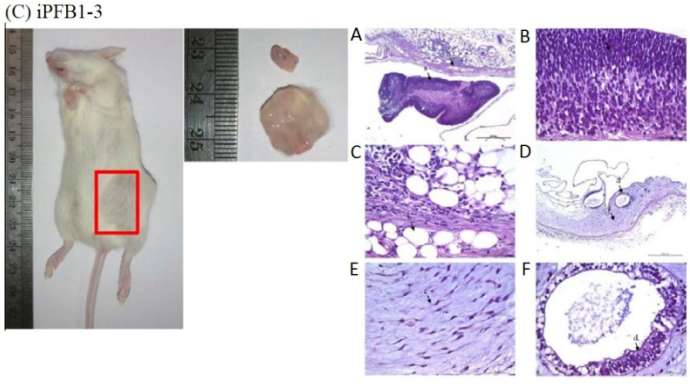

doi:10.6342/NTU202000313

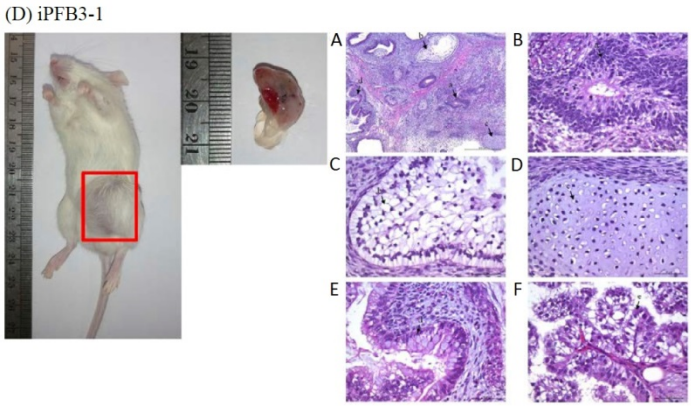

圖十六：以 NOD-SCID 小鼠實驗驗證 iPSC 的體內分化潛能。在小鼠身體注射 iPSC 之後可生成畸胎瘤，透過組織切片 H&E 染色分析，顯示出外胚層，中胚層和內胚層細胞均有被成功分化出來，例如：外胚層的神經上皮、色素上皮、視網膜樣結構和鱗狀上皮;中胚層的脂肪組織、透明軟骨和粘液樣結締組織(myxoid connective tissue);內胚層的腺體上皮 (glandular epithelium)。

圖十六 A：外胚層組織包括（A）神經上皮和（B）色素上皮。中胚層組織是（C）透明軟骨。內胚層組織包括（D）腺樣上皮和（E）具有亞核空泡的腺體結構（A：比例尺測量 500μm; B-E：比例尺測量 50μm）。

圖十六 B：外胚層組織包括(A) 色素上皮和 (B) 鱗狀上皮，其特徵在於具有空泡化細胞質的多角形細胞。中胚層組織是（C）透明軟骨。內胚層組織包括（D）腺樣上皮和(E)乳突狀腺樣上皮（A：比例尺測量 500μm; B-E：比例尺測量 50μm）。

圖十六 C：外胚層組織是（A）視網膜樣結構。 中胚層組織包括（B）脂肪組織和（C）粘液樣結締組織。 內胚層組織是（D）腺樣上皮（A 和 D：比例尺測量為 500μm; B，C，E 和 F：比例尺測量為 50μm）。

圖十六 D：外胚層組織包括（A）神經上皮和（B）鱗狀上皮，其特徵在於具有空泡化細胞質的多角形細胞。 中胚層組織是（C）透明軟骨。 內胚層組織包括（D）具有杯狀細胞的腺上皮，和（E）乳頭狀腺上皮（A：比例尺測量 500μm; B-F：比例尺測量 50μm）。

doi:10.6342/NTU202000313

圖十七

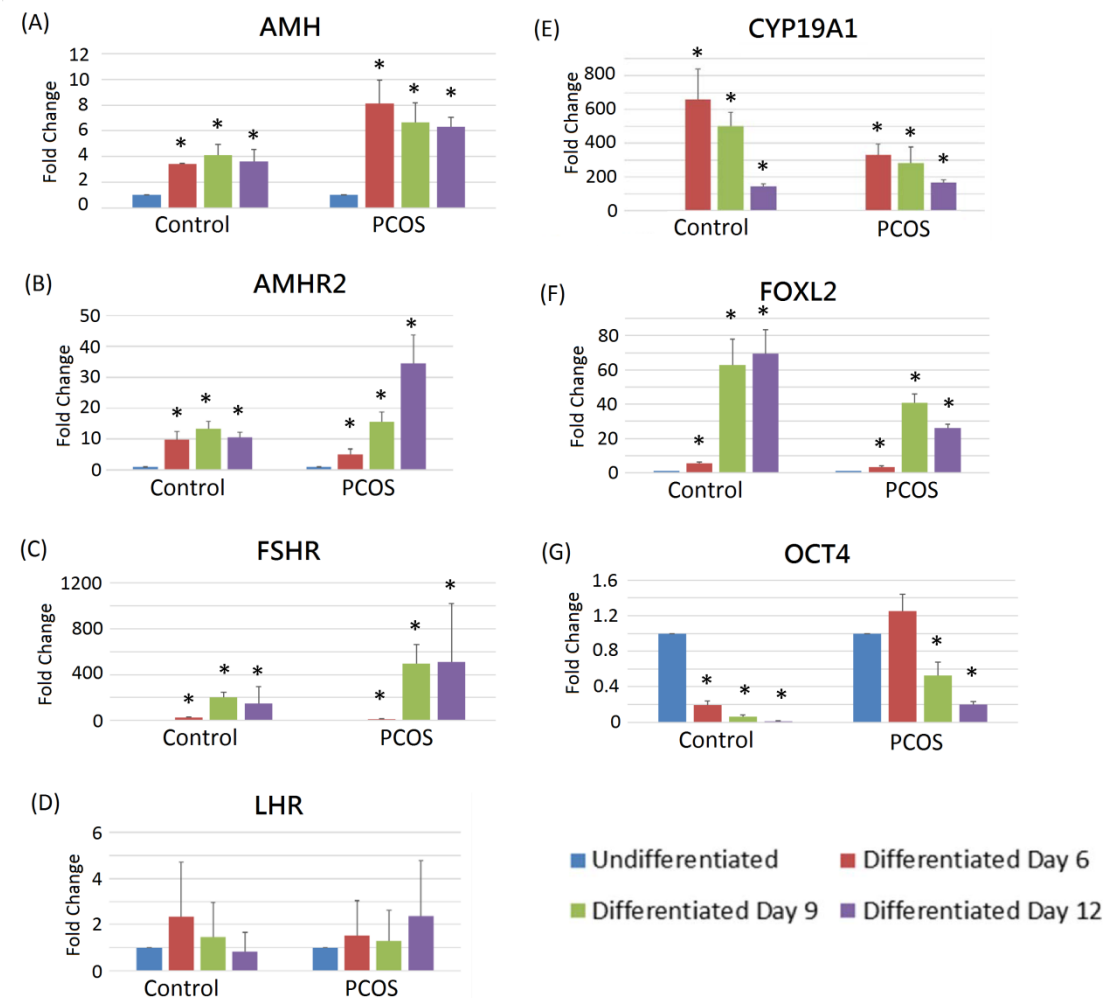

圖十七：iPSC 衍生顆粒細胞之相關基因表現。顯示了在不同時間點，來自多囊性卵巢症候群和非多囊性卵巢症候群對照組之 iPSC 所衍生顆粒細胞的相關基因表驗。在分化後第 0 天（未分化），6、9 和 12 天使用 qRT-PCR 檢查顆粒細胞特異性表現基因（*FOXL2*，*AMH*，*FSHR*，*LHR*，*AMHR2* 和 *CYP19A*）和多能性基因（*OCT4*）的表現。 Y 軸表示相對於第 0 天的基因表現的倍數變化 （fold change ；FC）。*GAPDH* 用作管家基因 (housekeeping gene)。*與未分化的 iPSC 相比 P <0.05。

doi:10.6342/NTU202000313

圖十八.

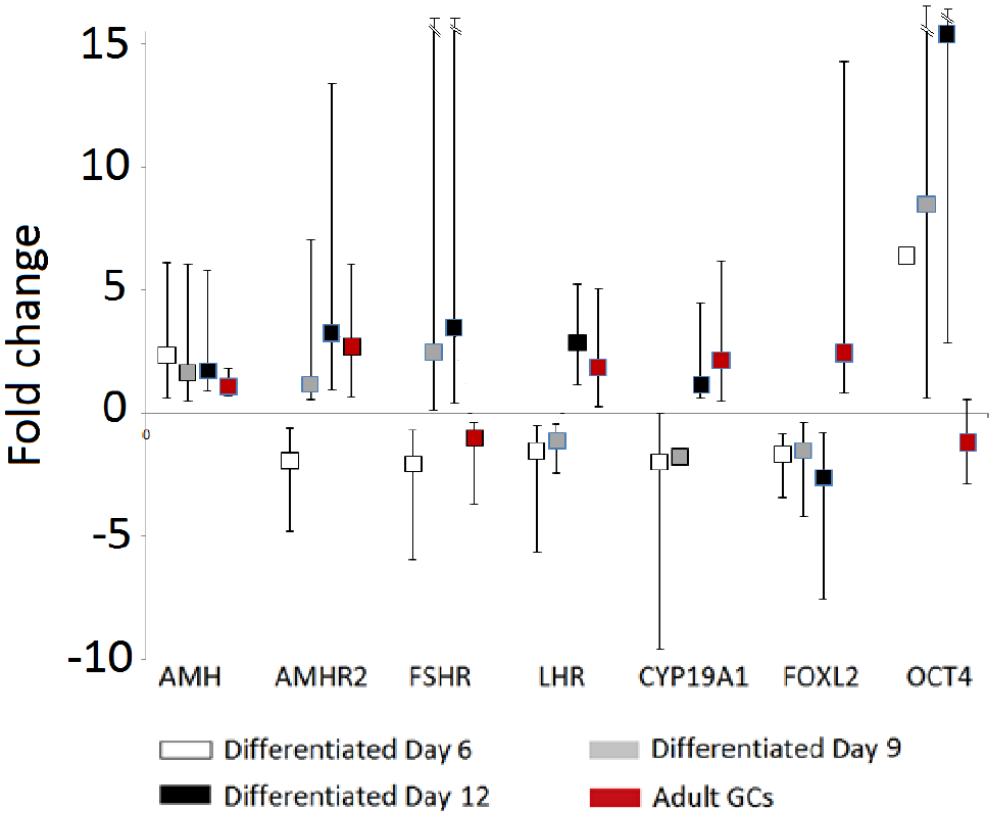

圖十八：比較顆粒細胞相關基因在多囊性卵巢症候群組和對照組的表現值。以對照組為基準 1，計算多囊性卵巢症候群組表現量為對照組的幾倍（縱向誤差線表示 90%信賴區間）。在 iPSC 衍生顆粒細胞的不同分化天數與成人顆粒細胞之間相比，顆粒細胞相關基因的表現量沒有顯著差異。iPSC 衍生顆粒細胞的基因表現量數據來自三重複之 qPCR 實驗（多囊性卵巢症候群組的 n = 2，對照組的 n = 2），成人顆粒細胞中的基因表現量來自基因表現晶片（多囊性卵巢症候群組的 n = 4，對照組的 n = 3）。

doi:10.6342/NTU202000313

圖十九.

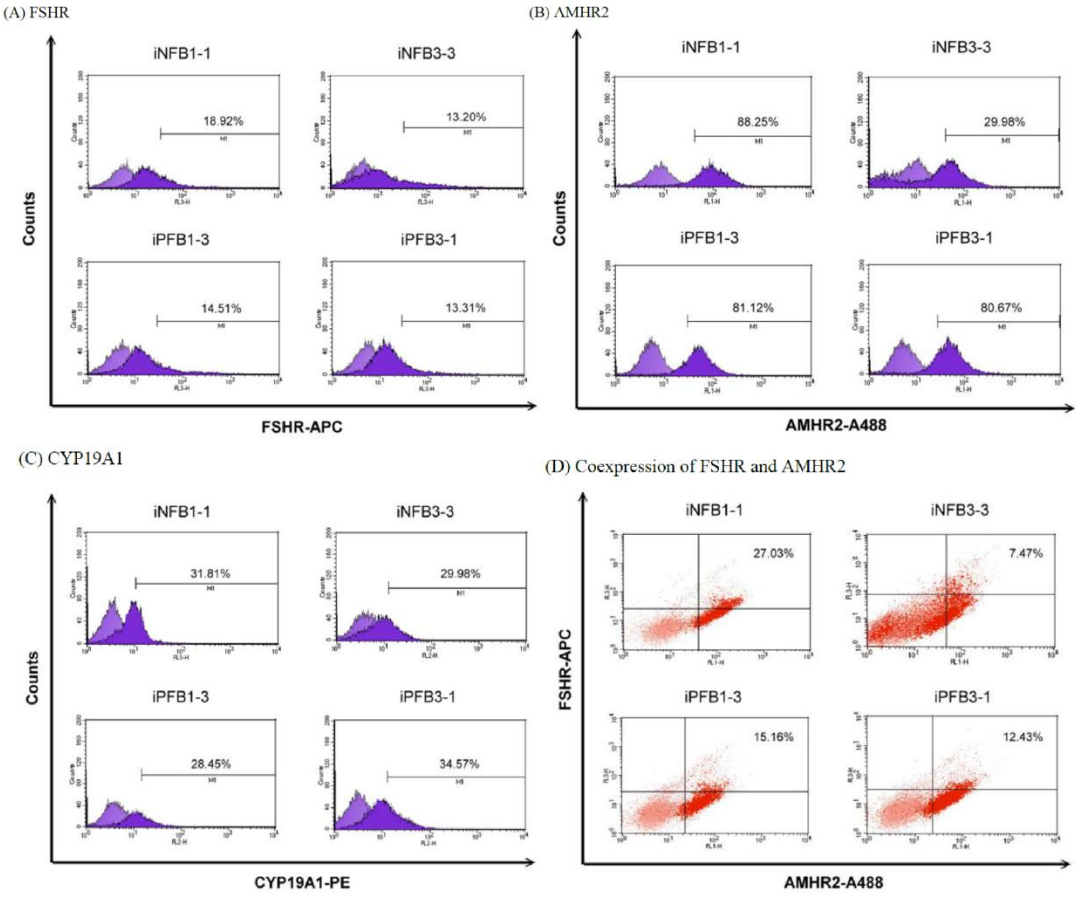

圖十九：以流式細胞儀分析 iPSC 衍生顆粒細胞中顆粒細胞特異基因的表現。多囊性卵巢症候群組和對照組相比，其 iPSC 所衍生顆粒細胞的 FSHR、CYP19A1 和 AMHR2 基因的表現比率相似，顯示其分化效率沒有顯著差異。 FSHR = follicle-stimulating hormone receptor; AMHR2 = antimullerian hormone receptor 2; CYP19A1 = aromatase.（對照組：iNFB1-1 和 iNFB3-3; 多囊性卵巢症候群組：iPFB1-3 和 iPFB3-1）。

doi:10.6342/NTU202000313

圖二十.

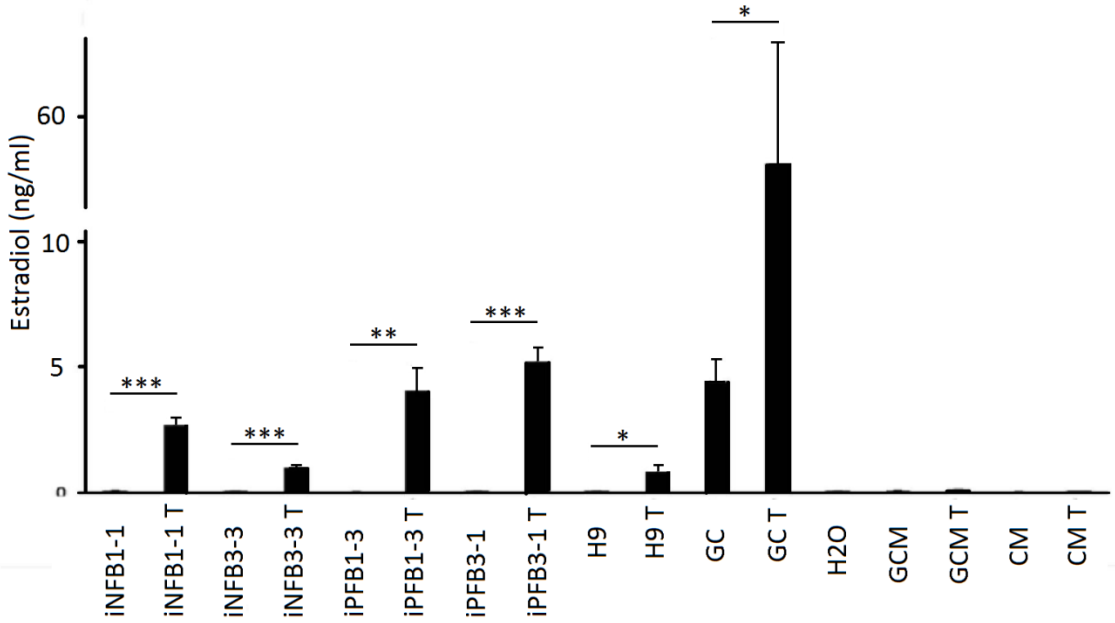

圖二十：iPSC 衍生顆粒細胞的芳香酶活性測定。由於顆粒細胞的芳香酶可將睪固酮轉化為雌激素，所有 iPSC 衍生顆粒細胞用 50ng / mL 睪固酮處理後，測量雌激素的濃度來測定細胞中芳香酶的活性。 * P <0.05，** P <0.01，*** P <0.001。 數據來自至少 3 次獨立實驗的平均值±標準偏差。H9 是從我們之前建立的人類胚胎幹細胞所重新分化得到的顆粒細胞。GCs 是在經取卵手術收集得到的顆粒細胞。T：睪固酮。GCM：人類顆粒細胞的培養基。 CM：iPSC 和 H9 所衍生顆粒細胞的培養基。(非多囊性卵巢症候群控制組：iNFB1-1 和 iNFB3-3; 多囊性卵巢症候群組：iPFB1-3 和 iPFB3-1)。

doi:10.6342/NTU202000313

圖二十一.

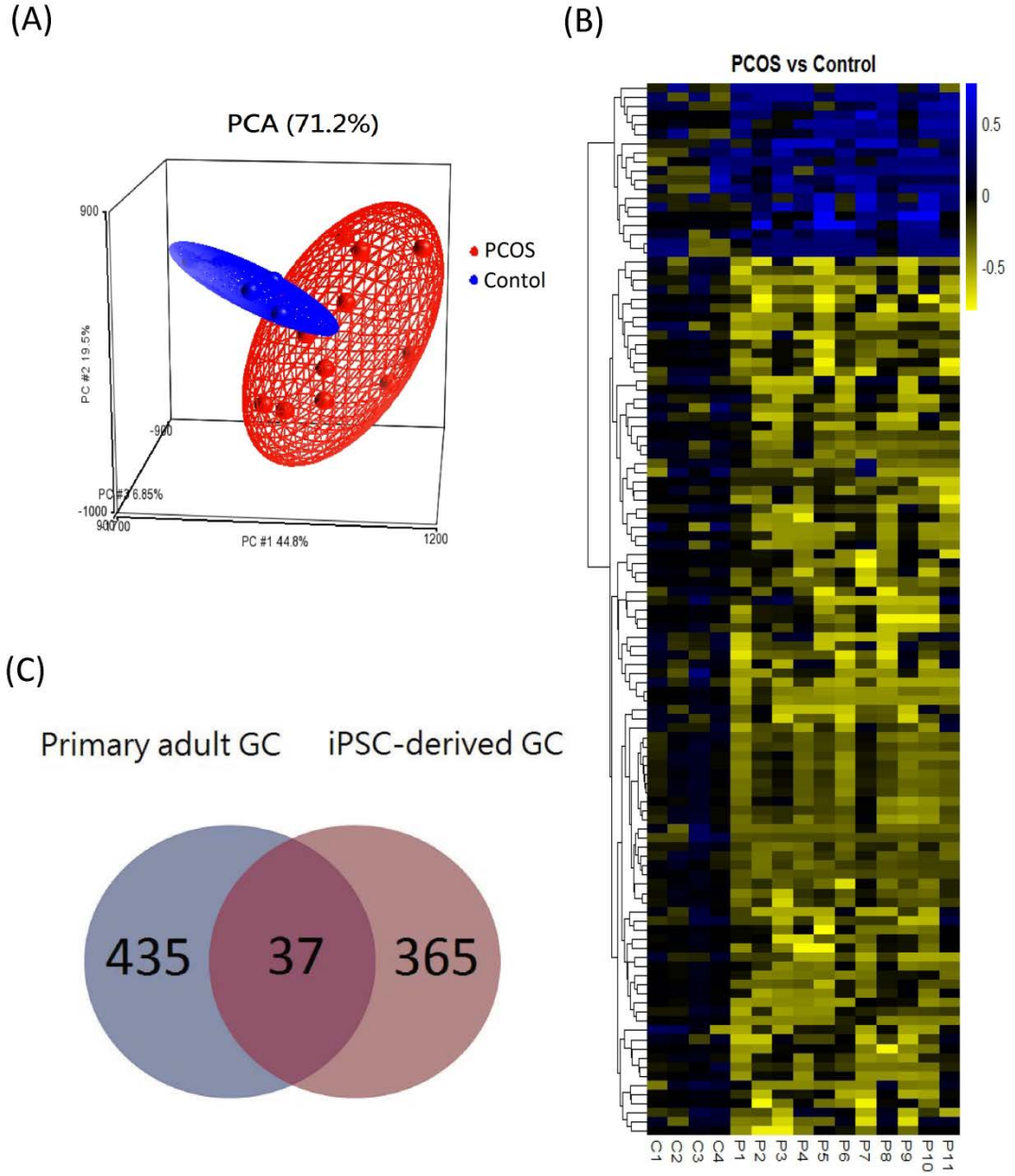

圖二十一：以晶片分析比較多囊性卵巢症候群與對照組之全基因體 DNA 甲基化表現。

圖二十一 A：從成人顆粒細胞（11 名多囊性卵巢症候群患者和 4 名對照受試者）中，對所有樣本之全基因體 DNA 甲基化表現進行主成份分析 (principle component analysis) 。圖中的每個點都是一個樣本，代表所有 CpG 位置的平均甲基化狀態。結果顯示多囊性卵巢症候群組和對照組的樣本的平均 CpG 甲基化狀態可以有明顯

doi:10.6342/NTU202000313

區分。

圖二十一 B：針對多囊性卵巢症候群和對照組之成人顆粒細胞的差異性甲基化基因，進行階層式分群法之分析（熱圖）。 每一行代表一個單獨的差異性甲基化基因，每一列代表一個受試者的樣本（列在熱圖下方）。 熱圖下方的色帶表示甲基化狀態：低度甲基化為黃色，高度甲基化為藍色。

圖二十一 C：將多囊性卵巢症候群和對照組相比較所找出之差異甲基化基因，在成人顆粒細胞和分化第 12 天之 iPSC 衍生顆粒細胞兩種不同細胞進行比較，繪出維恩圖(Venn diagram)。其中，分化第 12 天之 iPSC 衍生顆粒細胞只囊括前 10%的差異甲基化基因來分析。每個圓圈中的數字，代表差異甲基化基因的數量。重疊處的數字代表兩種不同顆粒細胞所共同出現的差異甲基化基因，非重疊處代表兩種不同顆粒細胞所各自有的差異甲基化基因。重疊的 37 個基因的名稱列表，列在表十中。

doi:10.6342/NTU202000313

圖二十二.

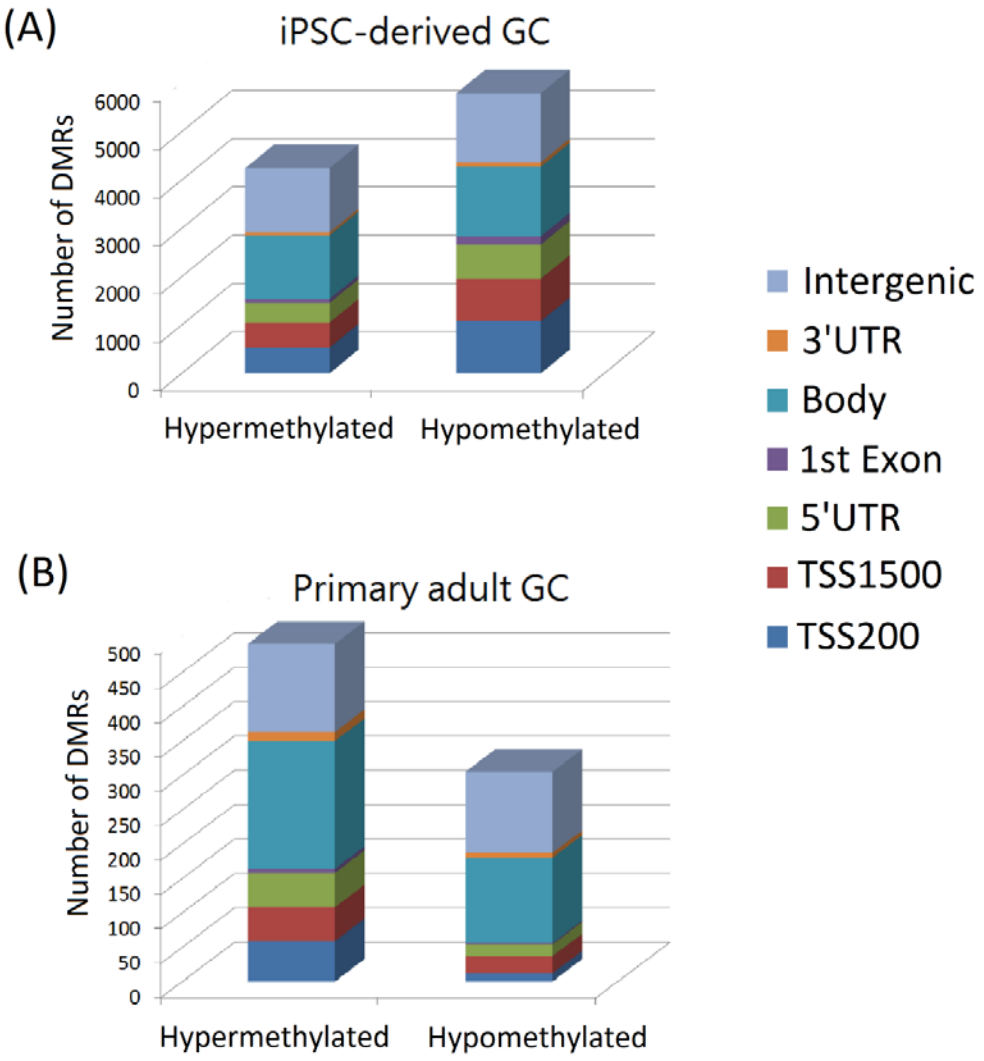

圖二十二：差異性甲基化區域在基因相對位置的分佈。

圖二十二 A：以柱狀圖顯示在多囊性卵巢症候群和對照組的成人顆粒細胞中，高度甲基化和低度甲基化的差異甲基化區域，位於不同基因構造的數量。 TSS = transcription start site; UTR = untranslated region。

圖二十二 B：以柱狀圖顯示在多囊性卵巢症候群和對照組的 iPSC 衍生顆粒細胞中，高度甲基化和低度甲基化的差異甲基化區域，位於不同基因構造的數量。

doi:10.6342/NTU202000313

圖二十三.

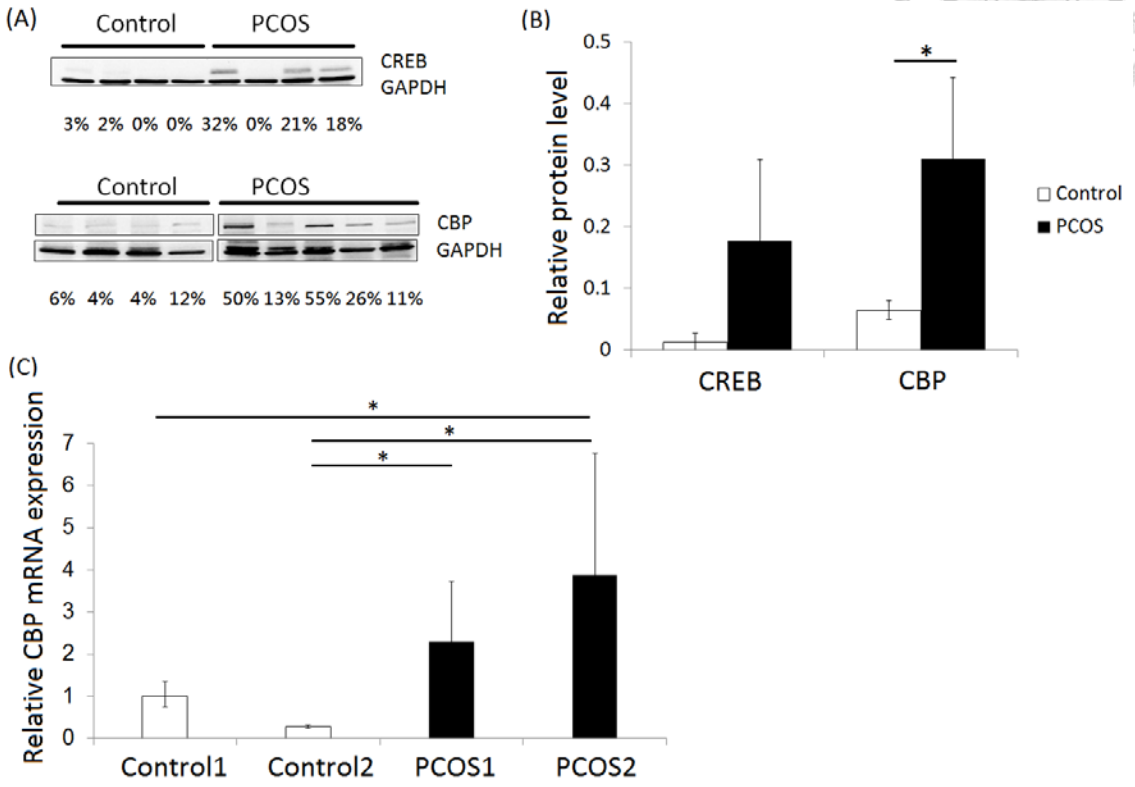

圖二十三：成人顆粒細胞和 iPSC 衍生顆粒細胞之 CREB 和 CBP 的表現。

圖二十三 A：以免疫沉澱法分析多囊性卵巢症候群組和對照組受試者的成人卵巢顆粒細胞的 CREB 和 CBP 蛋白的表現量。以 GAPDH 作為基準值。未切割的原始凝膠顯示在圖二十四中。(CREB：43kDa，CBP：220kDa，和 GAPDH：39kDa)。

圖二十三 B：將免疫沉澱法分析得到的成人卵巢顆粒細胞之 CREB 和 CBP 蛋白表現量進行量化。。* P <0.05。

圖二十三 C：以 rtPCR 分析分化第 12 天的 iPSC 衍生顆粒細胞的 CBP 基因表現量。先以流式細胞儀根據濾泡刺激素受體 (FSHR) 的陽性表現，來篩選純化出顆粒細胞並進行 rtPCR 分析。用 $2^{-\Delta\Delta CT}$ 方法計算出基因的相對表現值。每個數值代表三個獨立重複實驗的平均值和誤差。* P <0.05。 （非多囊性卵巢症候群控制組：IBMS-01-02 和 iNFB3-3; 多囊性卵巢症候群組：iPFB1-3 和 iPFB3-1。）

doi:10.6342/NTU202000313

圖二十四.

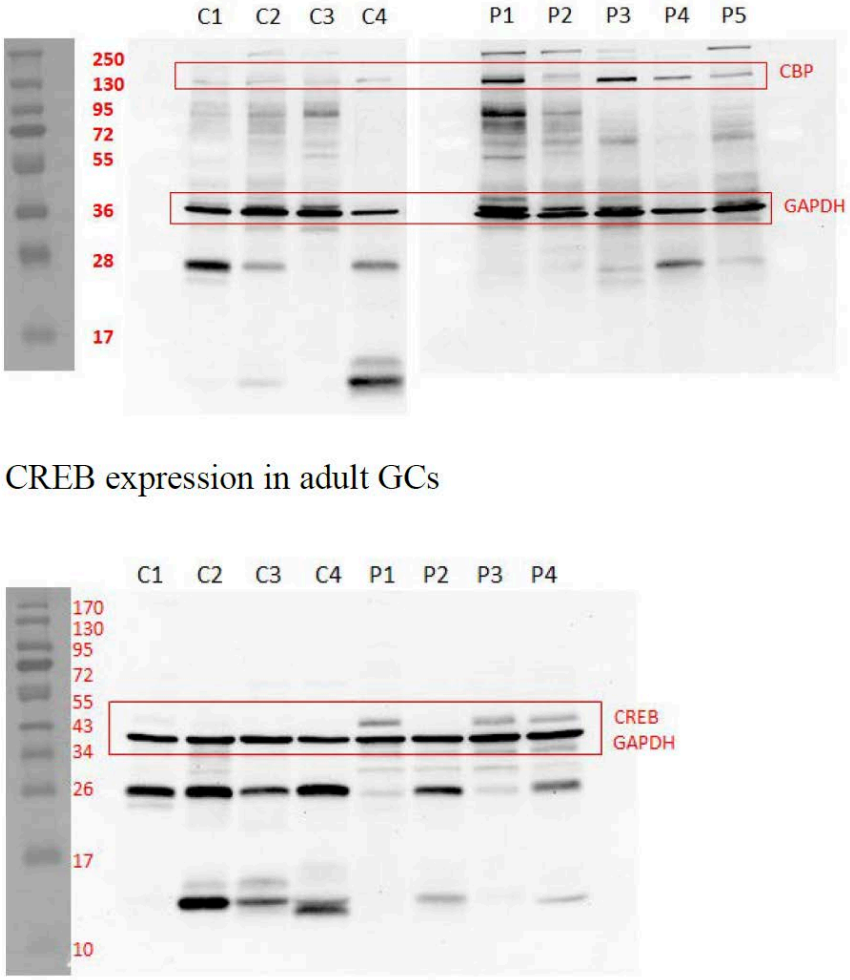

圖二十四：未經切割的西方墨點分析原始凝膠。

doi:10.6342/NTU202000313

圖二十五.

(A) miR-93

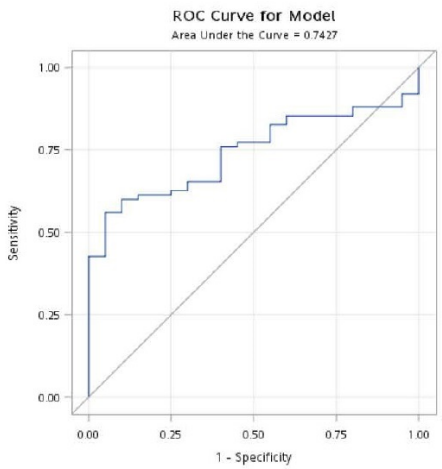

(B) miR-132

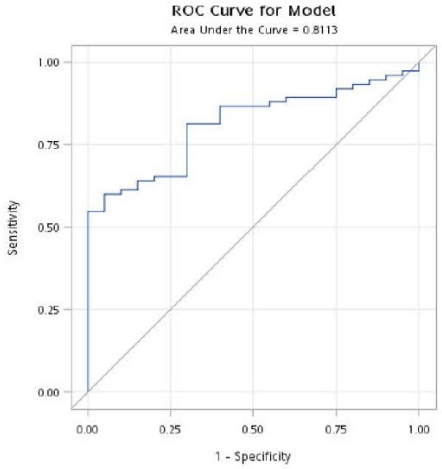

(C) miR-222

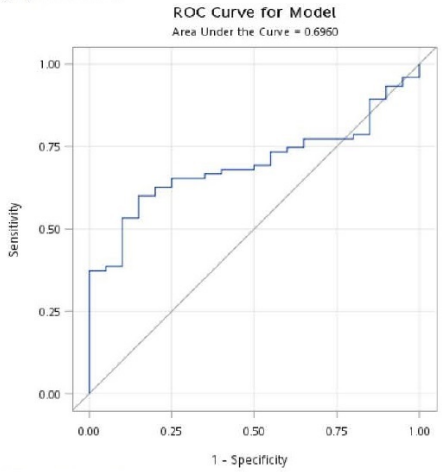

(D) miR-27a

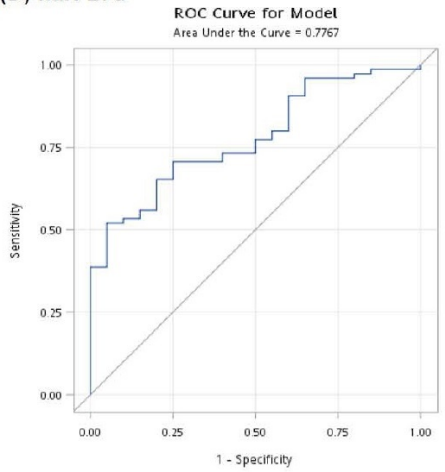

(E) miR-125b

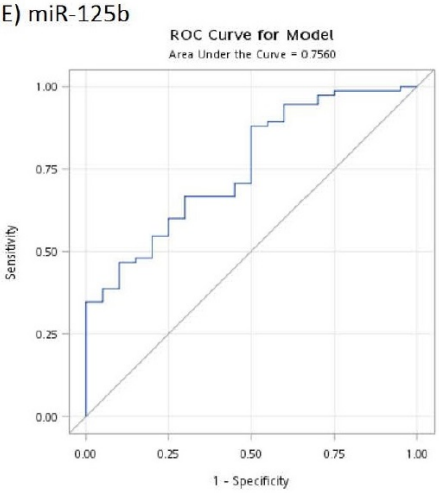

(F) miR-212

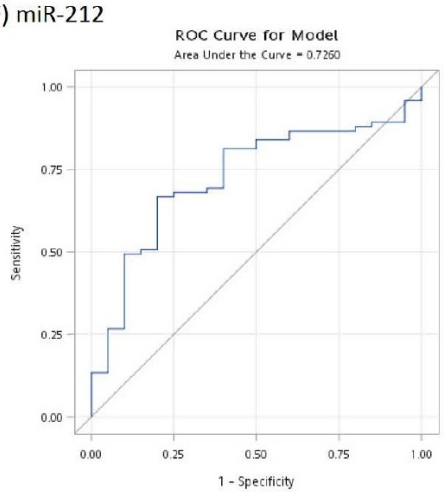

doi:10.6342/NTU202000313

圖二十五. (續)

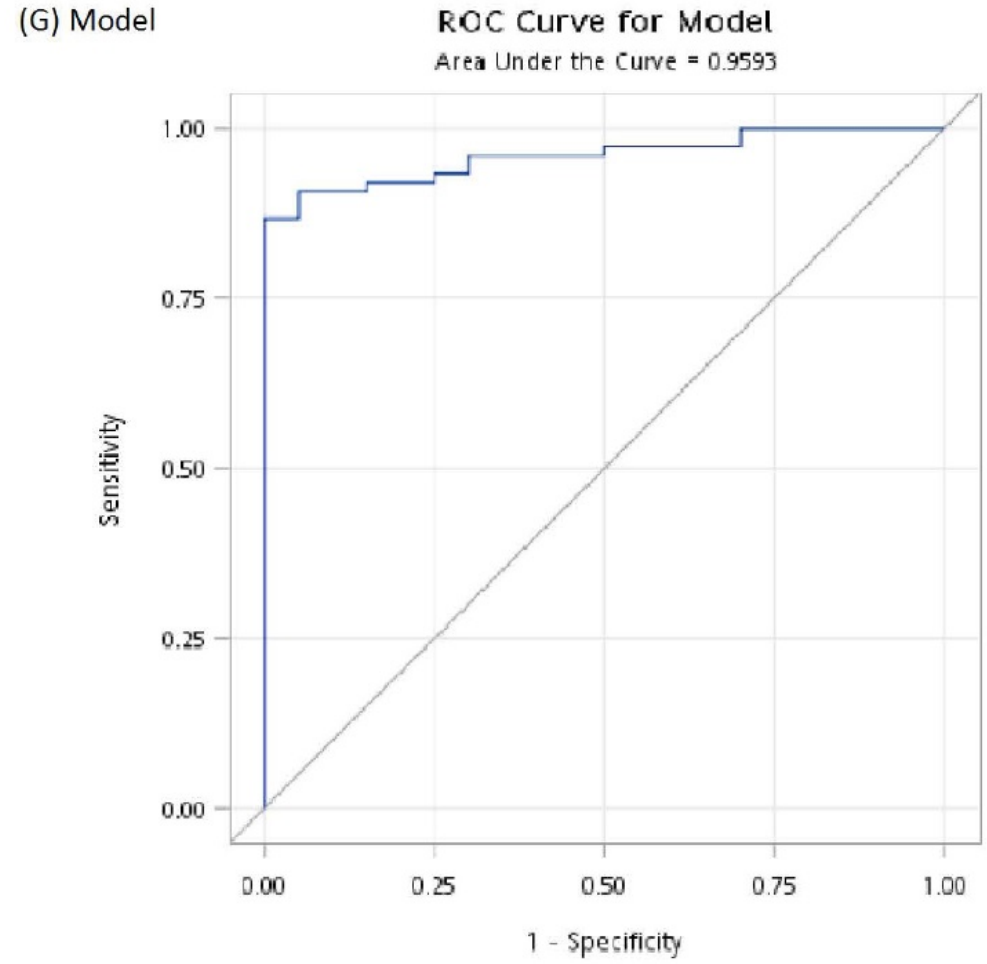

圖二十五：多囊性卵巢症候群診斷預測模型之 ROC 曲線圖。(A)到(F)顯示個別 miRNA 對於多囊性卵巢症候群診斷預測模型的 ROC 曲線，(G)則是綜合以上六個 miRNA 建立之預測模型之 ROC 曲線。詳細公式和各 ROC 曲線之特異性和敏感度列於表十五。

doi:10.6342/NTU202000313

圖二十六.

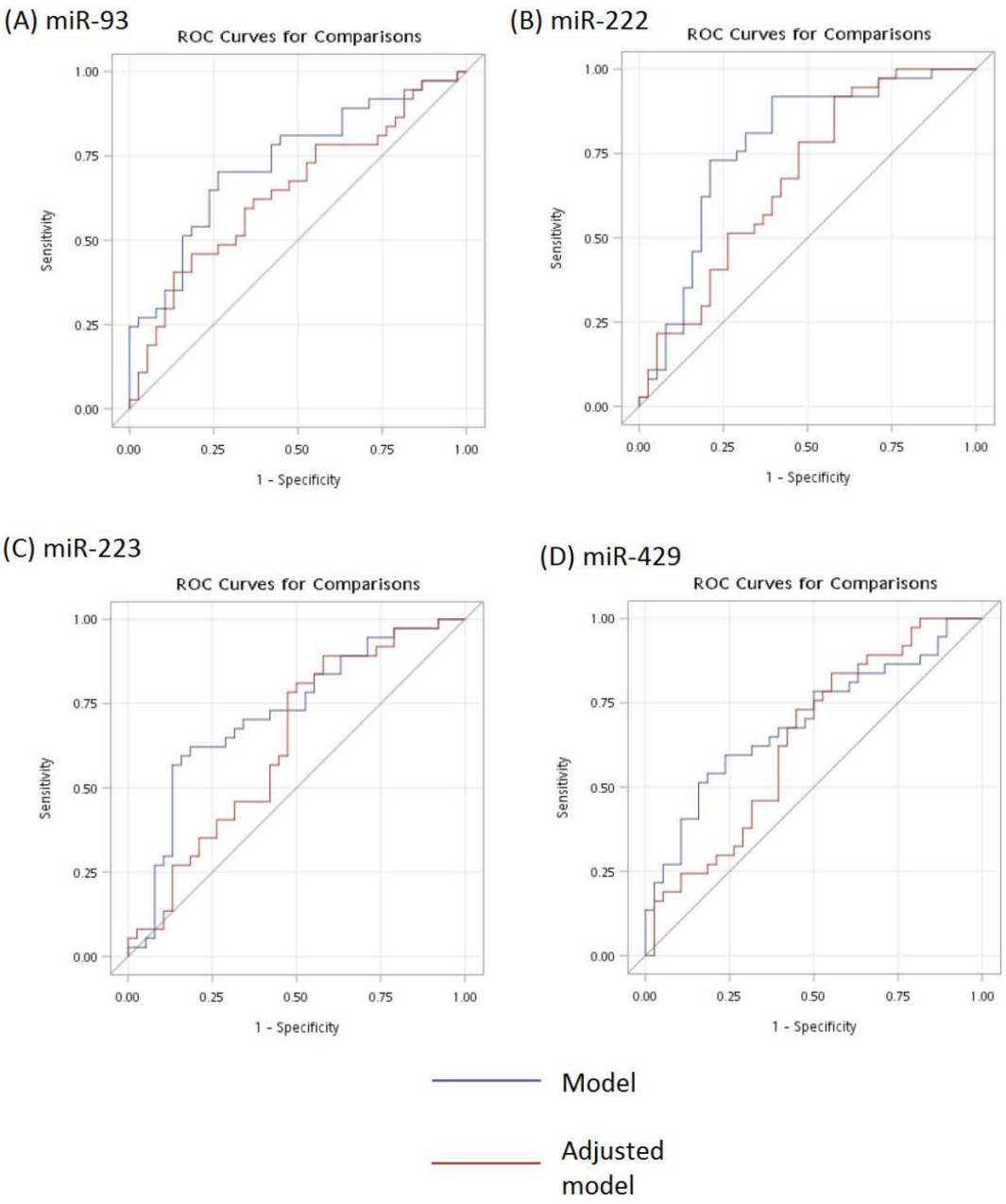

doi:10.6342/NTU202000313

圖二十六. (續)

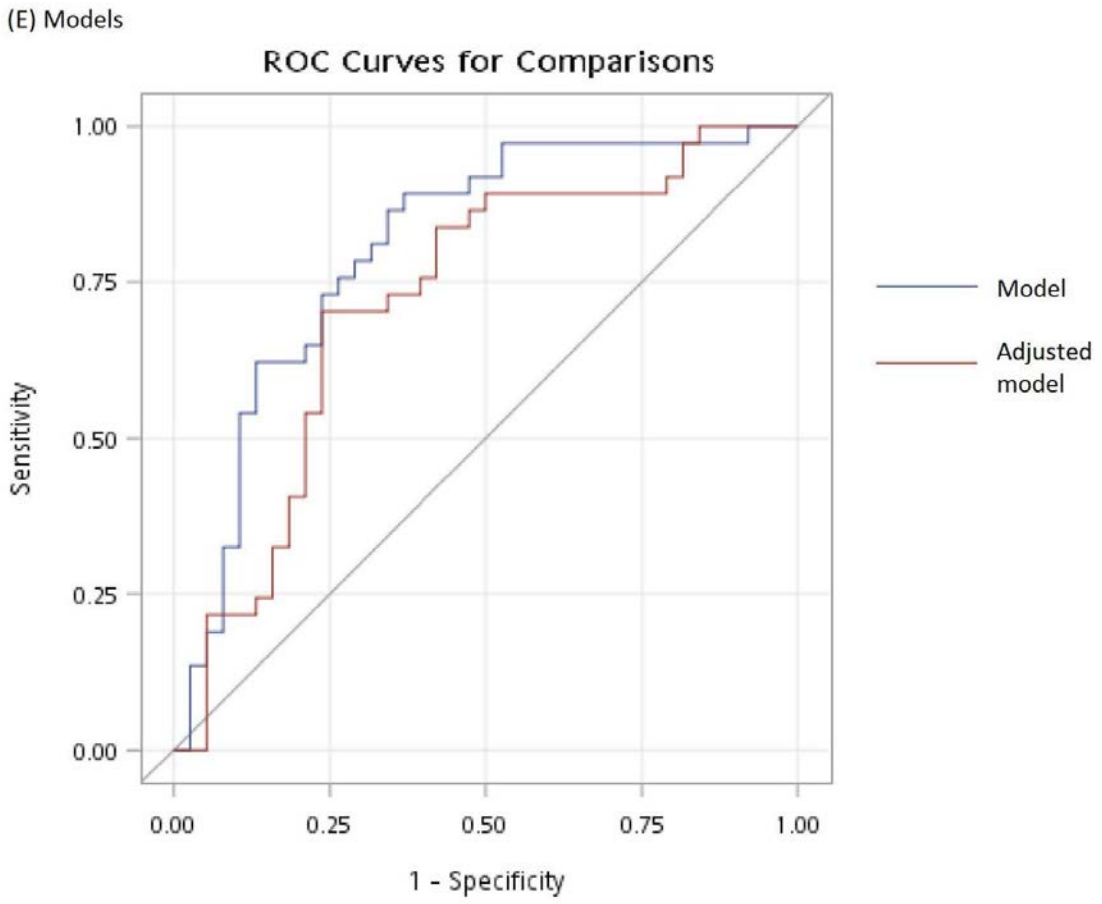

圖二十六：metformin 療效預測模型之 ROC 曲線圖。(A)到(D)顯示個別 miRNA 對於多囊性卵巢症候群診斷預測模型的 ROC 曲線，(E)則是綜合以上四個 miRNA 建立之預測模型之 ROC 曲線，其中藍色線代表僅用四個 miRNA 所建立之預測模型，紅色線為合併四個 miRNA 和四個臨床指標(年齡、月經週期、BMI、高雄性荷爾蒙症之有無)所建立之預測模型。詳細公式和各 ROC 曲線之特異性和敏感度列於表十六。

doi:10.6342/NTU202000313

表一：所用 PCR 和 qPCR 系統的 primer 序列和 TaqMan 探針 ID (Applied Biosystems)

Gene name	Assay ID (ABI)	Gene description
AFP	Hs01040598_m1	alpha-fetoprotein
AMH	Hs01006984_g1	Anti-mullerian hormone
AMHR2	Hs00179718_m1	Anti-mullerian hormone receptor, type II
CDH5	Hs00174344_m1	cadherin 5
c-Myc	Hs00153408_m1	v-myc avian myelocytomatosis
CYP19A1	Hs00903411_m1	Cytochrome P450, family 19, subfamily A, polypeptide 1
DNMT3B	Hs00171876_m1	DNA (cytosine-5-)-methyltransferase 3 beta
DPPA5	Hs00988349_g1	developmental pluripotency associated 5
FOXL2	Hs00846401_s1	Forkhead box L2
FSHR	Hs00174865_m1	Follicle stimulating hormone receptor
GAPDH	Hs02758991_g1	Glyceraldehyde-3-phosphate dehydrogenase
GDF3	Hs00220998_m1	growth differentiation factor 3
LCK	Hs00178427_m1	lymphocyte-specific protein tyrosine kinase
LHR	Hs00174885_m1	Luteinizing hormone/choriogonadotropin receptor
NANOG	Hs02387400_g1	Nanog homeobox
OCT-4	Hs00999632_g1	POU class 5 homeobox 1
SOX2	Hs01053049_s1	SRY (sex determining region Y)-box 2
TERT	Hs00972650_m1	telomerase reverse transcriptase
ZBTB16	Hs00232313_m1	zinc finger and BTB domain containing 16
CBP	Forward primer: CTCCTTCCCGAATGCCTCAG; reverse primer: CTGTGACACGCCTGTTTGGG (customized)	

doi:10.6342/NTU202000313

表二：廣義相關圖分析產生的四個次族群之身體指數、內分泌和新陳代謝指標

	第一組	第二組	第三組	第四組	所有人	P 值
變數	N=204	N=111	N=88	N=57	N=460	
年齡 (歲)	24.4(4.4)	25.4(5.4)	24.6(5.1)	24.3(6.1)	24.7(5.0)	0.381
身體指標						
身高 (公分)	160	159	161	161	160	0.105
體重 (公斤)	55.9(11.1)^{abc}	68.7(19.3)^{ad}	65.1(15.9)^{be}	79.5(14.5)^{cde}	63.7(16.8)	<0.001
BMI (公斤/平方公分)	21.9(3.9)^{abc}	26.9(6.9)^{ad}	25.1(5.9)^{be}	30.7(4.7)^{cde}	24.8(6.1)	<0.001
腰圍 (公分)	76.9(10.6)^{abc}	88.1(16.6)^{ad}	84.1(14.2)^{be}	95.5(12.1)^{cde}	83.3(14.7)	<0.001
臀圍 (公分)	90.1(8.4)^{abc}	99.5(13.3)^{ad}	97.2(10.9)^{be}	106.4(9.0)^{cde}	95.8(11.8)	<0.001
腰臀比	0.88(0.08)^{a}	0.87(0.10)	0.86(0.07)	0.83(0.08)a	0.87(0.08)	0.001
收縮壓 (毫米汞柱)	109(11)^{ab}	115(14)^{ac}	111(12)^{d}	124(13)^{bcd}	113(13)	<0.001
舒張壓 (毫米汞柱)	71(9)^{ab}	75(12)^{a}	72(10)^{c}	79(11)^{bc}	73(10)	<0.001
內分泌指標						
FSH (mIU/ml)	7.0(1.4)^{abc}	5.2(1.2)^{a}	5.2(1.0)^{b}	5.4(1.1)^{c}	6.0(1.5)	<0.001
LH (mIU/ml)	16.3(5.4)^{abc}	7.9(3.3)^{a}	7.2(3.4)^{b}	9.1(3.3)^{c}	11.6(6.0)	<0.001
LH/FSH 比值	2.5(1.1)^{abc}	1.6(0.9)^{a}	1.4(0.8)^{b}	1.7(0.7)^{c}	2.0(1.0)	<0.001
Estradiol (pg/dl)	47.7(20.5)^{a}	47.5(20.7)	40.9(19.0)^{a}	47.6(15.6)	46.3(19.8)	0.041
Testosterone (ng/ml)	0.84(0.35)^{a}	0.75(0.33)^{b}	0.83(0.41)^{c}	1.48(0.37)^{abc}	0.90(0.42)	<0.001
DHEA-S (ug/dl)	252.6(115.9)^{ab}	153.3(54.6)^{acd}	336.2(81.3)^{bce}	245.8(110.7)^{de}	243.8(114.2)	<0.001
SHBG (nmol/l)	43.9(19.7)^{abc}	34.4(21.2)^{ad}	33.6(19.9)^{be}	13.8(4.1)^{cde}	35.9(21.1)	<0.001
FAI (%)	8.6(6.6)^{a}	10.0(6.4)^{b}	10.9(6.5)^{c}	39.6(14.7)^{abc}	13.2(12.7)	<0.001
新陳代謝指標						
Glucose (mg/dl)	81.1(6.0)^{ab}	86.1(19.9)^{a}	83.5(7.0)^{c}	91.3(16.3)^{bc}	84.0(12.8)	<0.001
Insulin (uU/ml)	6.7(5.7)^{abc}	11.9(12.1)^{ad}	10.8(8.3)^{be}	21.0(12.2)^{cde}	10.5(10.1)	<0.001
HOMA-IR	1.4(1.2)^{abc}	2.8(3.5)^{ad}	2.3(1.9)^{be}	5.0(4.1)^{cde}	2.3(2.8)	<0.001
Uric acid (mg/dl)	5.3(1.1)^{a}	5.7(1.2)^{b}	5.7(1.1)^{c}	7.0(1.9)^{abc}	5.7(1.4)	<0.001
AST (IU/l)	20.8(7.0)^{ab}	26.6(19.3)^{ac}	22.7(11.0)^{d}	40.7(39.8)^{bcd}	25.0(19.2)	<0.001
ALT (IU/l)	18.3(15.2)^{ab}	31.9(37.4)^{ac}	24.9(28.3)^{d}	59.2(65.5)^{bcd}	27.9(35.8)	<0.001
T-CHO (mg/dl)	187.5(33.1)	188.3(33.2)	186.3(32.2)	192.0(39.4)	188.0(33.7)	0.783
LDL-C (mg/dl)	99.5(28.3)^{ab}	109.1(31.4)^{ac}	103.2(25.9)^{d}	123.6(35.8)^{bcd}	105.5(30.6)	<0.001
HDL-C (mg/dl)	54.6(12.6)^{abc}	47.8(11.8)^{ad}	48.8(12.0)^{be}	40.2(7.3)^{cde}	50.0(12.6)	<0.001
TG (mg/dl)	73.0(36.7)^{abc}	109.4(81.1)^{a}	93.7(49.1)^{bd}	131.8(63.6)^{cd}	93.0(59.6)	<0.001

1. $P<0.05$ 為統計顯著。事後比較檢定是以 Bonferroni 方法來進行。
2. 相同的上標英文字母代表在兩個變數之間出現統計顯著差異。
3. 縮寫：N: number, BMI: body mass index, FSH: follicle-stimulating hormone, LH: luteinizing hormone, DHEA-S: dehydroepiandrosterone sulfate, SHBG: sex hormone-binding globulin, FAI: free androgen index, HOMA-IR: homeostasis model assessment-insulin resistance, AST: aspartate aminotransferase, ALT: alanine aminotransferase, T-CHO: total cholesterol, LDL-C: low-density lipoprotein-cholesterol, HDL-C: high-density lipoprotein-cholesterol, TG: triglycerides.

doi:10.6342/NTU202000313

表三：廣義相關圖四個不同次族群的臨床表徵和所符合之鹿特丹診斷表型子群

變數	第一組 N=204	第二組 N=111	第三組 N=88	第四組 N=57	所有人 N=460	P 值
不同 PCOS 表徵						
慢性無排卵	92.6%	94.6%	85.2%	98.2%	92.4%	0.018
高雄性荷爾蒙症	78.9%	73.9%	81.8%	100.0%	80.9%	0.001
多毛症	47.1%	46.8%	55.7%	42.1%	48.0%	0.393
雄性禿	11.3%	19.8%	12.5%	21.1%	14.8%	0.095
高雄性荷爾蒙血症	51.0%	38.7%	44.3%	100.0%	52.8%	<0.001
多囊性卵巢超音波外觀	96.1%	91.9%	92.0%	96.5%	94.3%	0.289
鹿特丹診斷標準之四個表型子群						
完全表現子群	67.6%	60.4%	59.0%	94.7%	67.6%	<0.001
無多囊性卵巢外觀子群	3.9%	8.1%	8.0%	3.5%	5.7%	0.288
正常排卵子群	7.4%	5.4%	14.8%	1.8%	7.6%	0.019
無高雄性荷爾蒙症子群	21.1%	26.1%	18.2%	0	19.1%	0.001
其他 PCOS 診斷標準						
NIH	77.5%	75.7%	70.5%	98.2%	78.3%	0.001
AE-PCOS	84.8%	81.1%	85.2%	100.0%	85.9%	0.008

1. P<0.05 為統計顯著。
2. 事後比較檢定是用 Bonferroni 方法.
3. 縮寫：N: number, NIH: National Institutes of Health; AE-PCOS: Androgen Excess and PCOS Society.

doi:10.6342/NTU202000313

表四：在不同診斷標準和不同鹿特丹表型子群的新陳代謝症候群比率

		新陳代謝症候群比率
鹿特丹標準之表型子群		
完全表現子群	(HA+AO+PCOM)	19.9% (62/311)
無多囊性卵巢外觀子群	(HA+AO)	30.8% (8/26)
正常排卵子群	(HA+PCOM)	17.1% (6/35)
無高雄性荷爾蒙症子群	(AO+PCOM)	14.8% (13/88)
診斷標準		
NIH	(HA+AO)	20.8% (70/337)
AE-PCOS	(HA+AO or PCOM)	20.4% (76/372)
Rotterdam		19.3% (89/460)

縮寫：HA: hyperandrogenism; AO: chronic anovulation; PCOM: polycystic ovaries morphology, NIH: National Institutes of Health, AE-PCOS: Androgen Excess and PCOS Society

doi:10.6342/NTU202000313

表五：PF4 研究中試管嬰兒療程的病患特徵和治療情形

變數	PCOS (n=13)	對照組(n=11)	P 值
病患特徵			
年齡 (歲)	33.6 (3.1)	34.5 (3.5)	NS
BMI (公斤/平方公尺)	26.4 (7.4)	21.7 (3.0)	NS
未曾生育者人數(比例)	13 (100%)	10 (91%)	NS
月經週期間隔 (天數)	112.3 (95.4)	32.6 (9.5)	0.012
慢性無排卵人數	13 (100%)	0	-
高雄性荷爾蒙症人數	7 (54%)	0	-
月經第二天 FSH 值 (mIU/ml)	6.17 (1.72)	5.63 (1.16)	NS
月經第二天 LH 值 (mIU/ml)	9.17 (3.97)	3.99 (1.46)	<0.001
月經第二天 E2 值 (pg/ml)	36.4 (9.9)	39.0 (9.9)	NS
月經第二天 testosterone 值(ng/ml)	0.58 (0.2-1.4)	0.24 (0.2-0.28)	0.026
療程特色與結果			
試管嬰兒療程			
拮抗劑療程	13	10	
長療程	0	1	
總促性腺激素劑量	2028 (764)	1840 (526)	NS
排卵刺激天數 (天)	13.6 (1.1)	12.7 (1.0)	NS
促進排卵藥物			
hCG	4	6	
Triptorelin	9	5	NS
促進排卵當天 E2 值 (pg/ml)	5776 (3837)	5104 (3796)	NS
促進排卵當天 P4 值(ng/ml)	1.0 (0.4)	1.2 (0.6)	NS
總取卵數量	29.8 (14.4)	27.4 (8.0)	NS
總成熟卵子量	25.2 (14.6)	23.1 (9.1)	NS
受精率 (%)	67 (20)	68 (13)	NS

1. 所有連續變項以平均值 (標準變異) 來表示。.
2. P 值<0.05 為統計顯著。
3. 縮寫：BMI, body mass index; FSH, follicule-stimulating hormone; LH, luteinizing hormone; E2, estradiol; P4, progesterone; NS, non-significant

doi:10.6342/NTU202000313

表六：人類血管生成晶片之訊號值

	PCOS (n=14)	對照組 (n=11)	P 值
Angiogenin	1.18 (0.16)	1.24 (0.15)	NS
Angiopoietin-2	0.30 (0.22)	0.31 (0.27)	NS
Amphiregulin	0.27 (0.16)	0.20 (0.08)	NS
CXCL16	0.41 (0.40)	0.46 (0.42)	NS
DPPIV/CD26	0.40 (0.22)	0.39 (0.23)	NS
EG-VEGF/PK1	0.36 (0.23)	0.37 (0.22)	NS
Endostatin/collagen XVIII	0.18 (0.04)	0.20 (0.09)	NS
FGF-7/KGF	0.17 (0.09)	0.14 (0.08)	NS
HGF	0.28 (0.24)	0.20 (0.20)	NS
IGFBP-1	0.58 (0.32)	0.58 (0.35)	NS
IGFBP-2	0.73 (0.15)	0.72 (0.20)	NS
IGFBP-3	0.68 (0.23)	0.71 (0.17)	NS
Leptin	0.44 (0.27)	0.47 (0.26)	NS
MMP-9	0.34 (0.18)	0.27 (0.17)	NS
Pentraxin-3/TSG-14	0.33 (0.22)	0.24 (0.11)	NS
Platelet factor 4/CXCL4	0.31 (0.18)	0.16 (0.10)	0.004
Prolactin	0.41 (0.19)	0.37 (0.21)	NS
Serpin E1/PAI-1	0.58 (0.23)	0.67 (0.2)	NS
TIMP-1	0.75 (0.29)	0.75 (0.25)	NS
Thrombospondin-1	0.62 (0.39)	0.67 (0.33)	NS
TIMP-4	0.34 (0.37)	0.37 (0.37)	NS
VEGF	0.13 (0.03)	0.13 (0.07)	NS

1. 所有數項以平均值 (標準變異) 來表示。.

2. 統計分析是使用 Mann-Whitney U 檢定。P 值小於 0.05 為統計顯著

3. 縮寫：CXCL, C-X-C motif chemokine ligand; DPPIV, dipeptidyl peptidase-4; EG-VEGF, endocrine gland-derived vascular endothelial growth factor; PK, prokineticin; FGF, fibroblast growth factor; KGF, keratinocyte growth factor; IGF, hepatocyte growth factor; IGFBP, insulin-like growth factor-binding protein; MMP, matrix metalloproteinase; TSG, tumor necrosis factor-stimulated gene; PAI, plasminogen activator inhibitor; TIMP, tissue inhibitor of metalloproteinase; VEGF, vascular endothelial growth factor

doi:10.6342/NTU202000313

表七：DNA 甲基化晶片分析受試者的身體測量和生化特徵 (經取卵手術者)

	PCOS (n=11)	對照組 (n=4)	P 值
年齡 (歲)	33.5 ± 3.8	35.0 ± 2.2	NS
身高 (公分)	160.2 ± 6.5	159.8 ± 3.9	NS
體重 (公斤)	56.8 ± 7.3	52.3 ± 6.3	NS
BMI (公斤/平方公尺)	22.4 ± 3.0	20.5 ± 3.0	NS
月經週期間隔(天)	149.1 ± 75.1	31.3 ± 2.5	0.003
慢性無排卵	11/11	0	
多囊性卵巢超音波外觀	11/11	1/4	
高雄性荷爾蒙症 (no.)	5/11	0	
月經第二天 FSH 值 (mIU/ml)	6.1 ± 1.6	6.0 ± 1.0	NS
月經第二天 LH 值(mIU/ml)	10.0 ± 5.2	4.3 ± 1.9	0.026
月經第二天 E2 值(pg/ml)	42.1 ± 24.1	38.1 ± 9.3	NS
Testosterone (ng/ml)	0.57 ± 0.37	0.19 ± 0.06	0.033
DHEA-S (ug/dl)	201 ± 144	180 ± 141	NS
SHBG (nmol/L)	78.1 ± 60.0	67.6 ± 7.8	NS
Androstenedione (ng/ml)	2.0 ± 1.1	1.3 ± 0.5	NS
FAI (%)	4.5 ± 4.2	1.0 ± 0.4	NS
AC sugar (mg/dl)	85.8 ± 7.0	84.5 ± 3.1	NS
Insulin (uIU/ml)	10.2 ± 9.9	2.8 ± 0.6	0.028
HOMA-IR	2.2 ± 2.3	0.59 ± 0.13	0.024
Prolactin (ng/ml)	14.4 ± 10.0	15.5 ± 2.2	NS
TSH (uIU/ml)	1.55 ± 0.32	1.08 ± 0.76	NS
Free T4 (ug/dl)	0.91 ± 0.08	0.89 ± 0.05	NS
Cortisol (ug/dl)	20.2 ± 14.6	18.0 ± 2.6	NS
AST (U/L)	21.0 ± 7.8	17.8 ± 1.7	NS
LDL-C (mg/dl)	106.8 ± 36.8	112.0 ± 38.2	NS
HDL-C (mg/dl)	53.5 ± 15.1	72.4 ± 4.4	NS
Uric acid (mg/dl)	5.0 ± 1.4	4.6 ± 1.0	NS
TG (mg/dl)	144.0 ± 70.0	98.0 ± 4.2	NS
T-CHO (mg/dl)	210.1 ± 52.4	227.5 ± 7.8	NS

doi:10.6342/NTU202000313

試管嬰兒療程			
促進排卵當天 E2 值(pg/ml)	5065 ± 2415	5553 ± 4955	NS
促進排卵當天 P 值(ng/ml)	1.2 ± 0.7	1.2 ± 0.7	NS
促進排卵當天 LH 值(mIU/ml)	2.1 ± 1.5	1.6 ± 0.9	NS
總促性腺激素劑量 (IU)	2143 ± 827	1750 ± 509	NS
排卵刺激時間 (天)	12.1 ± 1.4	11.5 ± 0.6	NS
卵子數量	29.0 ± 15.1	23.5 ± 16.7	NS

1. 縮寫: NS: not significant; BMI: body mass index; SH: follicle-stimulating hormone; LH: luteinizing hormone; E2: estradiol; DHEA-S: dehydroepiandrosterone sulfate; SHBG: sex hormone binding globulin; FAI: free androgen index; HOMA-IR: homeostasis model assessment of insulin resistance; TSH: thyroid-stimulating hormone; T4: thyroxine; AST: aspartate transaminase; LDL-C: low-density lipoprotein cholesterol; HDL-C: high-density lipoprotein cholesterol; TG: triglycerides; T-CHO: total cholesterol; P: progesterone.
2. P 值小於 0.05 為統計顯著。

doi:10.6342/NTU202000313

表八：差異性甲基化基因的排名前 10 個富集途徑

富集途徑	P 值	比率	相關分子	分類
成人顆粒細胞				
Thromboxane A2 signaling pathway	3.069E-05	7/50	MEK1/2, MSK1/2 (RPS6KA5/4), PI3K reg class IA (p85), cPKC (conventional), PKA-reg (cAMP-dependent), PKC, PI3K reg class IA	Development
Antigen presentation by MHC class II	5.625E-05	10/118	MHC class II alpha chain, MHC class II beta chain, PKC-alpha, LY75, Dynein 1, cytoplasmic, intermediate chains, MHC class II, PIP5K1A, Rab-7, PSD4, PKC	Immune response
Nociceptin receptor signaling	6.844E-05	8/76	TY3H, PKC-alpha, MEK1/2, cPKC (conventional), PKA-reg (cAMP-dependent), p90Rsk, LIMK2, PKC	Nociception
Regulation of actin cytoskeleton organization by the kinase effectors of Rho GTPases	8.173E-05	7/58	MLCP (reg), PIP5KI, LIMK, Alpha-actinin, MRCKalpha, Paxillin, MRCK	Cytoskeleton remodeling
Activation of NADPH oxidase	9.132E-05	7/59	TRIO, PKC-alpha, MEK1/2, cPKC (conventional), PI3K cat class IB (p110-gamma), PKC, PI3K reg class IA	Oxidative stress
Activation of NOX1, NOX5, DUOX1 and DUOX2 NADPH Oxidases	1.027E-04	6/42	PKC-alpha, MEK1/2, FISH, cPKC (conventional), PKA-reg (cAMP-dependent), PKC	Oxidative stress
Histamine H1 receptor signaling in the interruption of cell barrier integrity	1.524E-04	6/45	MLCP (reg), PKC-alpha, Alpha-actinin, Alpha-catenin, LIMK2, Paxillin	Cell adhesion
CREB signaling pathway	2.463E-04	6/49	PKC-alpha, MSK1/2 (RPS6KA5/4), cPKC (conventional), PKA-reg (cAMP-dependent), p90Rsk, PI3K reg class IA	Transcription
Proinsulin C-peptide signaling	3.427E-04	6/52	PKC-alpha, PI3K reg class IA (p85), PI3K reg class IA (p85-alpha), PI3K cat class IB (p110-gamma), MEK2(MAP2K2), PI3K reg class IA	G-protein signaling
Plasmin signaling	3.966E-04	5/35	TGF-beta 1, TGF-beta receptor type III (betaglycan), TGF-beta receptor type I, PI3K reg class IA, Collagen IV	Cell adhesion
iPSC 衍生顆粒細胞				
TGF, WNT and cytoskeletal remodeling	5.827E-07	30/111	Talin, RhoA, PPAR-beta(delta), GRB2, FRAT1, Vinculin, IKK-alpha, Tcf(Lef), WNT, TCF7L2 (TCF4), DOCK1, eIF4E, ERK1/2, MDM2, FAK1, LRP5, Beta-catenin, Alpha-actinin, SOS, SMAD3, Caspase-9, Alpha-actinin 1, AKT(PKB), Collagen IV, Actin, p38 MAPK, ERK1 (MAPK3), Frizzled, mTOR, TGF-beta receptor type I	Cytoskeleton remodeling
Ephrin signaling	1.097E-06	17/45	RhoA, HGK(MAP4K4), GRB2, Kalirin, Ephrin-B, G-protein alpha-i family,	Cell adhesion

doi:10.6342/NTU202000313

			FAK1, Ephrin-A5, Fyn, Ephrin-A receptors, Ephexin, Ephrin-B receptor 1, Ephrin-A, ADAM10, Ephrin-B receptors, GRB10, Ephrin-A2	
Chemokines and adhesion	2.172E-06	27/100	TRIO, Talin, RhoA, B-Raf, GRB2, GCP2, CD44, PTEN, SERPINE2, Vinculin, Tcf(Lef), G-protein alpha-i family, Rap1GAP1, DOCK1, ERK1/2, ENA-78, MMP-2, FAK1, Beta-catenin, Alpha-actinin, SOS, Alpha-actinin 1, AKT(PKB), Collagen IV, IL8RA, Thrombospondin 1, Actin	Cell adhesion
NMDA-dependent postsynaptic long-term potentiation in CA1 hippocampal neurons	3.843E-06	23/80	NMDA receptor, Pyk2(FAK2), mGluR1, B-Raf, GRB2, PKC-alpha, NR2, NR1, GluR1, eIF4E, ERK1/2, PKA-reg (cAMP-dependent), RASGRF1, SOS, AKT(PKB), ERK1 (MAPK3), Ryanodine receptor 2, p90Rsk, NR2B, IP3 receptor, mTOR, GluR2, PLC-beta2	Neurophysiol ogical process
GABA-A receptor life cycle	5.855E-06	12/27	NSF, Dynein 1, cytoplasmic, heavy chain, GABA-A receptor, AP complex 2 medium (mu) chain, GABA-A receptor alpha-1/beta-2/gamma-2, GABA-A receptor alpha-1 subunit, Dynamin, GABA-A receptor gamma-2 subunit, Dynein 1, cytoplasmic, intermediate chains, GABA-A receptor beta-2 subunit, PLCL1, Tubulin (in microtubules)	Neurophysiol ogical process
PKA signaling	8.031E-06	17/51	LBC, G-protein alpha-12 family, AKAP3, G-protein alpha-s, PDE4D, G-protein alpha-i family, Adenylate cyclase, GABA-A receptor beta-1 subunit, Ryanodine receptor 1, PP2A regulatory, PKA-reg type II (cAMP-dependent), PKA-reg (cAMP-dependent), PCTK1, SMAD3, PDE3A, GABA-A receptor beta-2 subunit, AKAP8	Signal transduction
NF-kB signaling pathway	1.944E-05	14/39	TNF-R2, LTBR(TNFRSF3), PKC-theta, SUMO-1, LBP, IKK-alpha, TRAF6, IL1RAP, TOLLIP, IKK-gamma, IRAK1/2, AKT(PKB), NIK(MAP3K14), IKAP	Transcription
Integrin outside-in signaling	1.990E-05	16/49	TRIO, Talin, GRB2, Vinculin, PINCH, Tcf(Lef), ERK1/2, FAK1, Beta-catenin, WASP, Alpha-parvin, Alpha-actinin, SOS, Beta-parvin, AKT(PKB), Collagen IV	Cytoskeleton remodeling
A2B receptor: action via G-protein alpha s	2.648E-05	16/50	BETA-PIX, Pyk2(FAK2), B-Raf, G-protein alpha-s, GRB2, PLC-beta, TCF7L2 (TCF4), ERK1/2, Beta-catenin, PKA-reg (cAMP-dependent), SOS, AKT(PKB), p38 MAPK, Elk-1, IP3 receptor, MEKK4(MAP3K4)	Development
CREB pathway	4.884E-05	15/47	cPKC (conventional), G-protein alpha-s, Galpha(s)-specific amine GPCRs, GRB2, PKC-alpha, ERK1/2, IGF-1 receptor, MSK1/2 (RPS6KA5/4), PKA-reg (cAMP-dependent), SOS, AKT(PKB),	Transcription

doi:10.6342/NTU202000313

doi:10.6342/NTU202000313

表九：以 IPA 分析 PCOS 組和對照組的差異甲基化基因調控途徑

9-1 Top canonical pathways	**P value**	**Overlap**
Adult GCs		
Phagosome Maturation	8.70E-04	3.6 % 5/138
Germ Cell-Sertoli Cell Junction Signaling	2.13E-03	3.0 % 5/169
Semaphorin Signaling in Neurons	2.70E-03	5.8 % 3/52
Rac Signaling	3.47E-03	3.4 % 4/116
PTEN Signaling	3.81E-03	3.4 % 4/119
iPSC-derived GCs		
Antigen Presentation Pathway	1.11E-09	42.1 % 16/38
OX40 Signaling Pathway	1.68E-08	32.1 % 18/56
Allograft Rejection Signaling	2.45E-06	29.2 % 14/48
Nur77 Signaling in T Lymphocytes	8.84E-06	26.4 % 14/53
Calcium-induced T Lymphocyte Apoptosis	8.87E-06	25.0 % 15/60

doi:10.6342/NTU202000313

表九：以 IPA 分析 PCOS 組和對照組的差異甲基化基因調控途徑 (續)

9-2 Top upstream regulators	**Gene Ontology annotations**	**P value of overlap**
Adult GCs		
MKL1 (Megakaryoblastic Leukemia (Translocation) 1)	nucleic acid binding and actin binding	7.26E-03
SCAP (SREBF Chaperone)	protein complex binding and cholesterol binding	1.03E-02
CREBZF (CREB/ATF BZIP Transcription Factor)	DNA binding transcription factor activity and identical protein binding.	1.53E-02
SMYD2 (SET And MYND Domain Containing 2)	p53 binding and protein-lysine N-methyltransferase activity	1.53E-02
miR-148a-3p	mRNA binding involved in posttranscriptional gene silencing	1.53E-02
iPSC-derived GCs		
EBI3 (Epstein-Barr Virus Induced 3)	cytokine activity and interleukin-27 receptor binding	3.64E-05
TENM1 (Teneurin Transmembrane Protein 1)	protein homodimerization activity and heparin binding.	1.33E-04
HNRNPA2B1 (Heterogeneous Nuclear Ribonucleoprotein A2/B1)	nucleic acid binding and RNA binding	4.10E-04
MGEA5 (Meningioma Expressed Antigen 5 (Hyaluronidase))	histone acetyltransferase activity and beta-N-acetylglucosaminidase activity.	1.05E-03
ITPR2 (Inositol 1,4,5-Trisphosphate Receptor Type 2)	binding and phosphatidylinositol binding	1.14E-03

doi:10.6342/NTU202000313

表九：以 IPA 分析 PCOS 組和對照組的差異甲基化基因調控途徑 (續)

9-3 Top Associated Network Functions	**Score**
Adult GCs	
1 Cellular Movement, Embryonic Development, Organ Development	26
2 Cardiovascular System Development and Function, Cellular Movement, Cell Signaling	17
3 Cellular Development, Cellular Growth and Proliferation, Cellular Movement	13
4 Cell Morphology, Embryonic Development, Hematological System Development and Function	13
5 DNA Replication, Recombination, and Repair, Cell Cycle, Cell Death and Survival	13
iPSC-derived GCs	
1 Cell-To-Cell Signaling and Interaction, Hematological System Development and Function, Immune Cell Trafficking	38
2 Cellular Movement, Cancer, Connective Tissue Disorders	34
3 Organ Morphology, Organismal Injury and Abnormalities, Reproductive System Development and Function	30
4 Cardiovascular System Development and Function, Cellular Movement, Cellular Development	30
5 Endocrine System Disorders, Gastrointestinal Disease, Immunological Disease	28

doi:10.6342/NTU202000313

表九：以 IPA 分析 PCOS 組和對照組的差異甲基化基因調控途徑 (續)

9-4 Top Tox Lists	P value	Overlap
Adult GCs		
NRF2-mediated Oxidative Stress Response	6.06E-03	2.3 % 5/216
Negative Acute Phase Response Proteins	4.19E-02	12.5 % 1/8
PPAR/RXR Activation	6.37E-02	1.8 % 3/171
Increases Glomerular Injury	6.67E-02	2.5 % 2/79
TR/RXR Activation	9.65E-02	2.0 % 2/98
iPSC-derived GCs		
NRF2-mediated Oxidative Stress Response	6.97E-03	11.6 % 25/216
Increases Liver Damage	2.87E-02	11.7 % 15/128
PPAR/RXR Activation	4.53E-02	10.5 % 18/171
RAR Activation	5.45E-02	10.2 % 19/187
Increases Heart Failure	6.82E-02	17.4 % 4/23

doi:10.6342/NTU202000313

表九：以 IPA 分析 PCOS 組和對照組的差異甲基化基因調控途徑 (續)

9-5 Top analysis-ready molecules	**Adult GCs**	**iPSC-GCs**
Up regulated	*SLC25A37*	*MEIS1*
	ARHGAP22	*CCDC94*
	ITGA1	*POLR1B*
	PCID2	*TCF7L1*
	NSF	*CDH17*
	MYO16	*MYO10*
	PIK3CG	*FAM228B*
	LGALS7/LGALS7B	*DNAJC6*
	C2orf54	*FOXK2*
	MXI1	*CAT*
Down regulated	*GPR83*	*PCNT*
	VHL	*TRPV2*
	ADAMTS19	*C1orf94*
	AEBP1	*ZNF335*
	FAM213A	*ACTN3*
	DYDC1	*MEGF6*
	PSMA7	*EFCAB13*
	BRDT	*SORCS2*
	TMC7	*RFTN1*
	RNF39	*LRRTM4*

doi:10.6342/NTU202000313

表十：iPSC 衍生顆粒細胞與成人顆粒細胞共同出現的 37 個差異性甲基化基因

UCSC Gene Name	Probe id (PtGC /iPSC-GC)	基因區域	PtGC FC	iPSC-GC FC	染色體	Official Full name	Gene ontology class
Both hypermethylation							
RPTOR	cg17906851	Body	4.15	14.02	17	regulatory associated protein of MTOR complex 1	RNA polymerase III type 1 promoter DNA binding; cellular response to nutrient levels
MEIS1	cg14553323	Body	3.89	185.81	2	Meis homeobox 1	RNA polymerase II proximal promoter sequence-specific DNA binding; negative regulation of myeloid cell differentiation
ZMIZ1	cg04007726	Body	2.50	13.55	10	zinc finger MIZ-type containing 1	in utero embryonic development; vasculogenesis
RNF220	cg10329345/ cg08242458	Body/ Body	2.59	2.57	1	ring finger protein 220	ubiquitin-protein transferase activity
PTPRN2	cg17334266/ cg01394671	Body/ TSS200	2.64	4.28	7	protein tyrosine phosphatase, receptor type N2	transmembrane receptor protein tyrosine phosphatase activity; lipid metabolic process; insulin secretion involved in cellular response to glucose stimulus
PRDM16	cg17455155/ cg04882216	Body/ Body	2.53	6.33	1	PR/SET domain 16	negative regulation of transcription by RNA polymerase II; brown fat cell differentiation
ZHX2	cg06035200/ cg04845852	5'UTR/ 5'UTR	4.44	5.71	8	zinc fingers and homeoboxes 2	negative regulation of transcription by RNA polymerase II;
TNXB	cg07148038/ cg06002203	Body/ Body	2.70	2.74	6	tenascin XB	extracellular matrix structural constituent; integrin binding;
TSNARE1	cg24849373	Body	4.41	5.77	8	t-SNARE domain containing 1	intracellular protein transport; endomembrane system; SNARE complex
WWTR1	cg14557185/ cg11923296	Body/ Body	2.91	2.98	3	WW domain containing transcription regulator 1	negative regulation of protein phosphorylation; hippo signaling;
Both hypomethylation							
SORBS2	cg09120722	Body	0.24	0.04	4	sorbin and SH3 domain	RNA binding; structural constituent of cytoskeleton

doi:10.6342/NTU202000313

						containing 2	
ESRRB	cg07730622/ cg00929286	5'UTR/ 5'UTR	0.40	0.12	14	estrogen related receptor beta	RNA polymerase II proximal promoter sequence-specific DNA binding; stem cell population maintenance; positive regulation of glycogen biosynthetic process
B3GALT1	cg12624040/ cg18015625	5'UTR/ TSS1500	0.40	0.11	2	beta-1,3-galactosyltransferase 1	Golgi membrane; oligosaccharide biosynthetic process; lipid and protein glycosylation
RASA3	cg23168520	Body	0.28	0.07	13	RAS p21 protein activator 3	MAPK cascade; positive regulation of GTPase activity
ADARB2	cg20205188/ cg09867002	Body/ Body	0.21	0.07	10	adenosine deaminase, RNA specific B2	double-stranded RNA binding;
DIP2C	cg15986644/ cg24068006	Body/ Body	0.36	0.16	10	disco interacting protein 2 homolog C	catalytic activity; cellular component; biological process; metabolic process
MB21D2	cg16788857	Body	0.39	0.08	3	Mab-21 domain containing 2	protein-containing complex binding; cadherin binding
GALNT2	cg26303777	Body	0.26	0.13	1	Polypeptide N-acetylgalactosaminyltransferase 2	Golgi membrane; protein O-linked glycosylation, polypeptide N-acetylgalactosaminyltransferase activity;
Hypermethylation in patient GC and hypomethylation in iPSC-derived GC							
ADCK2	cg24022528	Body	2.61	0.17	7	aarF domain containing kinase 2	protein serine/threonine kinase activity; ATP binding
ZBTB7C	cg11823448	5'UTR	3.39	0.16	18	zinc finger and BTB domain containing 7C	DNA-binding transcription factor activity, RNA polymerase II-specific; positive regulation of fat cell differentiation
MYO10	cg02288345	Body	2.50	0.09	5	myosin X	Motor activity; protein binding
RPH3AL	cg04172345/ cg02661110	Body/ 5'UTR	3.07	0.11	17	rabphilin 3A like	intracellular protein transport; protein binding; exocytosis; glucose homeostasis
CCDC88B	cg15296767/ cg09619347	Body/ TSS200	2.68	0.30	11	coiled-coil domain containing 88B	positive regulation of cytokine production; positive regulation of T cell proliferation
ZIC5	cg23476830	TSS200	2.76	0.36	13	Zic family member 5	DNA-binding transcription factor activity, RNA

doi:10.6342/NTU202000313

							polymerase II-specific
PRRC2B	cg01192190/ cg13168499	5'UTR/ Body	2.87	0.13	9	proline rich coiled-coil 2B	RNA binding
KCNIP4	cg00688962/ cg07695835	TSS200 /Body	2.65	0.39	4	potassium voltage-gated channel interacting protein 4	potassium channel activity;
PRKAR1B	cg10127554/ cg11448166	Body/ Body	2.51	0.32	7	protein kinase cAMP-dependent type I regulatory subunit beta	cAMP-dependent protein kinase inhibitor activity; cellular response to glucagon stimulus
Hypermethylation in patient GC and hypomethylation in iPSC-derived GC							
YJU2	cg04158402	Body	0.39	132.44	19	YJU2 splicing factor homolog	RNA splicing; protein binding
FOXK2	cg12855313	Body	0.35	34.99	17	forkhead box K2	RNA polymerase II proximal promoter sequence-specific DNA binding
AK8	cg21425790	Body	0.37	16.47	9	adenylate kinase 8	adenylate kinase activity; protein binding
CAT	cg06508490	Body	0.33	37.23	11	catalase	response to reactive oxygen species
BTBD2	cg01688609	Body	0.39	18.08	19	BTB domain containing 2	Protein binding
TSGA10	cg26495595	Body	0.27	4.31	2	testis specific 10	Protein binding; spermatogenesis
DENND2A	cg26445985	Body	0.35	5.60	7	DENN domain containing 2A	Rab guanyl-nucleotide exchange factor activity; protein transport
JPH3	cg20107632/ cg09496634	Body/ Body	0.32	2.61	16	junctophilin 3	calcium-release channel activity; junctional membrane complex
ARSJ	cg06384865	Body	3.73	0.18	4	arylsulfatase family member J	arylsulfatase activity; metabolic process; metal ion binding

1. 基因富集分組的資訊可從官網查得 http://amigo.geneontology.org/amigo/landing.
2. 縮寫：GC: granulosa cell
3. 當成人顆粒細胞和 iPSC 衍生顆粒細胞的差異甲基化區域位於不同探針上時，表格中的前一個探針是成人顆粒細胞的，後一個探針是 iPSC 衍生顆粒細胞的。

doi:10.6342/NTU202000313

表十一：miRNA 研究中 PCOS 組和對照組之受試者特徵

	PCOS (n=75)	對照組 (n=20)	P 值
背景資料			
年齡 (歲)	24.5 (5.1)	25.8 (2.3)	NS
體重 (公斤)	64.0 (16.6)	55.2 (5.7)	<0.0001
BMI (公斤/平方公尺)	24.9 (6.2)	21.8 (1.6)	<0.0001
腰圍 (公分)	86.3 (13.9)	74.0 (6.5)	<0.0001
臀圍 (公分)	93.9 (12.5)	88.7 (5.5)	0.008
月經週期 (天)	205.1 (122.3)	29.9 (1.8)	<0.0001
內分泌指標			
高雄性荷爾蒙症	80%	0	<0.0001
Testosterone (ng/ml)	0.67 (0.32)	0.32 (0.12)	<0.0001
DHEA-S (μg/ml)	276.2 (115.8)		
SHBG (nmol/l)	37.5 (23.0)		
FAI (%)	8.4 (5.9)		
FSH (mIU/ml)	6.4 (1.8)	7.1 (1.8)	NS
LH (mIU/ml)	12.1 (5.9)	4.8 (2.4)	<0.0001
E2 (pg/ml)	49.9 (25.4)	31.8 (11.8)	0.003
新陳代謝指標			
Insulin (IU/ml)	9.0 (9.3)	7.7 (13.4)	NS
Glucose (IU/ml)	83.4 (6.5)	84.8 (7.3)	NS
HOMA-IR	1.92 (2.05)		
Uric acid (mg/dl)	5.56 (1.18)	4.72 (0.82)	0.003
LDL-C (mg/dl)	108.9 (34.9)	87.8 (33.5)	0.017
HDL-C (mg/dl)	55.9 (12.7)	58.0 (9.1)	NS
TG (mg/dl)	87.4 (51.3)	61.9 (21.8)	0.001
T-CHO (mg/dl)	192.4 (40.5)	183.8 (27.8)	NS
AST (U/l)	25.5 (21.3)	19.6 (13.4)	NS
ALT (U/l)	30.4 (41.6)	19.1 (23.6)	NS

1. P 值小於 0.05 為統計顯著
2. 縮寫：PCOS: polycystic ovarian syndrome; DHEA-S: dehydroepiandrosterone sulfate, SHBG: sex hormone-binding globulin, FAI: free androgen index, FSH: follicle-stimulating hormone, LH: luteinizing hormone, E2:estradiol, HOMA-IR: homeostasis model assessment-insulin resistance, LDL-C: low-density lipoprotein-cholesterol, HDL-C: high-density lipoprotein-cholesterol, TG: triglycerides. T-CHO: total cholesterol, AST: aspartate aminotransferase, ALT: alanine aminotransferase.

doi:10.6342/NTU202000313

表十二：PCOS 和對照組之血液游離微小核醣核酸表現

微小核醣核酸	**PCOS 組 (n=75)**	**對照組 (n=20)**	**P 值**
miR-21	2.09 (1.31)	1.84 (0.69)	NS
miR-93	0.25 (0.13)	0.15 (0.06)	<0.0001
miR-132	0.02 (0.016)	0.008 (0.003)	<0.0001
miR-193	2.01 (6.51)	1.54 (1.19)	NS
miR-221	1.62 (0.69)	1.39 (0.24)	0.02
miR-222	0.08 (0.04)	0.1 (0.03)	0.007
miR-223	6.97 (5.63)	4.73 (2.36)	0.009
miR-27a	1.39 (1.05)	0.59 (0.37)	<0.0001
miR-125b	0.21 (0.62)	0.04 (0.03)	NS
miR-200b	0.19 (0.52)	0.18 (0.22)	NS
miR-212	0.18 (0.53)	0.02 (0.04)	0.012
miR-320a	1.09 (0.31)	1.25 (0.4)	0.048
miR-429	0.001 (0.002)	0.003 (0.006)	NS
miR-483	0.01 (0.02)	0.02 (0.07)	NS

P 值小於 0.05 為統計顯著。

doi:10.6342/NTU202000313

表十三：Metformin 治療有效組和無效組之受試者特徵

	Metformin 治療無效組 (n=38)	Metformin 治療有效組 (n=37)	P 值
背景資料			
年齡 (歲)	24.4 (5.4)	24.5 (4.9)	NS
體重 (公斤)	62.9 (16.2)	65.2 (17.1)	NS
BMI (公斤/平方公尺)	24.4 (5.7)	25.4 (6.6)	NS
腰圍 (公分)	84.8 (12.1)	87.8 (15.6)	NS
臀圍 (公分)	92.7 (11.4)	95.1 (13.5)	NS
月經週期 (天)	240 (123)	169 (112)	0.01
內分泌指標			
高雄性荷爾蒙症	82%	78%	NS
Testosterone (ng/ml)	0.62 (0.26)	0.71 (0.37)	NS
DHEA-S (μg/ml)	276.1 (126.8)	276.4 (105.5)	NS
SHBG (nmol/l)	34.8 (20.1)	40.3 (25.5)	NS
FAI (%)	8.9 (7.0)	7.8 (4.6)	NS
FSH (mIU/ml)	6.3 (2.0)	6.7 (1.6)	NS
LH (mIU/ml)	12.1 (5.4)	12.1 (6.4)	NS
Estradiol (pg/ml)	47.0 (15.5)	52.9 (32.5)	NS
Prolactin (ng/ml)	8.95 (8.16)	8.03 (4.00)	NS
TSH (mIU/l)	1.62 (26.8)	1.84 (1.31)	NS
新陳代謝指標			
Insulin (IU/ml)	8.9 (9.5)	9.1 (9.2)	NS
Glucose (IU/ml)	83.2 (5.1)	83.6 (7.8)	NS
HOMA-IR	1.87 (2.01)	1.98 (2.12)	NS
Uric acid (mg/dl)	5.5 (1.4)	5.6 (1.0)	NS
LDL-C (mg/dl)	116.6 (40.4)	101.0 (26.3)	NS
HDL-C (mg/dl)	57.9 (12.6)	53.8 (12.6)	NS
TG (mg/dl)	88.5 (51.7)	86.3 (51.5)	NS
T-CHO (mg/dl)	202.5 (45.7)	182.0 (31.8)	0.028
AST (U/l)	27.1 (26.8)	23.9 (13.6)	NS
ALT (U/l)	32.8 (50.0)	28.0 (31.5)	NS

1. P 值小於 0.05 為統計顯著

2. 縮寫：PCOS: polycystic ovarian syndrome; DHEA-S: dehydroepiandrosterone sulfate, SHBG: sex hormone-binding globulin, FAI: free androgen index, FSH: follicle-stimulating hormone, LH: luteinizing hormone, HOMA-IR: homeostasis model assessment-insulin resistance, LDL-C: low-density lipoprotein-cholesterol, HDL-C: high-density lipoprotein-cholesterol, TG: triglycerides. T-CHO: total cholesterol, AST: aspartate aminotransferase, ALT: alanine aminotransferase.

doi:10.6342/NTU202000313

表十四：Metformin 治療有效組和無效組之血液微小核醣核酸表現

微小核醣核酸	Metformin 治療無效組 (n=38)	Metformin 治療有效組 (n=37)	P 值
miR-21	1.88 (1.19)	2.3 (1.42)	NS
miR-93	0.22 (0.12)	0.28 (0.13)	0.03
miR-132	0.021 (0.021)	0.017 (0.009)	NS
miR-193	2.97 (8.95)	1.01 (1.71)	NS
miR-221	1.56 (0.76)	1.68 (0.61)	NS
miR-222	0.06 (0.04)	0.09 (0.04)	0.012
miR-223	5.97 (5.52)	8.01 (5.63)	NS
miR-27a	1.14 (0.76)	1.64 (1.24)	0.04
miR-125b	0.29 (0.86)	0.12 (0.15)	NS
miR-200b	0.21 (0.7)	0.18 (0.22)	NS
miR-212	0.23 (0.61)	0.13 (0.45)	NS
miR-320a	1.08 (0.33)	1.09 (0.31)	NS
miR-429	0.001 (0.002)	0.002 (0.002)	NS
miR-483	0.01 (0.02)	0.01 (0.02)	NS

1. P 值小於 0.05 為統計顯著。

2. 縮寫：NS: not significant.

doi:10.6342/NTU202000313

表十五：微小核糖核酸表現對於 PCOS 診斷之 ROC 曲線分析值

微小核糖核酸	*敏感度*	*特異度*	*Youden index*	*曲線下面積*	*曲線下面積 (95% 信賴區間)*	*閾值*	*Probability*
miR-21	0.507	0.700	0.207	0.519	(0.400- 0.637)	1.9103	0.788
miR-93	0.560	0.950	0.510	0.743	(0.644- 0.841)	0.2392	0.848
miR-132	0.600	0.950	0.550	0.811	(0.723- 0.900)	0.0130	0.845
miR-193b	0.120	1.000	0.120	0.217	(0.128- 0.305)	5.2533	0.799
miR-221	0.360	1.000	0.360	0.597	(0.488- 0.707)	1.8221	0.822
miR-222	0.600	0.850	0.450	0.696	(0.590- 0.802)	0.0786	0.808
miR-223	0.453	0.950	0.403	0.586	(0.472- 0.700)	7.5987	0.821
miR-27a	0.520	0.950	0.470	0.777	(0.675- 0.878)	1.0902	0.854
miR-125b	0.880	0.500	0.380	0.756	(0.641- 0.871)	0.0269	0.652
miR-200b	0.547	0.600	0.147	0.459	(0.314- 0.603)	0.0747	0.788
miR- 212	0.667	0.800	0.467	0.726	(0.607- 0.845)	0.0070	0.725
miR-320a	0.613	0.650	0.263	0.617	(0.464- 0.770)	1.0630	0.813
miR-429	0.933	0.200	0.133	0.345	(0.175- 0.514)	0.0051	0.731
miR-483	1.000	0.050	0.050	0.325	(0.191- 0.459)	0.0865	0.728
預測模型＊	0.867	1.000	0.867	0.959	(0.924- 0.995)		0.862

標示網底處表示曲線下面積之 95%信賴區間大於 0.5，所對應之六個微小核糖核酸指標用來建立預測模型＊如下：Y = log (p/(1-p)) = 0.00148 – 10.8903 * **miR-93** + 28.6881 * **miR-132** - 48.8523 * **miR-222** + 2.4562 * **miR-27a +** 2.1320 * **miR-125b +** 18.2793 * **miR-212**

doi:10.6342/NTU202000313

表十六：微小核糖核酸表現對於 metformin 療效判定之 ROC 曲線分析值

微小核糖核酸	*敏感度*	*特異度*	*Youden index*	*曲線下面積*	*(95% 信賴區間)*	*閾值*	*Probability*	*P 值*
miR-21	0.946	0.263	0.209	0.588	(0.458- 0.718)	0.7943	0.411	
Adjusted miR-21[a]	0.703	0.684	0.387	0.706	(0.584- 0.827)		0.506	0.100
miR-93	0.459	0.816	0.275	0.645	(0.519- 0.771)	0.3258	0.571	
Adjusted miR-93[a]	0.703	0.737	0.440	0.733	(0.618- 0.847)		0.495	0.140
miR-132	1.000	0.132	0.132	0.436	(0.302- 0.570)	0.0418	0.452	
Adjusted miR-132[a]	0.568	0.816	0.383	0.679	(0.556- 0.801)		0.579	0.004
miR-193b	0.973	0.158	0.131	0.316	(0.187- 0.444)	6.0776	0.411	
Adjusted miR-193b[a]	0.541	0.816	0.356	0.682	(0.560- 0.804)		0.594	<0.001
miR-221	0.973	0.237	0.210	0.558	(0.425- 0.691)	0.8867	0.444	
Adjusted miR-221[a]	0.595	0.763	0.358	0.694	(0.572- 0.816)		0.562	0.083
miR-222	0.919	0.421	0.340	0.678	(0.556- 0.800)	0.0451	0.387	
Adjusted miR-222 [a]	0.919	0.605	0.524	0.773	(0.662- 0.884)		0.373	0.090
miR-223	0.892	0.421	0.313	0.634	(0.506- 0.762)	2.8557	0.425	
Adjusted miR-223 [a]	0.622	0.816	0.437	0.72	(0.601- 0.838)		0.567	0.193
miR-27a	0.324	0.895	0.219	0.61	(0.482- 0.739)	2.0691	0.583	
Adjusted miR-27a [a]	0.622	0.816	0.437	0.729	(0.614- 0.844)		0.565	0.058
miR-125b	0.946	0.132	0.078	0.489	(0.356- 0.623)	0.3175	0.470	
Adjusted miR-125b [a]	0.541	0.789	0.330	0.655	(0.529- 0.781)		0.587	0.041
miR-200b	1.000	0.053	0.053	0.307	(0.185- 0.428)	1.1205	0.469	
Adjusted miR-200b [a]	0.541	0.789	0.330	0.664	(0.539- 0.790)		0.582	<0.001
miR- 212	0.946	0.211	0.156	0.51	(0.375- 0.645)	0.1767	0.492	
Adjusted miR- 212[a]	0.541	0.816	0.356	0.68	(0.558- 0.802)		0.581	0.036
miR-320a	1.000	0.105	0.105	0.499	(0.365- 0.633)	0.6411	0.487	
Adjusted miR-320a [a]	0.568	0.737	0.304	0.671	(0.548- 0.795)		0.570	0.067
miR-429	0.838	0.447	0.285	0.641	(0.514- 0.767)	0.0003	0.453	
Adjusted miR-429 [a]	0.595	0.763	0.358	0.693	(0.573- 0.814)		0.565	0.508
miR-483	0.135	1.000	0.135	0.475	(0.341- 0.609)	0.0005	0.495	
Adjusted miR-483 [a]	0.568	0.816	0.383	0.676	(0.553- 0.800)		0.577	0.022
Model [b]	0.703	0.763	0.466	0.722	(0.602- 0.841)		0.496	
Adjusted Model [c]	0.892	0.632	0.523	0.807	(0.704- 0.909)		0.368	0.063

doi:10.6342/NTU202000313

[a] Adjusted miRNA was adjusted for MC interval, age, BMI and HA.

[b] Y = log (p/(1-p)) = -1.8255 + 4.1106 * **miR-93** + 18.0284 * **miR-222** - 0.1152 * **miR-223** + 145.8 * **miR-429**

[c] Y = log (p/(1-p)) = -2.0454 + 0.0242 * **Age** + 0.0219 * **BMI** + 0.1168 * **HA** - 0.00689 * **MC Interval** + 3.6416 * **miR-93** + 25.4973 * **miR-222** - 0.1253 * **miR-223** + 163.0 * **miR-429**

doi:10.6342/NTU202000313

表十七 Metformin 治療六個月後之臨床表徵與血漿微小核醣核酸變化

miRNA	檢測時間	Metformin 有效組 (n=37)		Metformin 無效組 (n=38)		有效 v.s. 無效
miR-21	治療前	2.3 (1.42)	P=0.003	1.88 (1.12)	NS	NS
	治療後	1.53 (1.04)		1.68 (1.26)		NS
miR-93	治療前	0.28 (0.13)	P<0.0001	0.22 (0.12)	NS	P=0.03
	治療後	0.18 (0.1)		0.18 (0.12)		NS
miR-222	治療前	0.09 (0.04)	P<0.0001	0.06 (0.04)	NS	P=0.012
	治療後	0.04 (0.03)		0.05 (0.04)		NS
miR-223	治療前	8.01 (5.63)	P<0.0001	5.97 (5.52)	NS	NS
	治療後	4.15 (3.23)		5.10 (4.30)		NS
miR-27a	治療前	1.64 (1.24)	P<0.0001	1.14 (0.76)	NS	P=0.04
	治療後	0.97 (0.61)		0.87 (0.52)		NS
Total testos-terone	治療前	0.71 (0.37)	P<0.0001	0.62 (0.26)	P<0.0001	NS
	治療後	0.44 (0.25)		0.47 (0.2)		NS
FAI	治療前	7.85 (4.63)	P=0.001	8.87 (7.0)	P=0.013	NS
	治療後	5.04 (3.31)		7.03 (7.7)		NS
FSH	治療前	6.66 (1.55)	NS	6.23 (2.04)	NS	NS
	治療後	6.11 (0.29)		6.02 (1.82)		NS
LH	治療前	12.1 (6.4)	P<0.0001	11.9 (5.4)	NS	NS
	治療後	7.9 (6.0)		11.4 (5.8)		P=0.041
DHEA-S	治療前	276.4 (105.5)	NS	276.1 (126.8)	NS	NS
	治療後	302.1 (139.9)		294.9 (127.2)		NS
體重	治療前	65.2 (17.1)	P<0.0001	62.9 (16.2)	P<0.0001	NS
	治療後	62.7 (15. 9)		60.8 (14.9)		NS
BMI	治療前	25.4 (6.8)	P<0.0001	24.4 (5.7)	P<0.0001	NS
	治療後	24.3 (6.1)		23.6 (5.2)		NS
腰圍	治療前	87.8 (15.6)	P<0.0001	84.8 (12.1)	P=0.005	NS
	治療後	84.4 (13.5)		82.2 (10.5)		NS
臀圍	治療前	95.1 (13.5)	P=0.007	92.7 (11.4)	P=0.01	NS
	治療後	92.7 (11.9)		90.3 (10.4)		NS

doi:10.6342/NTU202000313

血糖	治療前	83.6 (7.8)	NS	83.2 (5.1)	NS	NS
	治療後	83.4 (6.1)		82.9 (6.3)		NS
胰島素	治療前	9.07 (9.20)	P=0.036	8.93 (9.48)	NS	NS
	治療後	6.21 (7.33)		9.03 (9.86)		NS
HOMA-IR	治療前	1.98 (2.12)	P=0.037	1.87 (2.01)	NS	NS
	治療後	1.35 (1.72)		1.88 (2.07)		NS
總膽固醇	治療前	182.0 (31.8)	P=0.039	202.5 (45.7)	NS	P=0.028
	治療後	171.2 (34.6)		194.4 (44.0)		P=0.014
低密度脂蛋	治療前	101.1 (26.3)	NS	117. 2 (40.8)	NS	NS
白	治療後	99.6 (27.9)		113.6 (40.7)		NS
高密度脂蛋	治療前	53.8 (12.6)	NS	57.9 (12.6)	NS	NS
白	治療後	52.4 (9.3)		57.0 (11.8)		NS

- 數值之表現為平均值 (標準偏差)。
- 縮寫：NS: not significant; FAI: free androgen index; FSH: follicle-stimulating hormone; LH: luteinizing hormone; DHEA-S: dehydroepiandrosterone sulfate; BMI: body mass index; HOMA-IR: Homeostatic Model Assessment of Insulin Resistance.
- 微小核醣核酸數值以 P<0.0035 為統計顯著，其餘數值則以 P<0.05 為統計顯著。
- 藍色網底欄位之 P 值表示治療前和治療後相比，紅色網底欄位之 P 值表示 metformin 治療有效組和無效組相比。

doi:10.6342/NTU202000313

表十八 Gene ontology analysis of miR-132

	Gene numbers	Fold enrichment	FDR
GO biological process complete			
regulation of nitrogen compound metabolic process	251/5868	1.88	5.12E-25
regulation of primary metabolic process	256/6051	1.86	6.47E-25
regulation of macromolecule metabolic process	256/6180	1.82	8.62E-24
regulation of cellular metabolic process	255/6245	1.80	9.73E-23
regulation of metabolic process	266/6707	1.75	1.50E-22
regulation of RNA metabolic process	185/3826	2.13	1.22E-21
regulation of nucleobase-containing compound metabolic process	192/4080	2.07	1.39E-21
regulation of gene expression	202/4495	1.98	1.04E-20
regulation of macromolecule biosynthetic process	188/4082	2.03	5.56E-20
regulation of cellular macromolecule biosynthetic process	183/3952	2.04	1.62E-19
GO molecular function complete			
DNA-binding transcription factor activity	103/1715	2.64	8.43E-16
protein binding	367/11958	1.35	9.21E-16
regulatory region nucleic acid binding	73/966	3.33	1.55E-15
binding	425/15183	1.23	1.83E-15
transcription regulatory region DNA binding	73/965	3.33	1.83E-15
transcription regulator activity	113/2075	2.40	4.62E-15
DNA binding	126/2524	2.20	2.02E-14
sequence-specific DNA binding	78/1154	2.98	2.23E-14
proximal promoter sequence-specific DNA binding	50/562	3.92	1.02E-12
DNA-binding transcription factor activity, RNA polymerase II-specific	91/1609	2.49	1.16E-12

doi:10.6342/NTU202000313

GO cellular component complete			
intracellular part	411/14628	1.24	7.36E-14
intracellular	411/14638	1.24	8.05E-14
intracellular membrane-bounded organelle	342/11046	1.36	9.11E-14
nucleus	259/7437	1.53	1.05E-13
nuclear part	181/4506	1.77	2.70E-13
intracellular organelle	374/12834	1.28	7.00E-13
nuclear lumen	166/4109	1.78	4.04E-12
nucleoplasm	146/3491	1.84	2.38E-11
organelle	384/13654	1.24	5.70E-11
membrane-bounded organelle	361/12535	1.27	8.73E-11

FDR: false discovery rate

doi:10.6342/NTU202000313

表十九 Gene ontology analysis of miR-27a

	Gene numbers	Fold enrichment	FDR
GO biological process complete			
regulation of primary metabolic process	633/6051	1.55	1.90E-30
regulation of nitrogen compound metabolic process	613/5868	1.55	3.24E-29
regulation of metabolic process	676/6707	1.50	4.03E-29
regulation of cellular metabolic process	640/6245	1.52	5.57E-29
regulation of macromolecule metabolic process	635/6180	1.53	6.67E-29
positive regulation of cellular process	573/5409	1.57	3.86E-28
positive regulation of metabolic process	429/3614	1.76	5.49E-28
positive regulation of macromolecule metabolic process	401/3343	1.78	1.77E-26
positive regulation of biological process	622/6166	1.50	4.55E-26
multicellular organism development	533/5012	1.58	7.61E-26
GO molecular function complete			
protein binding	1019/11958	1.27	1.83E-26
binding	1197/15183	1.17	2.18E-23
molecular_function	1316/17634	1.11	1.26E-20
ion binding	573/6287	1.35	2.83E-13
sequence-specific double-stranded DNA binding	132/900	2.18	4.14E-12
regulatory region nucleic acid binding	137/966	2.11	7.66E-12
RNA polymerase II regulatory region DNA binding	121/807	2.23	8.01E-12
sequence-specific DNA binding	155/1154	2.00	8.06E-12
transcription regulatory region DNA binding	137/965	2.11	8.33E-12
transcription regulatory region sequence-specific DNA binding	125/850	2.19	8.92E-12

doi:10.6342/NTU202000313

GO cellular component complete			
intracellular	1180/14638	1.20	5.08E-28
intracellular part	1180/14628	1.20	7.33E-28
cell part	1293/17133	1.12	1.45E-21
cell	1294/17192	1.12	5.59E-21
intracellular membrane-bounded organelle	930/11046	1.25	8.70E-20
intracellular organelle	1043/12834	1.21	9.37E-20
membrane-bounded organelle	1022/12535	1.21	2.92E-19
organelle	1089/13654	1.19	5.79E-19
nucleoplasm	366/3491	1.56	4.39E-15
cytoplasm	946/11673	1.20	7.45E-15

FDR: false discovery rate

doi:10.6342/NTU202000313

表二十 Gene ontology analysis of miR-222

	Gene numbers	Fold enrichment	FDR
GO biological process complete			
regulation of cellular metabolic process	264/6245	1.75	5.14E-21
regulation of nitrogen compound metabolic process	254/5868	1.79	6.72E-21
regulation of macromolecule metabolic process	261/6180	1.75	1.15E-20
regulation of primary metabolic process	257/6051	1.76	1.28E-20
regulation of metabolic process	271/6707	1.67	3.42E-19
negative regulation of cellular process	207/4701	1.82	2.48E-16
negative regulation of metabolic process	149/2890	2.13	6.62E-16
negative regulation of macromolecule metabolic process	140/2644	2.19	1.37E-15
positive regulation of cellular process	225/5409	1.72	1.47E-15
negative regulation of biological process	245/6166	1.64	2.03E-15
GO molecular function complete			
protein binding	380/11958	1.31	3.53E-13
binding	446/15183	1.21	4.19E-13
molecular_function	483/17634	1.13	3.43E-11
RNA polymerase II regulatory region sequence-specific DNA binding	57/800	2.94	1.75E-09
RNA polymerase II regulatory region DNA binding	57/807	2.92	2.02E-09
sequence-specific DNA binding	70/1154	2.51	5.61E-09
regulatory region nucleic acid binding	62/966	2.65	6.29E-09
transcription regulatory region DNA binding	62/965	2.66	6.80E-09
double-stranded DNA binding	63/993	2.62	7.23E-09
sequence-specific double-stranded DNA binding	59/900	2.71	7.69E-09
GO cellular component complete			
nucleus	257/7437	1.43	3.79E-09
intracellular	423/14638	1.19	4.74E-09
cell	470/17192	1.13	5.84E-09
nucleoplasm	146/3491	1.73	6.23E-09

doi:10.6342/NTU202000313

cell part	469/17133	1.13	6.61E-09
intracellular part	423/14628	1.20	9.39E-09
nuclear part	173/4506	1.59	3.85E-08
nuclear lumen	161/4109	1.62	5.02E-08
intracellular membrane-bounded organelle	338/11046	1.26	9.62E-08
intracellular organelle	376/12834	1.21	3.38E-07

FDR: false discovery rate

doi:10.6342/NTU202000313

表二十一 Gene ontology analysis of miR-93

	Gene numbers	Fold enrichment	FDR
GO biological process complete			
regulation of cellular metabolic process	649/6245	1.57	5.78E-33
regulation of metabolic process	677/6707	1.52	1.31E-31
regulation of primary metabolic process	627/6051	1.56	3.34E-31
regulation of nitrogen compound metabolic process	604/5868	1.55	1.22E-28
regulation of cellular process	950/10941	1.31	2.18E-28
regulation of macromolecule metabolic process	624/6180	1.52	4.68E-28
biological regulation	1031/12352	1.26	7.65E-27
negative regulation of cellular process	506/4701	1.62	1.76E-26
regulation of cellular biosynthetic process	466/4216	1.66	5.03E-26
regulation of biosynthetic process	472/4296	1.65	5.10E-26
GO molecular function complete			
protein binding	996/11958	1.25	1.29E-23
binding	1176/15183	1.17	1.27E-21
enzyme binding	273/2238	1.84	5.62E-18
molecular_function	1286/17634	1.10	6.72E-16
DNA-binding transcription factor activity, RNA polymerase II-specific	205/1609	1.92	1.21E-14
DNA-binding transcription factor activity	211/1715	1.85	8.70E-14
transcription regulator activity	242/2075	1.76	9.53E-14
regulatory region nucleic acid binding	140/966	2.18	2.14E-13
transcription regulatory region DNA binding	140/965	2.19	2.25E-13
RNA polymerase II regulatory region DNA binding	123/807	2.30	5.26E-13
GO cellular component complete			
intracellular part	1154/14628	1.19	1.55E-24
intracellular	1155/14638	1.19	2.09E-24
intracellular organelle	1033/12834	1.21	3.46E-20
cell	1272/17192	1.11	4.00E-19
cell part	1267/17133	1.11	1.67E-18
nuclear lumen	422/4109	1.55	1.43E-17

doi:10.6342/NTU202000313

nucleus	663/7437	1.34	5.68E-17
organelle	1067/13654	1.18	5.70E-17
intracellular membrane-bounded organelle	905/11046	1.23	6.23E-17
membrane-bounded organelle	998/12535	1.20	7.41E-17

FDR: false discovery rate

doi:10.6342/NTU202000313

附錄 (Appendix)

臺灣大學醫學院臨床醫學研究所博士班修業期間所發表之相關論文清冊：

1. **Huang CC**, Tien YJ, Chen MJ*, Chen CH, Ho HN, Yang YS. Symptom patterns and phenotypic subgrouping of women with polycystic ovary syndrome: association between endocrine characteristics and metabolic aberrations. Human Reproduction 2015 Apr;30(4):937-46.

2. Wu MY, Chung CH, Pan SP, Jou GC, Chen MJ, Chang CH, Chen SU, **Huang CC***, Yang YS. Advantages of cumulative pregnancy outcomes in freeze-all strategy in high responders - A case-control matching analysis of a large cohort. J Formos Med Assoc. 2018 Aug;117(8):676-684. *correspondence

3. **Huang CC**, Chou CH, Chen SU, Ho HN, Yang YS, Chen MJ*. Increased platelet factor 4 and aberrant permeability of follicular fluid in PCOS. J Formos Med Assoc. 2019 Jan;118:249-259.

4. **Huang CC**, Chen MJ*, Lan CW, Wu CE, Huang MC, Kuo HC, Ho HN*. Hyperactive CREB signaling pathway involved in the pathogenesis of polycystic ovarian syndrome revealed by patient-specific induced pluripotent stem cell modeling. Fertil Steril. 2019 Sep;112(3):594-607.

doi:10.6342/NTU202000313